



# **Synthesis and Biological Studies of Cyclic Peptides**

by

**Haider Abdul-kareem Al-wafi**

A thesis submitted to Cardiff University

for the degree of

Doctor of Philosophy

School of Chemistry

Cardiff University

August 2018

## Declaration

This work has not been submitted in substance for any other degree or award at this or any other university or place of learning, nor is being submitted concurrently in candidature for any degree or other award.

Signed..... (Candidate) Date.....

### STATEMENT 1

This thesis is being submitted in partial fulfilment of the requirements for the degree of PhD

Signed..... (Candidate) Date.....

### STATEMENT 2

This thesis is the result of my own independent work/investigation, except where otherwise stated, and the thesis has not been edited by a third party beyond what is permitted by Cardiff University's Policy on the Use of Third Party Editors by Research Degree Students. Other sources are acknowledged by explicit references. The views expressed are my own.

Signed..... (Candidate) Date.....

### STATEMENT 3

I hereby give consent for my thesis, if accepted, to be available online in the University's Open Access repository and for inter-library loan, and for the title and summary to be made available to outside organisations.

Signed..... (Candidate) Date.....

## Acknowledgement

First and foremost, I would like to praise and thank GOD for helping me to complete this thesis.

I wish to express my gratefulness to my supervisor, **Dr James Redman** for his continuous supervision, positive discussions and valuable ideas through this research work.

**Prof. Rudolf Allemann** and his group, I would like to thank you for helping me throughout this research. I would also like to thank **Dr Mahmoud Akhtar** for his help while undertaking my PhD studies. My great thanks also extended to all technicians of the Mass laboratory and their help in offering me the facilities to complete my experiments. Special recognition to **Dr Tom Williams**. I would also like to thank other people in the group of **Prof. Wirth**. I would like to thank the staff of School of Chemistry especially.

I would like to extend my thanks to the **Iraqi Government** for sponsoring my PhD study, and many thanks to the staff of the **Iraqi cultural attaché** in London for their help during my stay in the UK.

My deepest thanks, love and gratitude for all of my family, **parents, brothers, sisters** and extraordinary thanks for my wife and my lovely kids (**Farah, Miar**).

## Abstract

Bax peptide **1c** (FLIMGWTLD) and two of its derivatives, 15-mer cyclic peptide **2c** (FLRELIRTIMGWTLD), 13-mer cyclic peptide **3c** (FLKSSKIMGWTLD) with their linear counterparts (**1b**, **2b**, **3b**) were prepared by a head-to-tail cyclisation strategy, purified (HPLC), characterised and identified (LCMS). Then the mass and concentration of the two derivatives (**2c**, **3c**) with their linear counterparts (**2b**, **3b**) were calculated. MS<sup>2</sup> mass spectra were used as evidence of synthesis of the cyclic peptides from their linear counterparts. There was a clear difference between each of the two cyclic peptides and its linear counterpart's mass spectra. A peak appeared for a fragment which has the two termini bonded together (Phe-Asp) in the cyclic peptide spectrum (**1c**, **2c**, **3c**) that did not appear in the linear peptide spectrum (**1b**, **2b**, **3b**).

The enzymatic degradation and kinetic study were undertaken for just the two derivatives (**2c**, **3c**) with their linear counterparts (**2b**, **3b**) using trypsin and chymotrypsin. Compound **1c** and its linear counterpart (**1b**) were excluded from these two studies and the stability studies of the peptide in fetal calf serum (FCS) medium because the 9-mer cyclic peptide (**1c**) had very low solubility in HPLC solvents and was hydrolysed during storage in the freezer.

Chymotrypsin cleaved the peptide bond between Trp and Thr but did not cleave the peptide bond between Phe and Asp in the 15-mer cyclic peptide (**2c**) and its linear counterpart (**2b**). Cyclisation of the linear peptide (**2b**) did not improve the stability of the peptide as the  $t_{1/2}$  of the cyclic peptide (**2c**) was less than the  $t_{1/2}$  of its linear counterpart (**2b**).

Trypsin cleaved the peptide bond between Arg and Thr in the linear peptide (**2b**), while in the cyclic peptide (**2c**) the cleavage was between Arg and Thr in addition to Arg and Glu. Stability of the cyclic peptide (**2c**) did not improve significantly as the  $t_{1/2}$  of compound **2c** increased slightly in comparison to the  $t_{1/2}$  of its linear counterpart (**2b**).

The effect of chymotrypsin on the two peptides (**3b**, **3c**) was the same. The peptide bond between Trp and Thr was hydrolysed in the two compounds (**3b**, **3c**), while between Phe and Leu did not break. Cyclisation of the linear peptide (**3b**) did not improve the stability of the peptide because the  $t_{1/2}$  of the

cyclic peptide (**3c**) increased slightly in comparison to the  $t_{1/2}$  of its linear counterpart (**3b**).

There was significant stability for the cyclic peptide (**3c**) against trypsin in comparison to its linear counterpart (**3b**). Compound **3c** did not hydrolyse for 30 min, while compound **3b** was hydrolysed at the peptide bond between Lys and Ile in the first few minutes of the enzymatic hydrolysis.

The stability of 15-mer cyclic compound (**2c**) was less than its linear counterpart (**2b**) in the medium of fetal calf serum (FCS) as the  $t_{1/2}$  of compound **2c** (120 h) was less than the  $t_{1/2}$  of compound **2b** (165 h). In contrast, the stability of the 13-mer cyclic compound (**3c**) was more than its linear counterpart (**3b**) as indicated by the  $t_{1/2}$  of compound **3c** (285 h) that was more than the  $t_{1/2}$  of **3b** (110 h).

# Contents

<b>1 Introduction</b>	<b>2</b>
1.1 Motivation	2
1.2 Bax protein	3
1.3 Binding of epitopes with MHC complex and TCR (T cell receptor)	4
1.4 Cyclic polypeptides in the medical field	6
1.5 The various types of cyclic polypeptides	8
1.6 Protecting groups in peptide synthesis	10
1.6.1 Main chain protecting groups	11
1.6.2 Side chain protecting groups	15
1.7 Methods to synthesise polypeptides	19
1.8 Cyclisation strategies of linear polypeptides	23
1.8.1 Head to tail cyclisation	23
1.8.2 Side chain-to-side chain cyclisation	29
1.8.3 Side chain-to-tail cyclisation	31
1.9 Important factors that affect the synthesis of cyclic polypeptides	32
1.9.1 Internal factors	32
1.9.2 External factors	34
1.10 Amino acids	36
1.11 Resin	38
1.12 Coupling reagents	39
<b>2 Cyclic Peptide Synthesis</b>	<b>44</b>
2.1 Introduction	44
2.2 Result and discussion of peptide synthesis	50
2.2.1 Synthesis of the 9-mer linear peptide allyl ester ( <b>1a</b> )	50
2.2.2 Synthesis of the 15-mer linear peptide allyl ester ( <b>2a</b> )	52
2.2.3 Synthesis of the 13-mer linear peptide allyl ester ( <b>3a</b> )	53

2.2.4 Synthesis of the 9-mer linear peptide ( <b>1b</b> ) as a precursor for the cyclic peptide ( <b>1c</b> )	55
2.2.5 Synthesis of the 15-mer linear peptide ( <b>2b</b> ) as a precursor for the cyclic peptide ( <b>2c</b> )	57
2.2.6 Synthesis of the 13-mer linear peptide ( <b>3b</b> ) as a precursor for the cyclic peptide ( <b>3c</b> )	58
2.3 Results and discussion of cyclisation reaction	60
2.3.1 Synthesis of the 9-mer cyclic peptide ( <b>1c</b> )	60
2.3.2 Synthesis of the 15-mer cyclic peptide ( <b>2c</b> )	63
2.3.3 Synthesis of the 13-mer cyclic peptide ( <b>3c</b> )	65
2.4 Synthesis of the linear peptide ( <b>2b</b> , <b>3b</b> )	69
2.4.1 Synthesis of the 15-mer linear peptide ( <b>2b</b> )	69
2.4.2 Synthesis of the 13-mer linear peptide ( <b>3b</b> )	70
2.5 Results of calculation of the concentration of polypeptides	72
2.5.1 Introduction	72
2.5.2 The 9-mer cyclic polypeptide ( <b>1c</b> )	73
2.5.3 The 9-mer linear peptide ( <b>1b</b> )	74
2.5.4 The 15-mer cyclic peptide ( <b>2c</b> )	74
2.6 Results of peptide fragmentation	76
2.6.1 Introduction	76
2.6.2 Comparison between fragmentation of the 9-mer cyclic peptide ( <b>1c</b> ) and its linear counterpart ( <b>1b</b> )	80
2.6.3 Comparison between fragmentation of the 15-mer cyclic peptide ( <b>2c</b> ) and its linear counterpart ( <b>2b</b> )	83
2.6.4 Comparison between fragmentation of the 13-mer cyclic ( <b>3c</b> ) peptide and its linear counterpart ( <b>3b</b> )	87
<b>3 Biological studies of the peptides</b>	<b>92</b>
3.1 Introduction	92

3.2 Results and discussion of the study of enzymatic degradation of peptides	92
3.2.1 Results of calculation of the concentration of trypsin and chymotrypsin	92
3.2.2 Results of the study of the activity of trypsin and chymotrypsin	94
3.2.3 Enzymatic degradation and kinetic study of the 15-mer linear peptide (2b) in the presence of chymotrypsin	95
3.2.4 Enzymatic degradation and kinetic study of the 15-mer cyclic peptide (2c) in the presence of chymotrypsin and the comparison with its linear counterpart (2b)	99
3.2.5 Enzymatic degradation and kinetic study of the 15-mer linear peptide (2b) in the presence of trypsin	105
3.2.6 Enzymatic degradation and kinetic study of the 15-mer cyclic peptide (2c) in the presence of trypsin and the comparison with its linear counterpart (2b)	110
3.2.7 Enzymatic degradation and kinetic study of the 13-mer linear peptide (3b) in the presence of chymotrypsin	116
3.2.8 Enzymatic degradation and kinetic study of the 13-mer cyclic peptide (3c) in the presence of chymotrypsin and the comparison with its linear counterpart (3b)	121
3.2.9 Enzymatic degradation and kinetic study of the 13-mer linear peptide (3b) in the presence of trypsin	126
3.2.10 Enzymatic degradation and kinetic study of the 13-mer cyclic peptide in the presence of trypsin and the comparison with its linear counterpart (3b)	131
<b>4 Stability of the peptides in fetal calf serum</b>	<b>136</b>
4.1 Introduction	136
4.2 Stability of the 15-mer linear peptide (2b) in 20% FCS	136
4.3 Stability of the 15-mer cyclic peptide (2c) in 20% FCS	139
4.4 Stability of the 13-mer linear peptide (3b) in 20% FCS	143
4.5 Stability of the 13-mer cyclic peptide (3c) in 20% FCS	145



<b>5 Conclusion</b>	<b>151</b>
5.1 Conclusion	151
5.1.1 Synthesis of peptides	151
5.1.2 Enzymatic degradation and kinetic study	155
5.1.3 Stability of the peptides ( <b>2b</b> , <b>2c</b> , <b>3b</b> , <b>3c</b> ) in fetal calf serum (FCS)	157
5.2 Future work	158
<b>6 Methods</b>	<b>160</b>
6.1 Analytical methods	160
6.1.1 RP-HPLC	160
6.1.2 LC-MS	160
6.1.3 Glass and plasticware	160
6.1.4 Chemicals	161
6.1.5 Instruments	161
6.2 Method to synthesise the cyclic peptide and their linear counterparts	161
6.2.1 Method to synthesise the linear peptide allyl esters ( <b>1a</b> , <b>2a</b> , <b>3a</b> )	161
6.2.2 Method to deprotect the allyl ester from the C-terminus	162
6.2.3 Cyclisation of the linear peptide ( <b>1c</b> , <b>2c</b> , <b>3c</b> )	163
6.2.4 Method to synthesise linear peptide ( <b>1b</b> , <b>2b</b> , <b>3b</b> )	163
6.2.5 Cleavage of the cyclised peptide	164
6.3 HPLC purification of the peptides	164
6.4 Fragmentation of the peptides	166
6.5 Preparation of the buffer solution	167
6.6 Calculating the concentration of the peptides ( <b>2b</b> , <b>2c</b> , <b>3b</b> , <b>3c</b> )	167
6.6.1 The 13-mer cyclic peptide ( <b>3c</b> )	167
6.6.2 The 13-mer linear peptide ( <b>3b</b> )	167
6.6.3 The 15-mer cyclic peptide ( <b>2c</b> ) and its linear counterpart ( <b>2b</b> )	168

6.6.4 Calculation of the percentage yield of the peptides ( <b>2b</b> , <b>2c</b> , <b>3b</b> , <b>3c</b> )	168
6.7 Calculation of the concentration of the enzymes	168
6.8 Preparation of the BSA solution	169
6.9 Checking the activity of the enzymes	169
6.9.1 Activity of the chymotrypsin	169
6.9.2 Activity of the trypsin	169
6.10 Enzymatic degradation and kinetics for the hydrolysis of peptides	169
6.10.1 Enzymatic degradation and calculation of the $t_{1/2}$ of 13-mer linear peptide ( <b>3b</b> ) in the presence of chymotrypsin	169
6.10.2 Enzymatic degradation and calculation of the $t_{1/2}$ of the 13-mer cyclic peptide ( <b>3c</b> ) in the presence of chymotrypsin	170
6.10.3 Enzymatic degradation and calculation of the $t_{1/2}$ of the 13-mer linear peptides ( <b>3b</b> ) in the presence of trypsin	171
6.10.4 Enzymatic degradation and calculation of the $t_{1/2}$ of the 13-mer cyclic peptide ( <b>3c</b> ) in the presence of trypsin	171
6.10.5 Enzymatic degradation and calculation of the $t_{1/2}$ of the 15-mer linear peptide ( <b>2b</b> ) in the presence of chymotrypsin	171
6.10.6 Enzymatic degradation and calculation of the $t_{1/2}$ of the 15-mer cyclic peptide ( <b>2c</b> ) in the presence of chymotrypsin	172
6.10.7 Enzymatic degradation and calculation of the $t_{1/2}$ of the 15-mer linear peptide ( <b>2b</b> ) in the presence of trypsin	172
6.10.8 Enzymatic degradation and calculation of the $t_{1/2}$ of the 15-mer cyclic peptide ( <b>2c</b> ) in the presence of trypsin	173
6.11 General procedures to study the stability of the peptides ( <b>2b</b> , <b>3b</b> , <b>2c</b> , <b>3c</b> ) in fetal calf serum (FCS)	173
6.11.1 Preparation of 20% FCS solution	173
6.11.2 Studying the stability of the 13-mer linear peptide ( <b>3b</b> ) in the presence of FCS	173

6.11.3 Studying the stability of the 13-mer cyclic peptide ( <b>3c</b> ) in the presence of FCS	174
6.11.4 Studying the stability of the 15-mer linear peptide ( <b>2b</b> ) in the presence of FCS	174
6.11.5 Studying the stability of the 15-mer cyclic peptide ( <b>2c</b> ) in the presence of FCS	175
6.11.6 General procedure to calculate the $t_{1/2}$ of the peptides ( <b>2b</b> , <b>2c</b> , <b>3b</b> , <b>3c</b> ) in the presence of FCS	175
<b>7 References</b>	<b>177</b>
<b>8 Appendix A</b>	<b>190</b>
<b>9 Appendix B</b>	<b>206</b>
<b>10 Appendix C</b>	<b>242</b>

## List of Figures

<b>Figure 1.1:</b> Structure of major histocompatibility complex class I (MHC). <sup>16</sup>	5
<b>Figure 1.2:</b> A-homodetic cyclic peptide, B-heterodetic cyclic peptide, C-complex cyclic peptide, D-Cyclotides (Kalata B1).	9
<b>Figure 1.3:</b> Structure of batenecin (A), cyclosporin A (B), largamide (C).	10
<b>Figure 1.4:</b> Structure of Cbz (carbobenzoxy) protecting group.	11
<b>Figure 1.5:</b> Structure of Troc (A), Bpoc (B), Nps (C) protecting groups attached to an amino acid.	12
<b>Figure 1.6:</b> Dmab protecting group structure.	15
<b>Figure 1.7:</b> Three types of arginine protecting group.	16
<b>Figure 1.8:</b> Structure of Lys(ivDde)-OH (A) and Lys(Dde)-OH (B).	17
<b>Figure 1.9:</b> Types of cysteine protecting group.	18
<b>Figure 1.10:</b> General structure of cyclic peptide via a lactam bond.	30
<b>Figure 1.11:</b> General structure of cyclic peptide via a disulfide bond.	30
<b>Figure 1.12:</b> Formation of a cyclic structure by two serine residues that are esterified to a dicarboxylic acid.	31
<b>Figure 1.13:</b> Types of additives to prevent racemisation.	35
<b>Figure 1.14:</b> L and D-isomers of amino acid.	37
<b>Figure 1.15:</b> Types of coupling reagents.	40
<b>Figure 2.1:</b> Location of peptide IMGWTLDFL in the Bax protein (1F16) highlighted in yellow. <sup>171</sup>	45
<b>Figure 2.2:</b> Structure of compounds <b>1a</b> , <b>2a</b> and <b>3a</b> .	47
<b>Figure 2.3:</b> Sequences of <b>1c</b> , <b>2c</b> and <b>3c</b> .	48
<b>Figure 2.4:</b> A = Structure of Fmoc-Asp (NovaSyn® TGA)-OAll. B = Structure of Fmoc-Trp(Boc)-Thr(ψMe, Mepro)-OH.	50
<b>Figure 2.5:</b> HPLC chromatogram of 9-mer crude linear peptide allyl ester ( <b>1a</b> ).	51
<b>Figure 2.6:</b> Total ion chromatogram of 9-mer purified linear peptide allyl ester ( <b>1a</b> ) ( $[M+H]^+$ $m/z = 1135.5$ ), collected peak at 22.53 min in Figure 2.5).	51
<b>Figure 2.7:</b> Structure of 9-mer linear peptide allyl ester ( <b>1a</b> ) in the +1 charge state ( $m/z = 1135.5$ ).	52
<b>Figure 2.8:</b> HPLC chromatogram of 15-mer crude linear peptide allyl ester ( <b>2a</b> ).	52
<b>Figure 2.9:</b> Total ion chromatogram of 15-mer crude linear peptide allyl ester ( <b>2a</b> ) ( $[M+2H]^{2+}$ $m/z = 952.5$ ).	53
<b>Figure 2.10:</b> Structure of 15-mer linear peptide allyl ester ( <b>2a</b> ) in the +2 charge state ( $m/z = 952.5$ ).	53

<b>Figure 2.11:</b> HPLC chromatogram of 13-mer crude linear peptide allyl ester ( <b>3a</b> ). .....	54
<b>Figure 2.12:</b> Total ion chromatogram of 13-mer crude linear peptide allyl ester ( <b>3a</b> ) ( $[M+3H]^{3+}$ $m/z = 522.6$ ). .....	54
<b>Figure 2.13:</b> Structure of 13-mer linear peptide allyl ester ( <b>3a</b> ) in the +3 charge state ( $m/z = 522.6$ ). .....	55
<b>Figure 2.14:</b> HPLC chromatogram of 9-mer crude linear peptide ( <b>1b</b> ). .....	55
<b>Figure 2.15:</b> Total ion chromatogram of 9-mer crude linear peptide ( <b>1b</b> ) ( $[M+H]^+$ $m/z = 1095.6$ ). .....	56
<b>Figure 2.16:</b> Structure of 9-mer linear peptide ( <b>1b</b> ) in the +1 charge state ( $m/z = 1095.6$ ). .....	56
<b>Figure 2.17:</b> HPLC chromatogram of 15-mer purified linear peptide ( <b>2b</b> ). .....	57
<b>Figure 2.18:</b> Total ion chromatogram of 15-mer purified linear peptide ( <b>2b</b> ) ( $[M+3H]^{3+}$ $m/z = 622.0$ ). .....	57
<b>Figure 2.19:</b> Structure of 15-mer linear peptide ( <b>2b</b> ) in the +3 charge state ( $m/z = 622.0$ ). .....	58
<b>Figure 2.20:</b> HPLC chromatogram of 13-mer crude linear peptide ( <b>3b</b> ). .....	58
<b>Figure 2.21:</b> Total ion chromatogram of 13-mer crude linear peptide ( <b>3b</b> ) ( $[M+3H]^{3+}$ $m/z = 509.3$ ). .....	59
<b>Figure 2.22:</b> Structure of 13-mer linear peptide ( <b>3b</b> ) in the +3 charge state ( $m/z = 509.3$ ). .....	59
<b>Figure 2.23:</b> HPLC chromatogram of 9-mer purified cyclic peptide ( <b>1c</b> ). .....	61
<b>Figure 2.24:</b> Total ion chromatogram of 9-mer purified cyclic peptide ( <b>1c</b> ) ( $[M-H]^-$ $m/z = 1075.5$ ). .....	62
<b>Figure 2.25:</b> Structure of 9-mer cyclic peptide ( <b>1c</b> ) in the -1 charge state ( $m/z = 1075.5$ ). .....	62
<b>Figure 2.26:</b> HPLC chromatogram of 15-mer purified cyclic peptide ( <b>2c</b> ). .....	64
<b>Figure 2.27:</b> Total ion chromatogram of 15-mer purified cyclic peptide ( <b>2c</b> ) ( $[M+2H]^{2+}$ $m/z = 923.5$ ). .....	64
<b>Figure 2.28:</b> Structure of 15-mer cyclic peptide ( <b>2c</b> ) in the +2 charge state ( $m/z = 923.5$ ). .....	65
<b>Figure 2.29:</b> HPLC chromatogram of 13-mer purified cyclic peptide ( <b>3c</b> ). .....	66
<b>Figure 2.30:</b> Total ion chromatogram of 13-mer purified cyclic peptide ( <b>3c</b> ) ( $[M+2H]^{2+}$ $m/z = 754.4$ ). .....	67
<b>Figure 2.31:</b> Structure of 13-mer cyclic peptide ( <b>3c</b> ) in the +2 charge state ( $m/z = 754.4$ ). .....	67
<b>Figure 2.32:</b> HPLC chromatogram of 15-mer purified linear peptide ( <b>2b</b> ). .....	69

<b>Figure 2.33:</b> Total ion chromatogram of 15-mer purified linear peptide ( <b>2b</b> ) ( $[M+3H]^{3+}$ $m/z = 622.0$ ).....	70
<b>Figure 2.34:</b> HPLC chromatogram of 13-mer purified linear peptide ( <b>3b</b> ).....	70
<b>Figure 2.35:</b> Total ion chromatogram of 13-mer purified linear peptide ( <b>3b</b> ) ( $[M+3H]^{3+}$ $m/z = 509.5$ ).....	71
<b>Figure 2.36:</b> HPLC chromatogram of 9-mer purified cyclic peptide ( <b>1c</b> ) after 15 days' storage in the freezer at $-20\text{ }^{\circ}\text{C}$ . ....	73
<b>Figure 2.37:</b> Total ion chromatogram of 9-mer purified cyclic peptide ( <b>1c</b> ) after 15 days' storage in the freezer at $-20\text{ }^{\circ}\text{C}$ , ( $[M+H]^+$ $m/z = 1077.5$ ).....	74
<b>Figure 2.38:</b> $MS^2$ mass spectrum of 9-mer cyclic peptide ( <b>1c</b> ) precursor ( $m/z = 1077$ ).....	80
<b>Figure 2.39:</b> $MS^2$ mass spectrum of 9-mer linear peptide ( <b>1b</b> ) precursor ( $m/z = 1095.7$ ).....	82
<b>Figure 2.40:</b> $MS^2$ mass spectrum of 15-mer cyclic peptide ( <b>2c</b> ) precursor ( $m/z = 924.0$ ).....	84
<b>Figure 2.41:</b> $MS^2$ mass spectrum of 15-mer linear peptide ( <b>2b</b> ) precursor ( $m/z = 933.0$ ).....	86
<b>Figure 2.42:</b> $MS^2$ mass spectrum of purified 13-mer cyclic peptide ( <b>3c</b> ) precursor ( $m/z = 754.9$ ).....	87
<b>Figure 2.43:</b> $MS^2$ mass spectrum of purified 13-mer linear peptide ( <b>3b</b> ) precursor ( $m/z = 509.6$ ).....	89
<b>Figure 3.1:</b> Calibration graph of the protein standard (BSA).....	93
<b>Figure 3.2:</b> HPLC chromatograms of the reaction between $25\text{ }\mu\text{L}$ of chymotrypsin ( $1.06\text{ }\mu\text{M}$ ) and $250\text{ }\mu\text{L}$ of <b>2b</b> ( $100\text{ }\mu\text{M}$ ) at $10\text{ }^{\circ}\text{C}$ and pH 8.6 for 0 and 30 min. ....	96
<b>Figure 3.3:</b> Total ion chromatogram of 15-mer linear peptide ( <b>2b</b> ) in the presence of chymotrypsin at $10\text{ }^{\circ}\text{C}$ and pH 8.6 for 20 min. ....	97
<b>Figure 3.4:</b> Suggested structure of peptide <b>2b1</b> ( $348.2\text{ }m/z$ ) in the +1 charge state produced by enzymatic hydrolysis of 15-mer linear peptide ( <b>2b</b> ) in the presence of chymotrypsin at $10\text{ }^{\circ}\text{C}$ and pH 8.6 for 20 min. ....	97
<b>Figure 3.5:</b> Enzymatic hydrolysis of 15-mer linear peptide ( <b>2b</b> ) by chymotrypsin at $10\text{ }^{\circ}\text{C}$ and pH 8.6.....	99
<b>Figure 3.6:</b> HPLC chromatograms of the reaction between $25\text{ }\mu\text{L}$ of chymotrypsin ( $1.06\text{ }\mu\text{M}$ ) and $250\text{ }\mu\text{L}$ of <b>2c</b> ( $100\text{ }\mu\text{M}$ ) at $10\text{ }^{\circ}\text{C}$ and pH 8.6 at 0 and 20 min.....	100
<b>Figure 3.7:</b> Total ion chromatogram of 15-mer cyclic peptide ( <b>2c</b> ) in the presence of chymotrypsin at $10\text{ }^{\circ}\text{C}$ and pH 8.6 for 20 min. ....	100
<b>Figure 3.8:</b> Suggested structure of peptide ( $m/z = 923.5$ ) in the +2 charge state produced from 15-mer cyclic peptide ( <b>2c</b> ) by trypsin catalysed hydrolysis of the	

peptide bond between Asp and Phe with elimination of one water molecule from one of the threonine residues. ....	101
<b>Figure 3.9:</b> Suggested structure of peptide <b>2c1</b> ( $m/z = 923.5$ ), in the +2 charge state produced from cyclic peptide ( <b>2c</b> ) by chymotrypsin catalysed hydrolysis of the peptide bond between Thr and Trp with elimination of a water molecule from one of the threonine residues. ....	102
<b>Figure 3.10:</b> Enzymatic hydrolysis of 15-mer cyclic peptide ( <b>2c</b> ) by chymotrypsin at 10 °C and pH 8.6. ....	104
<b>Figure 3.11:</b> HPLC chromatograms of the reaction between 25 $\mu\text{L}$ of trypsin (0.41 $\mu\text{M}$ ) and 250 $\mu\text{L}$ of <b>2b</b> (100 $\mu\text{M}$ ) at 10 °C and pH 6.2 for 0, 8, 15 min. ....	106
<b>Figure 3.12:</b> Total ion chromatogram of 15-mer linear peptide ( <b>2b</b> ) in the presence of trypsin at 10 °C and pH 6.2 for 20 min. ....	107
<b>Figure 3.13:</b> Suggested structure of peptide <b>2b4</b> (936.4 $m/z$ ) in the +1 charge state produced by enzymatic hydrolysis of 15-mer linear peptide ( <b>2b</b> ) by trypsin at 10 °C and pH 6.2 for 20 min. ....	107
<b>Figure 3.14:</b> Enzymatic hydrolysis of 15-mer linear peptide ( <b>2b</b> ) by trypsin at 10 °C and pH 6.2. ....	109
<b>Figure 3.15:</b> HPLC chromatograms of the reaction between 25 $\mu\text{L}$ of trypsin (0.41 $\mu\text{M}$ ) and 250 $\mu\text{L}$ of <b>2c</b> (100 $\mu\text{M}$ ) at 10 °C and the pH 6.2 for 0, 2, 30 min. ....	111
<b>Figure 3.16:</b> Total ion chromatogram of 15-mer cyclic peptide ( <b>2c</b> ) after its digestion by trypsin at 10 °C and pH 6.2 for 20 min. ....	112
<b>Figure 3.17:</b> Suggested structure of peptide <b>2c2</b> (676.9 $m/z$ ) in the +2 charge state produced by enzymatic hydrolysis of 15-mer cyclic peptide ( <b>2c</b> ) in the presence of trypsin where the peptide bonds between Arg and Thr, Arg and Glu were cleaved. ....	113
<b>Figure 3.18:</b> Suggested structure of peptide <b>2c3</b> ( $m/z = 530.3$ ) in the +1 charge state produced by enzymatic hydrolysis of 15-mer cyclic peptide ( <b>2c</b> ) in the presence of trypsin where the peptide bonds between Arg and Thr, Arg and Glu were cleaved. ....	114
<b>Figure 3.19:</b> Structure of 15-mer linear peptide ( <b>2b</b> ) in the +3 charge state ( $m/z = 622.0$ ). ....	114
<b>Figure 3.20:</b> Enzymatic hydrolysis of 15-mer cyclic peptide ( <b>2c</b> ) by trypsin at 10 °C and pH 6.2. ....	115
<b>Figure 3.21:</b> HPLC chromatograms of the reaction between 25 $\mu\text{L}$ of chymotrypsin (1.06 $\mu\text{M}$ ) and 250 $\mu\text{L}$ of 13-mer linear peptide ( <b>3b</b> ) (200 $\mu\text{M}$ ) at 10 °C and the pH 8.6 for 0, 4, 30 min. ....	117

<b>Figure 3.22:</b> Total ion chromatogram of 13-mer linear peptide ( <b>3b</b> ) after digestion by chymotrypsin at 10 °C and pH 8.6 for 20 min.....	118
<b>Figure 3.23:</b> Suggested structure of peptide <b>3b1</b> (399.6 m/z) in the +3 charge state produced by enzymatic hydrolysis of 13-mer linear peptide ( <b>3b</b> ) in the presence of chymotrypsin where the peptide bond between Trp and Thr was cleaved.....	119
<b>Figure 3.24:</b> Enzymatic hydrolysis of 13-mer linear peptide ( <b>3b</b> ) by chymotrypsin at 10 °C and pH 8.6.....	121
<b>Figure 3.25:</b> HPLC chromatograms of the reaction between 25 µL of chymotrypsin (1.06 µM) and 250 µL of <b>3c</b> (200 µM) at 10 °C and pH 8.6 for 0, 4, 20 min. ....	122
<b>Figure 3.26:</b> Total ion chromatogram of 13-mer cyclic peptide ( <b>3c</b> ) after its digestion with chymotrypsin at 10 °C and pH 8.6 for 20 min. ....	123
<b>Figure 3.27:</b> Suggested structure of peptide <b>3c1</b> (763.4 m/z) in the +2 charge state produced by enzymatic hydrolysis of <b>3c</b> in the presence of chymotrypsin where the peptide bond between Trp and Thr was cleaved.....	123
<b>Figure 3.28:</b> Enzymatic hydrolysis of 13-mer cyclic peptide ( <b>3c</b> ) in the presence of chymotrypsin at 10 °C and pH 8.6. ....	125
<b>Figure 3.29:</b> HPLC chromatograms of the reaction between 25 µL of trypsin (0.41 µM) and 250 µL of <b>3b</b> (200 µM) at 10 °C and the pH 6.2 over 0, 8 and 20 min. ....	127
<b>Figure 3.30:</b> Total ion chromatogram of 13-mer linear peptide ( <b>3b</b> ) during digestion by trypsin at 10 °C and pH 6.2 for 20 min. ....	128
<b>Figure 3.31:</b> Suggested structure of peptide <b>3b4</b> (835.4 m/z) in the +1 charge state produced by enzymatic hydrolysis of <b>3b</b> in the presence of trypsin where the peptide bond between Lys and Ile was cleaved.....	128
<b>Figure 3.32:</b> Suggested structure of peptide <b>3b3</b> (709.4 m/z) in the +1 charge state produced by enzymatic hydrolysis of 13-mer linear peptide ( <b>3b</b> ) in the presence of trypsin where the peptide bond between Lys and Ile was cleaved. ....	130
<b>Figure 3.33:</b> Enzymatic hydrolysis of 13-mer linear peptide ( <b>3b</b> ) by trypsin at 10 °C and pH 6.2. ....	131
<b>Figure 3.34:</b> HPLC chromatograms of the reaction between 25 µL of trypsin (0.41 µM) and 250 µL of <b>3c</b> (200 µM) with an internal standard (IS) at 10 °C and the pH 6.2 for 0, 30 min. ....	132
<b>Figure 3.35:</b> Structure of 13-mer cyclic peptide ( <b>3c</b> ) in the +2 charge state (m/z = 754.4).....	133



<b>Figure 3.36:</b> HPLC chromatograms of 13-mer cyclic peptide ( <b>3c</b> ) and its linear counterpart ( <b>3b</b> ) during their digestion with trypsin at 0, 20 min for <b>3b</b> and 0, 30 min for <b>3c</b> .	134
<b>Figure 4.1:</b> Stability of 15-mer linear peptide ( <b>2b</b> ) in 20% FCS at 37 °C and pH 7.4 (Replicate 1, 2, 3).	138
<b>Figure 4.2:</b> Stability of 15-mer cyclic peptide ( <b>2c</b> ) in 20% FCS at 37 °C and pH 7.4 (Replicate 1, 2, 3).	141
<b>Figure 4.3:</b> Stability of 13-mer linear peptide ( <b>3b</b> ) in 20% FCS at 37 °C and pH 7.4 (Replicates 1, 2, 3).	144
<b>Figure 4.4:</b> Stability of 13-mer cyclic peptide ( <b>3c</b> ) in 20% FCS at 37 °C and pH 7.4 (Replicates 1, 2, 3).	147

## List of Schemes

<b>Scheme 1.1:</b> The function of Bax in the apoptosis pathway. ....	3
<b>Scheme 1.2:</b> N-protected dipeptide (benzoyl glycylglycine) formation. ....	11
<b>Scheme 1.3:</b> Introduction of Fmoc group into an amino acid. ....	12
<b>Scheme 1.4:</b> Mechanism of Fmoc group removal by piperidine. ....	13
<b>Scheme 1.5:</b> Introducing Boc protecting group to the N-terminus of the amino acid. ....	13
<b>Scheme 1.6:</b> Mechanism of the Boc protecting group cleavage. ....	14
<b>Scheme 1.7:</b> Protection of C-terminus as an allyl ester. ....	14
<b>Scheme 1.8:</b> Deprotection of allyl protecting group by palladium catalyst. ....	15
<b>Scheme 1.9:</b> Homoserine lactone formation after methionine alkylation. ....	17
<b>Scheme 1.10:</b> $\beta$ -elimination of protected cysteine at the C-terminus. ....	18
<b>Scheme 1.11:</b> $\alpha$ and $\beta$ -peptide formation resulting from aspartimide formation. .	19
<b>Scheme 1.12:</b> Peptide bond formation reaction. ....	19
<b>Scheme 1.13:</b> Solution phase synthesis (SPS) fragment coupling method to synthesise a polypeptide. ....	20
<b>Scheme 1.14:</b> General scheme for synthesis of polypeptide using the solid phase Fmoc strategy. ....	21
<b>Scheme 1.15:</b> Principle of native chemical ligation (NCL) reaction. ....	25
<b>Scheme 1.16:</b> General mechanism of protein splicing by an intein. ....	27
<b>Scheme 1.17:</b> Mechanism of the Staudinger ligation mediated by phosphinothiol. ....	28
<b>Scheme 1.18:</b> Click chemistry procedure. ....	29
<b>Scheme 1.19:</b> Cyclisation of the linear peptide via the radical addition of the thiol group in the cysteine to the alkene group. ....	31
<b>Scheme 1.20:</b> Amino acids categorised according to polarity. ....	37
<b>Scheme 1.21:</b> General scheme for the coupling reaction. ....	39
<b>Scheme 1.22:</b> Dicyclohexylurea formation using the reagent DCC. ....	41
<b>Scheme 1.23:</b> Racemisation of a protected amino acid using DCC or DIC as a coupling reagent. ....	41
<b>Scheme 2.1:</b> General procedure to synthesise of the cyclic peptide ( <b>1c</b> ) by the head to tail method. ....	47
<b>Scheme 2.2:</b> Mechanism of peptide fragmentation using the CID method. ....	77
<b>Scheme 2.3:</b> Loss of ammonia from lysine-containing peptide forming a stable caprolactam derivative. ....	77

<b>Scheme 2.4:</b> Caprolactam derivative formed from lysine without loss of ammonia. ....	78
<b>Scheme 2.5:</b> Loss of ammonia from arginine-containing peptide. ....	78
<b>Scheme 2.6:</b> Caprolactam derivative formed by Arg side chain without loss of ammonia. ....	79
<b>Scheme 2.7:</b> Loss of water from Ser-containing peptide. ....	79
<b>Scheme 2.8:</b> Formation of a stable cyclic anhydride from an Asp residue.....	79
<b>Scheme 2.9:</b> Possible sites of cleaved peptide bonds during fragmentation of 9-mer cyclic peptide ( <b>1c</b> ) by MS <sup>2</sup> to result in the fragment of 946.6 m/z (b <sub>8</sub> , b <sub>8</sub> -H <sub>2</sub> O) which has a bond between F and D. ....	82
<b>Scheme 2.10:</b> Possible sites of cleaved peptide bonds in the 15-mer cyclic peptide ( <b>2c</b> ) during fragmentation by MS <sup>2</sup> to produce the fragment of MH <sub>2</sub> -NH <sub>3</sub> (915.0 m/z) which has a bond between F and D.....	85
<b>Scheme 2.11:</b> Possible sites of cleaved peptide bonds during fragmentation of 13-mer cyclic peptide ( <b>3c</b> ) by MS <sup>2</sup> to result in the fragment of 617.0 m/z (b <sub>5</sub> , y <sub>5</sub> ) which has a bond between F and D. ....	88
<b>Scheme 3.1:</b> Site of the peptide bond in 15-mer linear peptide ( <b>2b</b> ) that is cleaved by chymotrypsin at 10 °C and pH 8.6 for 20 min. ....	97
<b>Scheme 3.2:</b> Site of the cleaved peptide bond in 15-mer cyclic peptide ( <b>2c</b> ) by chymotrypsin at 10 °C and pH 8.6 for 20 min. ....	102
<b>Scheme 3.3:</b> Site of the peptide bond in the 15-mer linear peptide ( <b>2b</b> ) that is cleaved by trypsin at 10 °C and pH 6.2 for 20 min. ....	107
<b>Scheme 3.4:</b> Sites of the peptide bonds in the 15-mer cyclic peptide ( <b>2c</b> ) that are cleaved by trypsin at 10 °C and pH 6.2 for 20 min. ....	112
<b>Scheme 3.5:</b> Site of the peptide bond (Trp–Thr) cleaved by chymotrypsin in the 13-mer linear peptide ( <b>3b</b> ) at 10 °C and pH 8.6 for 20 min. ....	118
<b>Scheme 3.6:</b> Site of the peptide bond (Trp–Thr) cleaved by chymotrypsin in the 13-mer cyclic peptide ( <b>3c</b> ) at 10 °C and pH 8.6 for 20 min. ....	123
<b>Scheme 3.7:</b> Site of the peptide bond (Lys–Ile) cleaved by trypsin in the 13-mer linear peptide ( <b>3b</b> ) at 10 °C and pH 6.2 for 20 min. ....	128

## List of Tables

<b>Table 1.1:</b> Name and structure of some common resin linkers.....	38
<b>Table 2.1:</b> Attempts at cyclising <b>1b</b> under different conditions.....	61
<b>Table 2.2:</b> Comparison between the three cyclic peptides ( <b>1c</b> , <b>2c</b> , <b>3c</b> ). ....	68
<b>Table 2.3:</b> Properties of the two synthesised linear peptides ( <b>2b</b> , <b>3b</b> ). ....	72
<b>Table 2.4:</b> The value of concentration, weight, number of moles, and the percentage yield of the peptides ( <b>2b</b> , <b>2c</b> , <b>3b</b> , <b>3c</b> ) in their stock solutions.....	75
<b>Table 2.5:</b> The comparison between theoretically calculated peaks and the observed CID fragments of purified 9-mer cyclic peptide ( <b>1c</b> ). (See Figure 2.38) .....	81
<b>Table 2.6:</b> The comparison between theoretically calculated peaks and the observed CID fragments of purified 9-mer linear peptide ( <b>1b</b> ). (See Figure 2.39). ....	83
<b>Table 2.7:</b> The comparison between theoretically calculated peaks and the observed CID fragments of purified 15-mer cyclic peptide ( <b>2c</b> ). (See Figure 2.40). ....	84
<b>Table 2.8:</b> The comparison between theoretically calculated peaks and the observed CID fragments of purified 15-mer linear peptide ( <b>2b</b> ). (See Figure 2.41). ....	86
<b>Table 2.9:</b> The comparison between theoretically calculated peaks and the observed CID fragments of purified 13-mer cyclic peptide ( <b>3c</b> ). (See Figure 2.42). ....	87
<b>Table 2.10:</b> The comparison between theoretically calculated peaks and the observed CID fragments of purified 13-mer linear peptide ( <b>3b</b> ). (See Figure 2.43). ....	89
<b>Table 3.1:</b> Absorbance at 595 nm for the different concentrations of standard protein (BSA) with Bradford reagent.....	93
<b>Table 3.2:</b> Concentration of trypsin and chymotrypsin in 200 $\mu$ L ( $C_1$ ) and the stock solution ( $C_2$ ) with the mean of $C_2$ .....	94
<b>Table 3.3:</b> The comparison between theoretically calculated peaks and the observed CID fragments of precursor ion 348.1 m/z, (peptide <b>2b1</b> ) produced by hydrolysis of 15-mer linear peptide ( <b>2b</b> ) in the presence of chymotrypsin (See Figure B.6 in Appendix B). ....	98
<b>Table 3.4:</b> Areas of 15-mer linear peptide ( <b>2b</b> ) peaks in the HPLC chromatograms during its digestion with chymotrypsin at 10 °C and pH 8.6.....	98

<b>Table 3.5:</b> $t_{1/2}$ of 15-mer linear peptide ( <b>2b</b> ) during incubation with chymotrypsin at 10 °C and pH 8.6, including the rate constant ( $k \text{ min}^{-1}$ ) and the standard error (SE).....	99
<b>Table 3.6:</b> The comparison between theoretically calculated peaks and the observed CID fragments of the precursor ion 924.0 m/z (peptide <b>2c1</b> ) produced by hydrolysis of 15-mer cyclic peptide ( <b>2c</b> ) by chymotrypsin (See Figure B.8 in Appendix B). ....	103
<b>Table 3.7:</b> Areas of 15-mer cyclic peptide ( <b>2c</b> ) peaks in the HPLC chromatograms during digestion with chymotrypsin at 10 °C and pH 8.6. ....	104
<b>Table 3.8:</b> $t_{1/2}$ of 15-mer cyclic peptide ( <b>2c</b> ) during incubation with chymotrypsin at 10 °C and pH 8.6 including rate constant ( $k \text{ min}^{-1}$ ) and the standard error (SE). ....	104
<b>Table 3.9:</b> The comparison between theoretically calculated peaks and the observed CID fragments of the precursor ion 936.6 m/z (peptide <b>2b4</b> ) produced by trypsin digestion of <b>2b</b> (Figure B.10 in Appendix B). ....	108
<b>Table 3.10:</b> Areas of 15-mer linear peptide ( <b>2b</b> ) peaks in the HPLC chromatograms during trypsin digestion at 10 °C and pH 6.2. ....	109
<b>Table 3.11:</b> $t_{1/2}$ of 15-mer linear peptide ( <b>2b</b> ) in the presence of trypsin at 10 °C and pH 6.2, including the rate constant ( $k \text{ min}^{-1}$ ) and the standard error (SE). .	109
<b>Table 3.12:</b> The comparison between theoretically calculated peaks and the observed CID fragments of the precursor ion 676.6 m/z (peptide <b>2c2</b> ) produced by enzymatic hydrolysis of <b>2c</b> in the presence of trypsin (See Figure B.12 in Appendix B). ....	113
<b>Table 3.13:</b> Areas of 15-mer cyclic peptide ( <b>2c</b> ) peaks in the HPLC chromatograms during digestion with trypsin at 10 °C and pH 6.2.....	115
<b>Table 3.14:</b> $t_{1/2}$ of 15-mer cyclic peptide ( <b>2c</b> ) during digestion with trypsin at 10 °C and pH 6.2, including the value of rate the constant ( $k \text{ min}^{-1}$ ) and the standard error (SE). ....	116
<b>Table 3.15:</b> The comparison between theoretically calculated peaks and the observed CID fragments of the precursor ion 399.6 m/z (peptide <b>3b1</b> ) produced by enzymatic hydrolysis of 13-mer linear peptide ( <b>3b</b> ) in the presence of chymotrypsin (See Figure B.16 in Appendix B). ....	119
<b>Table 3.16:</b> Areas of 13-mer linear peptide ( <b>3b</b> ) peaks in the HPLC chromatograms during digestion with chymotrypsin at 10 °C and pH 8.6. ....	120
<b>Table 3.17:</b> $t_{1/2}$ of 13-mer linear peptide ( <b>3b</b> ) during digestion with chymotrypsin at 10 °C and pH 8.6, including the value of the rate constant ( $k \text{ min}^{-1}$ ) and the standard error (SE). ....	121

<b>Table 3.18:</b> The comparison between theoretically calculated peaks and the observed CID fragments of the precursor ion 763.5 m/z (peptide <b>3c1</b> ) produced by enzymatic hydrolysis of <b>3c</b> in the presence of chymotrypsin (See Figure B.18 in Appendix B).....	124
<b>Table 3.19:</b> Areas of 13-mer cyclic peptide ( <b>3c</b> ) peaks in the HPLC chromatograms during digestion with chymotrypsin at 10 °C and pH 8.6. ....	125
<b>Table 3.20:</b> $t_{1/2}$ of 13-mer cyclic peptide ( <b>3c</b> ) during digestion with chymotrypsin at 10 °C and pH 8.6, including value of rate constant ( $k \text{ min}^{-1}$ ) and the standard error (SE). ....	125
<b>Table 3.21:</b> The comparison between theoretically calculated peaks and the observed CID fragments of the precursor ion 835.6 m/z (peptide <b>3b4</b> ) produced by enzymatic hydrolysis of <b>3b</b> by trypsin (See Figure B.20 in Appendix B).....	129
<b>Table 3.22:</b> Areas of 13-mer linear peptide ( <b>3b</b> ) peaks in the HPLC chromatograms during digestion with trypsin at 10 °C and pH 6.2.....	130
<b>Table 3.23:</b> $t_{1/2}$ of 13-mer linear peptide ( <b>3b</b> ) during digestion with trypsin at 10 °C and pH 6.2, including the value of the rate constant ( $k \text{ min}^{-1}$ ) and the standard error (SE). ....	131
<b>Table 3.24:</b> The ratio of areas of 13-mer cyclic peptide ( <b>3c</b> ) peaks to areas of the internal standard peaks in the HPLC chromatograms during digestion with trypsin at 10 °C and pH 6.2.....	132
<b>Table 4.1:</b> HPLC peak areas for 15-mer linear peptide ( <b>2b</b> ) relative to the internal standard (IS) peak areas during incubation in 20% FCS at 37 °C and pH 7.4 for 0 – 48 h. Three replicates.....	137
<b>Table 4.2:</b> $t_{1/2}$ of 15-mer linear peptide ( <b>2b</b> ) in 20% FCS at 37 °C and pH 7.4 with the mean and standard deviation ( $\sigma$ ) of the triplicate. ....	139
<b>Table 4.3:</b> HPLC peak areas for 15-mer cyclic peptide ( <b>2c</b> ) relative to the internal standard (IS) during incubation in 20% FCS at 37 °C and pH 7.4 for 0 – 48 h. Three replicates. ....	139
<b>Table 4.4:</b> $t_{1/2}$ of 15-mer cyclic peptide ( <b>2c</b> ) in 20% FCS at 37 °C and pH 7.4 with the mean and standard deviation ( $\sigma$ ) of the triplicate. ....	142
<b>Table 4.5:</b> HPLC peak areas for the 13-mer linear peptide ( <b>3b</b> ) relative to the internal standard (IS) during incubation in 20% FCS at 37 °C and pH 7.4 for 0 – 48 h. Three replicates.....	143
<b>Table 4.6:</b> $t_{1/2}$ of 13-mer linear peptide ( <b>3b</b> ) in 20% FCS at 37 °C and pH 7.4 with the mean and standard deviation ( $\sigma$ ) of the triplicate. ....	145

<b>Table 4.7:</b> HPLC peak areas for 13-mer cyclic peptide ( <b>3c</b> ) relative to the internal standard (IS) during incubation in 20% FCS at 37 °C, and pH 7.4 for 0 – 48 h. Three replicates. ....	145
<b>Table 4.8:</b> $t_{1/2}$ of 13-mer cyclic peptide ( <b>3c</b> ) in 20% FCS at 37 °C and pH 7.4 with the mean and standard deviation ( $\sigma$ ) of the triplicate. ....	148
<b>Table 6.1:</b> Names of the suppliers of glassware and plasticware. ....	160
<b>Table 6.2:</b> Names of the chemical suppliers. ....	161
<b>Table 6.3:</b> Suppliers of instruments. ....	161
<b>Table 6.4:</b> HPLC method for purification of 9-mer cyclic peptide ( <b>1c</b> ), which has retention time 17.23 min. ....	165
<b>Table 6.5:</b> HPLC method for purification of 15-mer cyclic peptide ( <b>2c</b> ), which has retention time 12.29 min. ....	165
<b>Table 6.6:</b> HPLC method for the purification of 13-mer cyclic peptide ( <b>3c</b> ), which has retention time 14.49 min. ....	166
<b>Table 6.7:</b> Precursor ion $m/z$ for the $MS^2$ analysis which were obtained from MS scan. ....	166
<b>Table 6.8:</b> General HPLC method used to study the enzymatic degradation and $t_{1/2}$ of 13-mer cyclic peptide ( <b>3c</b> ) and its linear counterpart ( <b>3b</b> ) in the presence of chymotrypsin and trypsin. ....	170
<b>Table 6.9:</b> General HPLC method used to study the enzymatic degradation and $t_{1/2}$ of 15-mer cyclic peptide ( <b>2c</b> ) and its linear counterpart ( <b>2b</b> ) in the presence of chymotrypsin and trypsin. ....	172
<b>Table 6.10:</b> General HPLC method used to study the stability of 13-mer cyclic peptide ( <b>3c</b> ) and its linear counterpart ( <b>3b</b> ) in 20% FCS. ....	174
<b>Table 6.11:</b> General HPLC method used to study the stability of 15-mer cyclic peptide ( <b>2c</b> ) and its linear counterpart ( <b>2b</b> ) in 20% FCS. ....	174

## Abbreviations

Abs	Absorbance
Acm	Acetamidomethyl
Bax	Bcl-2-associated X protein
Boc	<i>tert</i> -Butoxycarbonyl
BSA	Bovine serum albumin
Cbz	Carbobenzoxy
DEPBT	3-(Diethoxyphosphoryloxy)-1,2,3-benzotriazin-4(3H)-one
DIPEA	<i>N,N</i> -Diisopropylethylamine
Dmab	4-{ <i>N</i> -[1-(4,4-Dimethyl-2,6-dioxocyclohexylidene)-3-methylbutyl]-amino} benzyl alcohol
DMPA	2,2-dimethoxy-2-phenylacetophenone
DMSO	Dimethyl sulfoxide
ESI	Electrospray ionisation
FCS	Fetal calf serum
Fmoc	Fluorenylmethoxycarbonyl
HATU	1-[Bis(dimethylamino)methylene]-1 <i>H</i> -1,2,3-triazolo[4,5-b]pyridinium 3-oxide hexafluorophosphate
HBTU	2-(1 <i>H</i> -benzotriazol-1-yl)-1,1,3,3-tetramethyluronium hexafluorophosphate
HEPES	4-(2-hydroxyethyl)-piperazine-1-ethanesulfonic acid
HLA	Human leukocyte antigen
HOAt	1-Hydroxy-7-azobenzotriazole
HOBt	1-Hydroxybenzotriazole
HODhbt	3-Hydroxy-3,4-dihydro-4-oxo-1,2,3-benzotriazine
IS	Internal standard
LCMS	Liquid chromatography mass spectrometry
MALDI-TOF	Matrix assisted laser desorption ionisation - time of flight
MHC	Major histocompatibility complex
MOMP	Mitochondrial outer membrane permeabilisation
Nle	Norleucine
NMM	<i>N</i> -methyl morpholine
NMP	<i>N</i> -Methyl-2-pyrrolidone
NMR	Nuclear magnetic resonance



PEG	Polyethylene glycol
PyBOP	(Benzotriazol-1-yloxy) tripyrrolidinophosphonium hexafluorophosphate
RCF	Relative centrifugal force
RP-HPLC	Reversed phase - high performance liquid chromatography
RPM	Revolutions per minute
RT	Retention time
SE	Standard error
SPPS	Solid phase peptide synthesis
SPS	Solution phase synthesis
TAP	Transporter associated with antigen processing
TCR	T cell receptor
tBu	tertiary-Butyl
TCR	T cell receptor
TFA	Trifluoroacetic acid
Tmob	Trimethoxybenzyl
Trt	Trityl
UV	Ultraviolet

# **Chapter 1**

# **Introduction**

# 1 Introduction

## 1.1 Motivation

Bax, one of the essential proteins that belongs to the Bcl-2 family of proteins, has a size of 21 kDa and a short half-life in the cell. It plays a key role in programmed cell death (apoptosis) and, in particular, can work to promote apoptosis. Two types of mammalian Bcl-2 family members have been characterised:<sup>1</sup>

a-Proapoptotic, e.g. Bax, which induce mitochondrial outer membrane permeabilisation (MOMP), releasing cytochrome *c*.

b-Antiapoptotic, e.g. Bcl-2 and Bcl-X<sub>L</sub>, which serves as the guardian of the outer membrane by opposing the induction of MOMP.

It has been observed that there is abnormal proteasomal degradation in cancer cells that has an adverse effect on the level of Bax, thus limiting apoptosis.<sup>2</sup> It has been hypothesised that proteasomal degradation of Bax leads to the presence and binding of Bax-derived peptides to the human leukocyte antigen which in turn leads to the activation of CD8<sup>+</sup> T cells.<sup>3</sup> These then have the ability to kill a variety of human leukocyte antigen (HLA) matched-cancer cells, including primary tumour cells from chronic lymphocytic leukaemia (CLL).

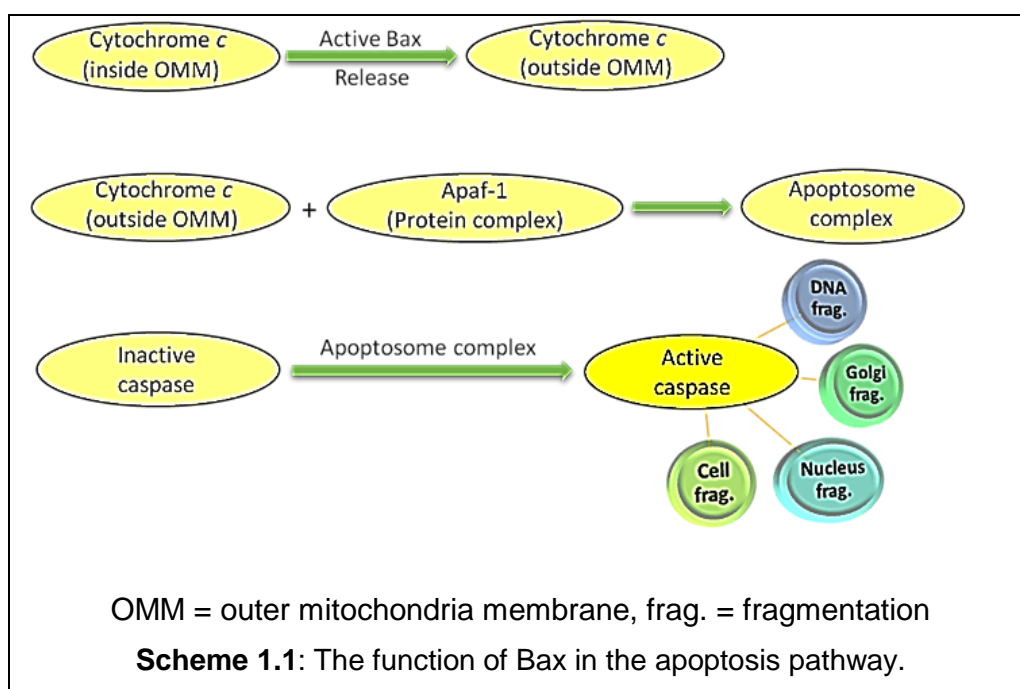
This study is concerned with the synthesis of a 9-mer cyclic Bax peptide (**1c**) with sequence FLIMGWTLD. This sequence is based upon cyclisation of a linear 9-mer, IMGWTLDFL, that had previously been identified as a potential tumour antigen originating from Bax<sub>136-144</sub>.<sup>3</sup> Two derivatives of this sequence were also investigated. The first (**2c**) was a 15-mer cyclic peptide (FLRELIRTIMGWTLD) in which the immunogenic 9-mer is surrounded by additional flanking residues from the wild-type Bax sequence. The second, (**3c**), was a 13-mer cyclic peptide (FLKSSKIMGWTLD) where the additional residues were designed to provide a flexible and solubilising linker.

In addition, the linear counterparts (**1b**, **2b**, **3b**) of these sequences were also investigated for comparison. Cyclic peptides are more highly ordered compounds than linear peptides in solution due to the constraints that

cyclisation places on their secondary structure. This is predicted to make them more resistant to enzymatic hydrolysis and proteolytic degradation in comparison to linear polypeptides, which have a poorly defined secondary structure.<sup>4</sup> In this study, two Bax cyclic peptide derivatives (**2c**, **3c**) were synthesised, resulting in cyclic peptides that are more soluble in aqueous solvents compatible with protease degradation assays and HPLC analysis. This allowed us to study their susceptibility to protease catalysed hydrolysis by performing an enzyme kinetic study, in addition to stability studies in serum.

## 1.2 Bax protein

Bax protein plays a critical role in the cell suicide programme (apoptosis). Bax anchors into the outer mitochondrial membrane (OMM) through the hydrophobic C-terminus<sup>5</sup> as a response, for instance, to DNA damage or growth factor deprivation, to release cytochrome c from the mitochondria. Cytochrome c in turn binds to a particular protein (Apaf-1) to form the apoptosome complex which controls the pathways of activation of caspases, enhancing the apoptosis process<sup>6</sup> as in Scheme 1.1. Therefore, the presence of Bax is necessary and plays a significant role in repressing cancer development. Changes in the level of Bax are associated with more than one type of cancer cell.



In tissue samples of human prostate adenocarcinoma, it was found that there was a good correlation between an increase of Bax protein degradation, decreased levels of Bax protein and increased Gleason scores of prostate cancer.<sup>7</sup> In addition, there were no significant changes in the level of Bcl-2 protein. Moreover, using a proteasome inhibitor increased the level of ubiquitinated forms of Bax protein without influence on the presence of Bax mRNA. Therefore, manipulation of this pathway (ubiquitin/proteasome-mediated Bax degradation method) of cancer cell survival is a possible approach to targeting cancers in humans, particularly those with elevated Bcl-2 expression.<sup>7</sup>

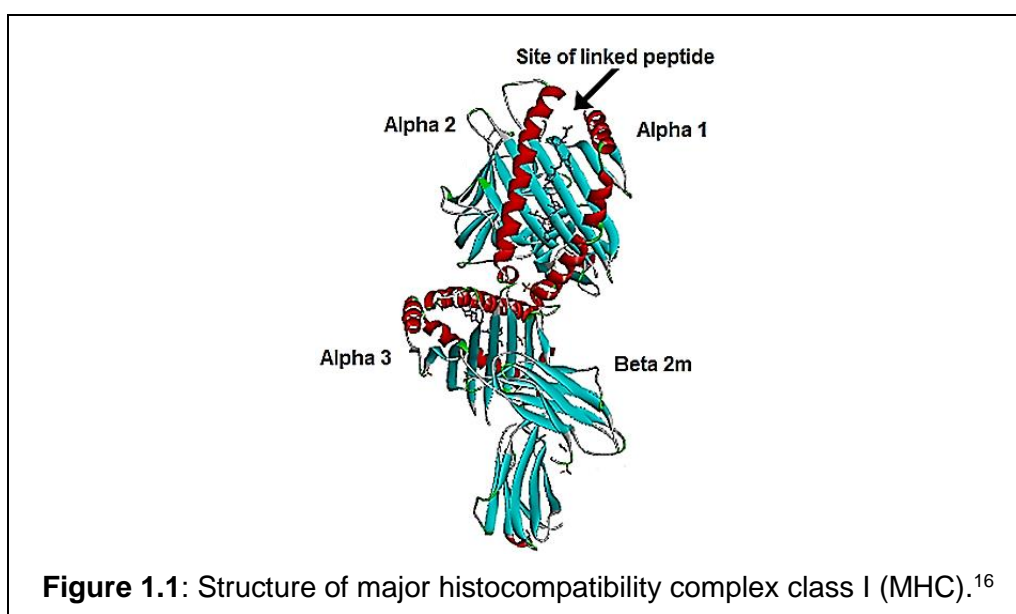
### **1.3 Binding of epitopes with MHC complex and TCR (T cell receptor)**

T-cells are activated by foreign antigen (peptides), only when the antigen is displayed on the surface of antigen presenting cell (B-cells, dendritic cells, macrophage cells). The fragments of protein antigens are degraded to peptides inside antigen presenting cells. The antigenic peptides are then carried to the surface of the antigen presenting cell to bind in a deep cleft in the HLA of the complex of MHC class I proteins (major histocompatibility complex). Small peptides, typically 7–10 amino acids in length, are loaded into the complex in the endoplasmic reticulum. The complex is secreted to the cell surface which presents these peptides to T-cells expressing the CD8 receptor. CD8 is one of the accessory receptors of T-cells that is expressed on cytotoxic T-cells and binds to the MHC class I protein. The T-cell receptor of the T-cells recognises antigenic peptides and binding triggers a cascade of events which leads to the destruction of pathogens and infected cells.<sup>8</sup> Therefore, peptides originating from the degradation of ubiquitinated-Bax could potentially serve as tumour-specific antigens of cancer cells.<sup>9, 10</sup>

The response of the immune system to a specific antigen is different between individuals due to their different patterns of MHC genes. There are three main types (A–C) of HLA class I and many HLA class II genes in each human individual. A large range of polymorphism has been identified for MHC genes (800 variants for HLA class I and more than 500 for HLA class II). It has been estimated that the number of peptide sequences which have the ability to

bind to a particular HLA class I molecule reaches between 1000 to 10000 when just 9–10 mer peptides are considered as T cell epitopes.<sup>11</sup> However, some peptides that are good binders to the MHC are not formed by processing of proteins and hence in reality are not presented by the MHC. Some peptides are presented by MHC molecules but do not stimulate the response system. Therefore, determining the sequences of the peptides that have an ability to bind MHC molecules and activate the immune system is a significant step for understanding the immune response with the goal to design and synthesise immunotherapies and peptide-based vaccines.<sup>12</sup> Pathogens produce a large number of peptides. Therefore, diagnosis of candidate T cell epitopes needs theoretical screening accompanied by experimental validation.

MHC class I complexes are noncovalently linked heterodimers<sup>13</sup> with the heavy chain oriented with its *N*-terminal major portion on the outside of the cell. The extracellular portion of the heavy chain was classified into three parts;  $\alpha_1$ ,  $\alpha_2$ ,  $\alpha_3$ .<sup>14</sup> The light chain is  $\beta_2$  microglobulin ( $\beta_2$  m).<sup>15</sup> Therefore, the sequence differences in the MHC complex led to restricted recognition by T cells and binding of the peptide to the MHC varies and mainly clusters in the  $\alpha_1$  and  $\alpha_2$  domains as in Figure (1.1). It was expected that these domains could include the part of the MHC class I molecule that binds to the both the peptide and TCR. It is concluded that the peptide-binding sites play a critical role in the prediction of which fragments will be antigenic or what conformation they would adopt when bound to a class I MHC molecule.



It could be said that two generalisations can be made about the interaction of a peptide with an MHC class I molecule; firstly, binding of the peptide chain occurs at its ends.<sup>17, 18</sup> This type of binding was considered as a universal peptide recognition element that is independent of MHC protein sequence. The second consideration is formation of hydrogen bonds from polymorphic MHC side chains to the peptide main chain and to peptide anchor side chains.

Several methods have been designed for prediction of the epitopes within protein sequences that have an ability to bind a TCR then activate the immune system. One of these computational methods supposed that the non-polar face of amphipathic helical structures of antigenic peptides contacts the class I MHC molecules, while the polar face is solvent exposed or binds the TCR.<sup>19</sup> Another method based on examination of the HLA-A<sub>2</sub> structure, suggested that the antigenic peptides bind the MHC molecule from three faces leaving the fourth directed towards solvent or contacting the TCR.<sup>20</sup> In addition, a search was performed for motifs within the primary sequence of a protein that have the ability to be T cell immunogens.<sup>21</sup> By analysis of 57 T cell epitopes the authors found the motif was a charged residue or glycine, followed by two or three hydrophobic residues, ending with a polar residue or glycine. Although this consensus sequence was quite degenerate because several peptides known to be T cell epitopes do not contain it.

Regarding the binding of the peptide to HLA-A<sub>2</sub>, using computational prediction to tether peptides into the HLA-A<sub>2</sub> site, it has been suggested that the standard helical conformation of the peptide is a very close fit in the binding site thus small movements of side chains or opening up of the site by displacing the  $\alpha$ -helices are potential requisites before binding or releasing a peptide in a helical conformation.<sup>22</sup>

## **1.4 Cyclic polypeptides in the medical field**

Living organisms have biochemical 'tools' to achieve their great number of physiological processes. Peptides are one of these powerful tools and play a crucial role throughout biology; for instance, they can act as hormones and are important factors in the nervous system as neurotransmitters.<sup>23</sup> Therefore, the functional and structural characteristics of biologically active peptides are widely studied and are of considerable interest in biological or medicinal

chemistry research. Cyclic peptides are one of these bioactive compounds. Many naturally occurring cyclic peptides are used in medical treatment; for example, a cationic cyclopeptide named TD-34 has the ability to decrease the level of sugar in the blood stream,<sup>24</sup> and vancomycin is a peptide-derived antibiotic.<sup>25</sup> Cyclic peptides tend to be highly resistant to the process of hydrolysis in the human digestive tract, and this property makes them an attractive material for designers of protein-based drugs, as they may be used as scaffolds for the delivery of other proteins that would otherwise be destroyed.<sup>26</sup>

Hundreds of cyclic peptides have been synthesised with different sizes of rings and types of building units (natural and unnatural amino acids, D or L-amino acids) giving a variety of conformations in solution. Many have also been investigated for their effectiveness against different diseases. For example, it was observed that the cyclic D-L- $\alpha$ -peptides, with six or eight residues have the ability to attack Gram positive and Gram-negative bacterial membranes, thus leading to rapid cell death.<sup>27</sup> A cyclic peptide named C1 containing D and L amino acids has the ability to reduce immune responses in models of arthritis and asthma.<sup>28</sup> Finally, it has been observed that the cyclic peptide (SGWTWRMY) can inhibit the NADPH-dependent dimerisation of the C-terminal binding proteins (CtBPs) which regulate the maintenance of mitotic fidelity in breast cancer cells.<sup>29</sup>

An important area of study of cyclic peptides in the field of medicine has been the search for a way to increase the half-life of peptides. This is considered a bottle neck in the development of new peptide drugs because endogenous proteases and peptidase degrade them before they can reach their target. Therefore, many attempts have been made to increase the stability and versatility of peptides.<sup>30</sup> One of the strategies employed is the conversion of linear peptides to cyclic peptides.

New findings demonstrate that cyclic decapeptides might represent novel anticancer agents, providing a new strategy for cancer therapy.<sup>31</sup> Studying the cytotoxicity of a library of antibacterial cyclodecapeptides on human carcinoma cell lines, and their effects on apoptosis and cell signalling proteins in cultured human cervical carcinoma cells, led to this discovery. Some of these sequences displayed specificity to, and high cytotoxicity against, HeLa cells



while showing low hemolytic activity and low cytotoxicity to non-malignant fibroblasts. Importantly, they were also stable to proteases in human serum and were able to induce apoptosis.

Inhibition of blood coagulation through anti-haemophilia Factor VIII–Factor IX interactions represents an attractive approach for the treatment and prevention of diseases caused by thrombosis. In this field, studies have indicated that the cyclic peptide analogues of the 558–565 sequence of the A2 subunit of Factor VIII provided a starting point for the development of new anticoagulant agents. These analogues displayed efficient inhibition of the Factor VIIIa–Factor IXa interaction.<sup>32</sup>

## 1.5 The various types of cyclic polypeptides

Cyclic polypeptides are polypeptide chains where the amino terminus and carboxyl terminus, and/or their equivalent side chain functionalities, are bonded together with a covalent bond, thereby producing a cyclic structure. Cyclic peptides can be found in nature in a number of different forms classified according to structural or physical characteristics.<sup>33, 34</sup> Thus, there is more than one method to classify cyclic peptides, and categories include:

A–Structure:

- 1) *Homodetic cyclic peptides*: this type is formed from head-to-tail cyclisation (Figure 1.2, A), where the ring is formed of a normal peptide bond ( $\alpha$ -carboxyl to  $\alpha$ -amine).<sup>35, 36, 37</sup>
- 2) *Heterodetic cyclic peptides*: a side chain is cyclised with another side chain or with one of the termini (head-to-side chain or side chain-to-tail). Here the bond is formed between the side chain functional group of the sequence and the *N*- or *C*-terminus (Figure 1.2, B).<sup>38</sup>
- 3) *Complex cyclic peptides*: this is a hybrid cyclic peptide containing both homodetic and heterodetic bonding (side chain-to-side chain and head-to-tail cyclisation). In this case, bonds are formed between two side chains of amino acids e.g. disulfide bonds and thioethers, in addition to the head-to-tail bond (Figure 1.2, C).<sup>39, 40, 41</sup>



3) *Mixed polarity cyclic polypeptides*: these cyclic polypeptides have amphoteric properties; for example, largamide (Figure 1.3, C). This type also often has antimicrobial properties.<sup>48, 49</sup>

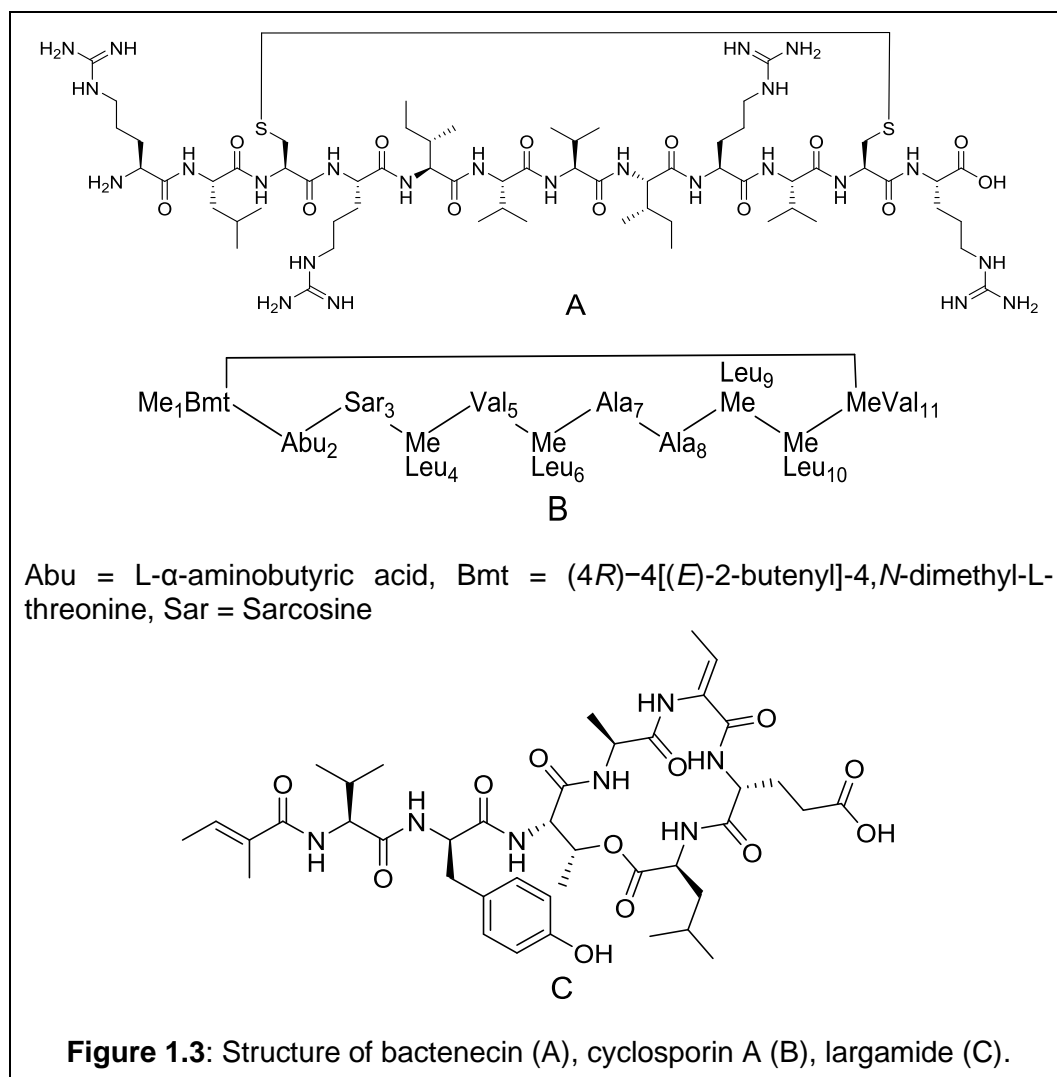


**Figure 1.3:** Structure of batenecin (A), cyclosporin A (B), largamide (C).

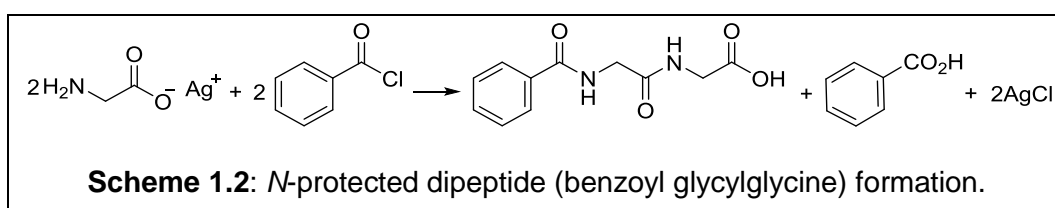
## 1.6 Protecting groups in peptide synthesis

A requirement of protecting groups is that they are easy to attach to the target functional group. Also, they must be stable in a diverse array of reaction conditions. In addition to that, they must be easily and selectively removed at the end of the synthesis.<sup>50</sup>

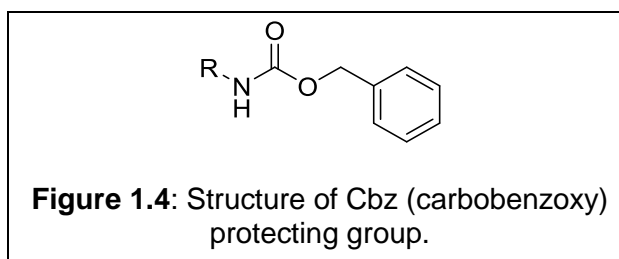
## 1.6.1 Main chain protecting groups

### 1.6.1.1 The $\alpha$ -amino protecting group

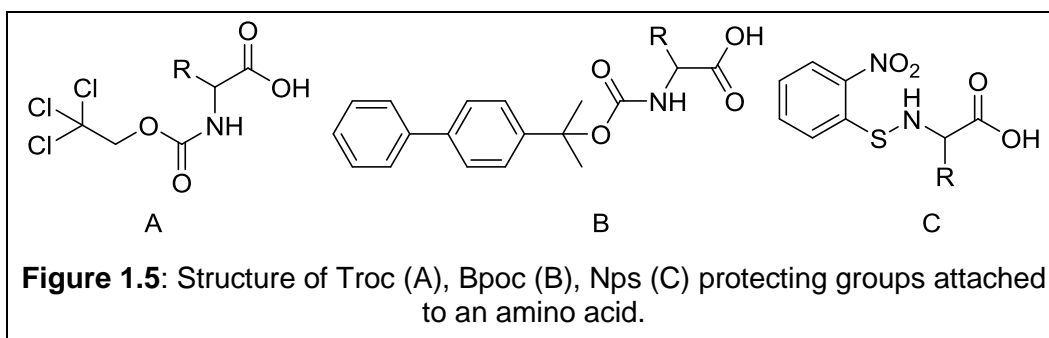
The history of  $\alpha$ -amino protecting groups dates back to 1882 when the first *N*-protected dipeptide (benzoyl glycylglycine)<sup>51</sup> was synthesised as in Scheme 1.2. Then, in 1901 the synthesis of a second *N*-protected dipeptide (glycylglycine) was published.<sup>52, 53</sup> However, there was a problem during that period in that the synthesis involved a free active amino group in the amino acid. Therefore, a mixture of products would be produced.



Consequently, amino protecting groups were investigated between 1930 and 1960 and discovered to solve this problem. Some amino protecting groups are now in common use; one such example is the Cbz (carbobenzoxy) group as in Figure 1.4,<sup>54</sup> which was then used as the *N*-protecting group in solid phase peptide synthesis (SPPS) launched by Merrifield in 1963.<sup>55</sup>

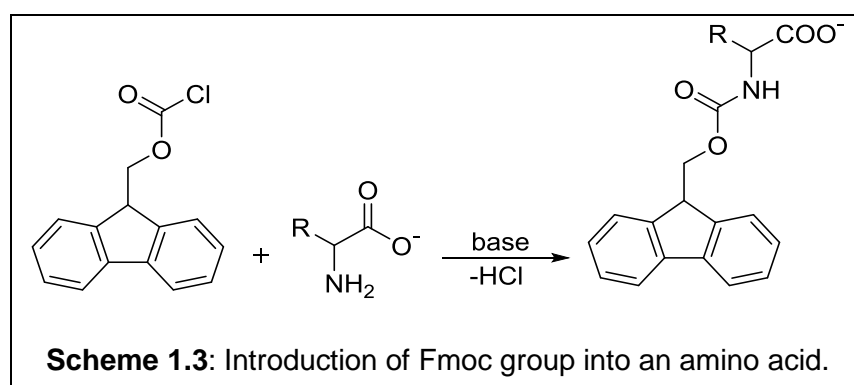


Various other protecting groups can also be used in solution phase synthesis (SPS) such as Troc (2, 2, 2-trichloroethoxycarbonyl), Bpoc (2-(4-biphenyl)-isopropoxy carbonyl) and Nps (2-nitrophenyl sulfenyl) as shown in Figure 1.5.<sup>50</sup>



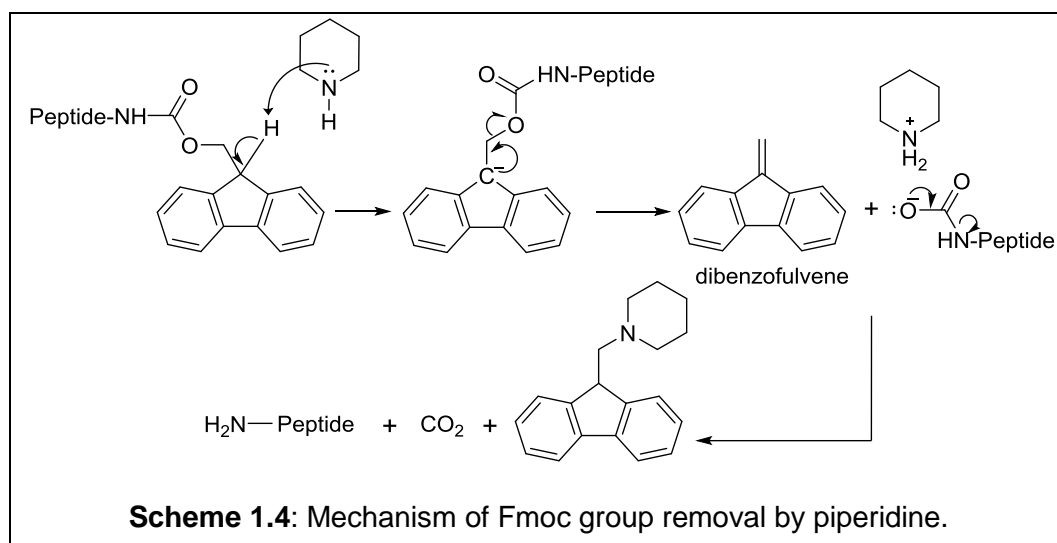
Two main types of  $\alpha$ -amino protecting groups used in the SPPS and SPS methods are Fmoc (fluorenylmethoxycarbonyl)<sup>56</sup> and Boc (*tert*-butoxycarbonyl).<sup>54</sup> The Fmoc group was launched as a protecting group for peptide synthesis in the 1970s.<sup>57</sup> It has since become the most common protecting group used to block the  $\alpha$ -amino group of every new incoming amino acid during the coupling reaction. The Fmoc group is stable under acidic conditions and a wide range of catalytic hydrogenation conditions.

More than one method is used to tether the amino acid to a Fmoc group. The most frequently used of these methods is where the free amino acid reacts with a haloformate analogue of the Fmoc protecting group.<sup>58</sup> The reaction can be hampered by the presence of a free C-terminus. Therefore, two approaches are used to overcome this problem. Using a protecting group is the first technique and the second is using less reactive electrophiles in the reaction.<sup>50</sup> Scheme 1.3 is an example of how an amino acid is protected by the Fmoc group using the reagent Fmoc-chloroformate.



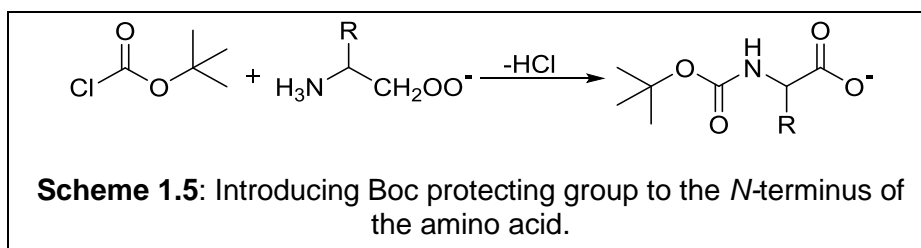
In the SPPS method, a piperidine reagent is used to remove the Fmoc group. This reagent also acts as a scavenger for the unstable dibenzofulvene intermediate compound, consequently converting it to a stable

fulvene–piperidine adduct. One of the standard conditions for removal of this protecting group is reaction with 20% piperidine–NMP for 18 min,<sup>59</sup> as displayed in Scheme 1.4.

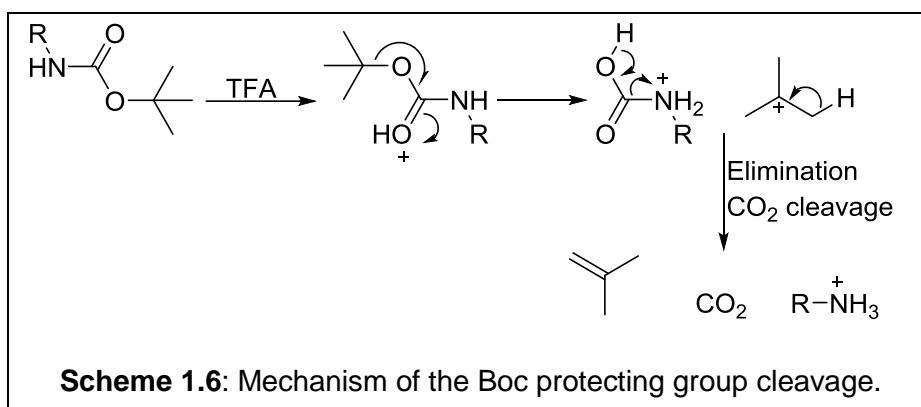


One of the popular methods of using the Fmoc protecting group is to rely on the combination of the Fmoc group for the *N*-terminus, and *tert*-butyl groups for the side chains. This strategy, denoted Fmoc/*tert*-butyl, is superior to the alternative Boc *N*- $\alpha$ -protection strategy because there is no accumulating loss of the side chain protection as a result of repetitive deblocking. Moreover, the presence of the Fmoc protecting group allows progress of the reaction to be followed using UV or fluorescence spectroscopy during automated peptide synthesis.

*Tert*-butoxycarbonyl (Boc)<sup>60</sup> was one of the most common *N*- $\alpha$ -protecting groups. The *N*-terminus of the amino acid is attached to the Boc protecting group in a similar way to the Fmoc group.<sup>58</sup> Scheme 1.5 indicates the product of introducing a Boc group to the *N*-terminus of the amino acid.

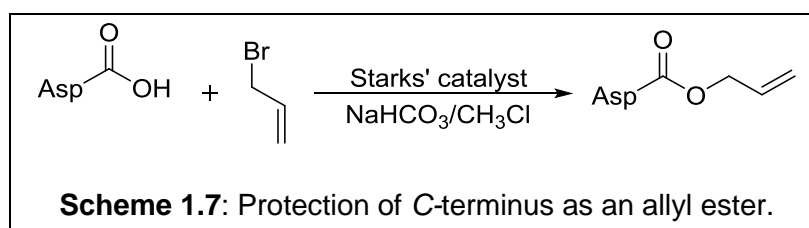


Acids quickly remove the Boc protecting group; for example, TFA, as in Scheme 1.6, or 1 M trimethylsilyl chloride (TMS-Cl).<sup>61</sup> The Boc group is stable under basic conditions and resistant to nucleophilic attack; in addition, it is unaffected by catalytic hydrogenation. Synthesis of polypeptides requires several deprotection cycles to remove the protecting group of the  $\alpha$ -amine and thus, mild conditions are favoured to deprotect this protecting group without affecting the remaining protecting groups on the C-terminus or side chains. The main problem when employing Boc as the *N*- $\alpha$  protecting group is that undesired side chain deprotection can occur during repetitive deprotection of the group by acid at each coupling reaction step. In addition, using HF as the deprotection reagent for the peptide from the resin is dangerous and requires expensive laboratory apparatus. Hence the Fmoc strategy has gained in popularity over the Boc strategy.

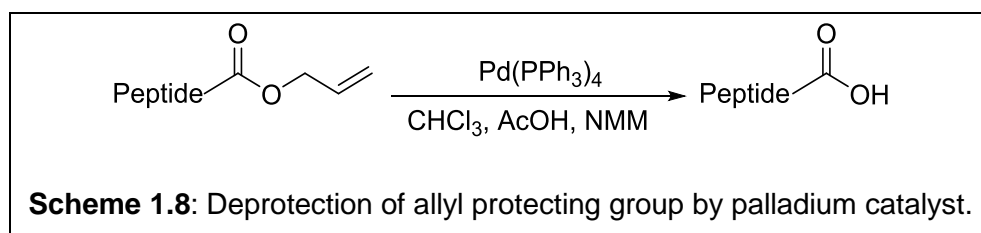


### 1.6.1.2 C-terminal protecting group

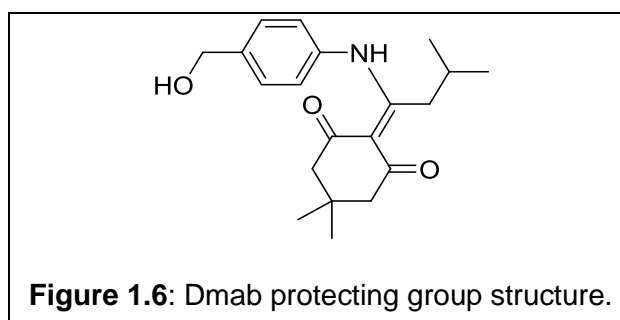
During solid phase synthesis of cyclic peptides, the resin support is commonly attached to an amino acid side chain or backbone nitrogen; therefore, protecting the C-terminus is very important.<sup>62</sup> Many methods are used to protect the C-terminus, including as an allyl ester. To that end, allyl bromide is one of the most commonly used reagents for this reaction<sup>63</sup> as shown in Scheme 1.7.



The palladium catalysed reaction of  $\text{Pd(PPh}_3)_4$  in  $\text{CHCl}_3$ , AcOH and NMM (*N*-methyl morpholine) can be used to remove the allyl ester protecting group from the C-terminus,<sup>64</sup> as in Scheme 1.8.



The Dmab group seen in Figure 1.6 is another C-terminal protecting group. This group is removed by hydrazine.<sup>65, 66</sup> In addition, trimethylsilyl ethyl ester is used as a carboxy protecting group which is removed under mild conditions by fluoride.<sup>67</sup>



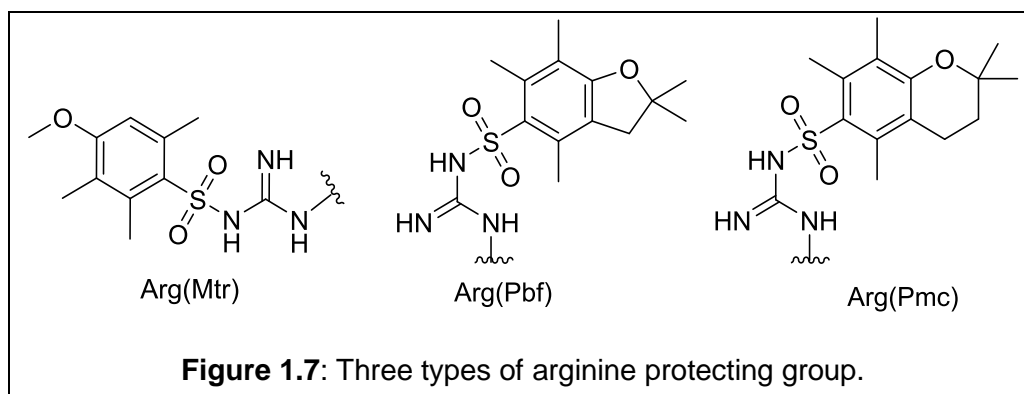
### 1.6.2 Side chain protecting groups

The methods which are used to synthesise peptides need to be high yielding to prevent accumulation of products from undesired bond formation and other unwanted side reactions. Thus, an important factor that plays a significant role in the success of these techniques is careful control of the amino acids used in the growing peptide chain. Some of these amino acids have a reactive side chain functional group, for instance, lysine has an amino group in the side chain that is of similar reactivity to the *N*-terminus. Additionally, aspartic acid has a carboxyl group in the side chain similar to that of the C-terminus. Therefore, protecting groups are employed to block these side chain groups until the end of the synthesis. These groups must be stable during repeated exposure to the basic conditions of the  $\alpha$ -*N*-deprotection step to prevent the reaction of these side groups; for example, in the coupling reaction.<sup>68</sup> Thus an orthogonal



protection strategy is used to achieve this task, i.e. the Fmoc group is removed by basic conditions while acidic conditions remove side chain protecting groups.

For arginine, there is a choice of more than one protecting group that can be used to block the guanidine side group during synthesis of polypeptides. The Mtr-protecting group (4-methoxy-2, 3, 6-trimethylbenzenesulfonyl) is one of these but requires extensive time for deprotection.<sup>69</sup> The Pmc-protecting group (2, 2, 5, 7, 8-pentamethyl-chroman-6-sulfonyl) is another that is removed within a much shorter time span than the Mtr-protecting group.<sup>70</sup> Finally, the Pbf-protecting group (pentamethyl-2,3-dihydrobenzofuran-5-sulfonyl) is often considered the best and is strongly recommended because of the shorter deprotection reaction time required, near to two hours, and because it is easy to scavenge.<sup>71</sup> Figure 1.7 shows the three types of arginine protecting group.

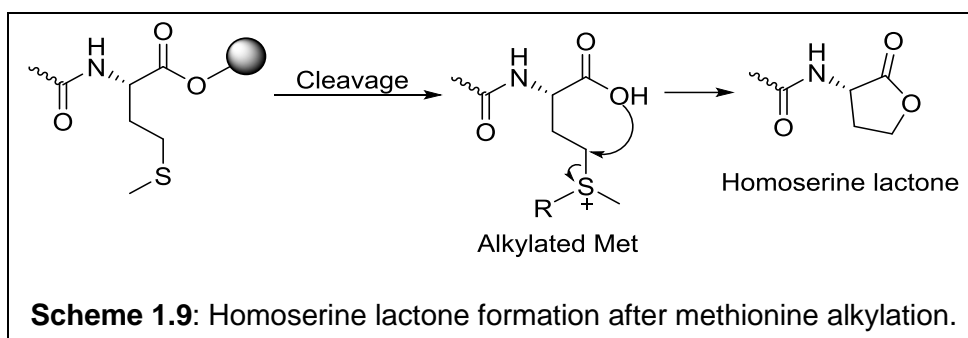


Some unscavenged protecting groups liberated by certain side chains in the deprotection of polypeptides lead to oxidation and alkylation of the indole ring of tryptophan.<sup>69</sup> Using the Boc protecting group to block this indole group will minimise the likelihood of its destruction.<sup>50</sup>

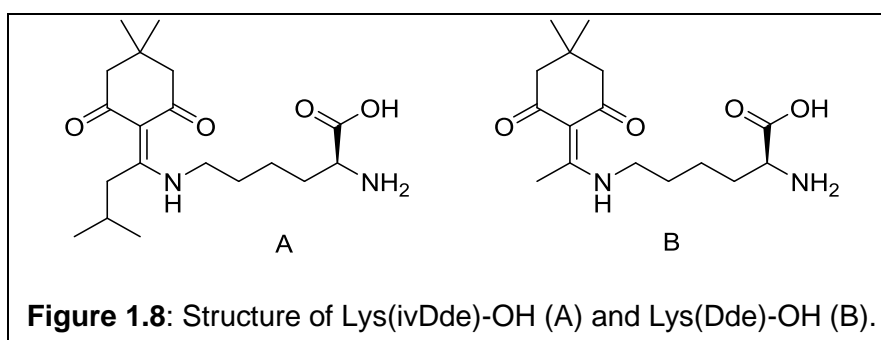
An unprotected methionine amino acid is employed in the Fmoc/*t*-Bu strategy. However, the thioether functionality of methionine has the potential for oxidation to the sulfoxide, or *S*-alkylation forms a homoserine lactone at the C-terminus,<sup>72</sup> as shown in Scheme 1.9. Ethylmethanethiol or thioanisole are used as scavengers to prevent formation of the lactone.<sup>73</sup>

When synthesising polypeptides, the unprotected hydroxyl groups of serine may undergo dehydration or *O*-acylation. Thus, protection is more

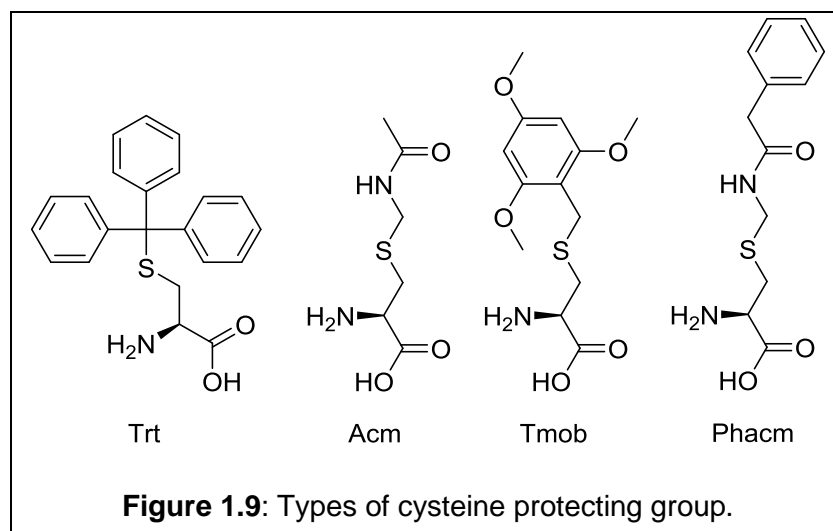
essential in SPPS than SPS, since an excess of acylating agents is used in SPPS. Therefore, solution-phase synthesis with unprotected serine may be successful with selection of appropriate activating reagents.<sup>50</sup>



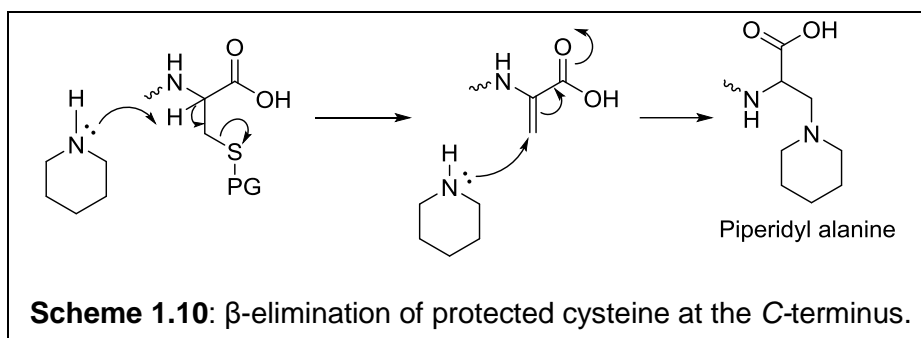
The active side chain of lysine must also be blocked because it will be prone to acylation resulting in the formation of undesired branched peptides. More than one protecting group is available to protect the side chain of lysine; Boc is the common acid-labile choice. The ivDde protecting group (Figure 1.8) is cleaved by hydrazine and this group possesses higher orthogonality to Boc and Fmoc in comparison to the Dde protecting group.<sup>74</sup>



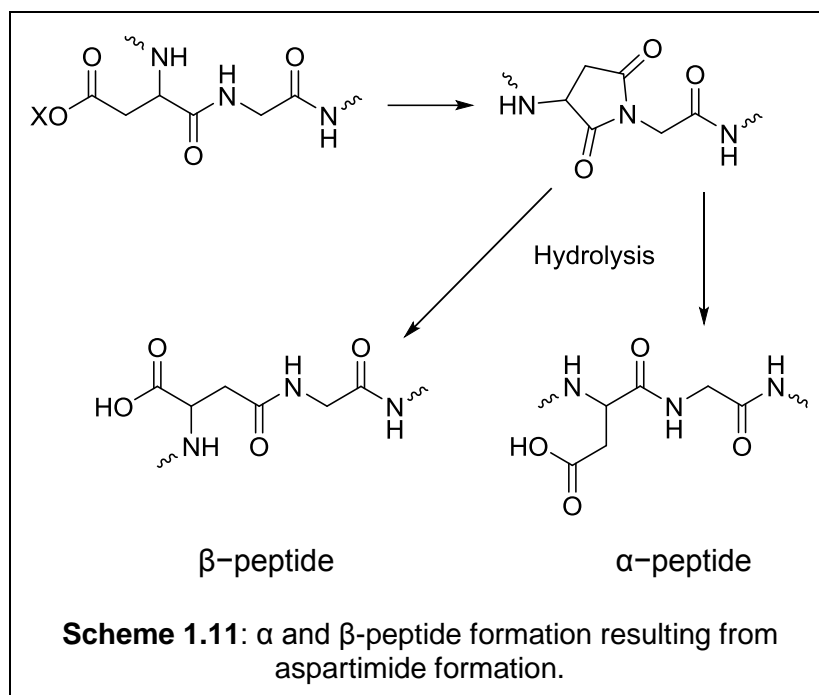
One other amino acid which has a reactive side chain is cysteine, which contains a thiol -SH. Consequently, cysteine containing peptides must also be protected to prevent the acylation, alkylation or oxidation of the thiol group to disulfide by atmospheric oxygen. Disulfide linked dimers are formed by oxidation of the cysteine side chain thiols to connect two chains. A cyclic peptide can form if there is more than one cysteine residue in the same sequence. Usually, oxidations take place more rapidly at a higher pH. Thus, the use of a protecting group, such as trityl (Trt)<sup>75</sup> or acetamidomethyl (Acm)<sup>76</sup> or trimethoxybenzyl (Tmob)<sup>77</sup> or S-phenylacetamidomethyl (Phacm)<sup>78</sup> is recommended. These groups are shown in Figure 1.9.



Even a protected cysteine could react with piperidine in the Fmoc/*t*-Bu strategy. The C-terminal protected cysteine residue undergoes  $\beta$ -elimination then reacts with the piperidine, resulting in the piperidylalanine residue as in Scheme 1.10.<sup>50</sup>

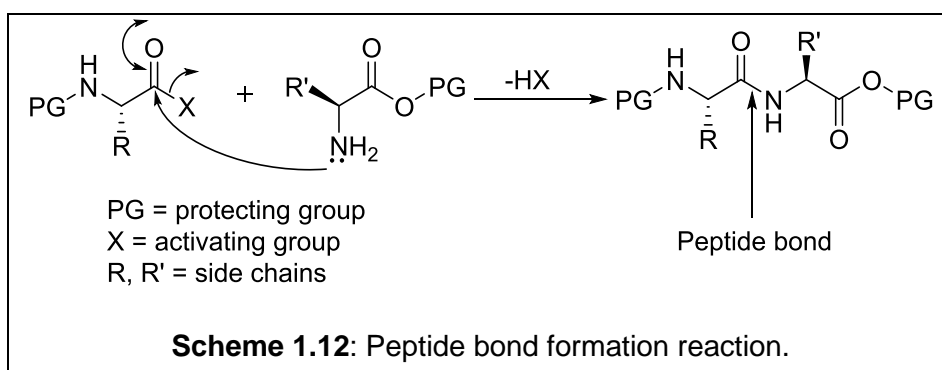


Undesired branched peptides could be formed from the unprotected active side chains of glutamic or aspartic acid in the SPPS strategy. Therefore, a protecting group is needed to prevent this issue as well as minimising the formation of aspartimide, hydrolysis of which causes two products, one of them undesired<sup>79</sup> as in Scheme 1.11. Pyroglutamate formation could also occur in the case of glutamic acid.<sup>80</sup> *t*-Butyl is the most commonly used protecting group for Asp and Glu side chains in the Fmoc/*t*-Bu strategy.



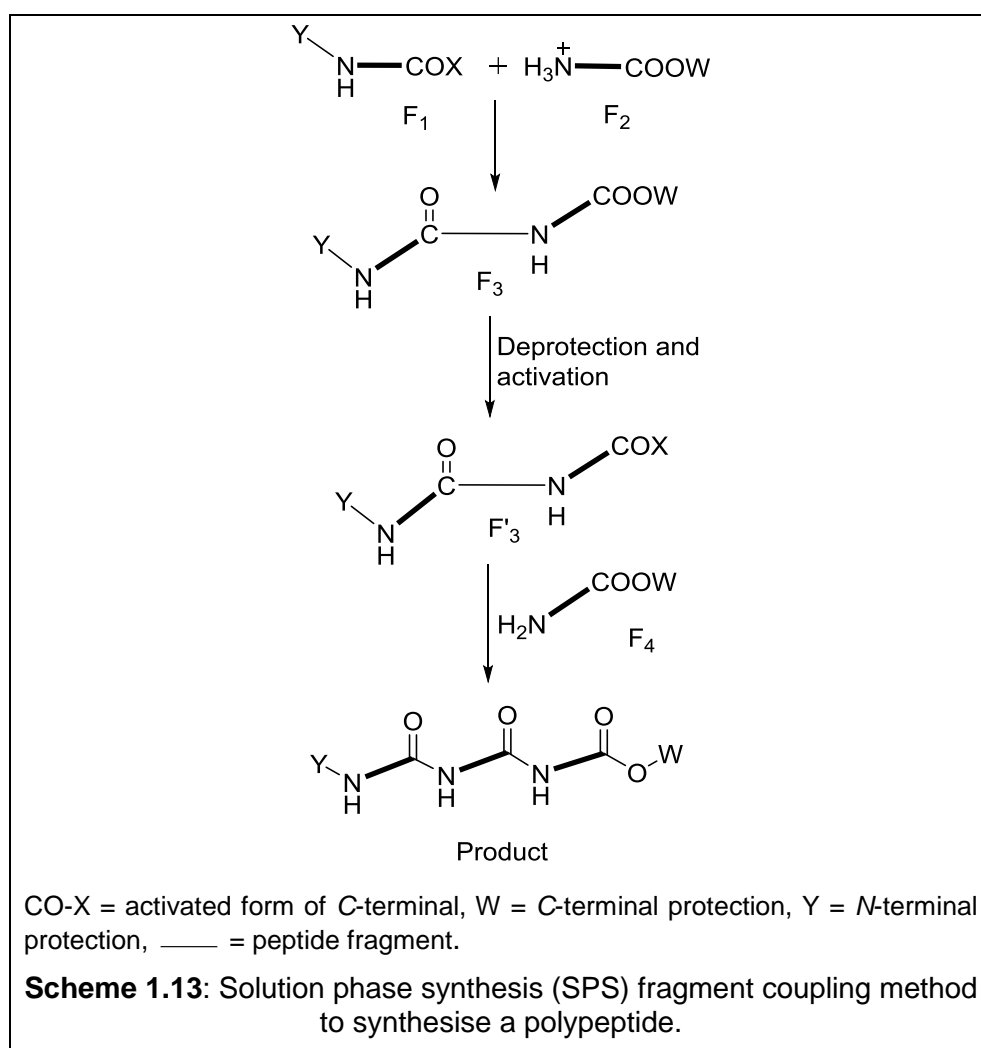
## 1.7 Methods to synthesise polypeptides

Two major chemical techniques are used to synthesise polypeptides: namely, SPPS (solid phase peptide synthesis), and SPS (solution phase synthesis).<sup>81</sup> Each technique has numerous advantages and disadvantages and the choice of one or the other depends on the properties of the resulting polypeptide combined with the quantity and quality required of the final product. The chemical synthesis of polypeptides requires a free amino group to react with the free carboxyl group of a second amino acid. Scheme 1.12 indicates the formation of an amide bond after activation of the carboxyl group.



The SPS technique is a classical method to synthesise polypeptides and has been widely used to form polypeptides since the pioneering research

performed by du Vigneaud in 1953.<sup>82</sup> Unlike SPPS, the coupling of amino acids takes place in the solution phase, not on a solid support. This method is most useful for preparation of polymers containing repeats of short sequences (3–10 amino acids). A long polypeptide chain can be formed by synthesising two short fragments as a first step, then coupling the two fragments.<sup>83</sup> This means that fewer equivalents of starting material are used in creating the full sequence, as displayed in Scheme 1.13. The SPS method has been used to generate many different compounds since the original research. For instance, the peptide hormone oxytocin was synthesised by this method.<sup>84</sup>

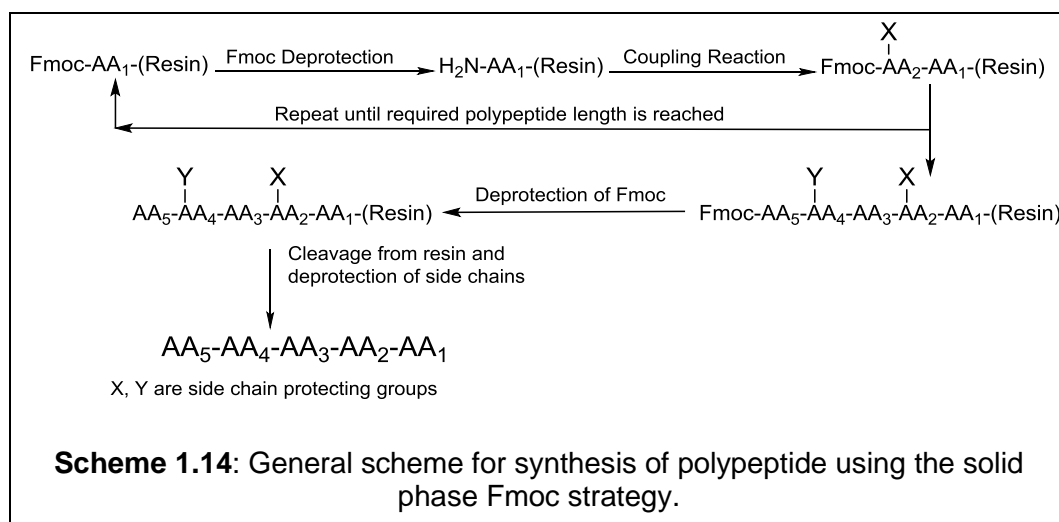


Although SPS has its own positive attributes, for example being easy and inexpensive to scale up, there are also disadvantages to this approach.<sup>55</sup> The first problem is that this method is tedious, laborious and slow. This is because the intermediate peptides need to be isolated after each amino acid addition. Typically, HPLC and mass spectrometry techniques are used to characterise

each fragment before continuing the synthesis of the chain. Thus, completion of the synthesis takes considerable time, and there is substantial labour involved. The second significant problem is the decreasing solubility of the growing polypeptide chain after each successful coupling step.

Since the introduction of the Fmoc group and the work of Merrifield, the SPPS method has become more popular and is now the standard method of polypeptide synthesis.<sup>85</sup> Furthermore, this approach can be used to synthesise other classes of polymer with a defined sequence, including oligosaccharides and oligonucleotides.<sup>86, 87</sup>

The general procedure to synthesise polypeptides by the SPPS method on a resin consists of first binding an *N*-protected amino acid to the resin via the *C*-terminal carboxyl group. The carboxyl group of the second amino acid must then be activated to couple with the first resin-bound residue via its *N*-terminus once the protecting group is removed. The resin then needs to be filtered and washed to remove the excess reagents and any undesired waste products. The previous step is then repeated, the *N*-protecting group of the newly attached residue is removed by a deprotection reagent, followed by filtration and washing, and the addition of another activated amino acid. Finally, the processes of deprotection and coupling are repeated for each successive amino acid until the peptide sequence is complete. Typically, all the protecting groups for the reactive side chains of the amino acids are then removed. The peptide can then be cleaved from the resin after filtration and washing of the resin. This process is shown schematically in Scheme 1.14.



SPPS has several advantages over SPS, one of these is that excess reagent can be used to ensure the reactions reach completion.<sup>55</sup> Another is that purification of the product peptide is rapid after each step, requiring a simple filtration and washing of the resin to remove excess reagents and waste products. Washing the resin is made possible as the growing polypeptide chain is covalently attached to an insoluble solid polymeric support during the chain assembly.<sup>88</sup> Additionally, the yield of desired products can be enhanced in otherwise poorly chemoselective reactions by attachment to an appropriate solid support.<sup>89</sup> Moreover, many compounds can be prepared at one time, since every bead of resin can be considered as a single isolated system for the reaction. Another important advantage of the SPPS method is that it is highly amenable to automation through simple robotic fluid handling. Finally, pseudo dilution can be exploited to render a cyclisation reaction more efficient in this method<sup>90</sup> and the final polypeptide can be detached from the polymer support and globally deprotected in one pot to simplify the work-up and isolation. However, despite these advantages, as with all techniques, there are several limitations to employing SPPS in the synthesis of polypeptides.

The first problem is a potential incompatibility between the resin and the growing peptide chain<sup>91</sup> leading to an incomplete reaction at each coupling step because of the aggregation of the peptide with the polymer of the resin. Consequently, resin-bound peptide side-products accumulate and, therefore, a complex mixture of products will be present upon cleavage from the resin. Furthermore, this method requires an excess of reagents and hence is wasteful.

SPPS has since been developed for use under microwave irradiation, becoming the aptly named technique microwave-assisted SPPS.<sup>92</sup> This approach is characterised as having limited racemisation and being high yielding. For this technique, both temperature and pressure are controlled over the course of the synthesis. Furthermore, Fmoc or Boc chemistry is compatible with this method, and it requires a much shorter cycle time in comparison to the traditional SPPS method for synthesising long polypeptides.

The primary requirement in the SPPS method is that the solid support is stable under all conditions of the synthesis. It is believed that there is a lower tendency of peptides to aggregate, especially with low resin loading, because

intermolecular peptide–peptide interactions are more limited when attached to a polymer compared to freely moving molecules in solution.<sup>93</sup> Avoidance of aggregation is an advantage of the SPPS technique.

## 1.8 Cyclisation strategies of linear polypeptides

Cyclic polypeptides are conformationally constrained relative to their linear counterparts.<sup>94</sup> Therefore, they are more resistant to enzymatic hydrolysis,<sup>95</sup> making them potentially more biologically active due to their increased likelihood of reaching the target under physiological conditions.<sup>96</sup> In addition, cyclic polypeptides are more selective than their linear counterparts for binding to specific targets.<sup>97</sup> Consequently, cyclic polypeptides have become attractive synthetic targets for medicinal and pharmaceutical chemistry.<sup>98</sup> Nevertheless, new synthetic strategies for these types of cyclic compounds are critical, as the current cost to produce them is inhibiting their application in industry. Therefore, the development of novel methodologies for the cyclisation reaction is urgently required for these molecules to increase their commercial potential.<sup>99</sup> Importantly, the same strategies that are used to form a peptide bond can also be used to synthesise cyclic polypeptides.

Depending on the functional groups in the linear compound, four different ways can be applied for cyclisation of the linear peptide,<sup>35, 38, 39</sup> head-to-tail (C-terminus to N-terminus), head-to-side chain,<sup>100</sup> side chain-to-tail or side-chain-to-side-chain<sup>101</sup> (See Figure 1.2). Therefore, more than one strategy has been used to improve methods for the cyclisation of the linear polypeptide to obtain high yields in a short time, fewer side reactions and lower cost.

### 1.8.1 Head to tail cyclisation

This method of cyclisation is one of the most important and has attracted the highest level of interest from chemists and pharmacologists over the last 30 years.<sup>102</sup> It has been observed that this strategy enhances biological activity by reducing flexibility and entropically increasing ligand binding affinity.<sup>103</sup> Thus, this method has been most applied to synthesise cyclic polypeptides from their linear counterparts, with only water being lost during the formation of the connective peptide bond. Initial strategies to achieve this began with the



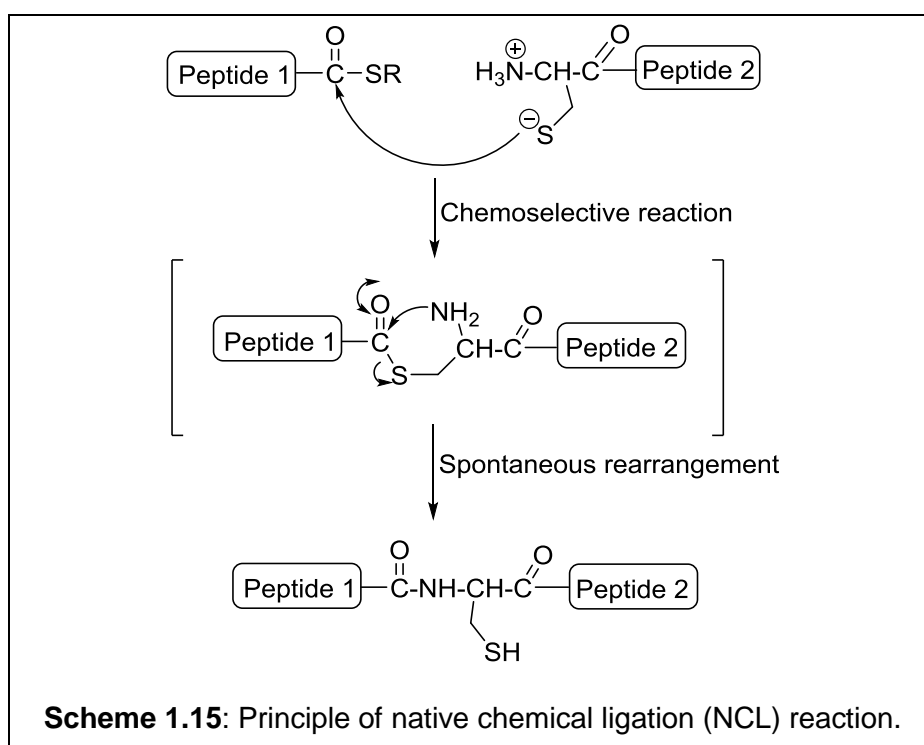
'classical' method, which is where the protected linear precursor is lactamised using high dilution in an organic solvent or under pseudo-dilution conditions on a solid support.<sup>81, 94</sup>

The formation of this amide bond between the two termini of the same linear precursor, without the need for any additional new amino acid or chain, means the cyclic polypeptide has the same sequence as its linear counterpart. Therefore, a direct and reliable comparison between the properties of the cyclic polypeptide and its linear counterpart is possible; for example, their relative stability to enzymatic degradation.  $\beta$ -sheet mimic structures are also formed using the head-to-tail cyclisation strategy, the presence of which in the linear peptide can, in turn, enhance the macrocyclisation.<sup>81</sup> Aspartic acid or glutamic acid is often used as the first amino acid in the sequence, both of which have two carboxyl groups. In this case, the side chain carboxyl group is bonded to the resin while the  $\alpha$ -carboxyl group, which is used to bond with the  $\alpha$ -amino group in the residue at the *N*-terminal, is protected with a temporary protecting group.

The cyclisation is slow, particularly if there is no turn structure-inducing amino acid in the linear precursor, such as glycine, proline or any D-amino acids. This delay in cyclisation leaves the active intermediate linear polypeptide able to react for a long time, increasing the opportunity to epimerise at the C-terminal residue.<sup>104, 105</sup> Furthermore the solubility of the protected peptide may become very low as its size increases. Therefore, synthesis of relatively large peptides by classical methods remains very difficult. Finally, it should be noted that there is no general, standard way to synthesise different peptides. The method used to synthesise a cyclic peptide depends on its properties, such as polarity and conformation, as well as the length and type of the sequence.

To overcome the above issues, alternative methods to the classical methods (indirect peptide bond formation) have been devised to form cyclic polypeptides, with the aim of direct peptide bond formation using completed unprotected linear precursors in aqueous solution.<sup>106</sup> These methods involve a process termed native chemical ligation (NCL),<sup>107</sup> which is considered a significant way of overcoming some of the size limitations of the SPPS method. In this technique, the cyclisation reaction consists of two steps: the first segment, an unprotected linear peptide  $\alpha$ -thioester<sup>108</sup> is reacted

chemoselectively with the second segment containing an *N*-terminal Cys residue. This results in a thioester linked intermediate. In the second step, an intramolecular acyl migration occurs in the transient compound. This molecular rearrangement forms a native peptide bond at the site of ligation, without any need to change the conditions of the reaction. The final desired product is thus formed without any further manipulation. Scheme 1.15 shows the principle of this strategy, of which the synthesis of collagen protein is an example. This strategy is particularly useful for collagen as it is difficult to synthesise this type of protein by the classical method because of its large size.<sup>109</sup> In this case, the SPPS method was used to prepare the cysteine and thioester peptide segments, then the polymerisation step between the two segments was undertaken using NCL under aqueous conditions to yield the polymer. Another example of NCL being used is in the synthesis of lipopeptide vaccine as treatment against group A streptococcal infection.<sup>110</sup>

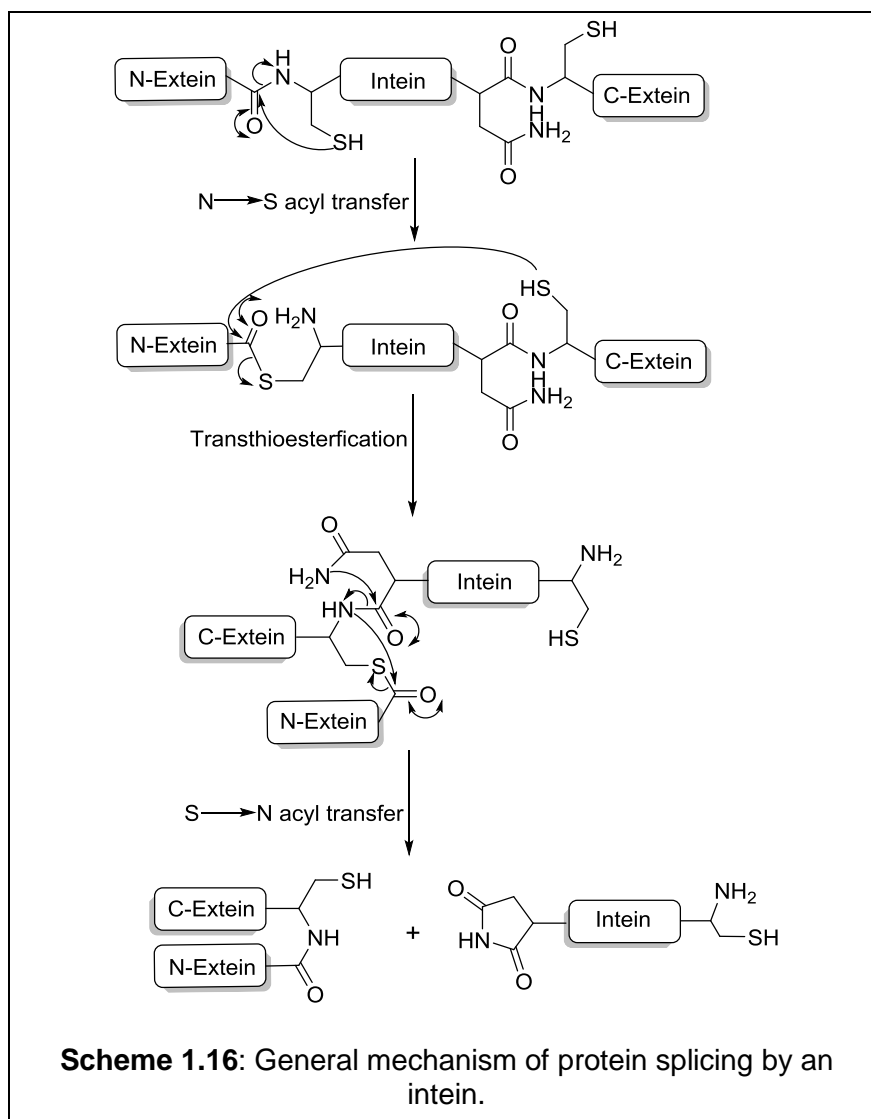


The NCL method is characterised by high chemoselectivity, permitting coupling of the segments without protection of the reactive side chain groups. However, this approach also has some limitations.<sup>111</sup> For example, the thioester peptide is usually prepared using Boc chemistry requiring repeated deprotections with TFA and an HF reaction for the cleavage of the thioester

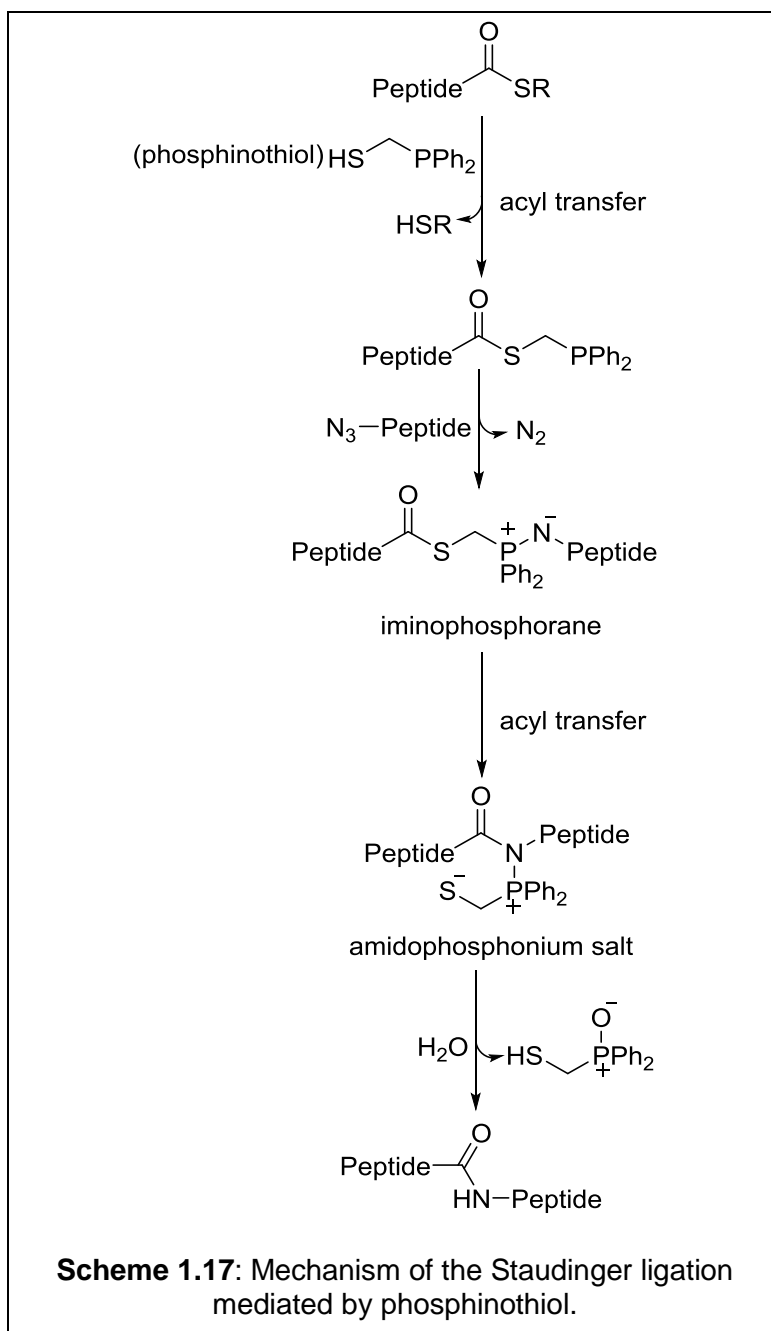
peptide product from the resin. Synthesis of the thioester peptide is one of the obstructions that can limit the use of this method. Consequently, more than one ligation technique has been designed to form the peptide bond, each one having been used to synthesise a certain problematic protein. Solid phase ligation is another example of a chemical ligation method that was introduced to increase the activity of ligation of multiple segments.<sup>112</sup>

The ligation of peptide hydrazides is an important strategy used to synthesise polypeptides and proteins.<sup>113</sup> It is one of the more modern chemical methods and does not require protecting groups. In this example, a two-step reaction is used to ligate two unprotected peptides. Firstly, a peptide azide is produced after mixing two peptides (one of the peptides has C-terminal hydrazide and the other has N-terminal cysteine) with  $\text{NaNO}_2$  (an oxidant) under acidic conditions. The thiols are added as a second reactant, followed by adjusting the pH of the reaction, leading to the formation of the required product.

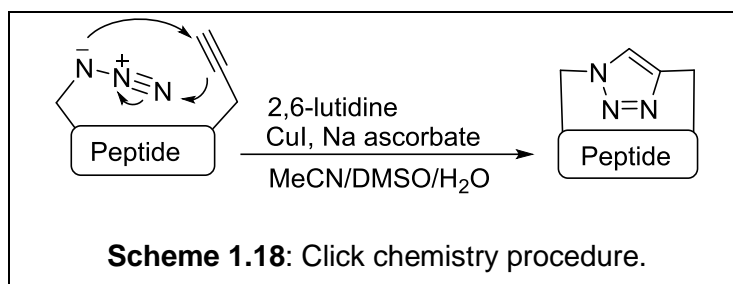
The aforementioned strategies have encountered some difficulties when used for ligating a recombinant peptide to a synthetic peptide or labelled peptide which could not be converted into peptide thioesters. As a result, expressed protein ligation (EPL) is a synthetic strategy that has been investigated to overcome this problem by employing an intein (Scheme 1.16). Notably in this strategy, the labelled fragments (intein) have no negative effect on peptide synthesis. This method has been used to synthesise many different proteins; for example, the synthesis of *Consensus* tetratricopeptide repeat.<sup>114</sup>



Another strategy, used as an alternative to NCL, is based on the Staudinger reaction.<sup>115</sup> Scheme 1.17 indicates the mechanism of the Staudinger ligation by mediation of phosphinothiol.<sup>116</sup>



Several attempts have since been made to overcome the problems of the methods mentioned and in the past decade, a strategy involving click chemistry (CuAAC), i.e. copper azide alkyne cycloaddition,<sup>117</sup> has emerged.<sup>118</sup> In this method, triazole cyclic polypeptides are generated by an aliphatic azide at the *N*-terminus reacting with an alkyne in the *C*-terminus of the linear polypeptide. This occurs through a 1, 3-dipolar cycloaddition and is catalysed by copper(I) to form a 1, 2, 3-triazole. Scheme 1.18 indicates the strategy of this click reaction.



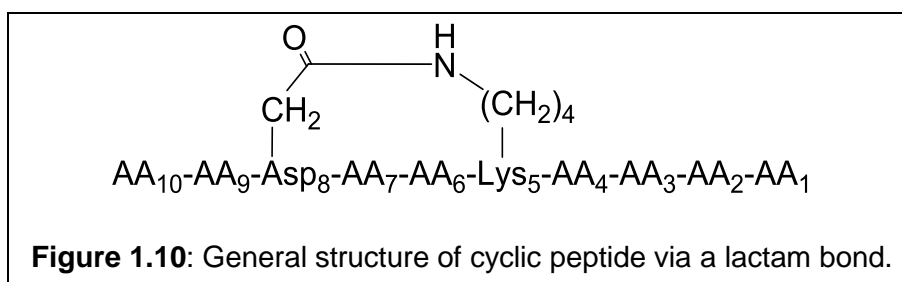
The main advantages of the click reaction are that it is a fast and irreversible method, the ligation generates high yields with a simple isolation procedure for the resulting products. Importantly, the method is also wide in scope. The starting materials and reagents are also readily available, and any solvents needed such as water, are easily removed. Chemically, the conditions of the reaction are mild compared to other methods. These qualities have resulted in the click reaction becoming a meaningful strategy towards the synthesis of polypeptides and proteins. In some complex biological environments, the by-products must be non-toxic, particularly in an *in vivo*-system,<sup>119</sup> therefore, the toxic copper catalyst can be considered a disadvantage of this strategy.

### 1.8.2 Side chain-to-side chain cyclisation

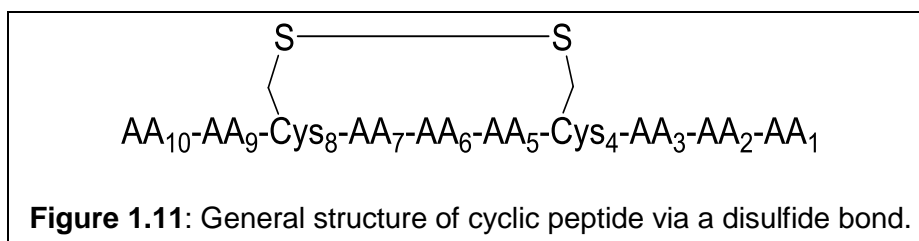
Side chain-to-side chain cyclisation is one of the most common procedures used to synthesise cyclic polypeptides from their linear counterparts, to upgrade their biological activity, pharmacokinetic characteristics and proteolytic stability.<sup>120</sup> In this case, a covalent attachment is formed between the side chain group on one amino acid residue and the side chain on another amino acid residue in the peptide. Therefore, there are many possibilities that form this type of tether. For example, cyclisation can occur via lactones (esters), lactams (amides), ethers, thioethers,<sup>121</sup> ring closing metathesis<sup>122</sup> or through the azide-alkyne click reaction.<sup>123</sup> Lactams have been the more widely used recently, with a side chain amino and a side chain carboxyl group being employed in this particular class.<sup>124</sup>

Stabilised helical structures, formed by specific sequences of polypeptides and proteins, play an essential role in the conformations of these compounds in nature, as seen by their relative frequency of occurrence.<sup>125</sup> Therefore, many chemical methods use the side chains of reactive amino acids

to form cross-links that stabilise an  $\alpha$ -helical segment of the peptide. An example of this strategy is a lactam cross-link between aspartate and lysine (Figure 1.10).<sup>126</sup>



A second important type of side chain–side chain bonding is a disulfide bridge. Disulfide bridges function naturally to strengthen the stability and conformational control of native peptides. This bond can also be used to protect protein–based therapeutics from fast enzymatic hydrolysis and to enhance the resistance of proteins from the effects of the environment during processes of chemical synthesis.<sup>127</sup> Therefore, chemical cyclisation of polypeptides via an S–S bond is of high interest to chemists and pharmacologists. Figure 1.11 indicates a polypeptide that has a cyclic structure formed by a disulfide bond.



Another example of side chain–side chain bonding to form a cyclic structure is by cross-linking the side chains of two residues of serine with a dicarboxylic acid. This ring forming cyclisation procedure was used to prepare the new constrained PTH (parathyroid hormone) analogue<sup>128</sup> as shown in Figure 1.12.

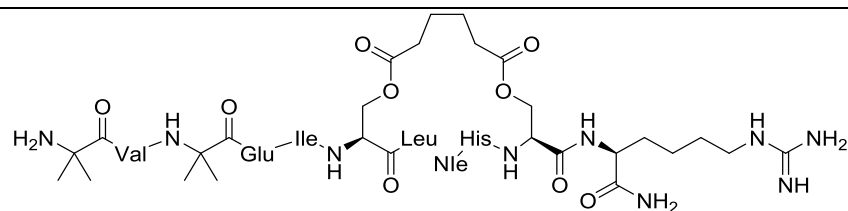
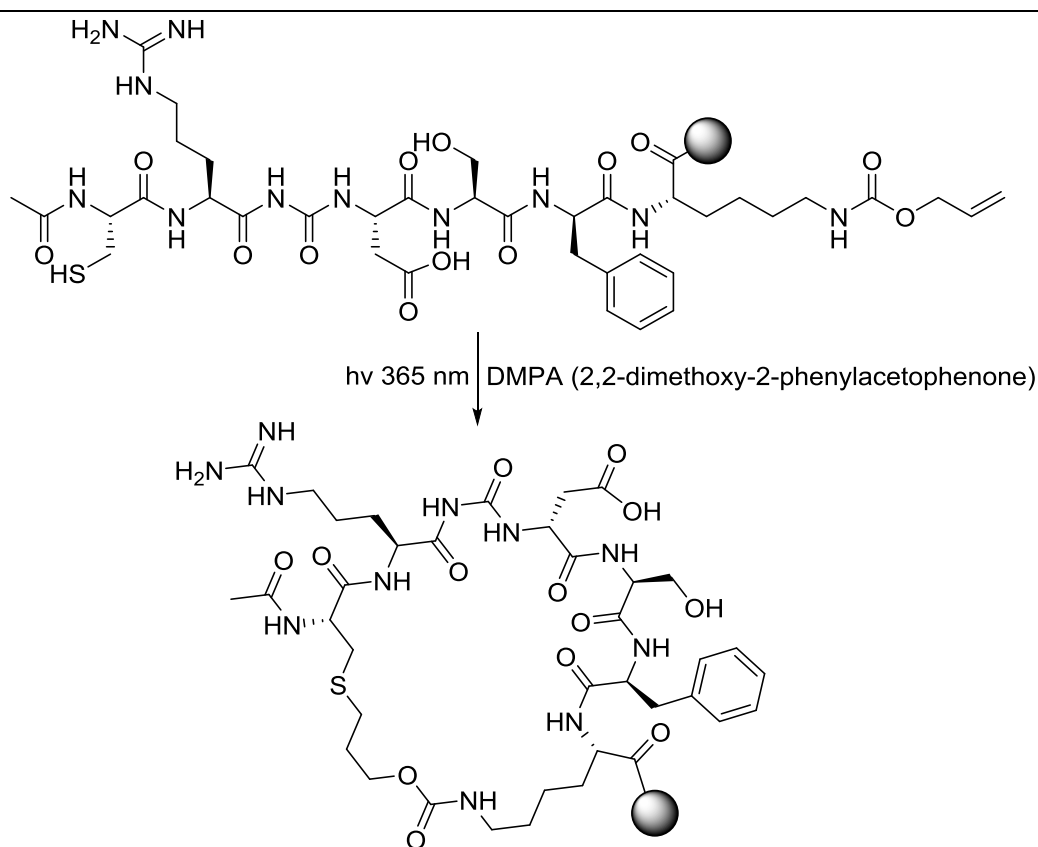


**Figure 1.12:** Formation of a cyclic structure by two serine residues that are esterified to a dicarboxylic acid.

### 1.8.3 Side chain-to-tail cyclisation

The third important method of macrocyclisation is the side chain-to-tail strategy. An example of this type of bonding is through a cysteine thiol functionality. The process involves the radical addition of the thiol group in the cysteine at the *N*-terminus to the alkene group attached to the side amino group of a lysine residue at the *C*-terminus,<sup>129</sup> as displayed in Scheme 1.19.



**Scheme 1.19:** Cyclisation of the linear peptide via the radical addition of the thiol group in the cysteine to the alkene group.



## 1.9 Important factors that affect the synthesis of cyclic polypeptides

An organisation of the reactive ends of the linear polypeptide, into a narrow molecular space before ring closure via the head-to-tail method, can be considered an essential step to the success of the macrocyclisation of the linear polypeptide precursor. Therefore, factors affecting cyclic polypeptide formation have attracted the attention of some research groups. These factors can be classified into two types:

### 1.9.1 Internal factors

The most important internal factor that controls the success of the cyclisation of the polypeptide is the resulting ring size,<sup>130, 131</sup> in particular, through the head-to-tail method. Polypeptides consisting of more than seven amino acids in the linear precursor are often favoured to close the ring successfully. The cyclisation is typically straightforward: this length or more can supply the requirements of reactive orientation for both termini with little ring strain. However, problems are observed during cyclisation of fewer than seven residue linear polypeptides, yet it is possible to cyclise peptides of this length.<sup>104</sup> The reason for the cyclisation difficulties is the absence of two crucial factors, hydrogen bonding and  $\beta$ -sheet structure, which both act as an accelerator to tether the residues of the sequence.<sup>132</sup>

It has been found that the presence of D-amino acid residues in a sequence of L-amino acids accelerates the cyclisation reaction of the linear polypeptide precursor. Their ability to induce a turn structure results in higher yields for many types of polypeptide cyclisation.<sup>133</sup>

The presence of a cis-amide bond in the middle of the linear polypeptide sequence can also result in a more efficient macrocyclisation. Thus, the presence of, *N*-methyl amino acids has a similar effect to a proline residue in the backbone of the peptide supporting the successful closure of the ring in high yields.<sup>134</sup> On the other hand, a polypeptide which does not contain any D-residue in the sequence, and hence has no turn-inducing structure, is consequently tricky to cyclise. To combat this, the  $\alpha$ -carbon of the C-terminal residue can be changed to the D-configuration.<sup>135</sup> Other research groups have

found that incorporation of a small heterochiral unit of diproline, D-Pro-L-Pro, in the linear polypeptide sequence results in a particularly efficient rate of cyclisation because this unit increases the presence of  $\beta$ -turn structures.<sup>136</sup>

In addition to the presence of proline in the sequence, glycine, when located in the middle of the sequence, also displays similar properties.<sup>137</sup> Glycine is a small residue and thus displays less steric hindrance, allowing for more bending of the linear peptide. In addition, it does not form side chain hydrogen bonds with neighbouring residues, leaving more degrees of freedom for the ends of the peptide to remain moving in the molecular space. Consequently, the likelihood of a ring-forming collision occurring is much higher.

Positive effects on, and higher yields for, the cyclisation reaction have also been found for particular amino acids at the termini of the linear peptide; for example, having a glycine at the C-terminus and a proline or alanine at the N-terminus, and vice-versa. The probable cause for this advantage is the difference in the conformations for each sequence, with certain combinations being more suitable for ring closings. On the other hand, having large residues at the termini results in less macrocyclisation.<sup>138</sup>

It has been found that using the amino acids serine, threonine or cysteine as protected oxazolidine/thiazolidine dipeptide derivatives in the SPSS techniques allows them to act as pseudo prolines, i.e. structural building blocks to prevent the aggregation and self-association of the linear polypeptide,<sup>139</sup> thus assisting the synthesis of short cyclic polypeptides without using turn-inducing factors.<sup>140</sup> The presence of protected pseudoproline dipeptide derivatives temporarily induces the establishment of  $\beta$ -turn structures, enhancing the cyclisation reaction.<sup>141</sup>

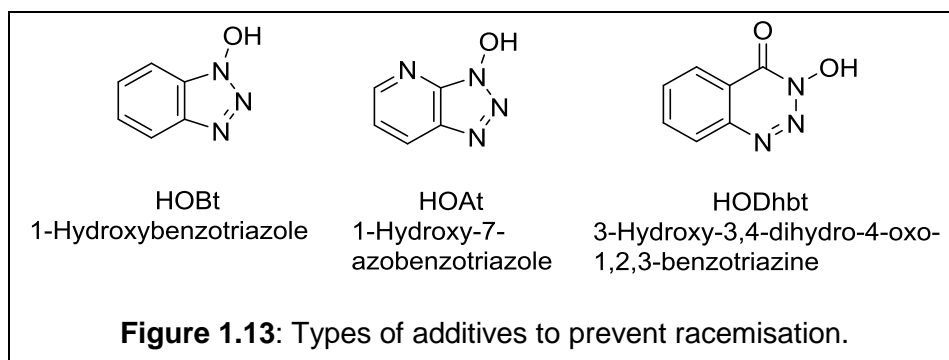
Some patterns have been found during the study into the effect of the size of the residue at the C-terminus or N-terminus on macrocyclisation efficiency. Linear polypeptides which have a small residue at the C-terminus have a greater ability to cyclise, and vice versa. With regards to the N-terminal residue, it has been found that the orientation of the side group of the N-terminus plays an important role in the success or failure of the cyclisation reaction.<sup>142</sup>

### 1.9.2 External factors

Multiple external factors play a significant role in the synthesis of polypeptides and their subsequent macrocyclisation. The first important factor is the choice of resin and how it swells, as there is often more than one type of resin with a particular property, such as high loaded resin or low loaded resin. Therefore, compatibility between the kind of peptide being produced and the properties of the resin is a key factor in the successful synthesis of the linear precursor of cyclic peptides. It has been observed that lower loaded resins are preferred for the synthesis of long peptide sequences, mainly due to increased accessibility to the  $\alpha$ -amine when using resin loading of less than 0.4 mmol/g. This type of resin also reduces interactions between individual growing sequences preventing interchain aggregation.<sup>143</sup> In addition, swelling of the resin prior to starting the synthesis must be performed in order to obtain the homogeneous presence of bound amino acids throughout the resin, resulting in a higher yield of the peptide.<sup>144</sup> Using a low-loading resin, decreases the potential for dimerisation or cyclodimerisation side reactions which would reduce the yield.<sup>142, 145</sup>

The second important factor is the choice of a coupling reagent, using high concentrations of the coupling reagent usually results in a high yield for the precursor peptide for the cyclisation reaction. It has also been observed that if not enough coupling reagent is added, the reaction may not reach completion, therefore, short, incomplete sequences are formed as a side product.<sup>146</sup>

Activation of the carboxylic acid before the amide bond forming step sometimes leads to racemisation; therefore, including certain additives (Figure 1.13) in the coupling reaction mixture is commonplace to overcome this problem; for example, adding HOBt (1-hydroxy benzotriazole) to a coupling reaction performed using PyBOP reagent.<sup>142</sup>



The third important factor is the choice of deprotection reagent. Multiple reagents can be used for this purpose. Cyclic secondary amines, e.g. piperidine and piperazine, are widely used as removal reagents for a 9-Fluorenylmethoxycarbonyl (Fmoc) group. Optimisation of the concentration of the reagent, the number of times the molecule is subjected to the deprotection procedure, and the duration of reaction may support the coupling reactions,<sup>147</sup> resulting in high quality and high yields of the linear peptide, thus affording more precursor to cyclise, giving a higher overall yield of cyclic peptide.

A critical factor in the synthesis of both linear and cyclic polypeptides is the cleavage reagent used for removing the peptide and side protecting groups from the resin.<sup>69</sup> The yield of the synthesis relies heavily on this step and the typical reagent for this cleavage when using the Fmoc protection method is TFA. Careful consideration of the TFA concentration and reaction time of the cleavage is important, as using too high a concentration could cleave the linker from the resin in addition to cleaving the peptide from the linker. The carbonium ion originating from the linker may react through alkylation with some side chains of the peptide, e.g. Trp or Cys, and consequentially, a side product is formed. In addition, leaving the reaction to occur for too long a time may result in the formation of the oxidised peptide. The addition of scavengers, such as ethanedithiol (EDT), triisopropyl silane (TIS), water and phenol, is essential to help prevent this problem.<sup>144, 148</sup>

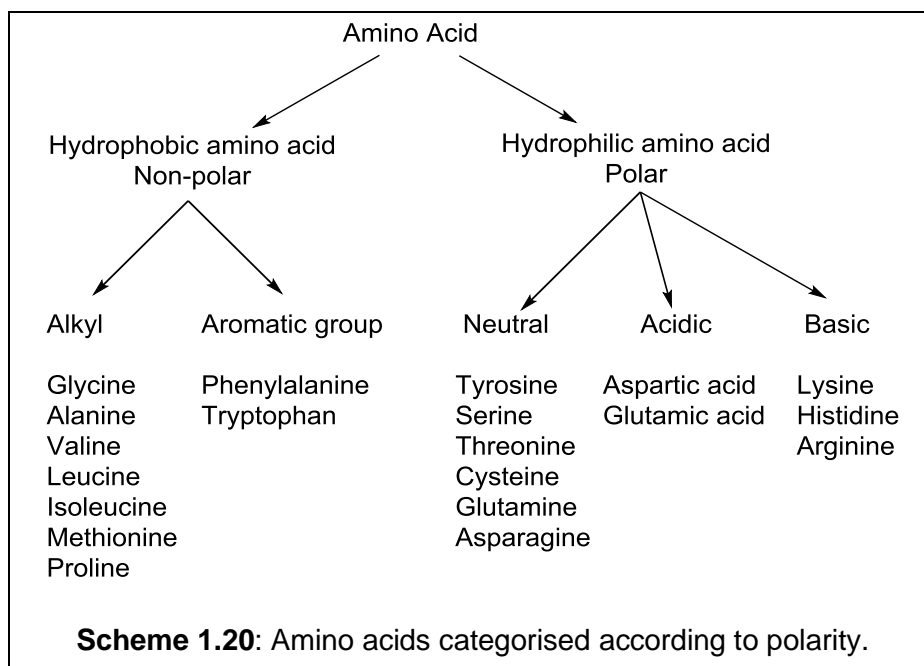
Finally, some other less obvious factors need to be considered in the synthesis of cyclic peptides, including the use of different metal ions as coordinators. These help to bend the peptide and reduce the distance between the two ends of the linear precursor before the cyclisation reaction. It has been

observed that lithium and cesium chloride are the best coordinators to obtain a high yield. However, solubility issues with the coupling reaction solvent can be a problem.<sup>138</sup> Changing the time for which the mixture is heated during the coupling reaction could also increase the yield of the cyclic peptide.<sup>142, 143</sup> In addition, increasing the number of times the coupling reaction is performed also affects the amount of the product. In the SPPS strategy, the number of occasions the resin bound peptide is washed after deprotection and coupling is important to remove excess quantities of reagents and side products. Finally, some cyclic peptides have poor solubility in certain solvents. Therefore, the purification of these cyclic peptides will be difficult. The choice of solvents are important factors for correct separation and purification of the peptide by high pressure liquid chromatography (HPLC). Meanwhile, trifluoroacetic acid (TFA) or formic acid is added to the solvents in a small percentage to boost the separation of the peptide, resulting in a higher yield.<sup>149</sup>

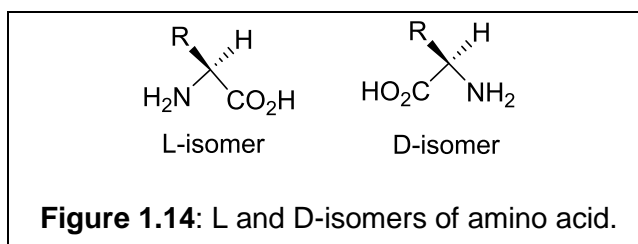
## 1.10 Amino acids

Amino acids are organic compounds containing two functional groups, an amine,  $\text{NH}_2$ , and a carboxyl,  $\text{COOH}$ , attached to the  $\alpha$ -carbon atom in addition to a side group. Twenty common amino acids are the building units of proteins. They are classified according to the structure of the side group as seen in Scheme 1.20.

The amino acids which contain nonpolar side chains, such as alkyl groups or aromatic groups, are called hydrophobic amino acids. Such examples include leucine or phenylalanine. The amino acids which have polar side chains, such as hydroxyl ( $\text{OH}$ ), or sulfhydryl ( $\text{SH}$ ), are called hydrophilic neutral amino acids; examples of these include serine or cysteine. Amino acids that have side chains such as a carboxylic acid ( $\text{COOH}$ ) are hydrophilic acidic amino acids and include aspartic acid or glutamic acid. Finally, in addition, the amino acids which have side chains containing an amino group ( $\text{RNH}_2$ ) are called hydrophilic basic amino acids and include arginine and lysine.



All the amino acids are optically active compounds as they have a  $\alpha$ -chiral carbon except glycine which has a hydrogen atom as its side group. There are two isomers of amino acids, known as the L and D-isomers. The L-isomers are prevalent in living organisms (Figure 1.14). The L-isomer generally corresponds to an S configuration of the stereocentre, with cysteine being an important exception.

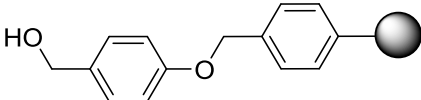
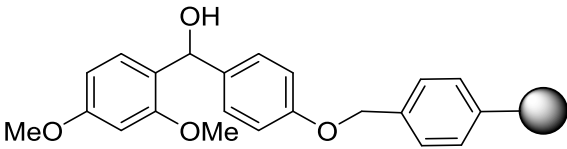
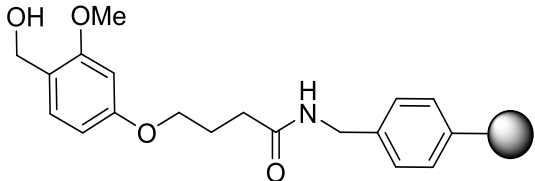
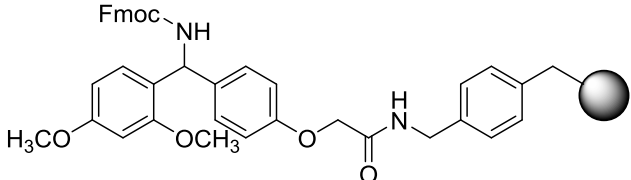
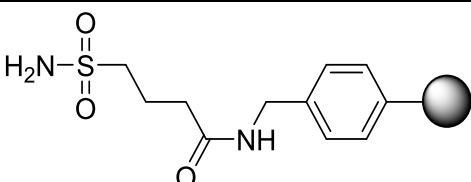


The sequence of amino acids in the peptide can be referred to by one or three letter abbreviations; for example, K or Lys for the amino acid lysine. Modified amino acids can also be found in some proteins; for instance, hydroxyproline or 5-hydroxylysine instead of proline or lysine respectively. Certain modifications in natural proteins help to boost their solubility, their stability, and their interaction with other proteins. Furthermore, the  $pK_a$  of amino acids can be changed with modifications; for example, the  $pK_3$  of selenocysteine (5.3) is lower than that of cysteine (8.3).<sup>150</sup>

## 1.11 Resin

Resins or insoluble polymer supports are used in the SPPS strategy to enhance the synthesis of polypeptides in comparison to the classical SPS method. The possible functions of the resin are widely extended because the linkers that anchor the resin to the growing polypeptide chain consist of different chemical groups. The main physical properties of the resin are a spherically shaped particle with a diameter of between 35–135  $\mu\text{m}$ . These days, the most commonly used resin is made of polystyrene cross-linked with 1% (divinylbenzene) DVB.<sup>151</sup> After swelling and opening up of the porosity of the resin by an appropriate solvent, the reagents enter the beads to react with the resin. Swelling factors rely on the type of resin.<sup>152</sup> Table 1.1 indicates some of the most common resin linkers for SPPS.<sup>153</sup> Two types of resin can be used to synthesise polar substances, polyamines and polyethylene glycol (PEG).<sup>154</sup> The latter has been used to form long, complex peptides with different solvents, including water.<sup>155</sup>

**Table 1.1:** Name and structure of some common resin linkers.

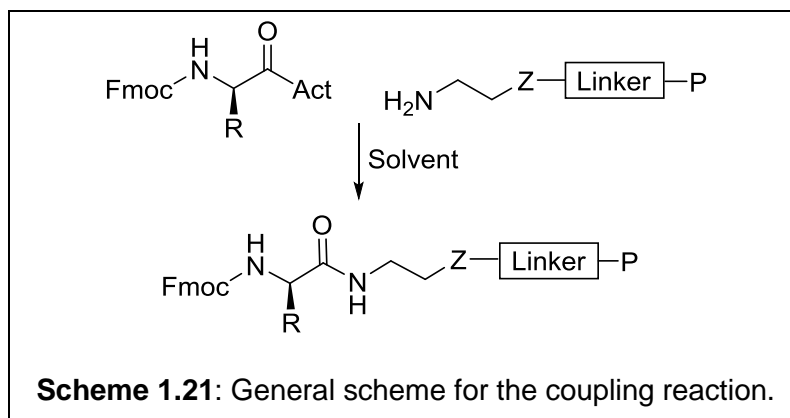
Name	Resin linker structure
Wang	
Rink acid	
HMPB	
Rink amide	
Sulfonamide	

## 1.12 Coupling reagents

One of the valuable reactions in organic synthesis and medicinal chemistry is amide bond formation. The amide bond has played a central role in the synthesis of drugs, especially for the creation of combinatorial libraries after the development of SPPS.<sup>156</sup> The coupling reagents that can reduce the racemisation of amino acids have attracted the attention of those interested in this field.<sup>157</sup>

The peptide bond formation reaction in the synthesis of peptides consists of two steps: the first is activation of the carboxyl of the new amino acid; the second step is acylation of the amino group. A reactive intermediate is formed in the first step following the reaction between the protected amino acid or peptide with the coupling reagent.

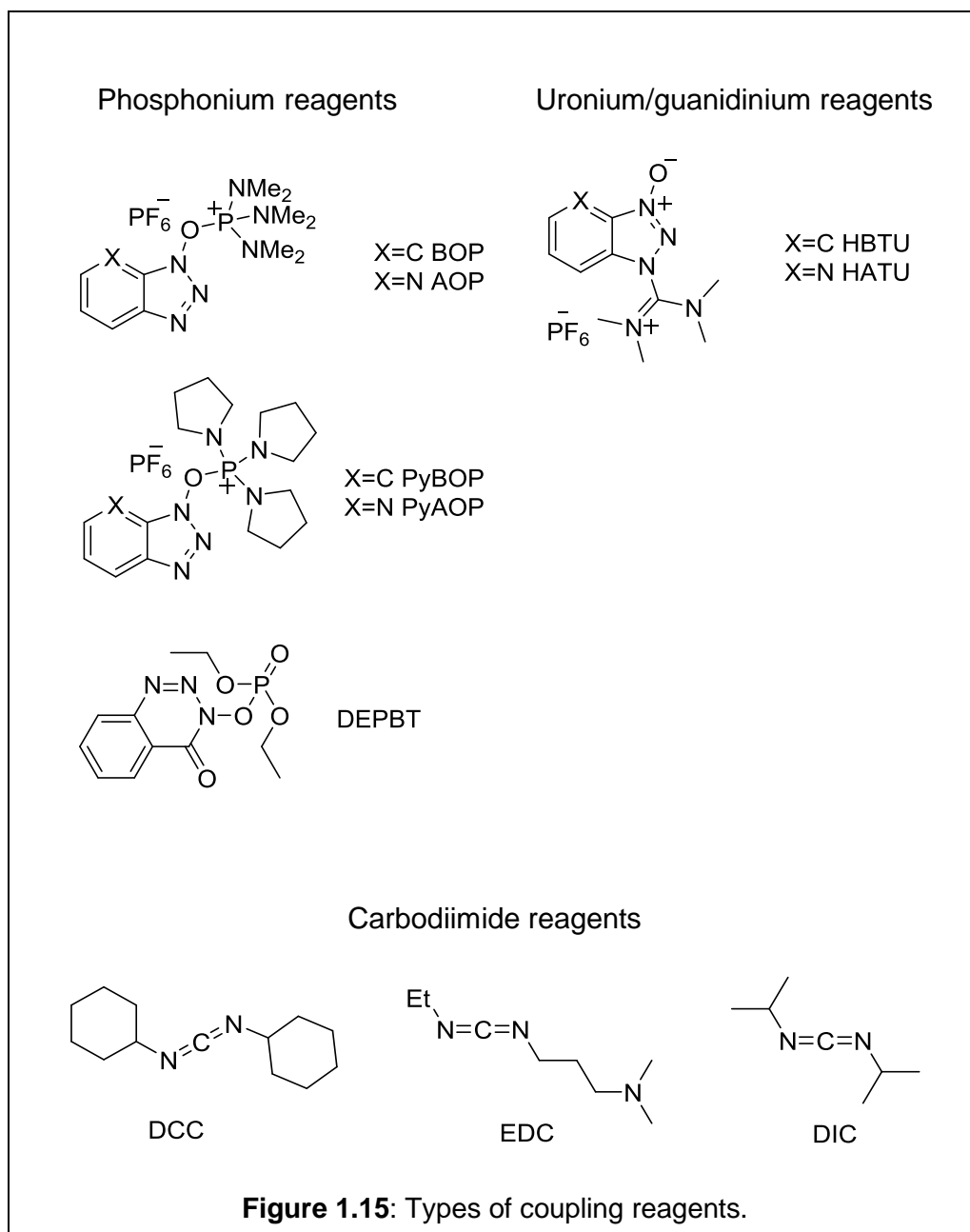
Some of the variables that have a direct effect on the efficiency of the coupling reactions are, for example, the choice of solvent which is used to swell the resin, steric hindrance resulting from side chains and their protecting groups, and reactivity of the activated carboxylic group, as in Scheme 1.21.



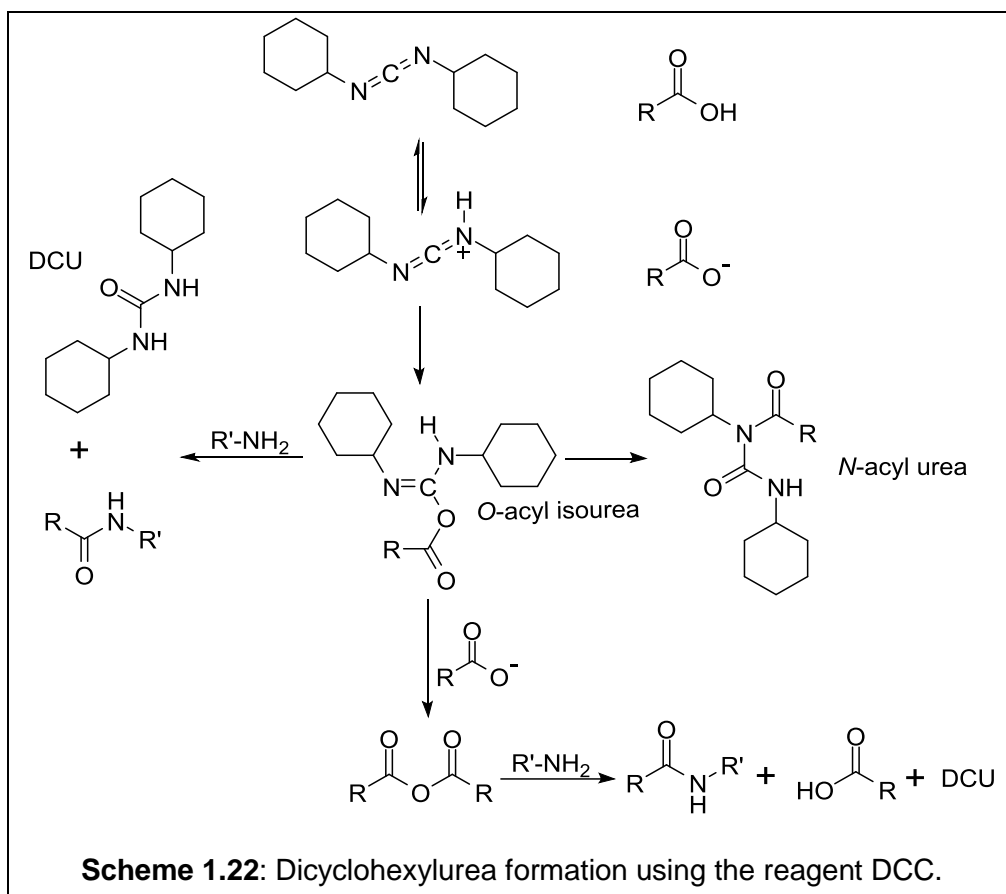
Racemisation could occur during poor coupling conditions which also may lead to forming unwanted products, such as truncated sequences.<sup>158</sup> Repeat of the coupling reaction with fresh reagents may result in a higher yield.

Different reagents have been prepared and used in the coupling reaction, for example, PyBOP, DEPBT, HATU, HBTU, DCC, DIC as in Figure 1.15.

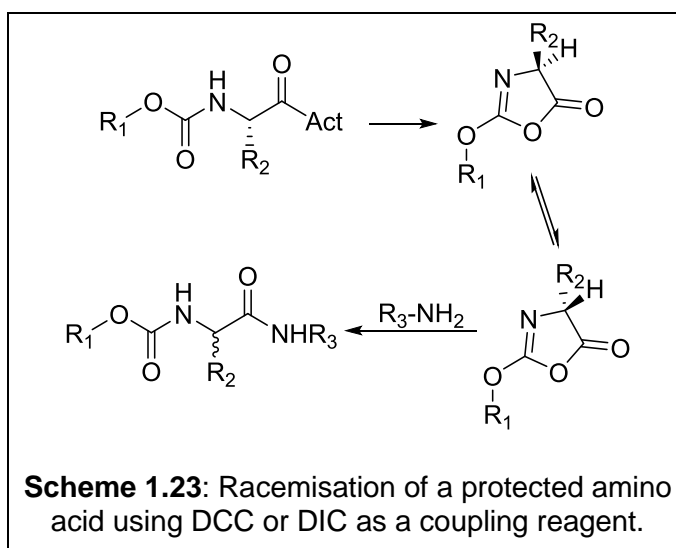




DCC (dicyclohexylcarbodiimide) is one of the carbodiimide reagents; it was used during the first days of SPPS strategy. Use of this reagent is limited in the SPPS strategy because the dicyclohexylurea side product is poorly soluble in most solvents.<sup>159</sup> (Scheme 1.22). Therefore, DIC (diisopropylcarbodiimide) is better than DCC in the SPPS method as the urea side product is soluble. DIC reagent was used to synthesis a cyclic undecapeptide, Wy-40,770 as an inhibitor for GH (growth hormone).<sup>160</sup>



Racemisation can occur resulting in epimers of the peptide, as in Scheme 1.23. This issue can be avoided by the presence of additives such as HOBt (1-hydroxybenzotriazole) in the reaction mixture.<sup>161</sup>



Recently, highly popular coupling reagents have been acylphosphonium salts, such as PyBOP (Benzotriazole-1-yl-oxy-tris-pyrrolidinophosphonium

hexafluorophosphate),<sup>162</sup> and acyluronium salts, such as TBTU (O-(Benzotriazol-1-yl)-N,N,N,N-tetramethyluronium tetrafluoroborate), HBTU (2-(1H-Benzotriazol-1-yl)-1,1,3,3-tetramethyluronium hexafluorophosphate).<sup>163</sup> BOP (Benzotriazol-1-yl-oxy-tris-(dimethylamino)-phosphonium hexafluorophosphate) is one of the phosphonium reagents which was prepared as an alternative to carbodiimide reagents to minimise the problems that can occur with carbodiimide, such as racemisation or side reaction.<sup>164</sup> Also, use of this reagent minimises asparagine or glutamine dehydration byproducts.<sup>165</sup> One of the disadvantages of this reagent is that it generates a carcinogenic by-product, which is hexamethylphosphoramide (HMPA). The PyBOP reagent is more efficient than BOP, as the coupling reaction is fast to complete and the by-product is less hazardous.

Uronium reagents, such as HBTU and TBTU, afford high coupling yields and fast reaction kinetics. Any excess of these reagents may lead to short sequences because they could react with free N-terminal of the peptide, forming a guanidine compound that blocks the elongation of the chain. Adding 1-hydroxybenzotriazole as an additive to the reaction mixture will reduce racemisation.<sup>166</sup>

DEPBT (3-(diethoxyphosphoryloxy)-1,2,3-benzotriazin-4(3H)-one) is an important coupling reagent in SPPS and SPS methods for synthesis of the polypeptides (linear and cyclic). It confers resistance to racemisation, and in addition, it is not necessary to protect the side chains of tyrosine, serine, threonine and histidine during the coupling reaction.<sup>167</sup>

**Chapter 2**

**Results and**

**Discussion of Cyclic**

**Peptide Synthesis**

## 2 Cyclic Peptide Synthesis

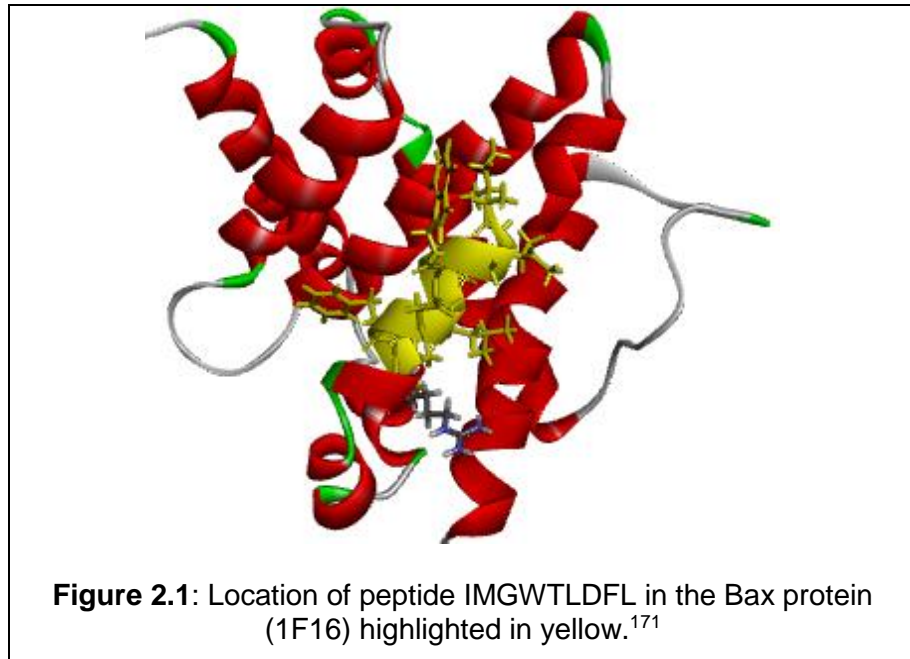
### 2.1 Introduction

As a goal of this project was the synthesis of a cyclised tumour antigen peptide, an important consideration was the design of the peptide sequence.

It has been found that many of the peptides that have the ability to bind HLA-A<sub>2</sub> are composed of 9 amino acids with a Leu residue in position 2 of the sequence.<sup>168</sup> It has been observed that the amino acid sequence of peptides is responsible for the conformation of the peptide in the HLA-A<sub>2</sub> complex which thus presents the side chains that affect the binding of the complex to the T cell receptor (TCR). Also, the length of the bound peptide to HLA-A<sub>2</sub> affects the orientation of the side chains of the residues giving different conformations for the complex that impact on recognition by the TCR.<sup>169</sup>

Several algorithms have been developed for computational prediction of peptide epitopes and these are implemented in more than one software package (NetCTL, WAPP, SMM and EpiJen). The EpiJen server aims to select the true epitope that activates CD8<sup>+</sup> T cells by modelling the processing of proteins to peptides, peptide transport and MHC binding.<sup>170</sup> A proportion of non-epitopes of the source protein are excluded in the first three steps (proteasome cleavage, TAP transport and MHC binding), leaving only 5% of peptides from the whole protein sequence. This small percentage has 85% of the true epitopes.

In an experimental approach to epitope discovery, libraries of synthetic 9-mer peptides derived from the Bax protein were screened at Cardiff University School of Medicine.<sup>2</sup> Bax was chosen for investigation as it was hypothesised that degradation of Bax in tumours would lead to presentation by HLA class I of Bax-derived peptides on the cell surface. A peptide, IMGWTLDFL, derived from the Bax<sub>136-144</sub> sequence was found to bind to HLA and then to activate CD8<sup>+</sup> T-cells to recognise and kill a variety of HLA-matched cancer cells.<sup>2</sup> The location of the antigenic peptide within the intact Bax protein is depicted in Figure 2.1. This peptide forms the basis of the work described in this thesis, where the goal is to increase its stability in serum while permitting uptake into cells followed by processing and display.



The functions of the peptide residues are different; some of them contact the HLA, while others make contact with the TCR. The sequence of the Bax peptide IMGWTLDFL is terminated with the hydrophobic residues leucine and isoleucine, which play an important role in anchoring the peptide to the HLA. The residues in the interior of the sequence will contact the TCR.

The cyclic peptide will no longer exhibit the helical structure found in the full length Bax protein and will not display any function of Bax. The 9-mer linear peptide could bind directly to the HLA-A<sub>2</sub>. However, it is likely that the cyclic peptides must be taken up by the cell and undergo processing (cleavage) inside the cell before binding to HLA-A<sub>2</sub>. Thus, the cyclic peptide must survive hydrolysis by extracellular proteases, so that it can be taken up by an antigen presenting cell (dendritic cell), processed by intracellular proteases in a similar way to Bax, to give the required fragment (9-mer) to be displayed on the MHC protein.

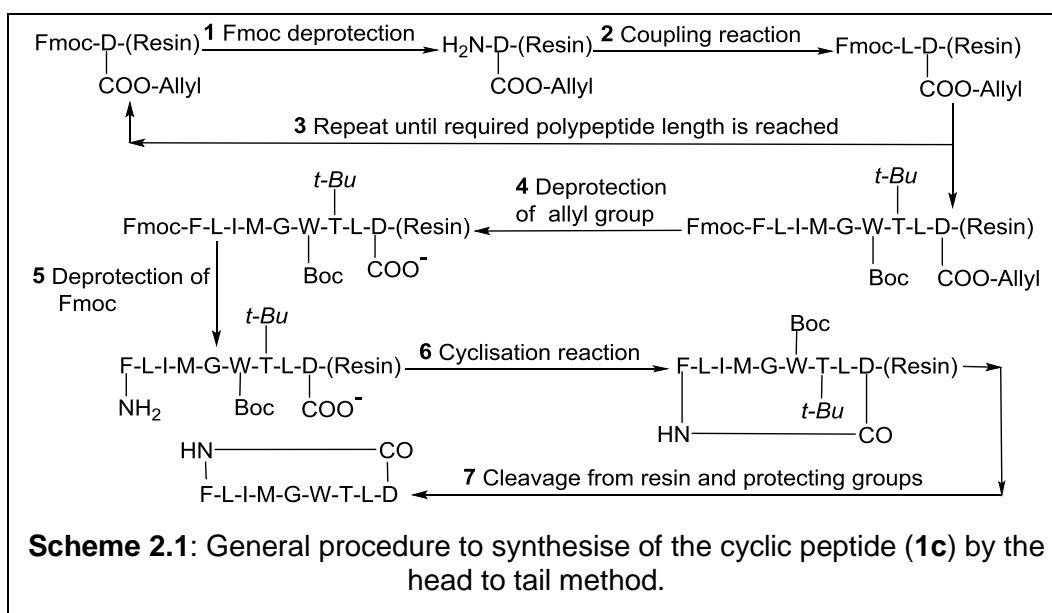
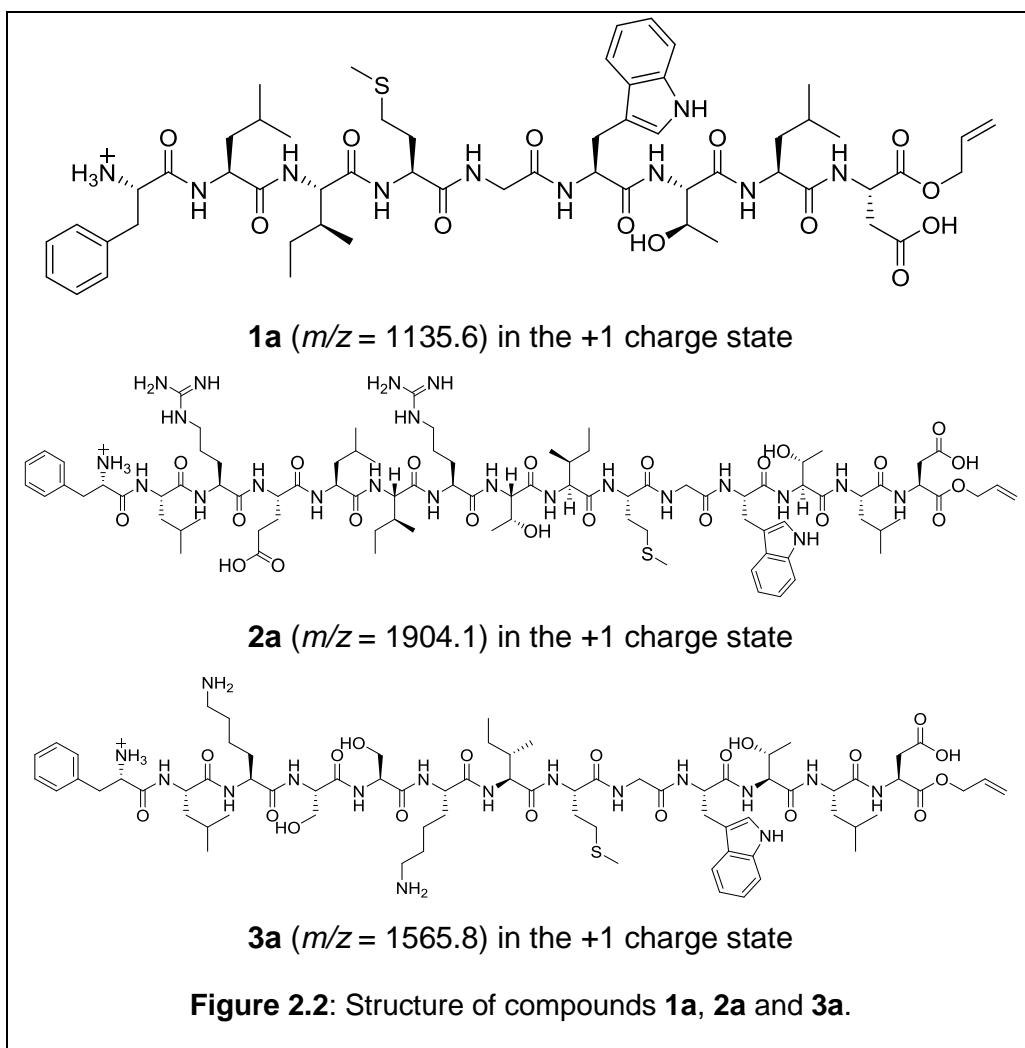
Extending the original 9-mer sequence with a short linker comprising flanking residues from Bax or residues chosen for solubility or cell permeability was another possibility to create cyclic peptides that could be processed within cells to generate the epitope. One of the reasons for choosing a 15-mer polypeptide length was that it had been found that B-cells loaded with 15-mer

polypeptide libraries have the ability to activate T-cells against human papillomavirus (HPV)-associated tumour.<sup>172, 173</sup>

For the purposes of synthesis of cyclic derivatives of this sequence, the terminal residues of IMGWTLDFL are not ideal as leucine lacks side chain functionality for resin-anchoring and the bulky side chains may slow the cyclisation reaction. To avoid these drawbacks, the sequence can be circularly permuted to place residues at the termini that are more conducive to cyclic peptide synthesis.

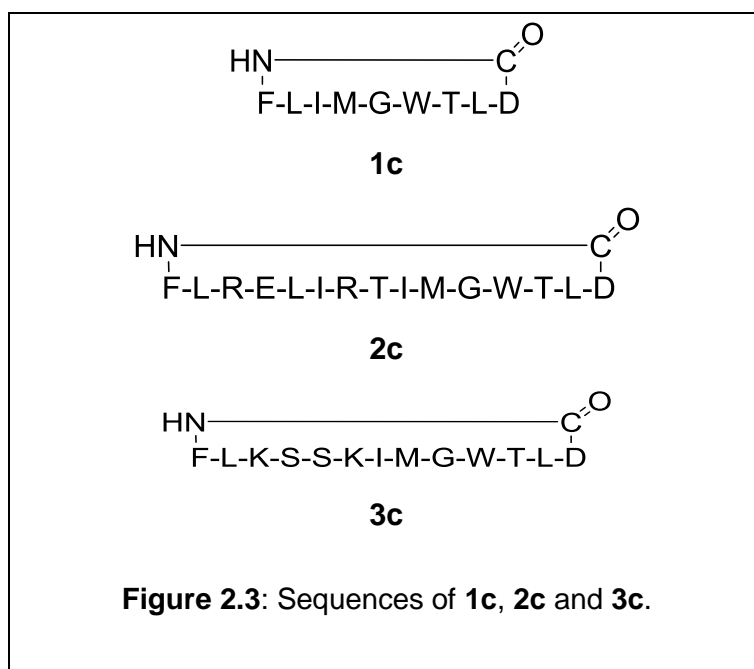
The 9-mer linear peptide allyl ester **1a** with sequence FLIMGWTLTD was prepared along with its derivatives, the 15-mer linear peptide allyl ester **2a** and 13-mer linear peptide allyl ester **3a** (Figure 2.2). The linear peptide allyl ester compounds (**1a**, **2a**, **3a**) were used as precursors for the synthesis of cyclic compounds **1c**, **2c**, and **3c** respectively, starting with aspartic acid (D) and ending with phenylalanine (F). Therefore, the epitope sequence after cyclisation is still the same as the original. The purpose of this permutation is to shift the aspartic acid residue to the C-terminus so that it can be anchored to the resin through its side chain. Wang resin pre-loaded through the side chain of the allyl ester protected derivative of aspartate (Section 1.6.1.2) is commercially available for this purpose. Once deprotected with the aid of a Pd(PPh<sub>3</sub>)<sub>4</sub> catalyst, the alpha carboxyl group of the aspartic acid residue at the C-terminus can be cyclised onto the amino group of the N-terminus to afford a cyclic peptide by a head-to-tail strategy (See Scheme 2.1).

In addition, this permutation shifted the glycine residue into the middle of the peptide sequence, increasing the flexibility of the peptide and providing a greater chance for the termini of the peptide to be close together during the cyclisation reaction.<sup>136</sup>





The importance of the epitope sequence for various aspects of immunotherapy<sup>174, 175</sup> and the poor physical properties of the 9-mer cyclic Bax peptide (very poor solubility in the HPLC and LCMS solvents) were the reasons to design and synthesise the two derivatives **2c** and **3c** (Figure 2.3) using the SPPS method.



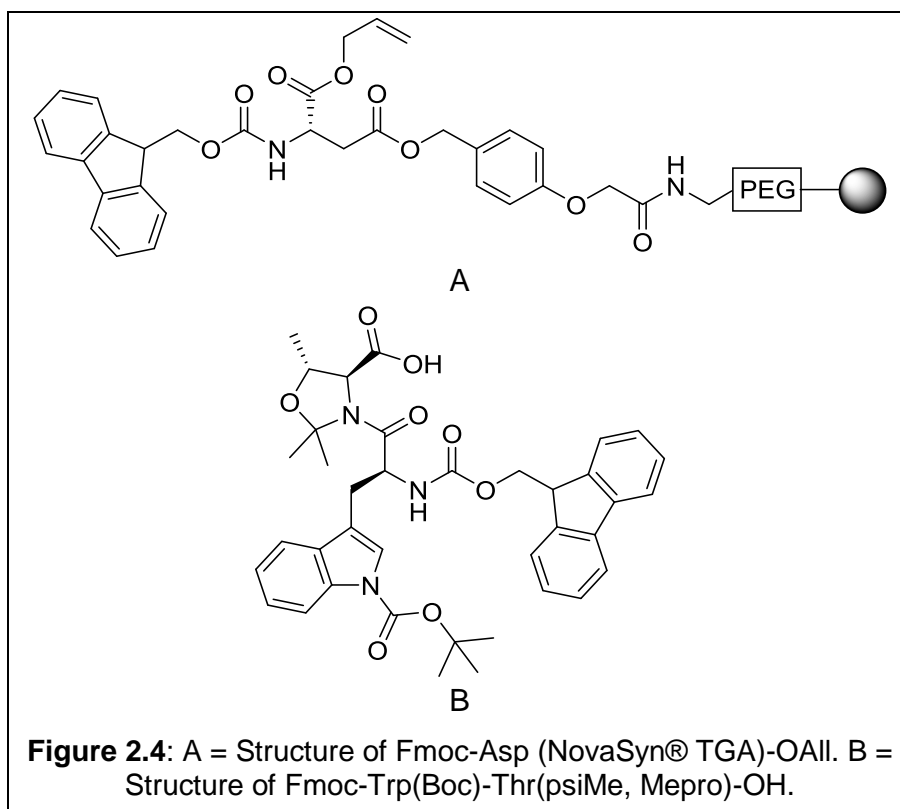
The cyclic peptide derivative **2c** included insertion of a fragment consisting of six amino acids, RELIRT, that flank the 9-mer epitope in the sequence of Bax (ELIRTIMGWTLDFLR). The flexibility arising from the greater length of the cyclic peptide (15-mer) enhances the chances of cyclic peptide formation.<sup>130, 131</sup> This fragment has three polar amino acids, one glutamic acid and two arginine residues. Thus, this peptide has two positive charges from the side chains of arginine, and two negative charges from the side chains of glutamate and aspartate. The polarity is greater than that of cyclic Bax peptide (**1c**) which has a single negative charge and, consequently, water solubility was expected to be enhanced. The presence of this fragment gives an amphipathic property to the cyclic peptide, supporting the ability of the compound to cross a biological membrane to enter the target cell.<sup>176</sup> In addition to that, this new fragment gives further synthetic options for forming a cyclic structure by linking the side chain of an Arg residue with the carboxyl group of the C-terminus (tail to side chain reaction) or linking the side chain of the Arg residue to the side chain of the Glu residue (side chain to side chain).<sup>38</sup> Moreover, this fragment

introduced the option to bind the peptide with the resin by the Glu residue instead of the Asp residue which may influence the yield of the cyclisation reaction.

The cyclic peptide **3c** included insertion of a fragment consisting of the four amino acids KSSK. This polar fragment introduces two additional positive charges. Consequently, compound **3c** is more hydrophilic than **1c** and thus more soluble in water. In addition to that, the presence of the positively charged sequence KSSK will create an overall cationic charge state at physiological pH, thus increasing the chance of crossing the membrane of the target cell.<sup>177</sup> Moreover, this new fragment leads to further options for cyclisation by binding of a Lys side chain with the C-terminus of the peptide (side chain to tail).<sup>126</sup> Furthermore, lysine can provide other synthetic routes, thus, 13-mer linear peptide (**3b**) can be anchored to the resin through the side chain of Lys. The Ser residue was chosen as this has been applied in flexible hydrophilic linkers for fusion of protein domains such as multivalent antibodies.<sup>178</sup>

Fmoc-Asp(NovaSyn® TGA)-OAll resin (Figure 2.4, A) with a low loading of 0.2 mmol/g, was used to synthesise the cyclic peptides (**1c**, **2c**, **3c**) and their linear counterparts (**1b**, **2b**, **3b**) by Fmoc methodology. The main reasons for using low loading resin is to increase the probability of intramolecular cyclisation and to reduce interactions between the individual growing sequences preventing interchain aggregation (intermolecular dimer formation).<sup>144</sup>

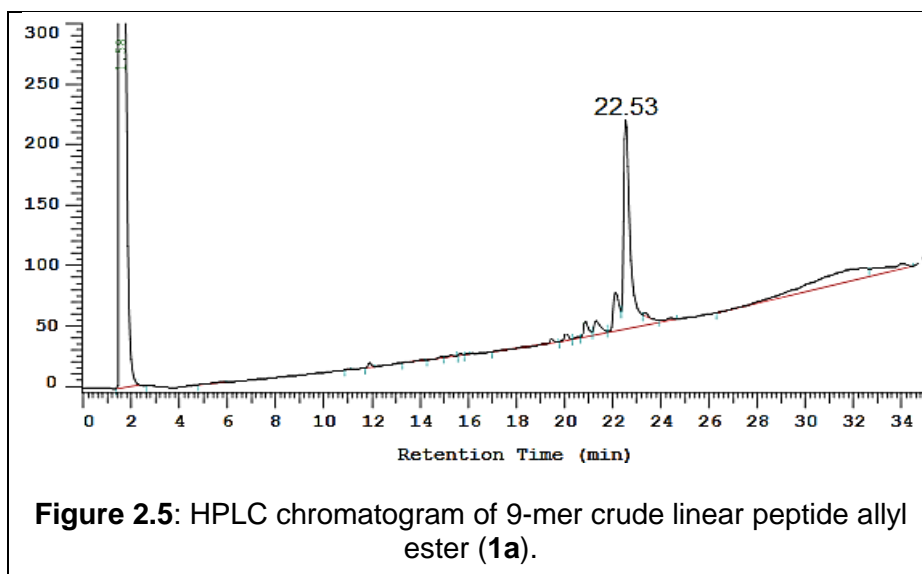
In the synthesis of the linear peptide allyl ester (**1a**, **2a**, **3a**), Fmoc-Trp(Boc)-Thr(ψMe, Mepro)-OH (Figure 2.4, B) was used instead of Fmoc-Trp(Boc)-OH and Fmoc-Thr(*t*-Bu)-OH residues. This secondary amino acid surrogate can positively support the synthesis of the cyclic peptide as it induces a turn in the peptide chain which was intended to assist with the cyclisation reaction by bringing the termini of the peptide closer together. The secondary amino acid surrogates are like proline or *N*-alkylamino acids; they work to disrupt the formation of the secondary structures during synthesis of peptides.<sup>179</sup>



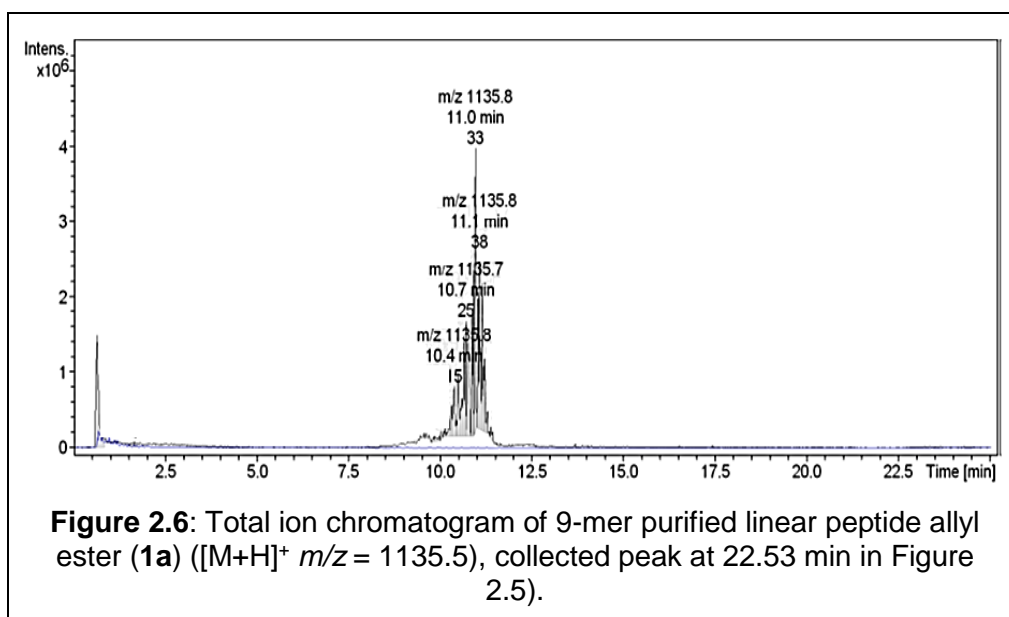
## 2.2 Result and discussion of peptide synthesis

### 2.2.1 Synthesis of the 9-mer linear peptide allyl ester (**1a**)

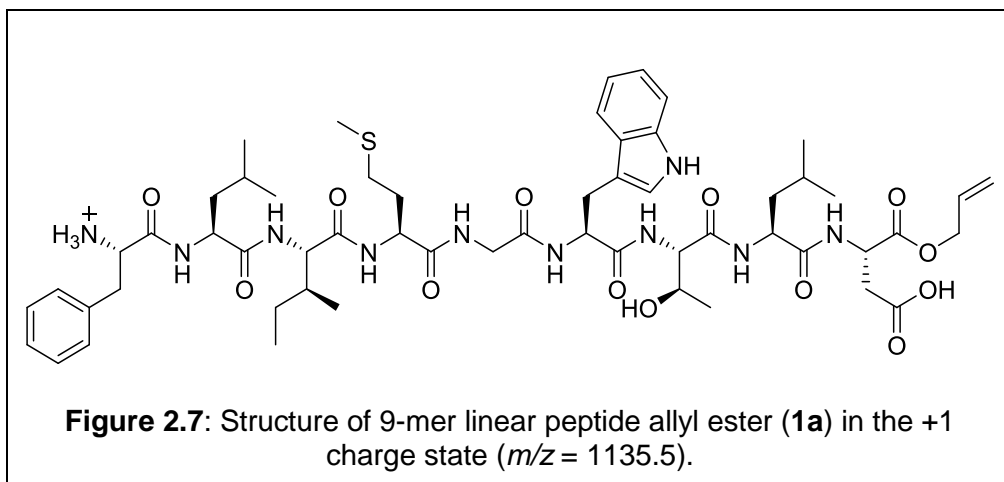
Subsequent to an investigation of the linear peptide allyl ester (**1a**) by HPLC, as in Figure 2.5, the crude sample gave a strong peak at retention time of 22.53 min; the peak width was less than one minute. It was eluted at a solvent composition containing more acetonitrile than water (41%:49% water to acetonitrile); this retention time is evidence that the peptide is a hydrophobic compound due to the presence in the sequence of more hydrophobic amino acids than hydrophilic. This peak was the target compound (**1a**).



The LC–MS analysis for the collected peak at the retention time 22.53 min in Figure 2.5 supported the HPLC result; the total ion chromatogram clearly showed a peak of 1135.8  $m/z$  with the retention time of 11.0 min (Figure 2.6). This peak was consistent with the theoretically calculated value of 1135.5  $m/z$  for the compound in the +1 charge state.

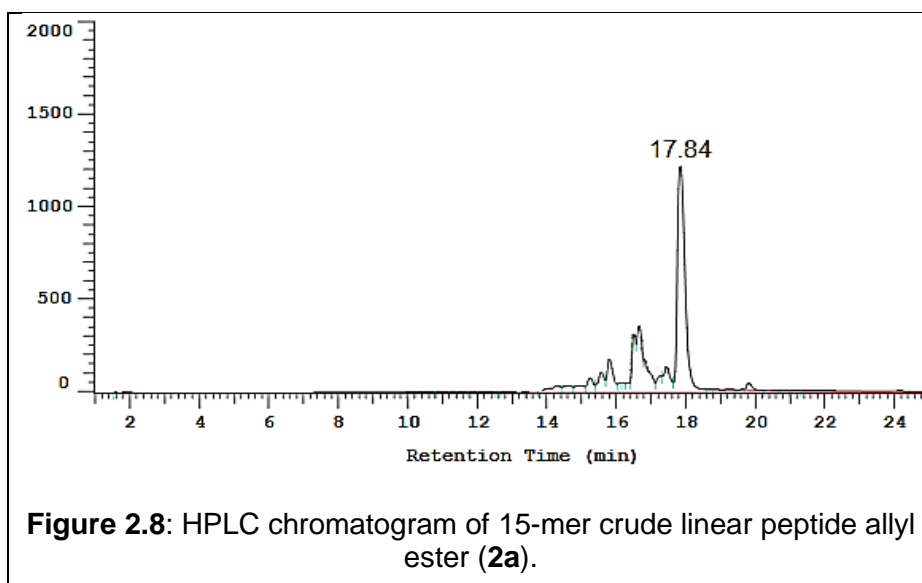


The structure of this compound (**1a**) is presented in Figure 2.7. This result provided evidence that the coupling reactions were successful and that the linear peptide allyl ester compound (**1a**) was formed in its entirety.

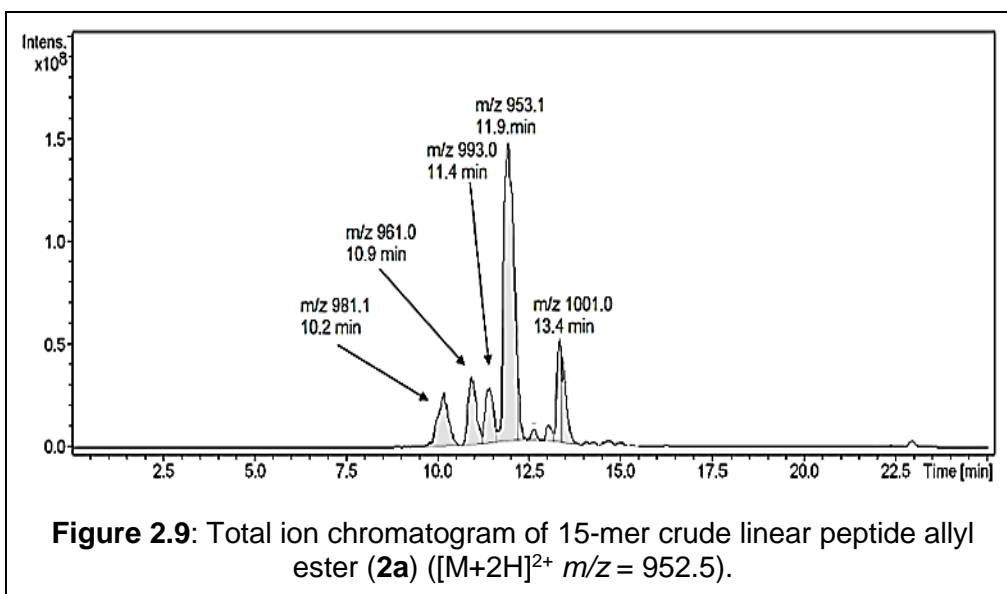


### 2.2.2 Synthesis of the 15-mer linear peptide allyl ester (**2a**)

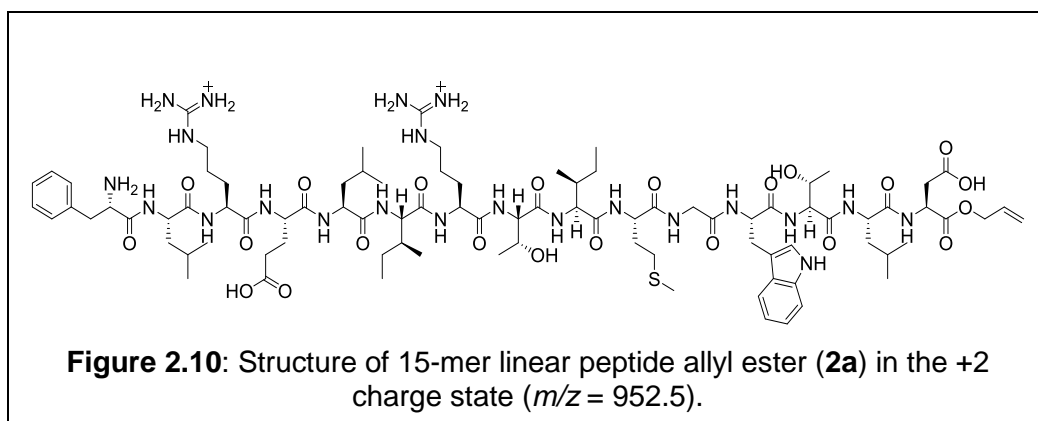
The investigation of the 15-mer linear peptide allyl ester (**2a**) by HPLC, as in Figure 2.8, showed that the crude sample gave a high-intensity sharp peak without any overlap and less than 1 min width at the retention time of 17.84 min. This peak was potentially compound **2a**.



The mass spectrum of the same sample supported the HPLC result. The total ion chromatogram (Figure 2.9) distinctly showed a peak of 953.1  $m/z$  at the retention time 11.9 min. This peak matches the theoretically calculated value of the target compound **2a** (952.6  $m/z$ ) in the +2 charge state.



The structure of compound **2a** is shown in Figure 2.10. This result is significant evidence of successful coupling reactions and that all the 15 residues were bonded together to form the linear peptide allyl ester (**2a**).

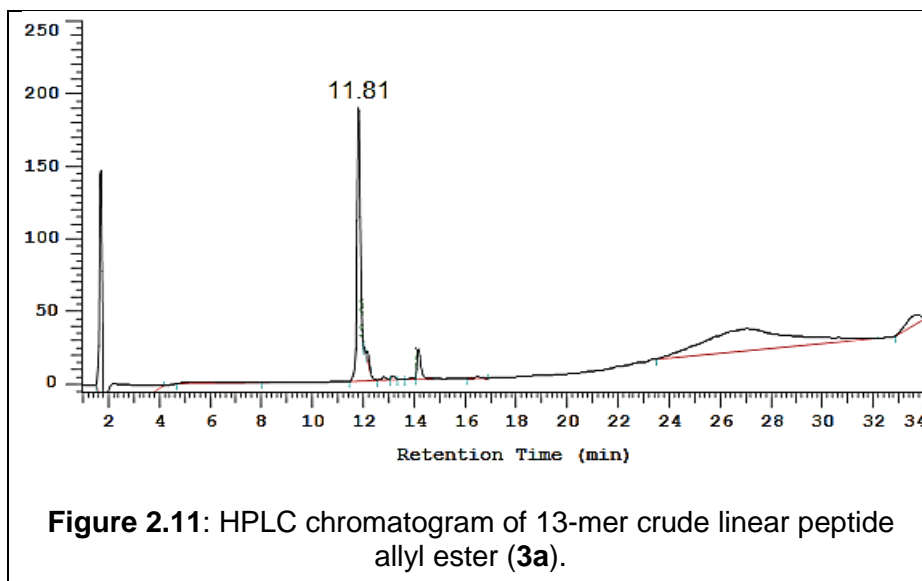


The other four peaks 981.1, 961.0, 993.0, 1001.0  $m/z$  at 10.2, 10.9, 11.4, 13.4 min respectively potentially represented: compound **2a** still bonded with one or two side chain protecting groups on a threonine residue (*t*-Bu) and tryptophan residue (Boc); oxidation of the sulfur (S) to a sulfoxide (S=O) at the side chain of the methionine residue; or linear peptide allyl ester with one or more amino acid deletions.

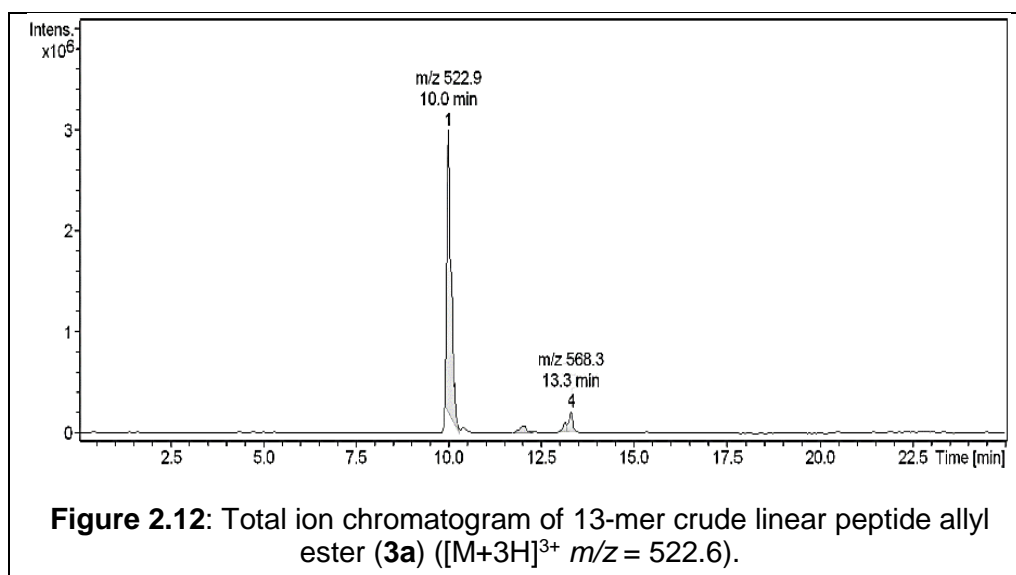
### 2.2.3 Synthesis of the 13-mer linear peptide allyl ester (**3a**)

Figure 2.11 shows the HPLC chromatogram of the crude sample of 13-mer linear peptide allyl ester (**3a**); the main result is a strong, sharp peak without

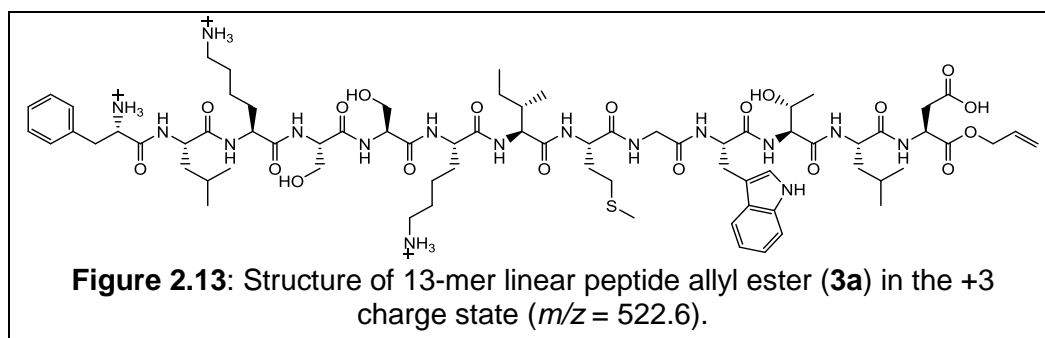
any overlap and less than 1 min width at the retention time 11.81 min. This peak was considered to be the target compound (**3a**).



The HPLC result was supported by the LC-MS analysis for the same sample; Figure 2.12 indicates the total ion chromatogram of the crude sample of compound **3a**. The peak of 522.9  $m/z$  at the retention time 10.0 min is consistent with the theoretically calculated value of 522.6  $m/z$  for the target compound in the +3 charge state.



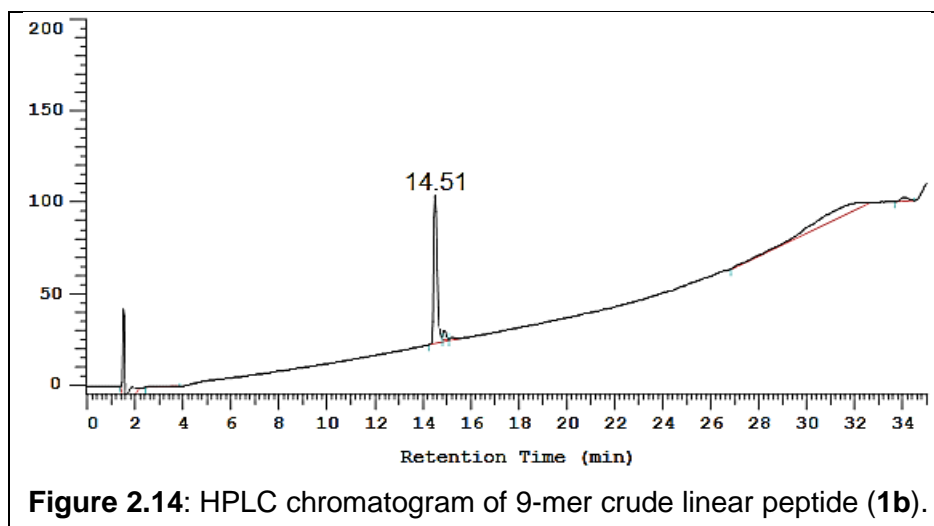
The structure of 13-mer linear peptide allyl ester (**3a**), is illustrated in Figure 2.13. The mass spectrometry result is clear evidence of the success of all the coupling reactions.



The peak of 568.3  $m/z$  at 13.3 min was possibly due to a side product in which compound **3a** was still bonded to hydrophobic protecting groups. It potentially represented the same species that appeared at retention time 14.17 min in the HPLC chromatogram (Figure 2.11)

## 2.2.4 Synthesis of the 9-mer linear peptide (**1b**) as a precursor for the cyclic peptide (**1c**)

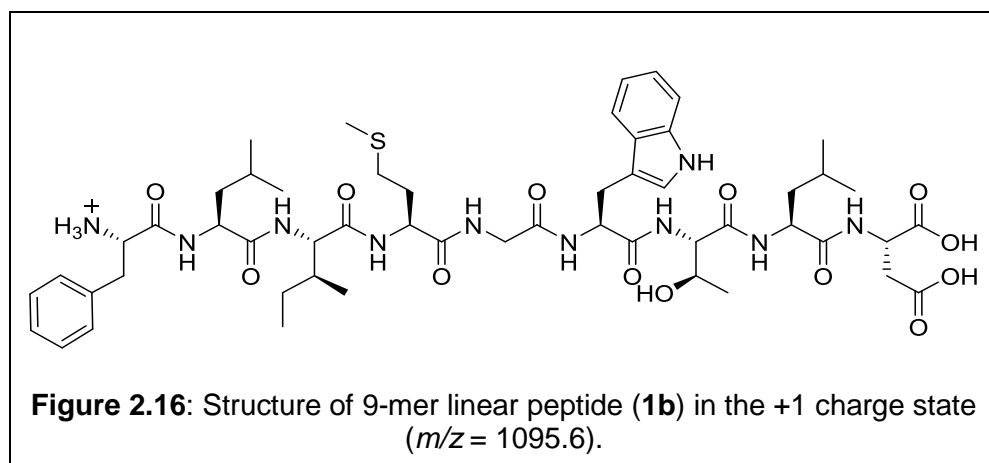
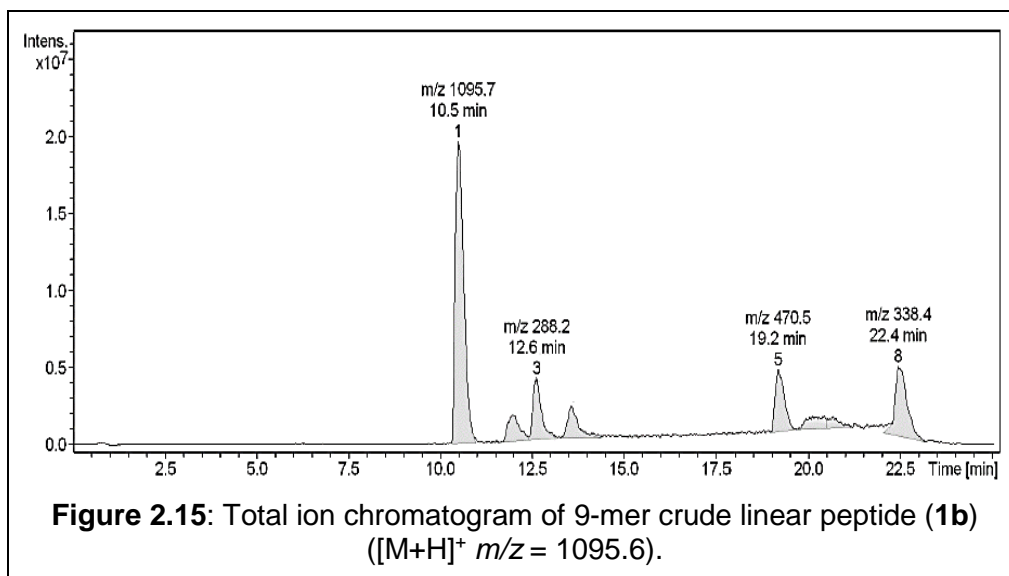
The data in Figure 2.14 show the HPLC chromatogram of a crude sample of 9-mer linear peptide (**1b**). The main result is the intense peak at the retention time of 14.51 min. This peak was considered to be the target compound (**1b**).



The result of the HPLC analysis was supported by LC-MS analysis of the same sample. As revealed in the total ion chromatogram of crude **1b** (Figure 2.15), the clear peak corresponding to 1095.7  $m/z$  at retention time 10.5 min was evidence that the deprotection reaction of the allyl group using  $\text{Pd}(\text{PPh}_3)_4$  as a catalyst was successful. The observed peak (1095.7  $m/z$ ) was consistent



with the theoretically calculated value of 1095.6  $m/z$  for the compound in the +1 charge state as in Figure 2.16.

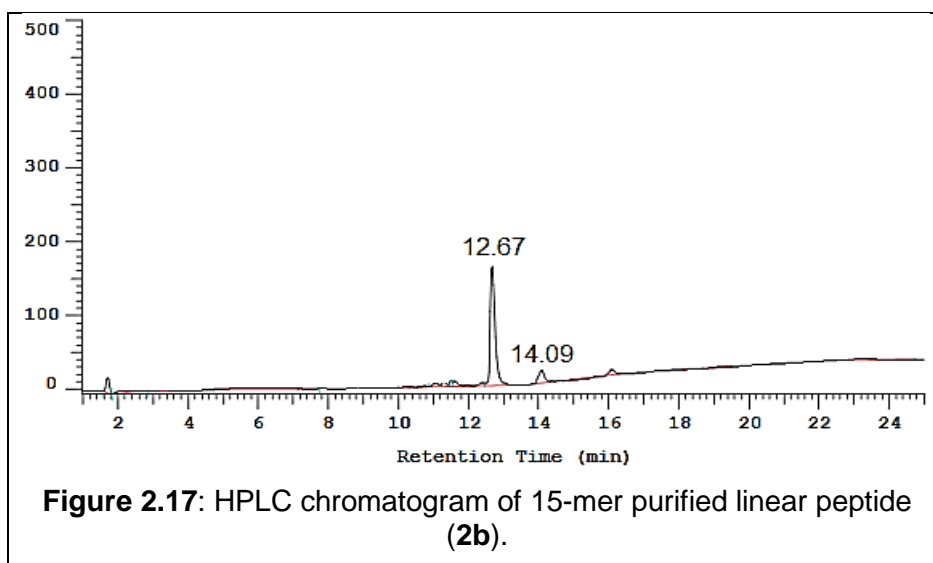


It should be noted that the retention time of this peak (14.51 min) was indicative of the successful conversion of compound **1a** to **1b** because the retention time of the first compound (**1a**) was 22.53 min (Figure 2.5), which was expected due to the lower polarity because of the allyl group compared to the carboxylic acid of **1b**.

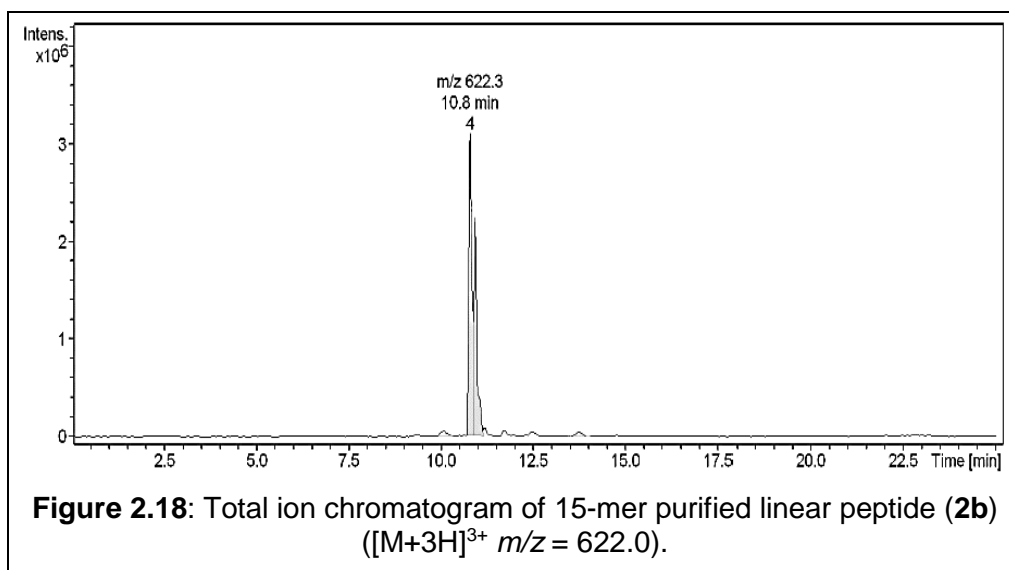
The low  $m/z$  peaks (288.2, 470.5, 338.4  $m/z$ ) at the retention times 12.6, 19.2 and 22.4 min respectively are probably contamination originating from the column.

## 2.2.5 Synthesis of the 15-mer linear peptide (2b) as a precursor for the cyclic peptide (2c)

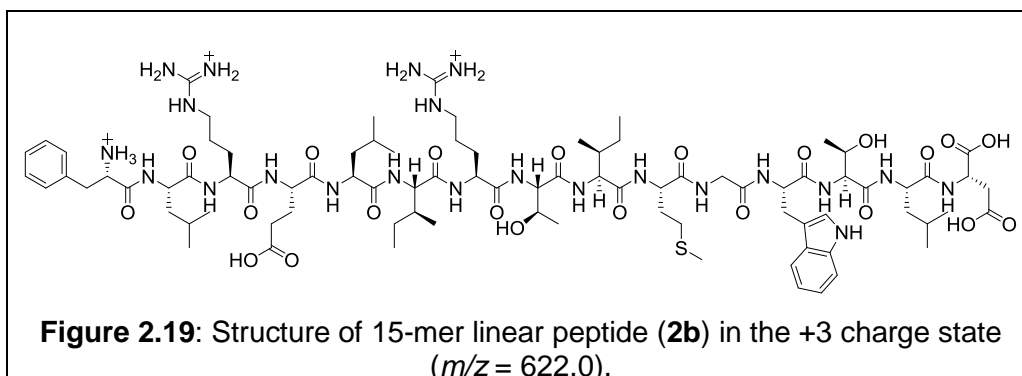
Figure 2.17 shows the HPLC chromatogram of the purified sample of 15-mer linear peptide (**2b**); the main apparent result is the strong sharp peak at the retention time 12.67 min. This peak was considered to be the target compound (**2b**)



Mass spectral analysis for the same sample (Figure 2.18) supported the HPLC result. The single peak of 622.3  $m/z$  at the retention time 10.8 min is consistent with the theoretically calculated value of 622.0  $m/z$  for **2b** in the +3 charge state.



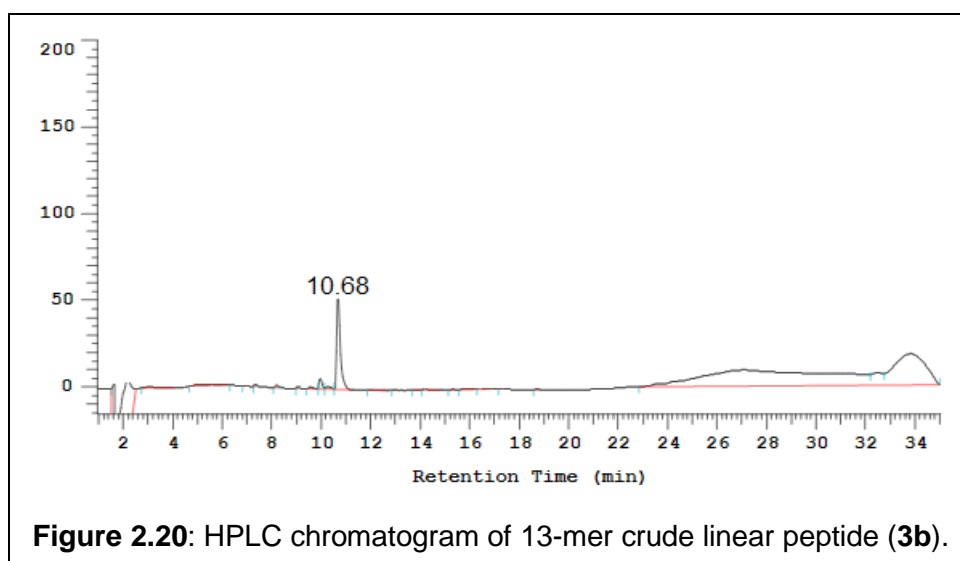
The structure of this peptide (**2b**) is in Figure 2.19. This result is evidence of the successful deprotection reaction of the allyl group by using  $\text{Pd(PPh}_3)_4$  as a catalyst to form the linear peptide (**2b**).



It is significant that the retention time of this peak (12.67 min) is less than the peak of **2a** (17.84 min) as in Figure 2.8. This result was expected because the polarity of the compound **2a** is less than compound **2b**. The small peak at the retention time 14.09 min was potentially a contaminant from the column.

## 2.2.6 Synthesis of the 13-mer linear peptide (**3b**) as a precursor for the cyclic peptide (**3c**)

As shown in Figure 2.20, the HPLC chromatogram of the crude sample for 13-mer linear peptide (**3b**) displays a strong, sharp peak at the retention time 10.68 min that was considered to be the linear peptide (**3b**).



The total ion chromatogram in Figure 2.21 for the same sample supports the HPLC result. The peak of 509.6  $m/z$  at the retention time 8.9 min is consistent with the theoretically calculated value of 509.3  $m/z$  for the linear peptide (**3b**) in the triply charged state. The structure of this compound (**3b**) is shown in Figure 2.22.

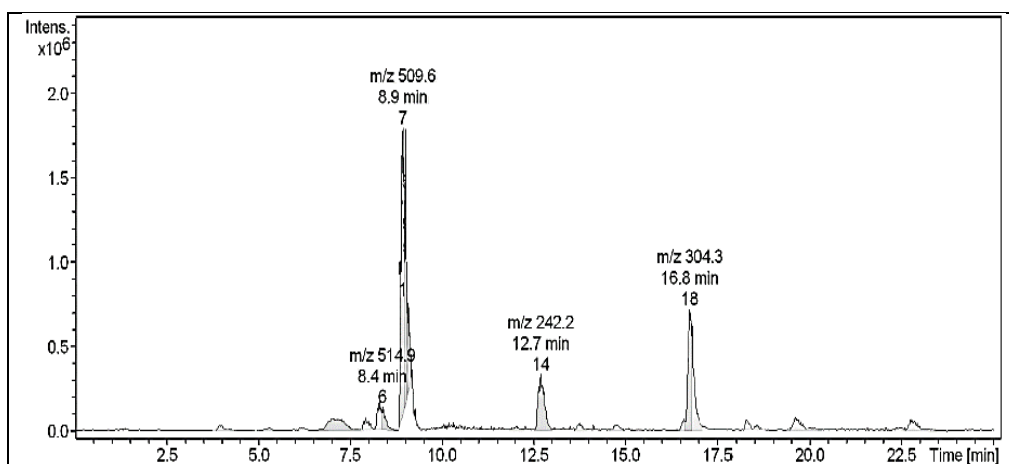


**Figure 2.21:** Total ion chromatogram of 13-mer crude linear peptide (**3b**) ( $[M+3H]^{3+}$   $m/z$  = 509.3).

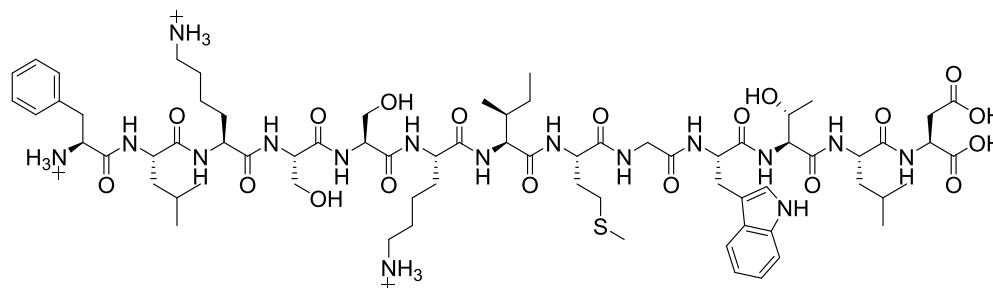


**Figure 2.22:** Structure of 13-mer linear peptide (**3b**) in the +3 charge state ( $m/z$  = 509.3).

This result is evidence of successful formation of the target compound (**3b**) by using  $\text{Pd}(\text{PPh}_3)_4$  as a catalyst. The HPLC result reveals an important point that must be taken into account; the retention time of this compound (**3b**) is less than the retention time of **3a** (11.81 min) as in Figure 2.11. This result is evidence that compound **3a** was converted to **3b**. The decrease in the retention time of **3b** in comparison with compound **3a** was expected, as the polarity of an allyl ester is less than a carboxylic acid.

The peak of 514.9  $m/z$  at the retention time 8.4 min is potentially compound **3b** that has undergone oxidation, by atmospheric oxygen, of the sulfur in the side group of methionine to form a sulfoxide (S=O). The other two peaks 242.2, 304.3  $m/z$  at 12.7, 16.8 min respectively are potentially due to contamination from the column.

## 2.3 Results and discussion of cyclisation reaction

In the following three experiments, the resin-bound side chain protected linear peptides (**1b**, **2b**, **3b**) were used as precursors for the synthesis of the cyclic peptides (**1c**, **2c**, **3c**).

### 2.3.1 Synthesis of the 9-mer cyclic peptide (**1c**)

Six attempts were conducted to convert the side chain protected 9-mer linear peptide (**1b**) to compound **1c** as in Table 2.1. Three different reagents (PyBOP, HBTU, HATU) were used in the first four of these six attempts. At each one a different number of repeats (2, 3), reaction time (1, 2, 24, 48 h), temperature (20, 25 °C), speed of the shaker (100, 150 RPM) were tried. In addition, lithium ions were used as a coordinator to fold the peptide, but the reactions failed. The reason for this failure possibly resulted from the length of the 9-mer cyclic peptide (**1c**), for which the flexibility might have been insufficient to bring the termini close enough together to support the coupling reaction successfully. These three reagents with the different conditions were not adequate in overcoming this problem. The final two attempts (fifth and sixth) were successful, a different reagent (DEPBT) was used for the coupling reaction. It appears that the use of the DEPBT reagent with an initial reaction time of 2 h, followed by an overnight reaction with fresh reagent, at 20 °C, 100 RPM shaker, with or without lithium ions, resulted in a successful cyclisation reaction (Table 2.1).

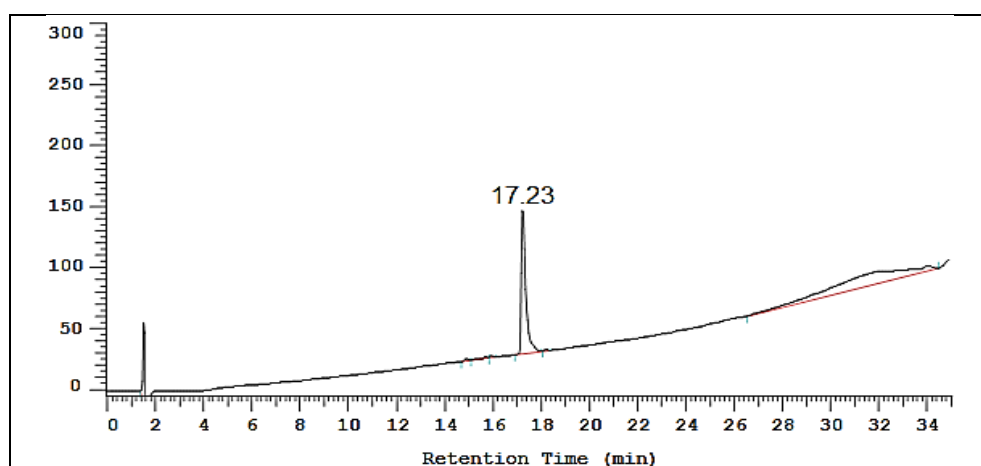
**Table 2.1:** Attempts at cyclising **1b** under different conditions.

No	Reagent	No of repeats	Time (h)	Temp (°C)	RPM*	MI <sup>‡</sup>	Result (LCMS)
1	PyBOP	2	1 <sup>st</sup> (2), 2 <sup>nd</sup> (overnight)	25	100	Li <sup>+</sup>	Failed
2	PyBOP	3	1 <sup>st</sup> (1), 2 <sup>nd</sup> (2), 3 <sup>rd</sup> (48)	20	150	Li <sup>+</sup>	Failed
3	HBTU	2	1 <sup>st</sup> (1), 2 <sup>nd</sup> (overnight)	25	100	Li <sup>+</sup>	Failed
4	HATU	2	1 <sup>st</sup> (1), 2 <sup>nd</sup> (overnight)	25	100	Li <sup>+</sup>	Failed
5	DEPBT	2	1 <sup>st</sup> (1), 2 <sup>nd</sup> (overnight)	20	100	Li <sup>+</sup>	Successful
6	DEPBT	2	1 <sup>st</sup> (2), 2 <sup>nd</sup> (overnight)	20	100	No	Successful

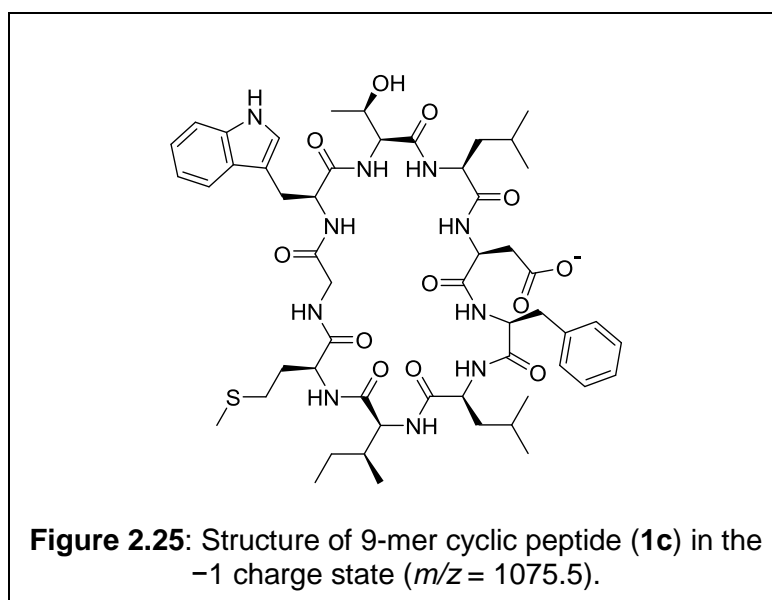
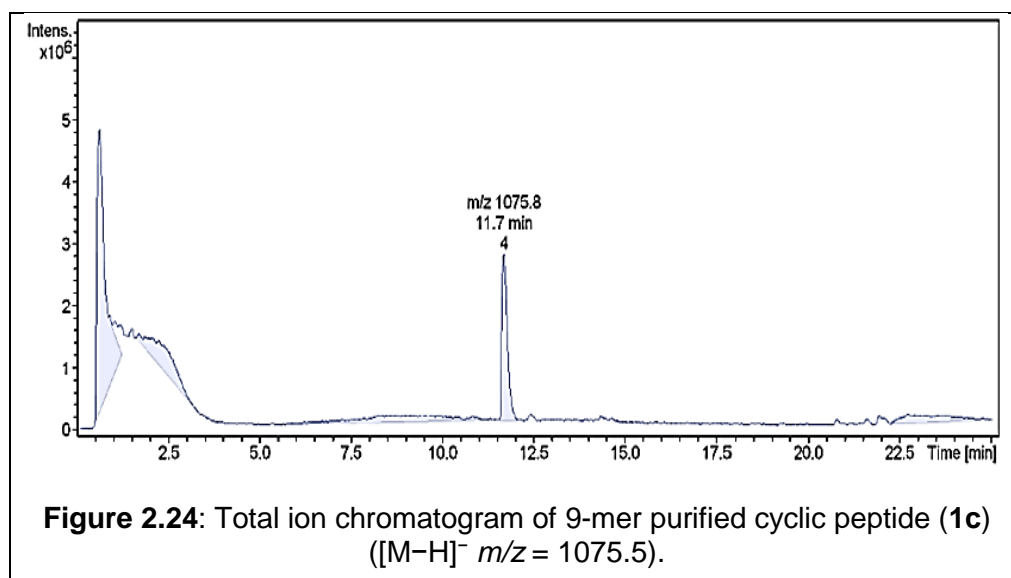
\* MI = Metal ion, \* RPM = shaker revolutions per min

Although the cyclisation reaction of the Bax peptide (**1b**) succeeded twice by using the DEPBT reagent, the yield was very low (less than 0.5 mg, for both reactions combined). The solubility of the compound (**1c**) was very poor in HPLC solvents; therefore, a small amount (1–5  $\mu$ L) of DMSO was always added for each sample that was analysed by HPLC or LCMS.

The investigation of the sample of the purified cyclic peptide (**1c**), by HPLC, is given in Figure 2.23. The single strong, sharp peak without any overlap at the retention time 17.23 min was considered to be the 9-mer purified cyclic peptide (**1c**).

**Figure 2.23:** HPLC chromatogram of 9-mer purified cyclic peptide (**1c**).

LCMS analysis of the same sample supported the HPLC result; as shown in Figure 2.24, the total ion chromatogram of compound **1c** has a clear peak corresponding to 1075.8  $m/z$  at the retention time 11.7 min that is consistent with the theoretically calculated value of 1075.5  $m/z$  for **1c** in the  $-1$  charge state. The structure of this compound (**1c**) is in Figure 2.25. It was evident that the cyclisation reaction between the two termini of the linear peptide (**1b**) using DEPBT coupling reagent was successful.



It should be noted that the width of the cyclic peptide peak in HPLC chromatogram is less than 1 min, with no overlap with other peaks, and no shoulders; thus, the purity of this cyclic peptide (**1c**) was deemed to be

acceptable. The retention time of this peak is significant as an item of evidence for conversion of the linear compound (**1b**) to the cyclic compound (**1c**). The retention time of this peak (17.23 min) was higher than the peak of **1b** (14.51 min) as in Figure 2.14. This result was expected because the polarity of the cyclic compound (**1c**) is less than the linear compound (**1b**). The reason for the decrease of the polarity in the cyclic compound is bonding of the free polar termini of the peptide together.

### 2.3.2 Synthesis of the 15-mer cyclic peptide (**2c**)

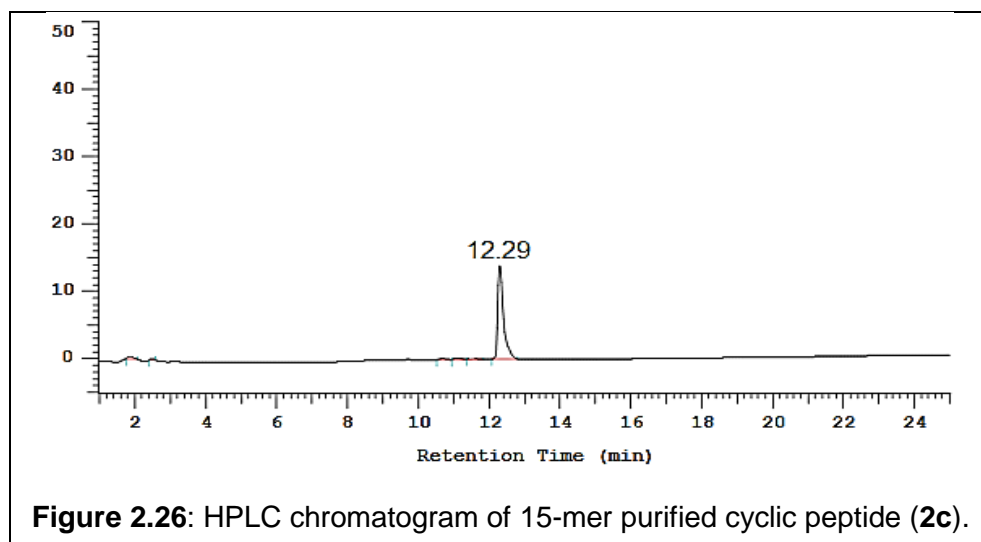
The 15-mer cyclic peptide synthesis was undertaken using the same method and conditions for the synthesis of the 9-mer cyclic peptide (**1c**) in entry five of Table 2.1. Two attempts were conducted to synthesise this cyclic compound; the first one failed during synthesis of the precursor (**2a**). In the second attempt, the on-resin cyclisation of protected **2b** was successful. Therefore, it provided clear evidence that insertion of the RELIRT fragment in the Bax peptide sequence between isoleucine and leucine residues was a successful proposal to enhance the cyclisation reaction.

The length and flexibility of the compound (15-mer) was potentially the reason for the precursor **2b** adopting new conformations having the termini closer together than in compound **1b**. Another possibility was hydrogen bonds between the side chains of the linker sequence pulling the termini of the peptide close together to enhance the coupling reaction.

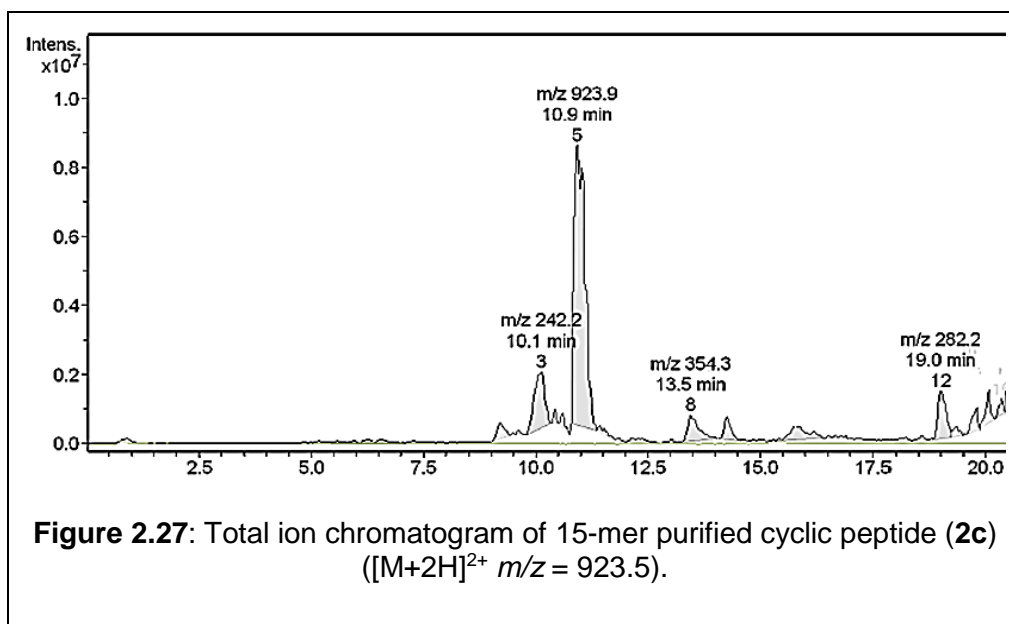
Collection and purification of **2c** by the HPLC was straightforward because the solubility of the compound in the HPLC solvent (a mixture of water and acetonitrile) was acceptable. Centrifuging of the sample dissolved in the HPLC solvent at 19450 RCF for 5 minutes led to a very small amount of precipitate being visible in the bottom of the Eppendorf tube, in comparison to **1c** which resulted in extensive precipitate being visible.

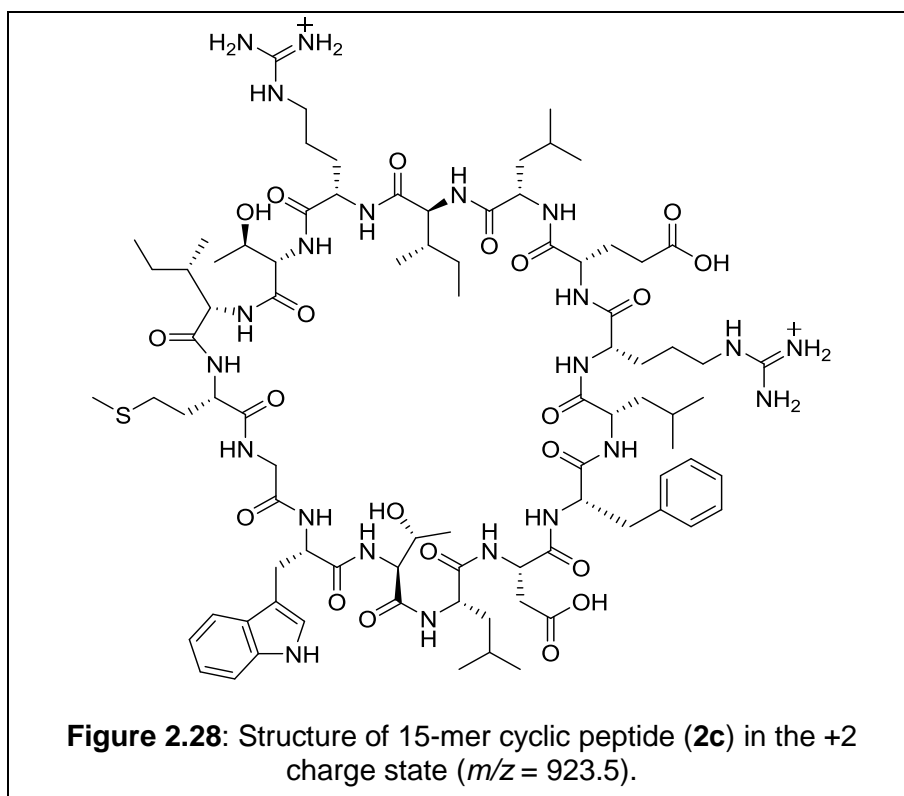
As can be seen from Figure 2.26, the HPLC chromatogram of the sample of the purified 15-mer cyclic peptide (**2c**), shows a single sharp peak without any overlap and less than 1 min width at the retention time 12.29 min that is considered to be the purified cyclic compound (**2c**).





LCMS analysis for the same sample of purified 15-mer cyclic peptide (**2c**) reinforced the HPLC results. As is demonstrated in Figure 2.27, showing the total ion chromatogram of a cyclic peptide (**2c**), here the peak of 923.9  $m/z$  at the retention time 10.9 min was a significant result because it matched the theoretically calculated value of 923.5  $m/z$  for **2c** in the +2 charge state, as in Figure 2.28.





This result provides evidence of the success of the cyclisation reaction converting the protected linear compound (**2b**) to **2c** (cyclic form) using the DEPBT reagent.

It is important to note that the retention time of **2c** (12.29 min) is less than that of **2b** (12.67 min), as in Figure 2.17. This result was not expected because the polarity of the linear peptide (**2b**) was predicted to be higher than the cyclic compound (**2c**); the reason could be that the restricted conformation of the cyclic peptide (**2c**) results in a more polar shape than the linear peptide (**2b**). The other peaks 242.2, 354.3, 282.3  $m/z$  at the retention times 10.1, 13.5, 19.0 min respectively could be attributed to impurities from the column.

### 2.3.3 Synthesis of the 13-mer cyclic peptide (**3c**)

Synthesis of compound **3c** was conducted using the same reagent, method, and conditions as entry five in Table 2.1. One attempt was needed to convert resin-bound protected **3b** to **3c** successfully. This result is evidence that the insertion of the fragment KSSK in the Bax peptide sequence was also successful in rearranging the linear peptide (**3b**) to permit adoption of

conformations that bring the two termini close to each other, supporting the coupling reaction.

As shown in Figure 2.29, the HPLC chromatogram of the sample of 13-mer purified cyclic peptide (**3c**) has a single strong peak at the retention time 14.69 min that represented the target compound (**3c**).

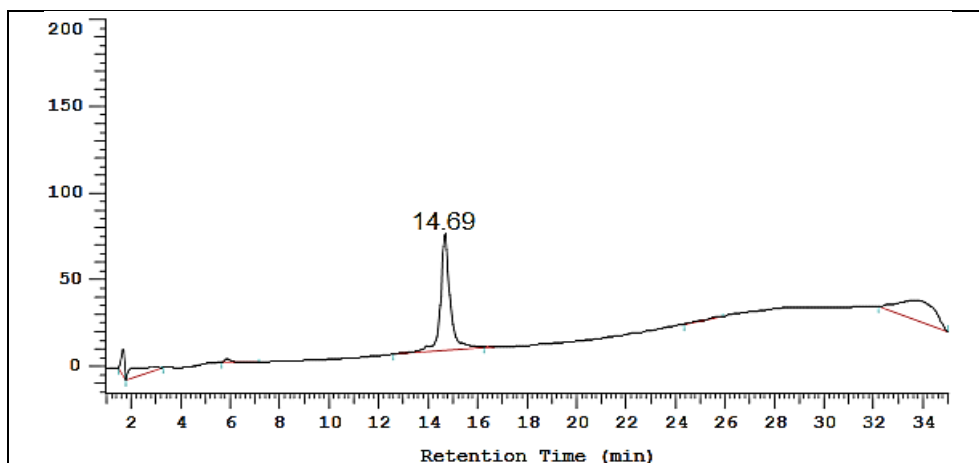
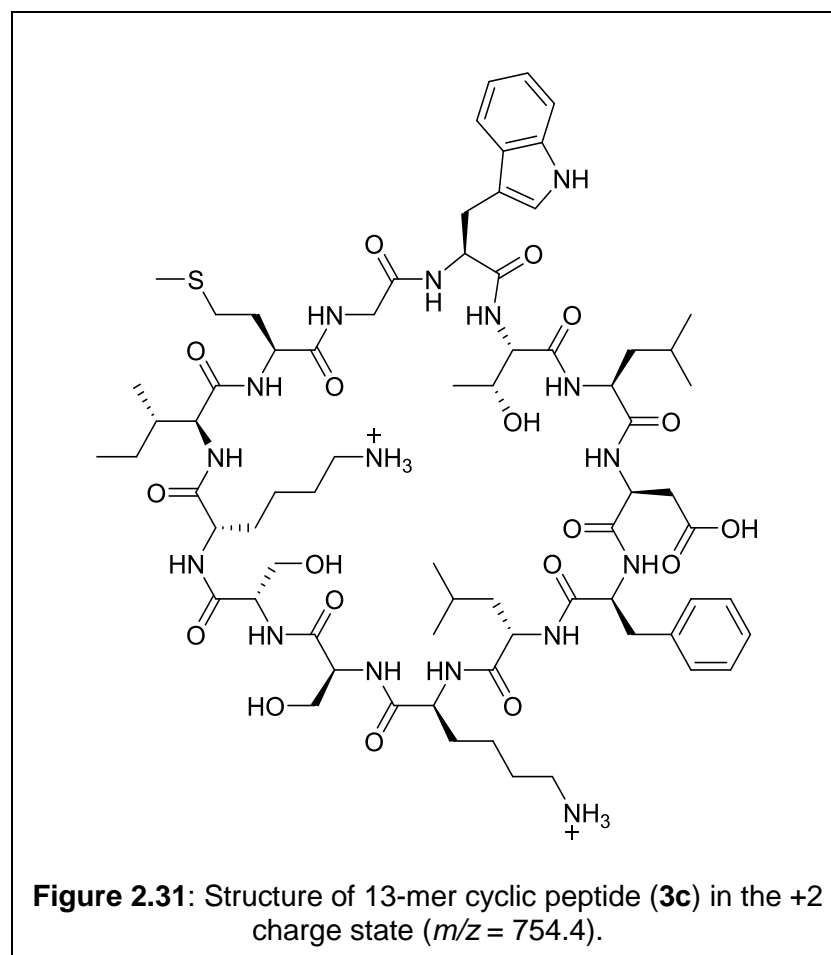
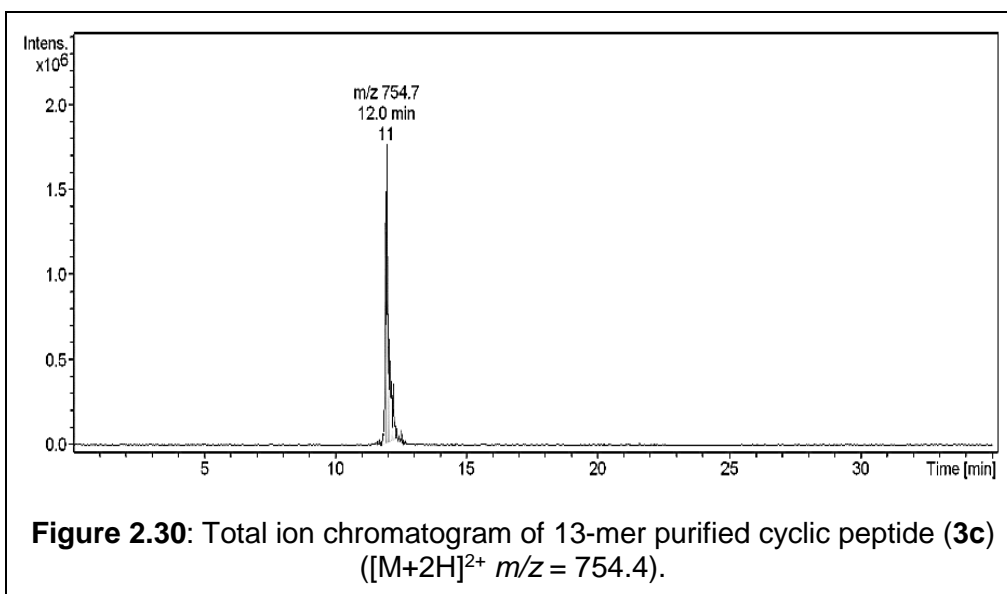


**Figure 2.29:** HPLC chromatogram of 13-mer purified cyclic peptide (**3c**).

The total ion chromatogram for the same sample shown in Figure 2.30 reinforced the HPLC result. In the total ion chromatogram of the purified sample for compound **3c**, here the peak of 754.7  $m/z$  at the retention time 12.0 min matches the theoretically calculated value of 754.4  $m/z$  for the cyclic peptide (**3c**) in the +2 charge state. The structure of this cyclic peptide (**3c**) is shown in Figure 2.31. This result provides further evidence for the success of DEPBT as a cyclisation reagent.



There is a possibility that the length of the peptide (13-mer) may assist in allowing the termini of the peptide to approach close together. In addition, the presence of two Lys residues in the backbone of the peptide may have

contributed to drawing the termini of the peptide close together, forming more intramolecular hydrogen bonding with carbonyl groups of the peptide bonds.

It should be noted that purification of compound **3c** by HPLC was more straightforward than compound **2c** because the solubility of **3c** in the HPLC solvent (a mixture of water and acetonitrile) was greater than **2c**. It appears that the insertion of the KSSK fragment in the sequence of the Bax peptide was a more decisive factor than the RELIRT fragment in increasing the yield (the yield of **2c** was  $0.4 \times 10^{-3}$  mmole, 2%, while the yield of **3c** was  $1.8 \times 10^{-3}$  mmole, 9%) and the solubility of the cyclic peptide in the HPLC solvents (See Table 2.2). The retention time of **3c** is an indicator that the cyclic compound (**3c**) has formed from its linear counterpart (**3b**) because the retention time of **3c** (14.69 min) is higher than compound **3b** (10.68 min), as in Figure 2.20. This result was expected as the polarity of the linear compound (**3b**) which has five free charged groups is greater than the cyclic compound (three ionisable groups).

**Table 2.2:** Comparison between the three cyclic peptides (**1c**, **2c**, **3c**).

Peptide	1c	2c	3c
Inserted fragment	-	RELIRT	KSSK
Yield (mg)	Crude* = 19.2 Purified† = <0.5	Crude = 31.5 Purified = 0.76	Crude = 43.6 Purified = 2.7
Yield mmole (purified)	-	$0.4 \times 10^{-3}$	$1.8 \times 10^{-3}$
Yield%	-	2	9
Coupling reagent	DEPBT	DEPBT	DEPBT
Solubility in H <sub>2</sub> O	Insoluble	Trace precipitate	No precipitate
Solubility in MeCN	Clearly visible precipitate	Trace precipitate	No precipitate
Solubility in (H <sub>2</sub> O+MeCN)	Insoluble	Trace precipitate	No precipitate
Solubility in methanol	Insoluble	Trace precipitate	Trace precipitate
Solubility in isopropanol	Insoluble	Clearly visible precipitate	Trace precipitate

\* Mass of crude sample measured by analytical balance.

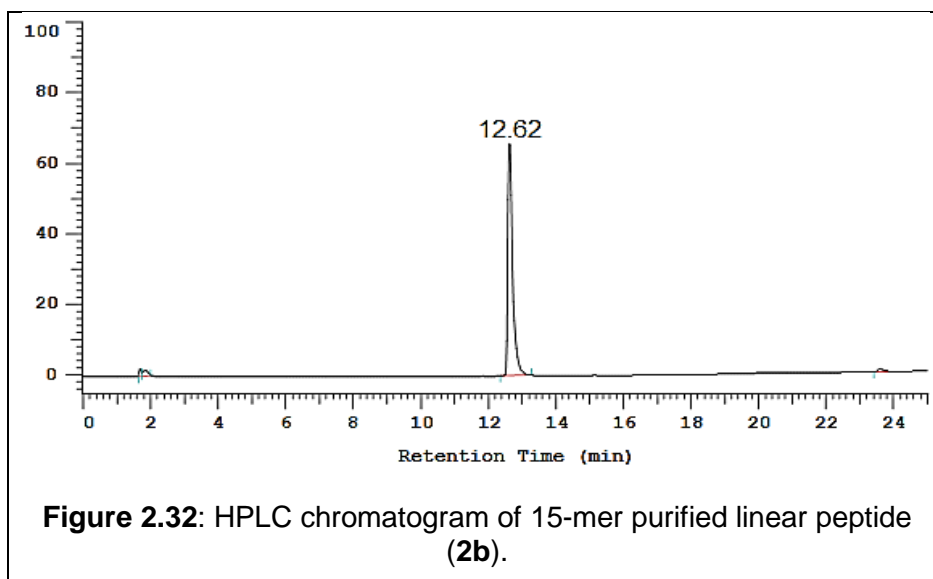
† Mass of the purified sample calculated from abs at 280 nm.

## 2.4 Synthesis of the linear peptide (2b, 3b)

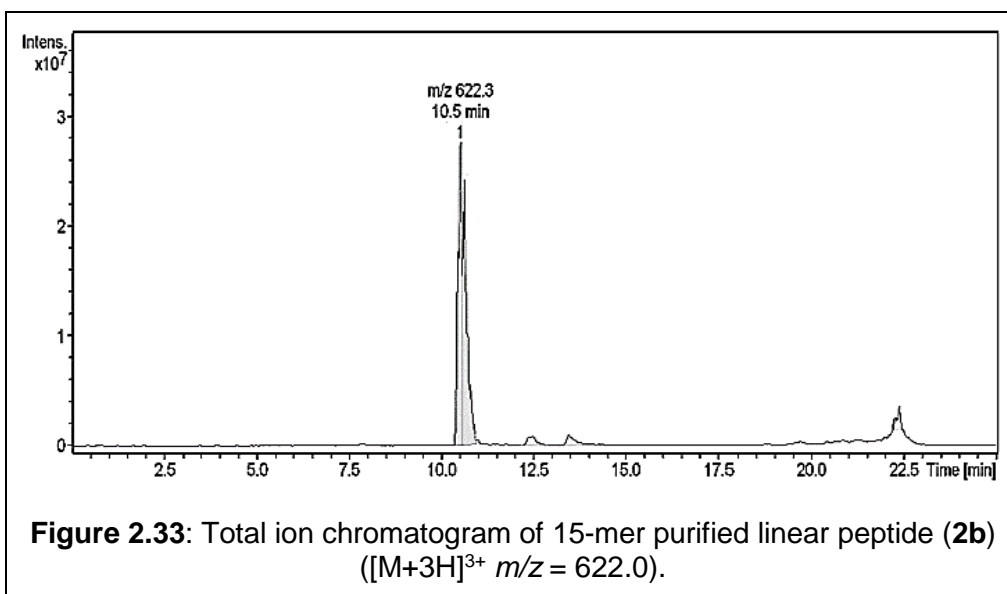
In the following two experiments, dedicated syntheses of linear peptides (**2b**, **3b**) were performed. The peptides were cleaved from the resin and purified to obtain sufficient amounts of these peptides for studies of their enzymatic degradation and stability in serum as a comparison with their cyclic counterparts (**2c**, **3c**).

### 2.4.1 Synthesis of the 15-mer linear peptide (2b)

The HPLC chromatogram of the sample of the purified 15-mer linear peptide (**2b**) after deprotection from the resin and removal of the side protecting groups of the amino acids is shown in Figure 2.32. The single sharp peak at the retention time 12.62 min without any overlap was consistent with the peak of 12.67 min in Figure 2.17 for the same intermediate compound (**2b**) during synthesis of the cyclic peptide (**2c**). Therefore, this peak was considered to be the target compound (**2b**).

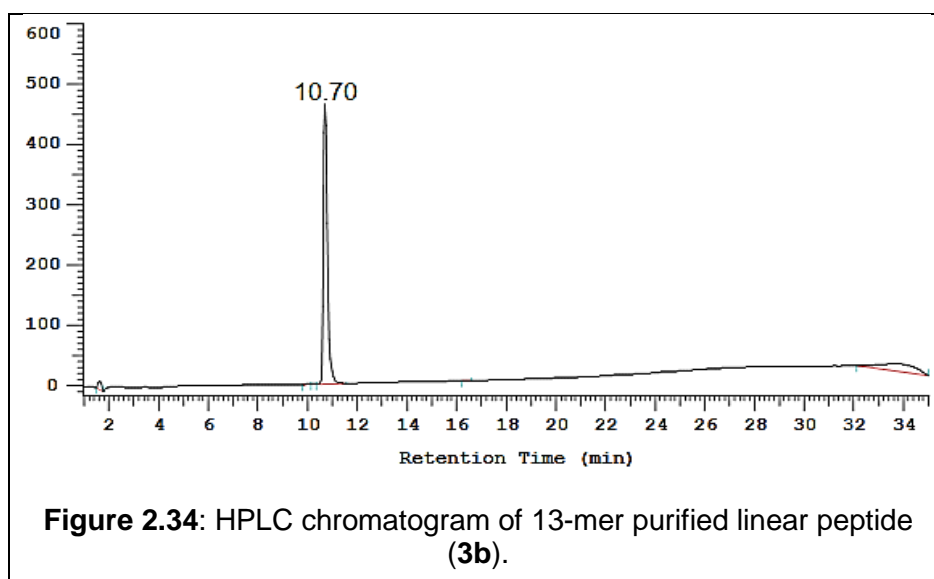


LCMS analysis (Figure 2.33) supported the HPLC result; the mass of 622.3  $m/z$  at the retention time 10.5 min was consistent with the theoretically calculated value of 622.0  $m/z$  for the 15-mer linear peptide (**2b**) in the +3 charge state (Figure 2.19). It is important to observe that the synthesis of this linear peptide using DEPBT as a coupling reagent was successful after the first attempt. In addition, the purification of this compound was also straightforward because of its good solubility in the HPLC solvent (water + acetonitrile).

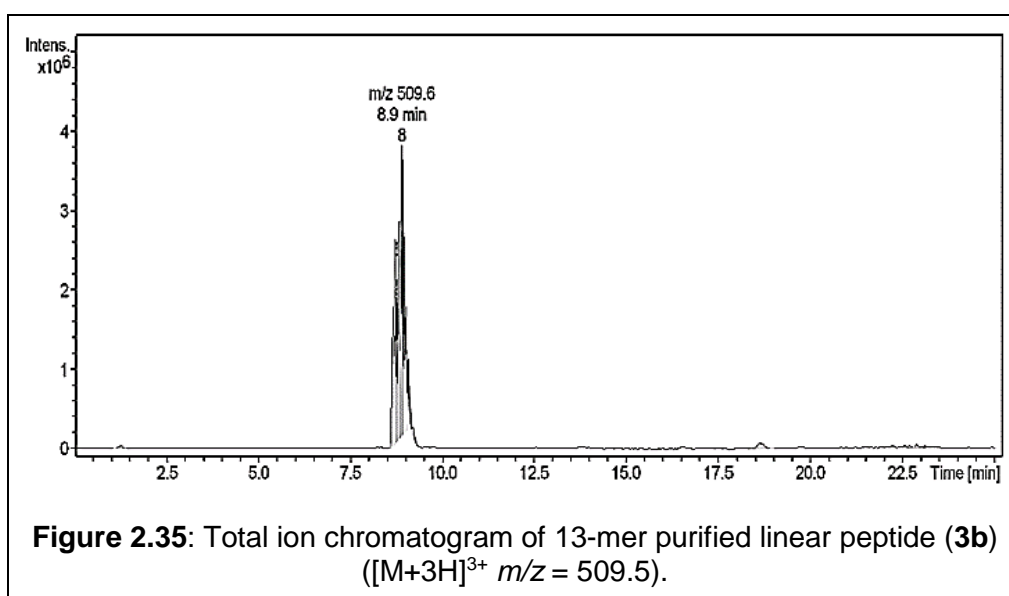


## 2.4.2 Synthesis of the 13-mer linear peptide (**3b**)

Figure 2.34 shows the HPLC chromatogram of the sample for the purified 13-mer linear peptide (**3b**) after deprotection from the resin and removal of the side chain protecting groups of the amino acids. The peak at the retention time 10.70 min was consistent with the peak of 10.68 min in Figure 2.20 for the same sample of the peptide (**3b**) after deprotection of the allyl group during synthesis of the cyclic peptide (**3c**). Therefore, this peak was considered to be the target compound (**3b**).



The mass spectral analysis reinforced the HPLC result; the total ion chromatogram in Figure 2.35 gave a peak of 509.6  $m/z$  at the retention time 8.9 min, which is the same peak observed in Figure 2.21 during synthesis of the cyclic peptide (**3c**). This peak matched the theoretically calculated value of 509.3  $m/z$  for the 13-mer linear peptide (**3b**) in the +3 charge state (Figure 2.22). This result is an indicator that the process of synthesis for this linear peptide (**3b**) using DEPBT as a coupling reagent was successful. The purification of the peptide was also straightforward because its solubility was acceptable (no precipitate) in the HPLC solvents (water, acetonitrile).



Both of the linear peptides (**2b**, **3b**) exhibited acceptable solubility (no precipitate) in HPLC solvents, as indicated in Table 2.3. The cause for this solubility in a range of different solvents is that they have more than one polar side chain added to the free polar termini of the two compounds.



**Table 2.3:** Properties of the two synthesised linear peptides (**2b**, **3b**).

Linear peptide	2b	3b
Mass ( <i>m/z</i> )	622.3	509.5
RT (min)	12.62	10.70
Solubility in H <sub>2</sub> O	No precipitate	No precipitate
Solubility in MeCN	No precipitate	No precipitate
Solubility in MeCN+H <sub>2</sub> O	No precipitate	No precipitate
Solubility in methanol	Trace precipitate	Trace precipitate
Solubility in isopropanol	Trace precipitate	Trace precipitate

## 2.5 Results of calculation of the concentration of polypeptides

### 2.5.1 Introduction

It has been found that significant amounts (10–70%) of salt and bound water or counterion remain in lyophilised peptides.<sup>180</sup> Thus, calculation of the concentration based on the mass is inaccurate. The number and type of counterions are affected by the sequence of the peptide therefore the concentration of peptides is best calculated based upon spectroscopic means.

The concentration of the peptides was calculated according to the following equation (Beer's law);

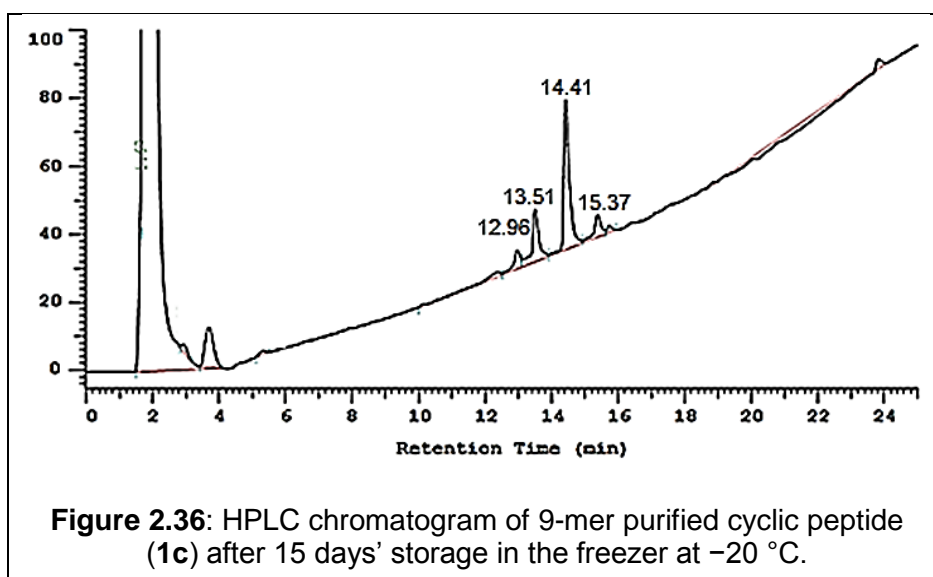
$$[\text{Peptide concentration}] = (A_{280} / \epsilon)$$

$A_{280}$  is the absorbance of the peptide solution at 280 nm in a 1 cm cell.  
 $\epsilon$  is the molar extinction coefficient of Tryptophan and/or Tyrosine at 280 nm.

$$\epsilon(\text{Trp}) = 5690 \text{ M}^{-1}\text{cm}^{-1}$$

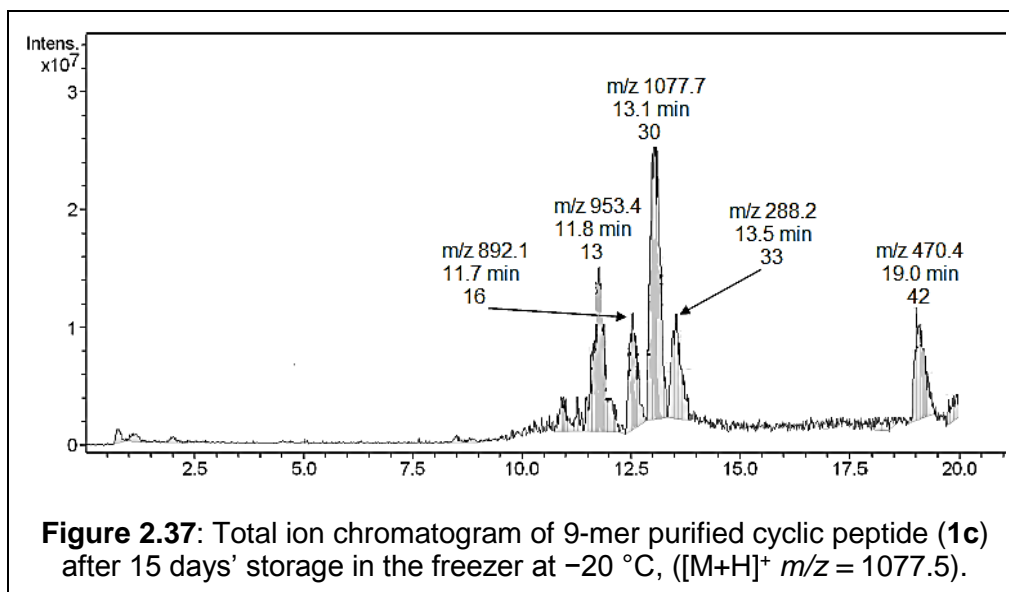
## 2.5.2 The 9-mer cyclic polypeptide (1c)

The concentration of the 9-mer cyclic peptide (**1c**) has not been calculated, for several reasons: the first was that a very small amount was collected, which was insufficient to prepare many samples to study the enzymatic degradation and to perform kinetic and stability studies in serum. The second reason was that some of this cyclic peptide was potentially exposed to hydrolysis during storage in the freezer at  $-20\text{ }^{\circ}\text{C}$  after 15 days. Figure 2.36 presents the HPLC chromatogram of **1c** after 15 days' storage in the freezer at  $-20\text{ }^{\circ}\text{C}$ . The appearance of three small peaks at the retention times 12.96, 13.51, 15.37 min around the peak of the cyclic compound (**1c**) at the retention time 14.41 min was an indicator of hydrolysis of **1c**.



A total ion chromatogram for the same sample, as shown in Figure 2.37, supported the HPLC result. In addition to the peak of  $1077.7\text{ }m/z$  at the retention time 13.1 min for the cyclic peptide (**1c**), there is more than one peak around the cyclic peptide peak such as  $953.4\text{ }m/z$  at the retention time 11.8 min, and the peak of  $892.1\text{ }m/z$  at the retention time 11.7 min. The stability of this compound (**1c**) was very low under these storage conditions. Possibly the reason was the short length of compound **1c**. Therefore, repurification of the cyclic peptide would cause a problem by reducing the yield further. The third important reason for not calculating the 9-mer cyclic peptide (**1c**) concentration is that the solubility of this compound in water was very low. Therefore, it will precipitate in the buffer solution; for example, ammonium bicarbonate

(NH<sub>4</sub>)HCO<sub>3</sub> (0.01 M) during the study of enzymatic hydrolysis by trypsin or chymotrypsin.



### 2.5.3 The 9-mer linear peptide (**1b**)

The project focused on the study of the synthesis of the cyclic peptides and the biological activity of these cyclic compounds, therefore, this linear peptide (**1b**) was excluded from this experiment and the biological study, due to there being an insufficient amount of compound **1c** (as was mentioned in section 2.5.2), in addition to that, the solubility of **1c** in water (which was used for preparation of the buffer solution) was very low.

### 2.5.4 The 15-mer cyclic peptide (**2c**)

$$A = 0.052, \text{MW} = 1864.2 \text{ g/mol}, \epsilon(\text{Trp}) = 5690 \text{ M}^{-1}\text{cm}^{-1}$$

Utilizing Beer's law;

$$[\text{9-mer cyclic peptide}] = 0.052/5690$$

$$= 9.1 \times 10^{-6} \text{ M}$$

This concentration,  $C_1$ , was in  $10^3 \mu\text{L}$  ( $V_1$ , volume of UV cuvette) which had been prepared by dilution of stock solution ( $V_2$ ,  $4 \mu\text{L}$ ) of concentration  $C_2$ . The concentration of the stock solution is then given by:  $C_1 \times V_1 = C_2 \times V_2$

$$9.1 \times 10^{-6} \times 10^3 = C_2 \times 4$$

$$C_2 \text{ (mol/L)} = 2.2 \times 10^{-3} \text{ (conc. of the stock solution)}$$

$$\text{Weight (mg)} = [2.2 \times 10^{-3} \times 1846.2 \times 180 \times 10^{-3} / 10^3] \times 10^3$$

$$= 0.76 \text{ mg}$$

$$\text{Number of mmoles} = \text{concentration of the stock solution} \times \text{stock solution volume} \times 10^3$$

$$= 2.2 \times 10^{-3} \times 180 \times 10^{-3}$$

$$= 0.4 \times 10^{-3}$$

$$\text{Percentage of yield} = \text{number of mmoles of peptide} \times 100 / \text{meq of resin (0.02)}$$

$$= 0.4 \times 10^{-3} \times 100 / 0.02$$

$$= 2$$

The above procedure was used to calculate the weight, concentration, number of moles, and the percentage of the yield for **2b**, **3b**, and **3c**. All the results are presented in Table 2.4.

**Table 2.4:** The value of concentration, weight, number of moles, and the percentage yield of the peptides (**2b**, **2c**, **3b**, **3c**) in their stock solutions.

Peptide	2b	2c	3b	3c
Absorbance	0.032	0.052	0.206	0.131
MW (g/mol)	1864.2	1846.2	1526.8	1508
Con. (M) in $10^3 \mu\text{L}^*$	$5.6 \times 10^{-6}$	$9.1 \times 10^{-6}$	$3.5 \times 10^{-5}$	$2.3 \times 10^{-5}$
Con. (M) in stock solution	$5.6 \times 10^{-3}$	$2.2 \times 10^{-3}$	$3.5 \times 10^{-3}$	$7.7 \times 10^{-3}$
Weight (mg)	1.1	0.76	0.74	2.7
Number of mmoles	$0.6 \times 10^{-3}$	$0.4 \times 10^{-3}$	$0.5 \times 10^{-3}$	$1.8 \times 10^{-3}$
Percentage yield	3	2	2.5	9

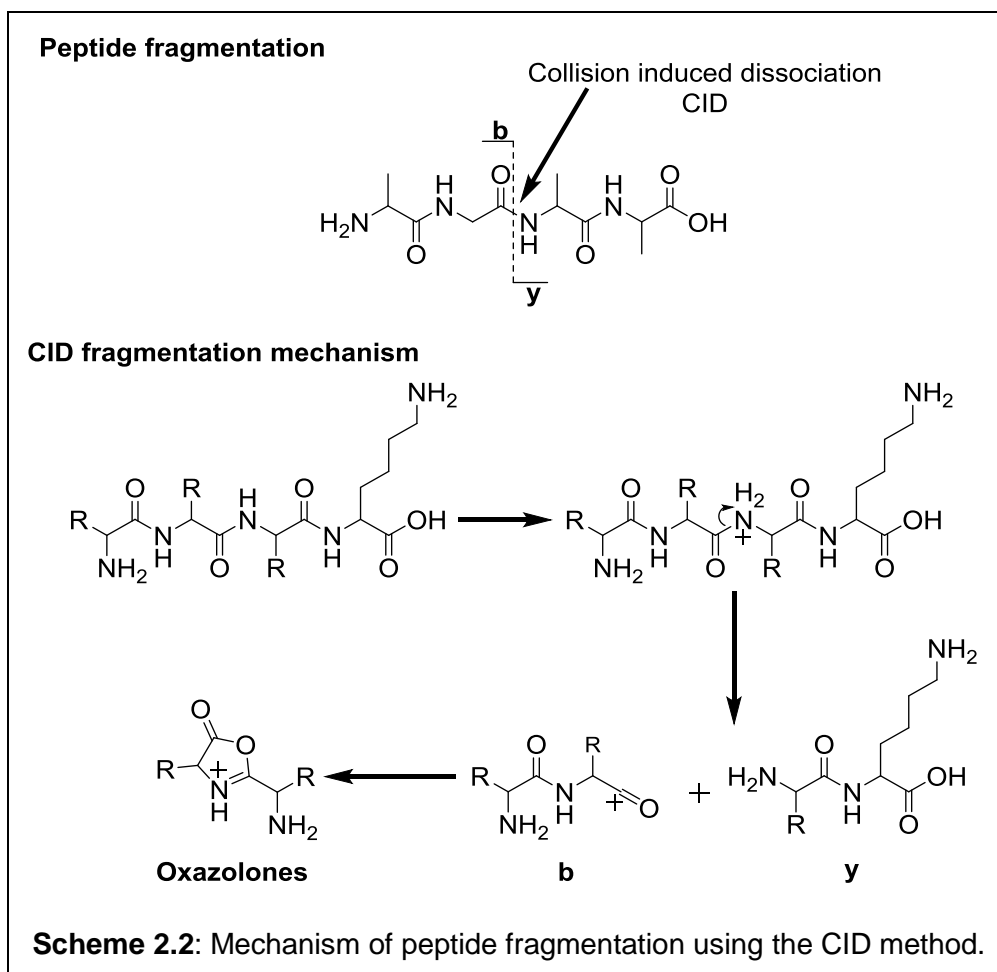
\*  $10^3 \mu\text{L}$  = UV cuvette volume

## 2.6 Results of peptide fragmentation

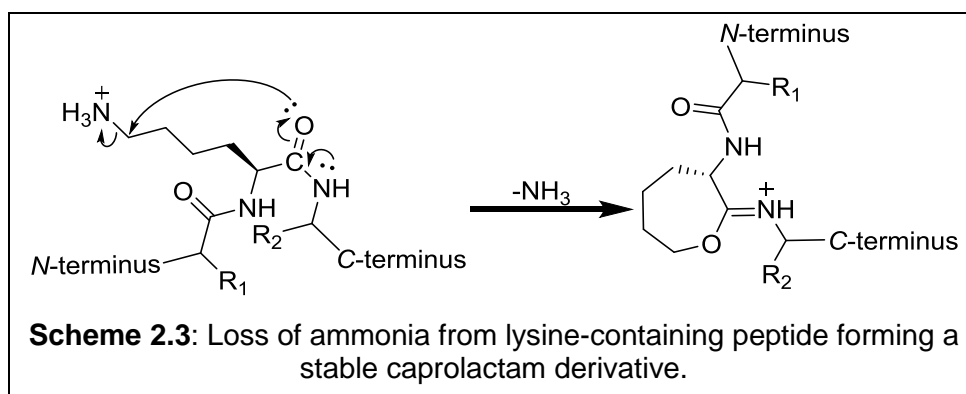
### 2.6.1 Introduction

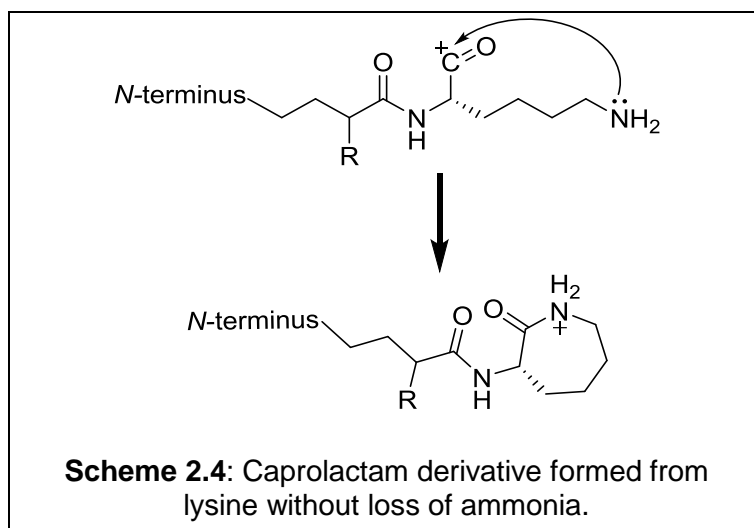
MS analysis is one of the most important techniques used to study and characterise the sequence of amino acids in peptides and proteins. Determination of the sequence of these compounds is undertaken after ionisation, converting them to charged compounds (mainly positive ions) in the gas phase. ESI (electrospray ionisation)<sup>181</sup> or MALDI (matrix-assisted laser desorption/ionisation)<sup>182</sup> are used as an ionisation technique to form these ions without fragmentation. The mass to charge ratio ( $m/z$ ) of these ions can be measured accurately.

The MS<sup>2</sup> method is usually used for deriving sequence information of peptides and proteins.<sup>183</sup> It is an attractive alternative method to NMR (nuclear magnetic resonance) for two main reasons: the first is that NMR technique requires large amounts of sample (milligrams), while in MS<sup>2</sup>, picograms are sufficient. The second is that a highly purified sample is used to verify structure by NMR, while in MS<sup>2</sup>, a non-purified sample can be employed.<sup>184</sup> In addition, interpretation of NMR spectra is time consuming. In the MS<sup>2</sup> method, the ions are exposed to excitation and dissociation after passing from the analyser to measure the value of  $m/z$  for the dissociation products. Low energy is used to excite the precursor ion by using an inert gas, such as argon, to create energetic collisions; this process is called collision induced dissociation (CID).<sup>185</sup> Under this low energy collision, protonated peptides are often fragmented by peptide bond cleavage to produce b ions (*N*-terminal fragment) and y ions (*C*-terminal fragment)<sup>186</sup> as shown in Scheme 2.2.

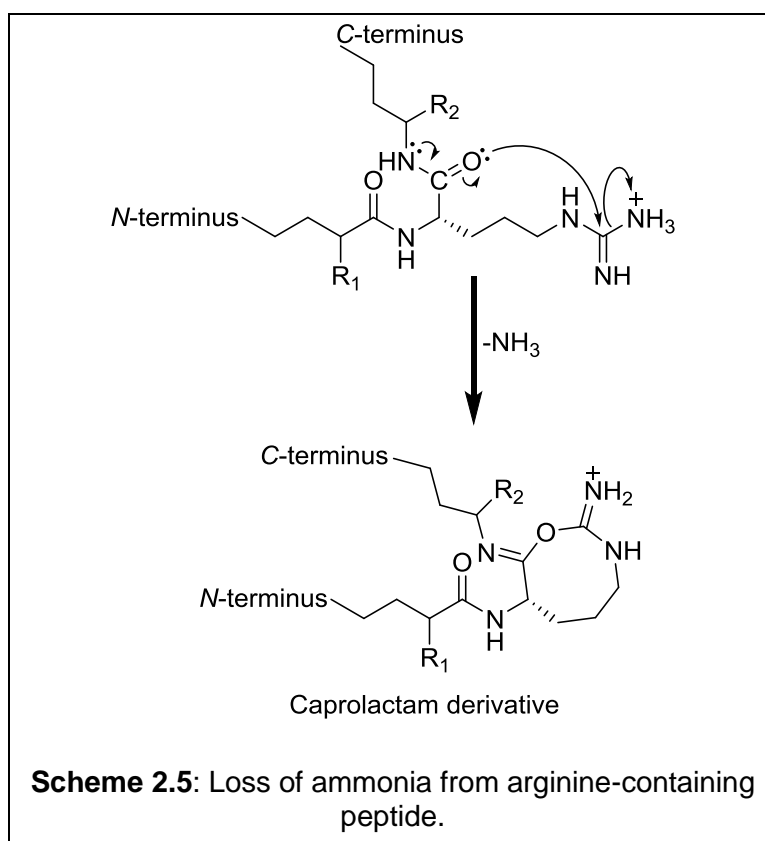


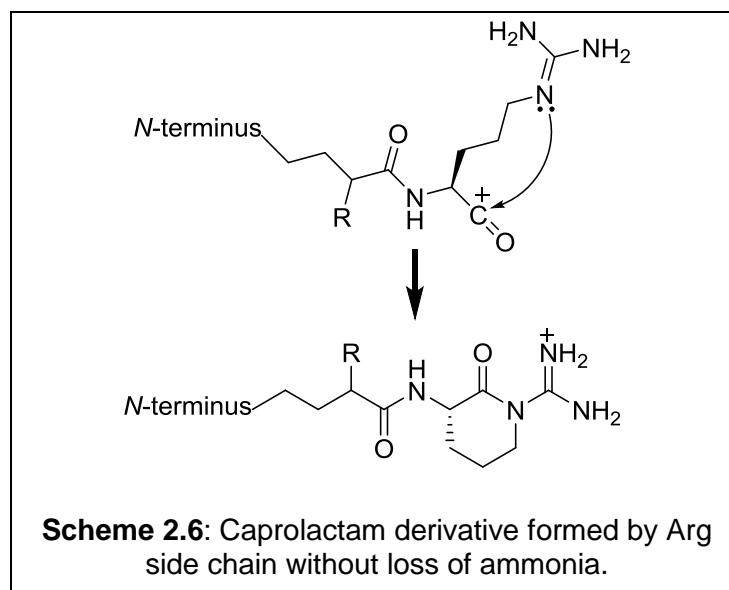
It was observed that there is an alternative, more stable structure (non-oxazolone) for the fragments (acyl  $b_1$ ,  $b_2$ ) where certain amino acids such as Lys or Arg are present in the sequence of the fragment.<sup>184</sup> A caprolactam derivative is formed with or without loss of ammonia from the side chain of Lys<sup>187</sup> as in Schemes 2.3 and 2.4.



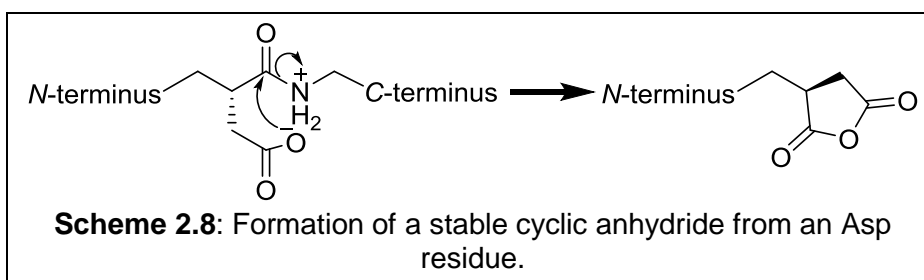
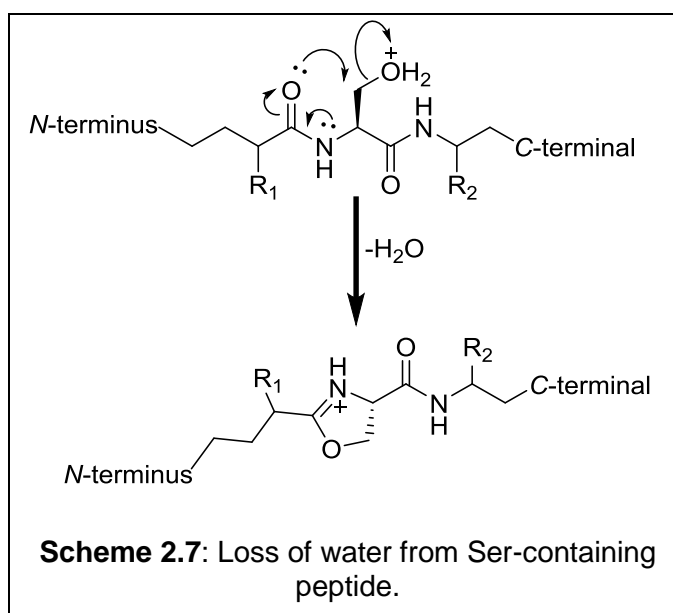


Regarding Arg, an ammonia molecule is eliminated from the guanidino side chain of arginine,<sup>188</sup> providing a stable structure as in Scheme 2.5. Without loss of ammonia, the cyclic structure is formed as in Scheme 2.6.





Loss of water molecules and formation of a cyclic structure in the gas phase was observed when Ser or Met residues were present in the sequence,<sup>189</sup> as in Scheme 2.7 for Ser, while in the presence of aspartic acid at the C-terminus,<sup>190</sup> the cyclic structure is formed as in Scheme 2.8.





One of the significant advantages to the MS<sup>2</sup> mass spectrometry is that this technique is used to provide evidence of the conversion of the linear form to the cyclic compound. The linear compound could eliminate a water molecule during measurement of the mass spectrum when it has a threonine or serine residue, giving the same mass of its cyclic counterpart. On the other hand, the process of cyclisation of the linear peptide by the head to tail method also involves loss of a water molecule. Therefore, the result of MS mass for the putative cyclic compound has the potential to be misleading. The MS<sup>2</sup> technique has the ability to resolve this issue. There is not a fragment that contains the two termini (C-terminal residue and N-terminal residue) bonded together in the MS<sup>2</sup> mass spectrum of the linear compound, while the presence of this fragment is possible in the MS<sup>2</sup> mass spectrum of the cyclic compound.

### 2.6.2 Comparison between fragmentation of the 9-mer cyclic peptide (1c) and its linear counterpart (1b)

The MS<sup>2</sup> mass spectrum of the 9-mer purified cyclic peptide (1c) is shown in Figure 2.38. The observed masses of the fragments were consistent with the theoretically calculated values. The possible sequences of these fragments are suggested in Table 2.5. The structures of these fragments are given in Table A.1 in Appendix A.

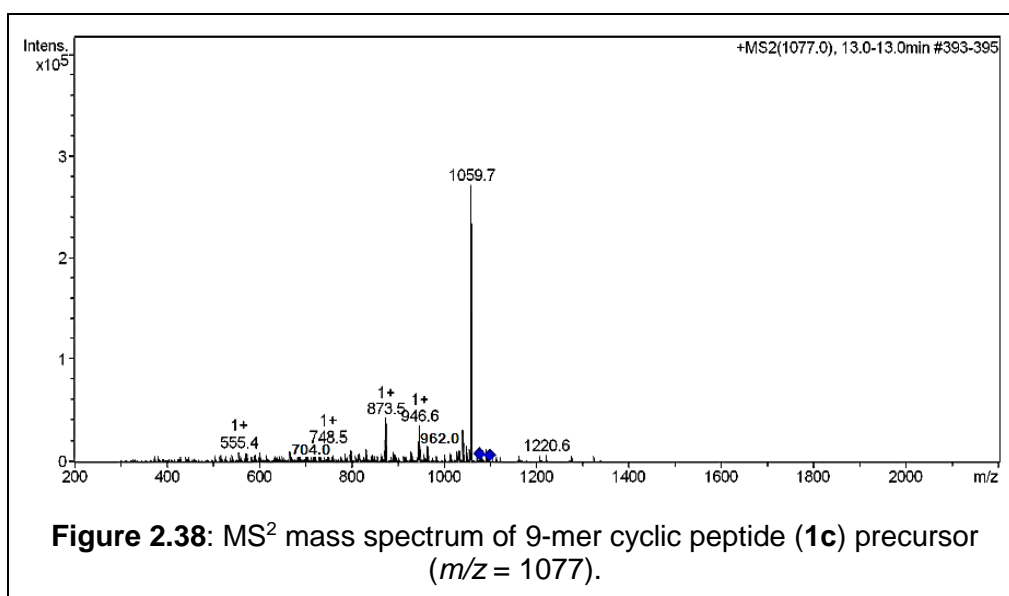
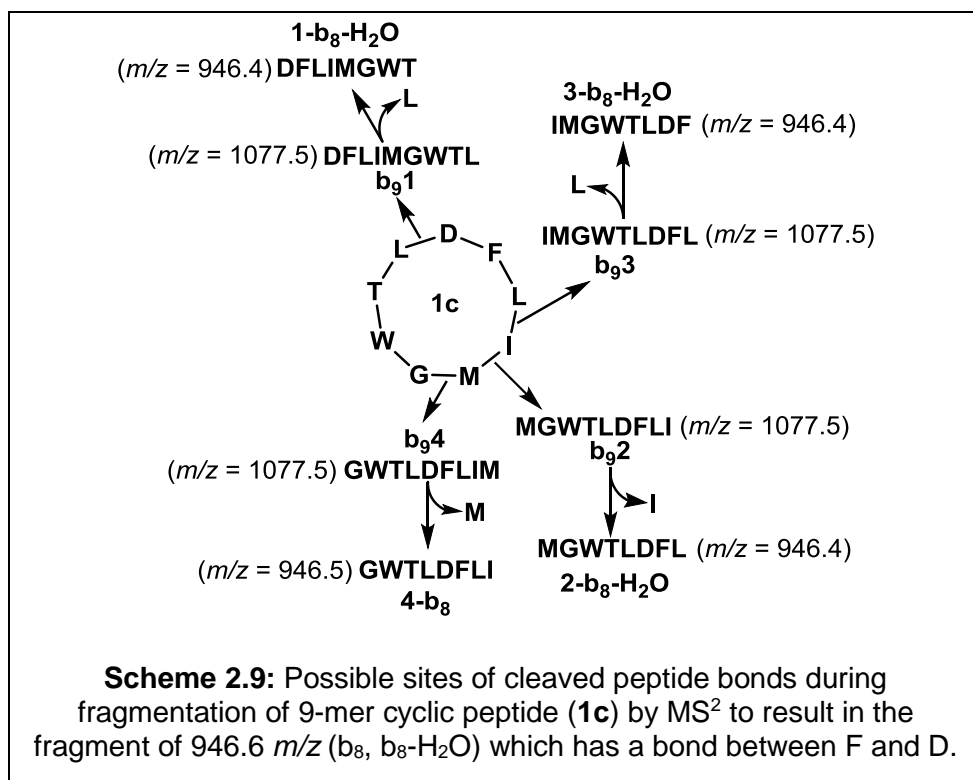


**Table 2.5:** The comparison between theoretically calculated peaks and the observed CID fragments of purified 9-mer cyclic peptide (**1c**). (See Figure 2.38)

No	Observed $m/z$	Calculated $m/z$	Suggested sequence
1	1059.7	1059.5	MH-2H <sub>2</sub> O
2	962.0	962.5	b <sub>8</sub>
3	946.6	946.5 946.4	b <sub>8</sub> b <sub>8</sub> -H <sub>2</sub> O
4	831.5	831.4	b <sub>7</sub> -H <sub>2</sub> O
5	748.5	748.4	b <sub>6</sub>
6	704.0	704.3	b <sub>6</sub>
7	555.4	555.3	b <sub>5</sub> -H <sub>2</sub> O

Notably, the observed mass of 946.6  $m/z$  was consistent with the theoretically calculated values of 946.5 and 946.4  $m/z$  for the fragments which have the possible sequences of b<sub>8</sub> and b<sub>8</sub>-H<sub>2</sub>O respectively. There are three proposed structures for the fragment of b<sub>8</sub>-H<sub>2</sub>O, as in entry 3 in Table A.1 in Appendix A. These four fragments were expected to exist among the other fragments because there were several possibilities for the site of the initially cleaved amide bond in the cyclic peptide (**1c**). All four fragments have the two residues Phe and Asp bonded together (Scheme 2.9).



As a comparison with the 9-mer linear peptide (**1b**), a fragment with 946.6 *m/z* did not appear in the MS<sup>2</sup> mass spectrum of **1b** (See Figure 2.39, Table 2.6 and Table A.2 in Appendix A) because it is impossible to find a fragment that has Asp and Phe residues bonded together. These two residues are each found at opposing termini of the linear peptide.

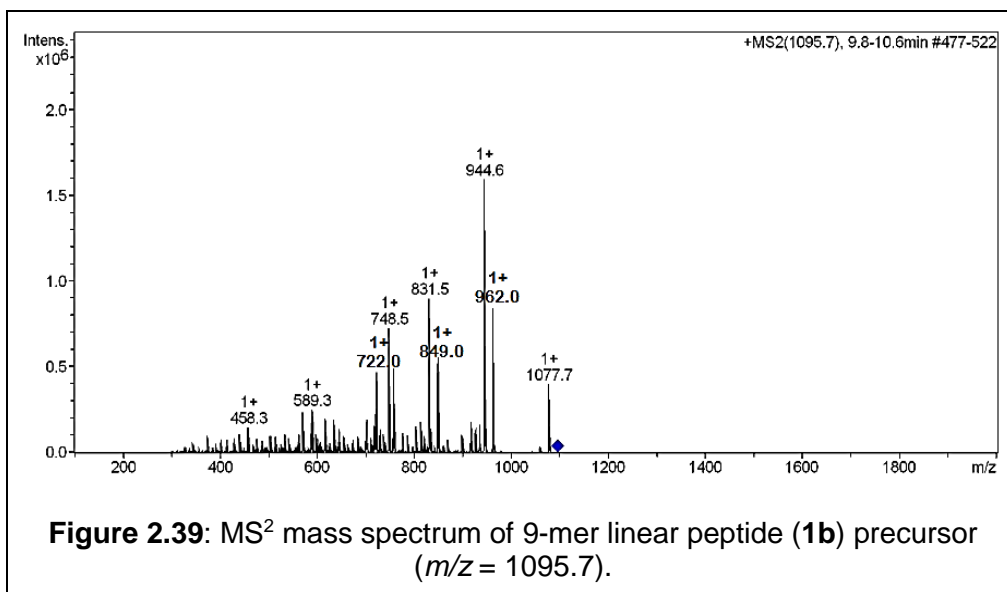


**Table 2.6:** The comparison between theoretically calculated peaks and the observed CID fragments of purified 9-mer linear peptide (**1b**). (See Figure 2.39).

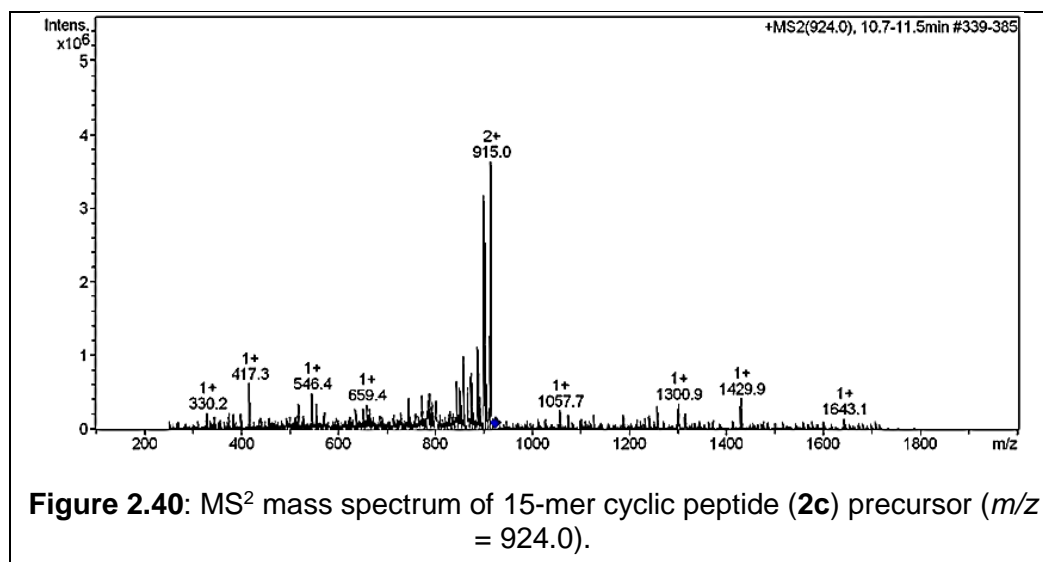
No	Observed $m/z$	Calculated $m/z$	Suggested sequence
1	1077.7	1077.5	MH-H <sub>2</sub> O
2	962.0	962.5	b <sub>8</sub>
3	944.6	944.5	b <sub>8</sub> -H <sub>2</sub> O
4	849.0	849.4	b <sub>7</sub>
5	831.5	831.4	b <sub>7</sub> -H <sub>2</sub> O
6	748.5	748.4	b <sub>6</sub>
7	722.0	722.3	y <sub>6</sub>

The observed mass of 1077.7  $m/z$  was consistent with the theoretically calculated value of 1077.5  $m/z$  for the linear peptide (**1b**); the mass of this peptide was reduced by the mass of a water molecule (See fragment 1 in Table 2.6). The structure of this fragment is entry number 1 in Table A.2 in Appendix A.

It should be noted that some of the observed fragments in the MS<sup>2</sup> mass spectrum of **1c** were observed in the MS<sup>2</sup> mass spectrum of **1b**; for example, b<sub>6</sub> and b<sub>7</sub>-H<sub>2</sub>O. On the other hand, some of the observed fragments in the MS<sup>2</sup> mass spectrum of **1c** did not appear in the MS<sup>2</sup> mass spectrum of **1b**; for example, y<sub>6</sub>-H<sub>2</sub>O and b<sub>5</sub>-2H<sub>2</sub>O. This result was expected because the first fragmentation of the cyclic peptide (**1c**) to the linear compound (**1b**) gives a different sequence in comparison with its linear counterpart (**1b**). Therefore, this fragment produces different sub-fragments compared to the fragments of its linear counterpart (**1b**).

### 2.6.3 Comparison between fragmentation of the 15-mer cyclic peptide (**2c**) and its linear counterpart (**2b**)

Figure 2.40 reveals the MS<sup>2</sup> mass spectrum of the 15-mer cyclic peptide (**2c**). The observed masses of the fragments were matched to theoretically calculated values (See Table 2.7).



The possible sequences of these fragments are suggested in Table 2.7. The structures of these possible sequences are given in Table A.3 in Appendix A.

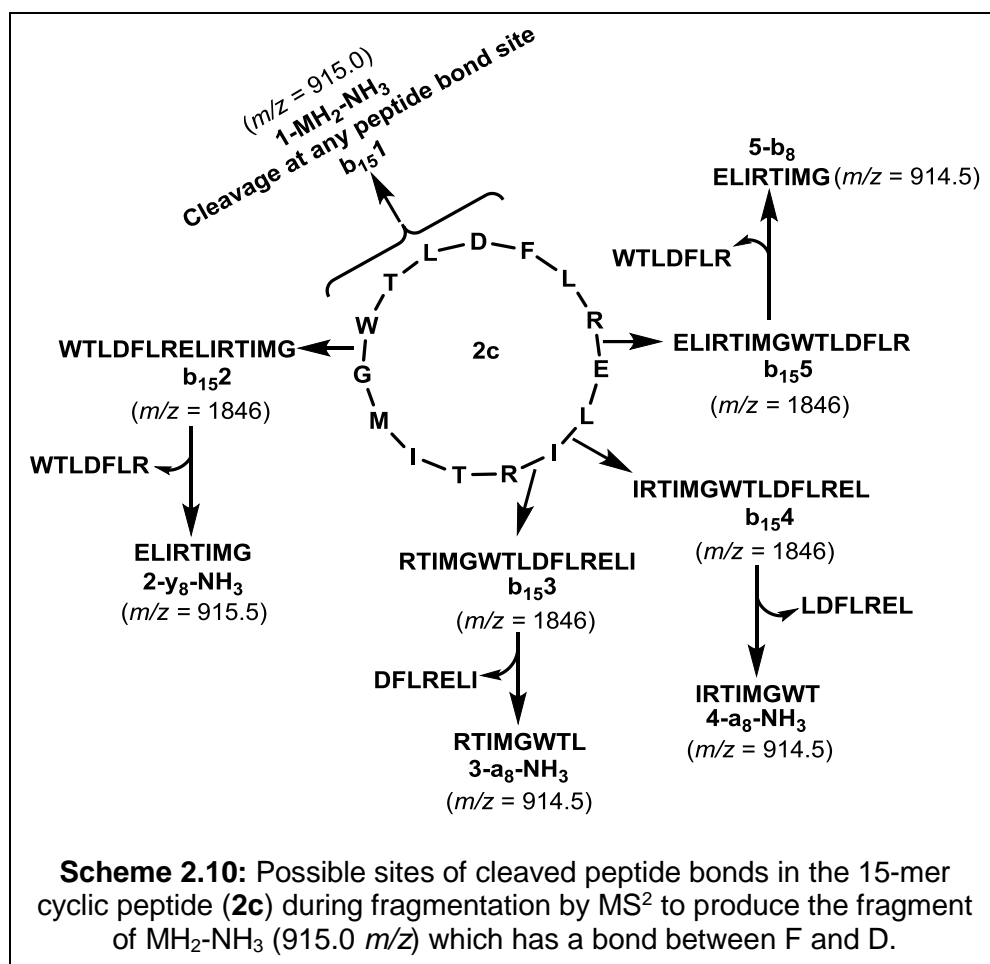
**Table 2.7:** The comparison between theoretically calculated peaks and the observed CID fragments of purified 15-mer cyclic peptide (**2c**). (See Figure 2.40).

No	Observed $m/z$	Calculated $m/z$	Suggested sequence
1	1300.9	1300.7	b <sub>11</sub>
2	915.0	915.0	1-MH <sub>2</sub> -NH <sub>3</sub>
		915.5	2-y <sub>8</sub> -NH <sub>3</sub> ,
		914.5	3-a <sub>8</sub> -NH <sub>3</sub>
		914.5	4-a <sub>8</sub> -NH <sub>3</sub> <sup>*</sup>
		914.5	5-b <sub>8</sub>
3	659.4	659.4	b <sub>5</sub>
4	546.4	546.3	b <sub>4</sub>
5	417.3	417.3	b <sub>3</sub> <sup>†</sup>
6	330.2	330.2	b <sub>3</sub>

a<sub>8</sub>-NH<sub>3</sub><sup>\*</sup> and b<sub>3</sub><sup>†</sup> are sequences were formed from fragmentation of a different ring-opened sequences in comparison to the a<sub>8</sub>-NH<sub>3</sub> and b<sub>3</sub> sequences respectively.

Notably, the observed mass of 915.0  $m/z$  was consistent with the theoretically calculated values of 915.0, 915.5, 914.5, 914.5, 914.5  $m/z$  for the fragments that have the possible sequences MH<sub>2</sub>-NH<sub>3</sub>, y<sub>8</sub>-NH<sub>3</sub>, a<sub>8</sub>-NH<sub>3</sub>,

$a_8\text{-NH}_3^+$ ,  $b_8$  respectively as in above Table 2.7. The structures of these fragments are in entry 2 in Table A.3 in Appendix A. Scheme 2.10 includes the possible sites for the cleaved peptide bonds in compound **2c** to give the fragment that has an observed mass of 915.0  $m/z$  in Figure 2.40. None of the observed fragments except doubly charged  $\text{MH}_2\text{-NH}_3$  contain both the Asp and Phe residues that were at the termini of the linear peptide precursor.



The presence of this fragment ( $\text{MH}_2\text{-NH}_3$ ) was evidence for successful coupling reaction between two termini of 15-mer linear peptide (**2b**) forming the cyclic compound (**2c**). As a comparison with compound **2b**, the corresponding fragment is not observed (See Figure 2.41, Table 2.8, Table A.4 in Appendix A). Phe represents the last residue at the *N*-terminus while Asp represents the last residue at C-terminus of **2b**.

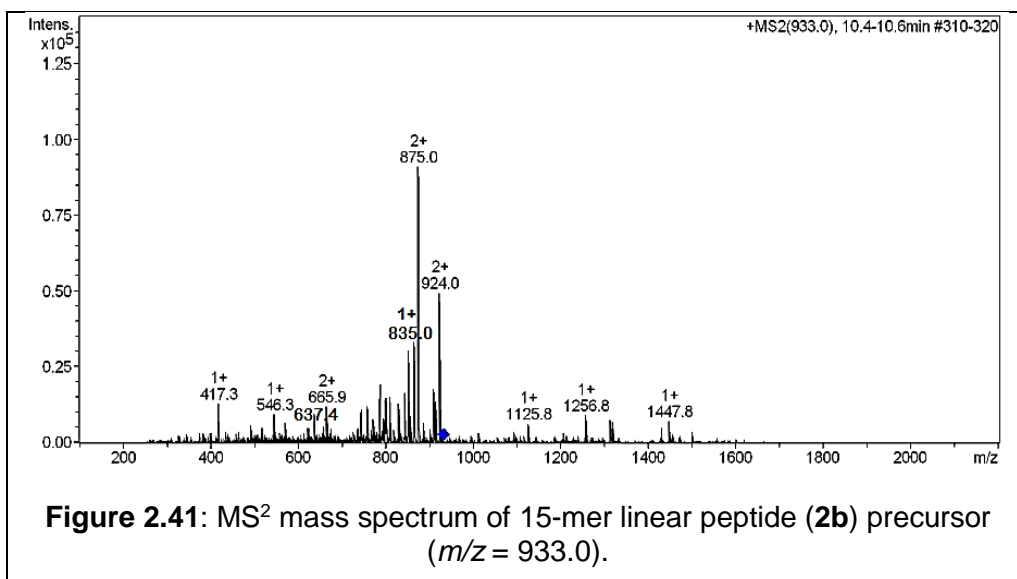


**Table 2.8:** The comparison between theoretically calculated peaks and the observed CID fragments of purified 15-mer linear peptide (**2b**). (See Figure 2.41).

No	Observed $m/z$	Calculated $m/z$	Suggested sequence
1	1447.8	1447.8	$y_{12}$
2	1256.8	1256.7	$b_{10}\text{-NH}_3$
3	1125.8	1125.7	$b_9\text{-NH}_3$
4	924.0	923.5	$\text{MH}_2\text{-H}_2\text{O}$
5	835.0	835.4	$y_7$
6	637.4	637.4	$b_{10}$
7	546.3	546.3	$b_4$
8	417.3	417.3	$b_3$

The presence of Arg at the C-terminal of a  $b_2$  ion led to formation of an alternative cyclic structure to the oxazolone involving a side chain of arginine acting as a nucleophile to attack an acylium ion (Entry 5 in Table A.3 in Appendix A). Also, a  $b_2$  ion which has Asp at the C-terminal has an alternative cyclic structure to the oxazolone (entry 6 in Table A.3 in Appendix A), where the side chain of the aspartic acid has made a nucleophilic attack on an acylium ion.

## 2.6.4 Comparison between fragmentation of the 13-mer cyclic (3c) peptide and its linear counterpart (3b)

The MS<sup>2</sup> mass spectrum of the 13-mer cyclic peptide (3c) can be seen in Figure 2.42. The observed masses of the fragments were consistent with the theoretically calculated values. The sequences of these fragments are suggested in Table 2.9. The proposed structures of these fragments are given in Table A.5 in Appendix A.

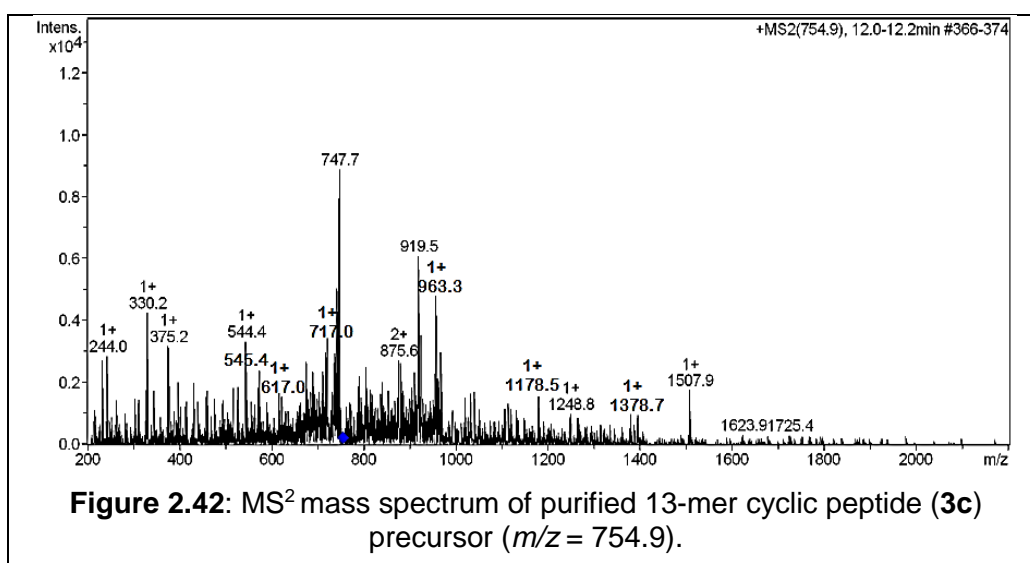
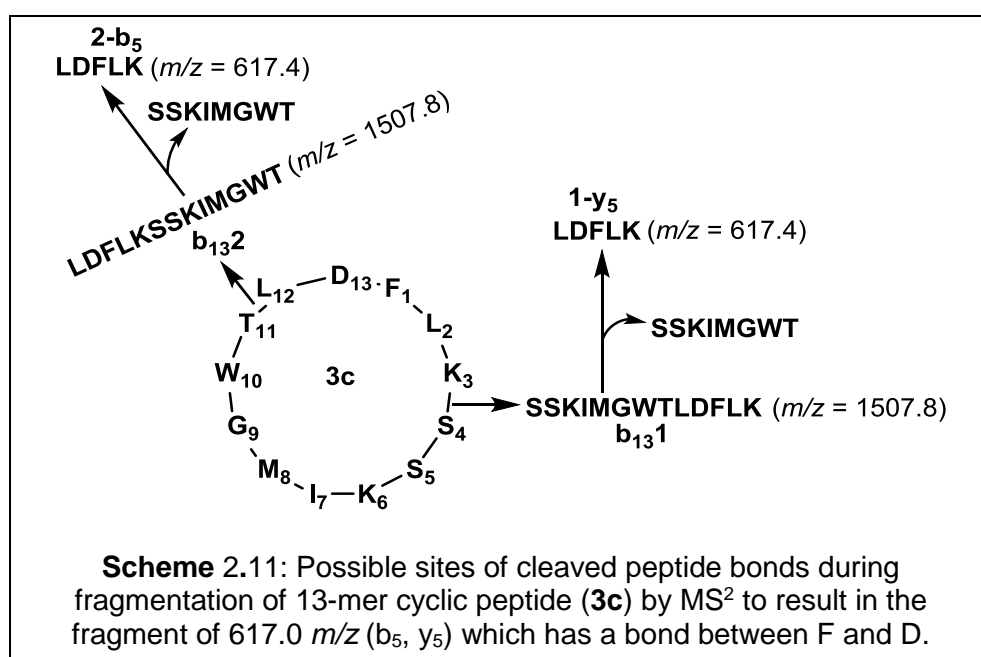


**Table 2.9:** The comparison between theoretically calculated peaks and the observed CID fragments of purified 13-mer cyclic peptide (3c). (See Figure 2.42).

No	Observed $m/z$	Calculated $m/z$	Suggested sequence
1	1507.9	1507.8	MH
2	1378.7	1378.7	$y_{12}+H_2O$
3	1178.5	1178.6	$b_{10}$
4	963.3	963.5	$y_8$
5	717.0	717.4	$b_6$
6	617.0	617.4	$y_5$ $b_5$
7	545.4	545.3	$b_5-H_2O$
8	330.2	330.2	$y_3$



Of all the fragments appearing, the fragment of 617.0  $m/z$  was consistent with the theoretically calculated value of 617.4  $m/z$  with the suggested sequences of  $b_5$  and  $y_5$  in Table 2.9. The structure of this fragment is entry 6 in Table A.5 of Appendix A. Appearance of the  $b_5$  and  $y_5$  fragments provide evidence for the presence of the cyclic peptide (**3c**) because the sequence of these fragments included Asp and Phe bonded together by a peptide bond, indicating there was a successful cyclisation reaction between the two termini of the linear peptide (**3b**). The presence of these fragments ( $b_5$ ,  $y_5$ ) was expected, as more than one site of peptide bond cleavage was expected during fragmentation. It appears that the cleavage was at the peptide bond between  $K_3$  and  $S_4$  then loss of the fragment SSKIMGWT producing the  $y_5$  fragment. Initial cleavage between  $L_{12}$  and  $T_{11}$ , then loss of the same fragment (SSKIMGWT) produced the  $b_5$  fragment as in Scheme 2.11.



In comparison with **3c**, this fragment (617.0  $m/z$ ) did not appear in the MS<sup>2</sup> mass spectrum of **3b** (Figure 2.43, Table 2.10 and Table A.6 in Appendix A), as was expected because there was no bond between Asp and Phe in compound **3b**.

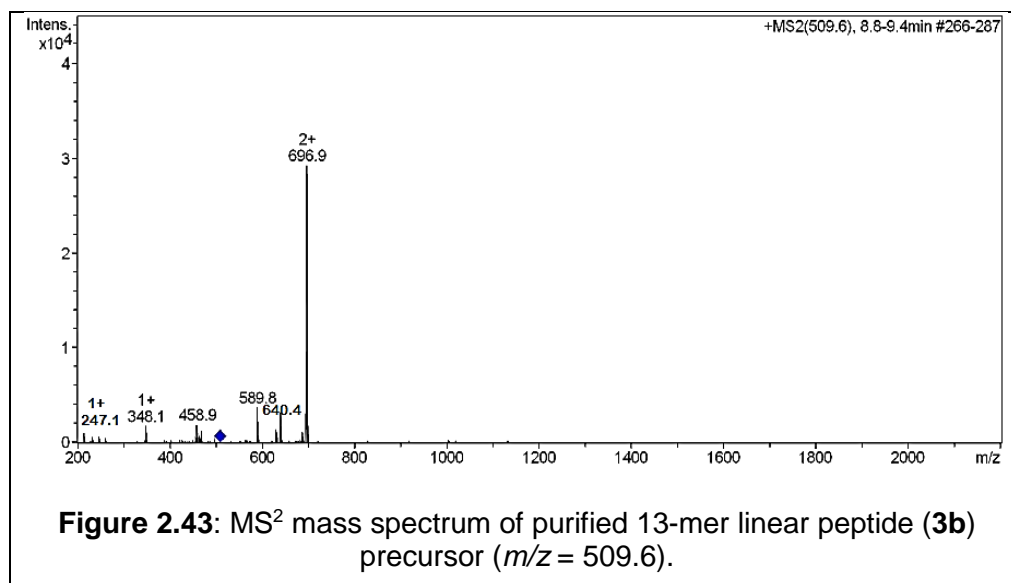


**Table 2.10:** The comparison between theoretically calculated peaks and the observed CID fragments of purified 13-mer linear peptide (**3b**). (See Figure 2.43).

No	Observed $m/z$	Calculated $m/z$	Suggested sequence
1	696.9	696.9	$b_{12}$
2	640.4	640.3	$b_{11}$
3	589.8	589.8	$b_{10}$
4	458.9	459.3	$b_4\text{-NH}_3$
5	348.1	348.2	$y_3$
6	247.1	247.1	$y_2$

Alternative cyclic structures to the oxazolone can be proposed in some  $b_2$  ion fragments (linear and cyclic) resulting from the presence of Asp, Lys, or serine at the C-terminal of the  $b_2$  ion, as mentioned for compounds **1c** or **2c**.

As was referred to in the study of fragmentation of compound **1c** and its linear counterpart (**1b**), here some of the fragments were also observed in both MS<sup>2</sup> mass spectra of **3b** and **3c**. In addition, some of the fragments were not seen in the MS<sup>2</sup> mass spectrum of **3b** that had been seen in the MS<sup>2</sup> mass spectrum of **3c**, for example,  $y_8$ .

The three cyclic peptides (**1c**, **2c**, **3c**) with their linear counterparts (**1b**, **2b**, **3b**) have been synthesised and identified. The first, Bax peptide (**1c**) was

excluded from the next experiments (enzymatic degradation and stability of the peptides in FCS) because of its yield being very low and its low solubility in water. In addition, it was hydrolysed during storage in the freezer. Therefore, its linear counterpart (**1b**) was also excluded from these experiments. MS<sup>2</sup> mass spectra for each cyclic peptide (**1c**, **2c**, **3c**) demonstrated different peaks from its linear counterpart (**1b**, **2b**, **3b**) in addition to the possibility of a fragment that has a bond between Phe and Asp. Insertion of a new fragment (RELIRT or KSSK) between the Ile and Leu residues of the Bax peptide sequence to form new derivatives (**2c** or **3c**) respectively increased the solubility of the peptides (**2c**, **3c**) in HPLC solvents and enhanced the synthesis yield following purification.

**Chapter 3**

**Biological Studies of  
the Peptides**

### 3 Biological studies of the peptides

#### 3.1 Introduction

The degradation experiments and kinetic study of the peptides (**2b**, **2c**, **3b** and **3c**) used two members of the serine protease family of enzymes, chymotrypsin and trypsin. This type of enzyme is one of the six families that are classified according to the nature of their catalytic residues<sup>191</sup> (serine acts as a nucleophilic residue at the active site of the enzyme) which can be found in the digestive tract and serum of humans, in addition to the bovine pancreas. They are endopeptidases that can cleave the internal peptide bonds with high specificity; for example, trypsin cleaves the peptide bond at the carboxyl side of the Arg or Lys amino acids by the addition of a water molecule.<sup>192</sup> The commercial availability of this type of enzyme was an advantage to their use in these experiments. Additionally, there is precedent for their use in many well-documented studies.<sup>193</sup> The source of the two enzymes was the bovine pancreas.

The reaction rate for the disappearance of the starting material during the enzyme catalysed peptide hydrolysis was modelled using first order kinetics. Therefore, the  $t_{1/2}$  of the peptides (**2b**, **3b**, **2c**, **3c**) was calculated using the following equation:

$$t_{1/2} = \ln 2 / k$$

where  $k$  = rate constant

#### 3.2 Results and discussion of the study of enzymatic degradation of peptides

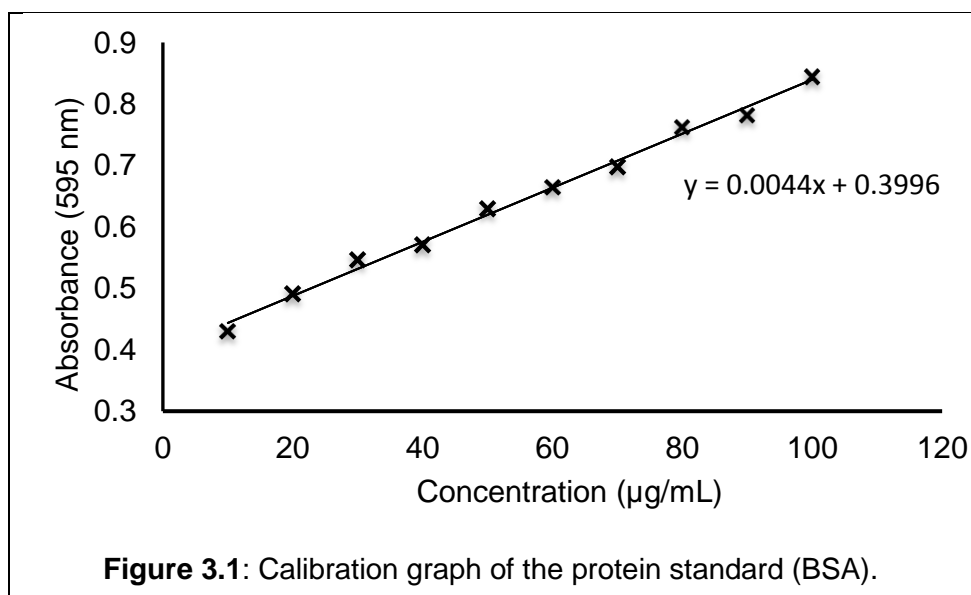
##### 3.2.1 Results of calculation of the concentration of trypsin and chymotrypsin

The concentration of the trypsin and chymotrypsin was determined using the Bradford assay using BSA as a standard protein. The absorbance of the Bradford reagent after addition of BSA at known concentration is given in Table 3.1.

**Table 3.1:** Absorbance at 595 nm for the different concentrations of standard protein (BSA) with Bradford reagent.

BSA $\mu\text{L}$	[BSA] $\mu\text{g/mL}$ in 200 $\mu\text{L}$	Absorbance 595 nm
2	10	0.429
4	20	0.490
6	30	0.546
8	40	0.570
10	50	0.628
12	60	0.663
14	70	0.698
16	80	0.761
18	90	0.781
20	100	0.844

The calibration curve of the concentration of BSA ( $\mu\text{g/mL}$ ) against the absorbance at 595 nm was plotted in Figure 3.1. The x parameter in the equation ( $y = 0.0044x + 0.3996$ ) represents the concentration of the protein ( $C_1$ ) in 200  $\mu\text{L}$  of solution prior to addition of the Bradford reagent.



After measuring the absorbance of the enzyme (trypsin, chymotrypsin) at the wavelength 595 nm, which is represented by the letter y in the equation, the concentration of the enzyme ( $C_1$ ) was calculated and the results are shown in Table 3.2.

**Table 3.2:** Concentration of trypsin and chymotrypsin in 200  $\mu\text{L}$  ( $C_1$ ) and the stock solution ( $C_2$ ) with the mean of  $C_2$ .

Enzyme	MW	μL	Abs (595 nm)	C <sub>1</sub> (μg/mL)	C <sub>2</sub> (μM)	Mean of C <sub>2</sub> (μM)
Chymotrypsin	25000	4	0.6123	48.032	96.064	106
Chymotrypsin	25000	6	0.7844	87.157	116.21	
Trypsin	23800	2	0.4261	5.704	23.969	41
Trypsin	23800	4	0.5208	27.225	57.195	

Subsequently, the concentration of the enzymes ( $\mu\text{M}$ ) in the stock solution ( $C_2$ ) and the mean of the two measurements were calculated for the two enzymes (See above Table 3.2), according to the following equation:

$$C_1 \times V_1 = C_2 \times V_2$$

$C_1$  = concentration of the enzyme in 200  $\mu\text{L}$

$V_1$  = 200  $\mu\text{L}$

$C_2$  = concentration of the enzyme in the stock solution ( $\mu\text{g/mL}$ )

$V_2$  = the withdrawn volume of the stock solution

Then  $C_2$  ( $\mu\text{g/mL}$ ) was converted to  $C_2$  ( $\text{g/L}$ ), according to:

$$C_2 (\text{g/L}) = C_2 \times 10^{-6}/10^{-3}$$

Then  $C_2$  ( $\text{g/L}$ ) was converted to  $C_2$  ( $\mu\text{M}$ ), by the following relationship:

$$C_2 (\mu\text{M}) = (C_2 (\text{g/L}) / \text{MW}) \times 10^6$$

MW = molecular weight of the enzyme (trypsin, chymotrypsin)

### 3.2.2 Results of the study of the activity of trypsin and chymotrypsin

#### 3.2.2.1 Mass spectrum of standard BSA

Figure B.1 and B.2 in Appendix B show the total ion chromatogram and mass spectrum of the bovine serum albumin (BSA) analysed as a positive control to check the proteolytic activity of the enzymes. The peak at the retention time

8.29 min in Figure B.1 is for the BSA. The observed mass in Figure B.2 (66.418 kDa) was consistent with the theoretically calculated value (66.46 kDa).

### 3.2.2.2 Result of BSA degradation with chymotrypsin

Figure B.3 in Appendix B is a total ion chromatogram of the hydrolysis products of the BSA by chymotrypsin at 37 °C and pH 7.4 for 15 min. The chromatogram has many peaks due to hydrolysis of the bovine serum albumin by the enzyme at a peptide bond on the C-terminal side of an aromatic amino acid residue. The chromatogram should be compared to the control chromatogram of BSA before digestion (Figure B.1 in Appendix B). This result provides evidence that the chymotrypsin was active and ready for use in the enzymatic degradation experiments.

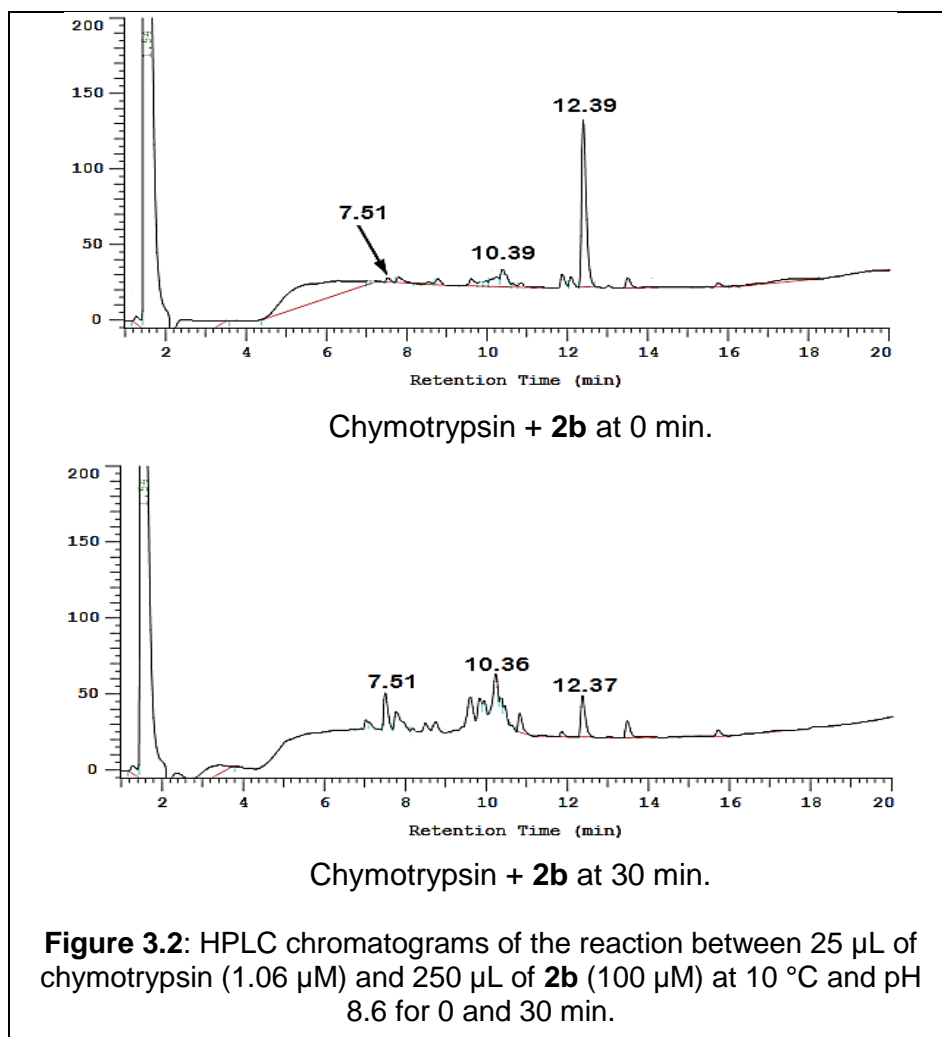
### 3.2.2.3 Result of BSA degradation with trypsin

The total ion chromatogram of the trypsin digest of BSA that is shown in Figure B.4 of Appendix B was evidence for the presence of active trypsin. The peak of the protein (BSA), as in Figure B.1 in Appendix B, was converted to many peaks when the BSA was incubated in the presence of trypsin under the same conditions for the chymotrypsin digest.

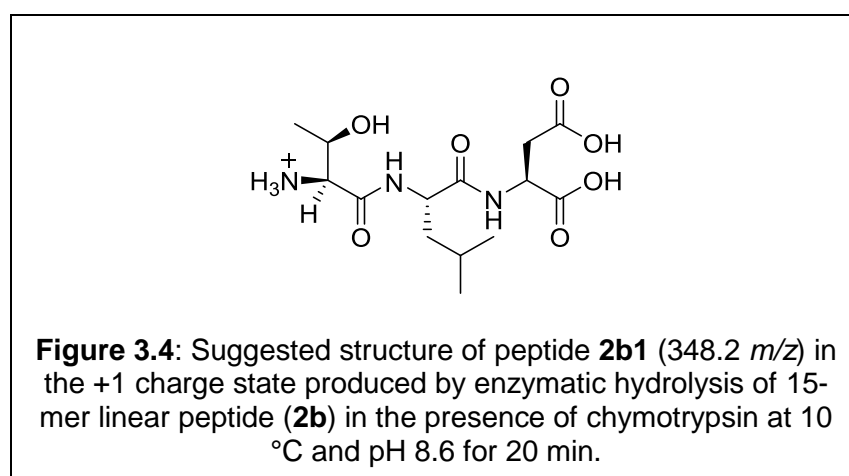
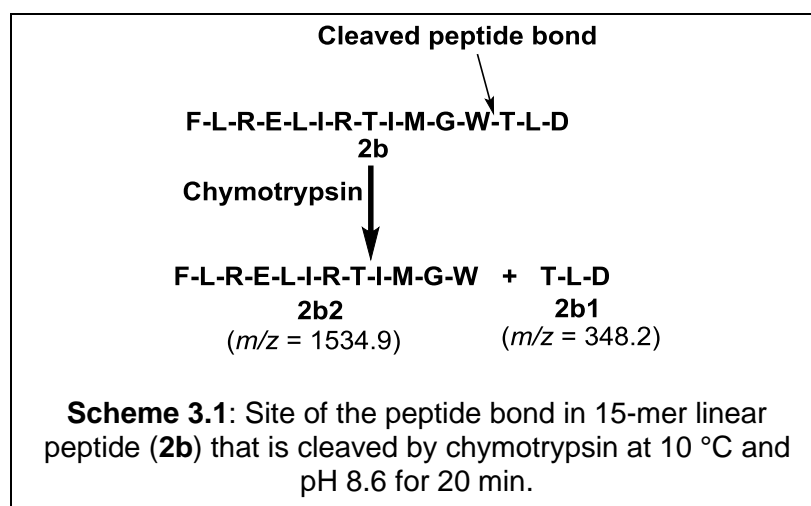
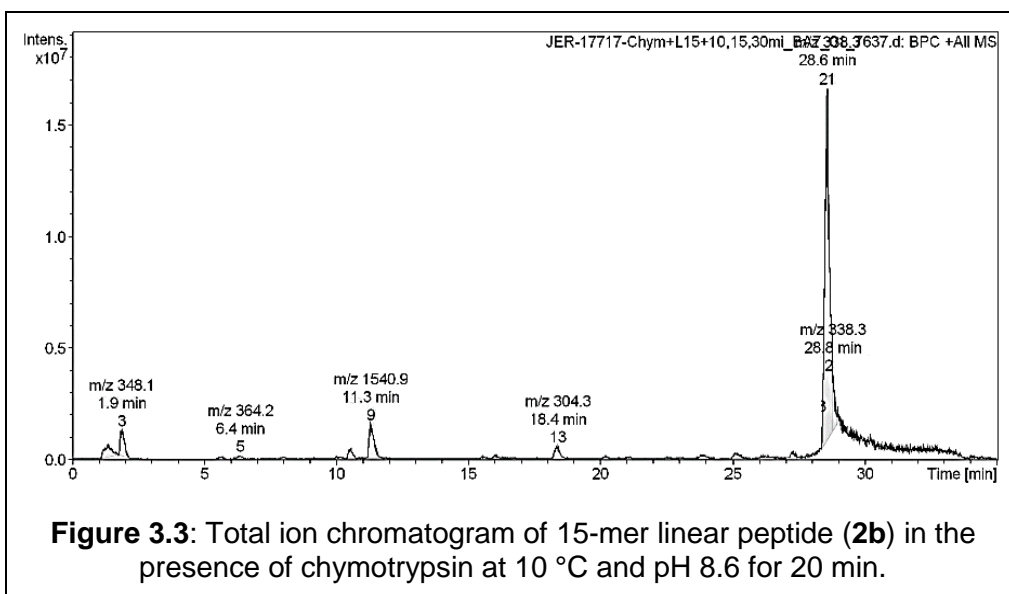
## 3.2.3 Enzymatic degradation and kinetic study of the 15-mer linear peptide (2b) in the presence of chymotrypsin

Figure B.5 in Appendix B depicts HPLC chromatograms of the reaction between chymotrypsin and 15-mer linear peptide (**2b**) at 10 °C, and pH 8.6 over 0–30 min. The purpose of these conditions was to obtain a lower rate of enzymatic hydrolysis for the peptides, consequently allowing the degradation of the peptides to be followed more precisely, as the reaction was very rapid under the standard conditions of 37 °C and pH 7.4. The peak at the retention time 12.39 min is for **2b**. The hydrolysis products were observable as new peaks even at the initial time point, shown in Figure 3.2. By the time the peak of **2b** began to decrease, several overlapping peaks with lower retention time had appeared; for example, a peak at the retention time of 7.51 min and a peak at the retention time of 10.39 min. The intensity of **2b** decreased to less than half at 30 min (See Figure 3.2).





The total ion chromatogram of the sample at 20 min of enzymatic reaction (Figure 3.3) demonstrated many peaks, 348.1, 364.2, 1540.9, 304.3  $m/z$  at the retention time 1.9, 6.4, 11.3, 18.4 min respectively. Also, a contamination peak was visible (338.3 at the retention time 28.8 min). None of the peaks matched the mass of any of the expected products (Table B.1 in Appendix B), except the peak of 348.1  $m/z$ . This was consistent with the theoretically calculated value of 348.2  $m/z$  for the protonated peptide (+1) which is peptide **2b1** in Scheme 3.1. As was expected, chymotrypsin cleaved the peptide bond between Trp and Thr. The structure of peptide **2b1** is shown in Figure 3.4. Hydrolysis of the *N*-terminal peptide bond between Phe and Leu may be slower than the hydrolysis of the bond between Trp and Thr.



The MS<sup>2</sup> mass analysis (Figure B.6 in Appendix B) for the peak of 348.1 *m/z* was evidence of the validity of the proposed structure for peptide **2b1** due to the observed peaks for the precursor ion (348.1 *m/z*) having masses consistent with the theoretically calculated values of peptide **2b1** (Table 3.3). The structures of the suggested fragments are in Table B.2 in Appendix B.

**Table 3.3:** The comparison between theoretically calculated peaks and the observed CID fragments of precursor ion 348.1 *m/z*, (peptide **2b1**) produced by hydrolysis of 15-mer linear peptide (**2b**) in the presence of chymotrypsin (See Figure B.6 in Appendix B).

No	Observed <i>m/z</i>	Calculated <i>m/z</i>	Suggested sequence
1	215.0	215.1	b <sub>2</sub>
2	247.0	247.1	y <sub>2</sub>
3	348.5	348.2	MH

The area of **2b** peaks in the HPLC chromatograms during its incubation with chymotrypsin at 10 °C and pH 8.6 for 0–30 min are reported in Table 3.4.

**Table 3.4:** Areas of 15-mer linear peptide (**2b**) peaks in the HPLC chromatograms during its digestion with chymotrypsin at 10 °C and pH 8.6.

Time (min)	Area	ln(area)
0	773347	13.558
2	601518	13.307
4	459869	13.038
6	418205	12.943
8	388694	12.87
10	374717	12.833
15	259918	12.468
20	186154	12.134
30	176984	12.083

The *t*<sub>½</sub> of **2b** was calculated by plotting the logarithm of the area of **2b** peaks against time, employing the Excel program. The value of *k* (0.0491 min<sup>-1</sup>) is the slope of the linear equation in Figure 3.5. The standard error (SE) was calculated from the linear regression using the LINEST function in the Excel program. Table 3.5 reveals the value of *t*<sub>½</sub> (14.11 ± 1.7 min).

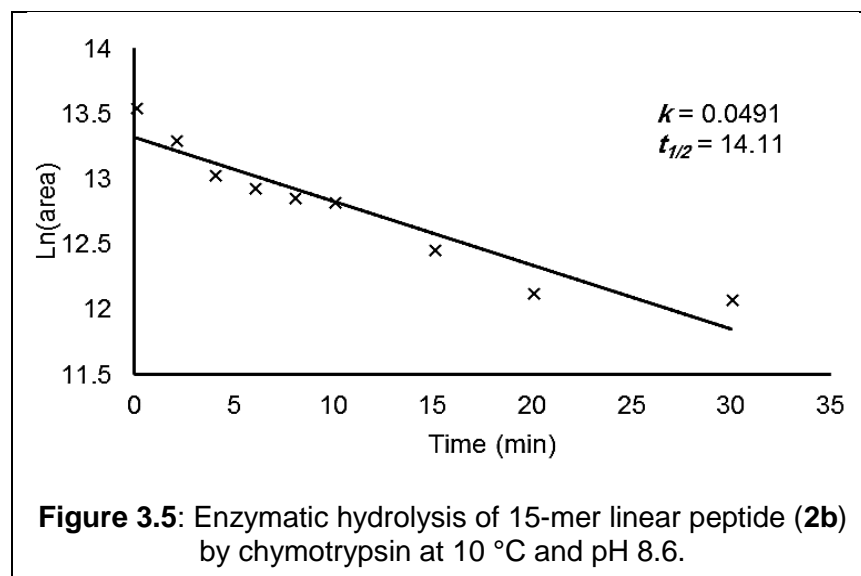


**Table 3.5:**  $t_{1/2}$  of 15-mer linear peptide (**2b**) during incubation with chymotrypsin at 10 °C and pH 8.6, including the rate constant ( $k \text{ min}^{-1}$ ) and the standard error (SE).

$k \text{ (min}^{-1}\text{)}$	SE	%Error of $k$	$t_{1/2} \text{ (min)}$	Error of $t_{1/2} \text{ (min)}$
0.0491	0.006	12	14.11	1.7

%error of  $k = 100 \times \text{SE} / k$

error of  $t_{1/2} = \% \text{error } k \times t_{1/2} / 100$

### 3.2.4 Enzymatic degradation and kinetic study of the 15-mer cyclic peptide (**2c**) in the presence of chymotrypsin and the comparison with its linear counterpart (**2b**)

Figure B.7 in Appendix B indicates the HPLC chromatograms of enzymatic hydrolysis of **2c** by chymotrypsin under the same conditions for hydrolysis of its linear counterpart (**2b**). The single sharp peak at the retention time 11.77 min is for **2c**. By the time the peak of **2c** began to decrease, a new peak had appeared with retention time of 13.99 min. The intensity of the new peak reached approximately the same intensity of **2c** at 10 min; then it became more intense at 20 min (See Figure 3.6).

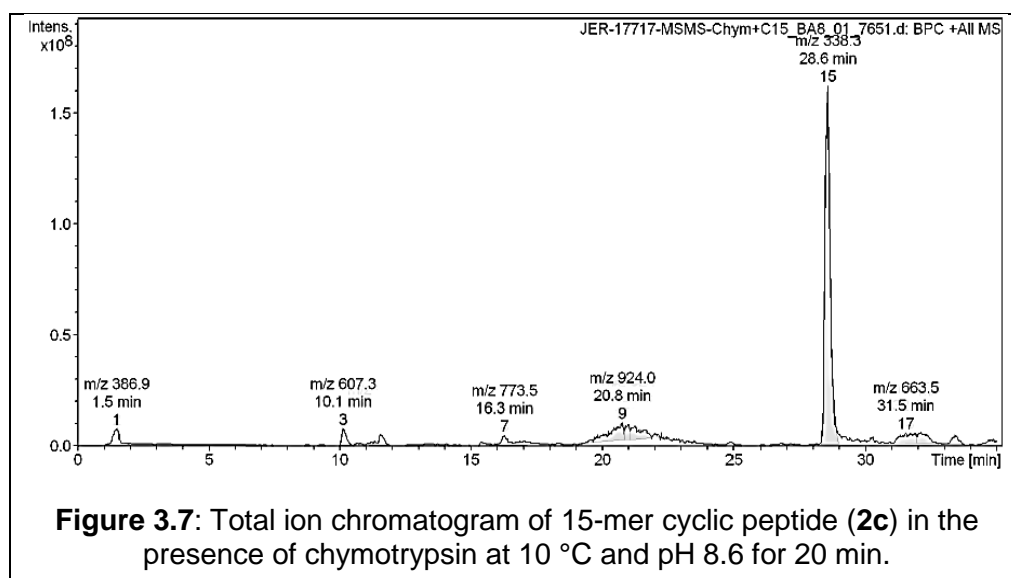
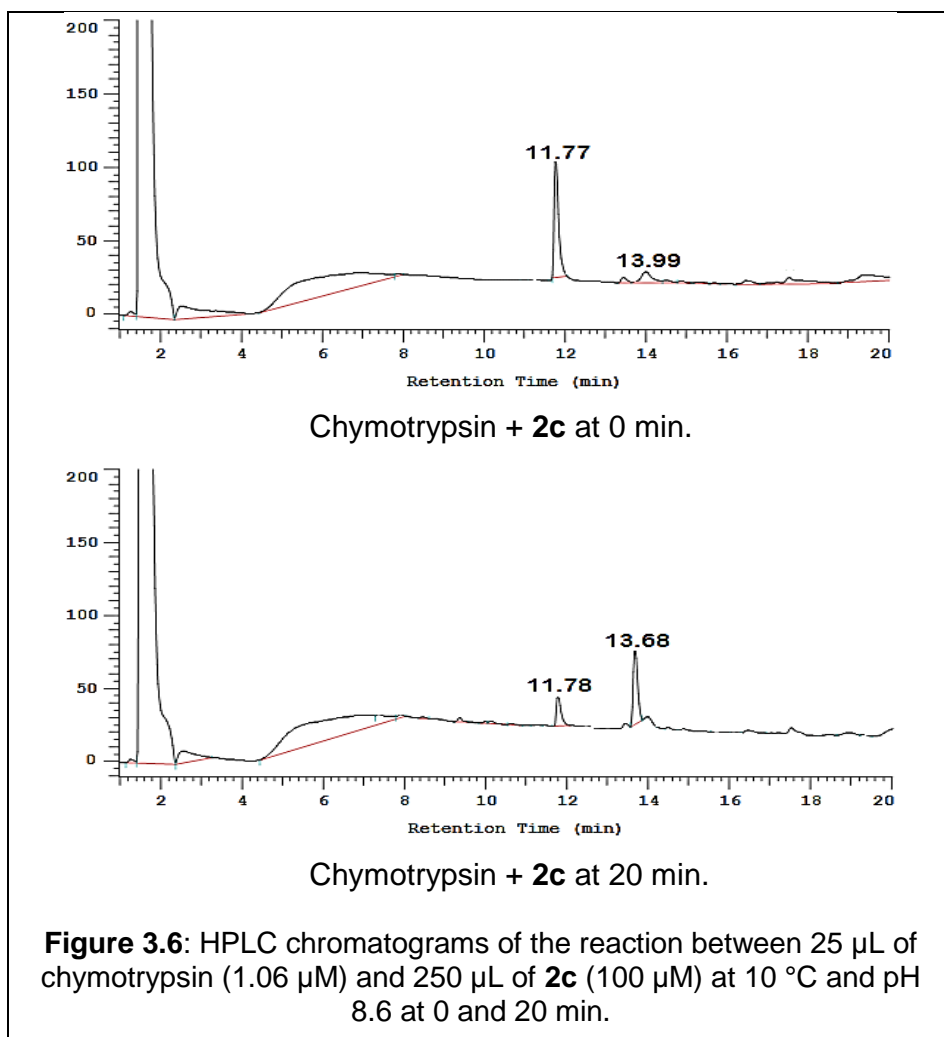
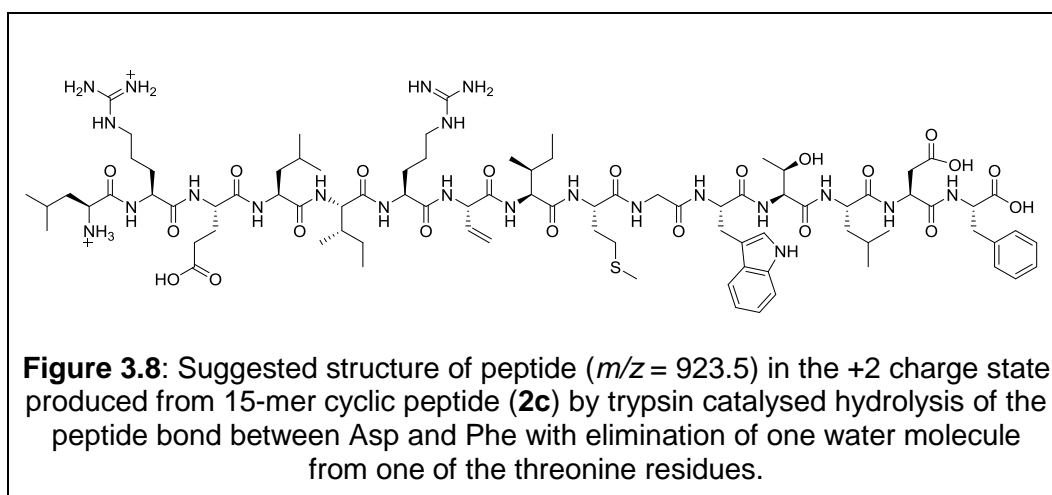
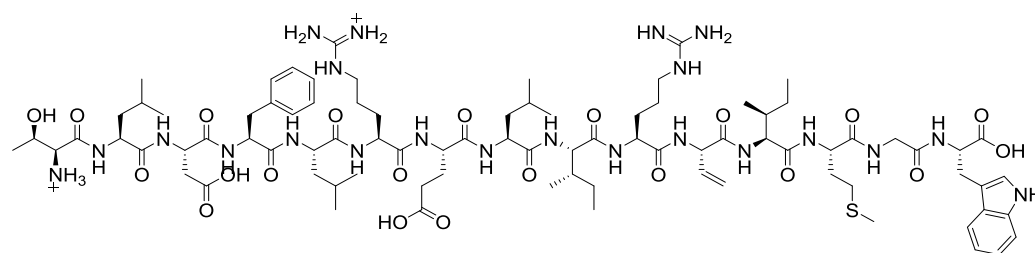


Figure 3.7 shows the total ion chromatogram of the 15-mer cyclic peptide (**2c**) at 20 min of the enzymatic reaction with chymotrypsin. The peak of 924.0

$m/z$  at the retention time 20.8 min could represent compound **2c**, as it was very close to the theoretically calculated value of 923.5  $m/z$  for **2c** in the +2 charge state as in Figure 2.28. However, this suggestion is inconsistent with the retention time of the genuine compound **2c** (See Figure 2.27) using the same method. Furthermore, this peak could represent the peptide in Figure 3.8 produced by the enzymatic cleavage of the peptide bond between Phe and Leu providing a 15-mer linear compound with elimination under the LC-MS conditions of one water molecule from a threonine residue. The mass of this peptide (923.5  $m/z$ ) was very close to the observed mass (924.0  $m/z$ ) in Figure 3.7. This suggestion is also unlikely because the HPLC retention time of this peptide (13.68 min) is different to the retention time of the very similar 15-mer linear peptide (**2b**) with the same enzyme (12.39 min) as shown in Figure 3.2. Moreover, the retention time of this peptide is different to the retention time of the genuine compound **2b** (12.67 min) as shown in Figure 2.17.

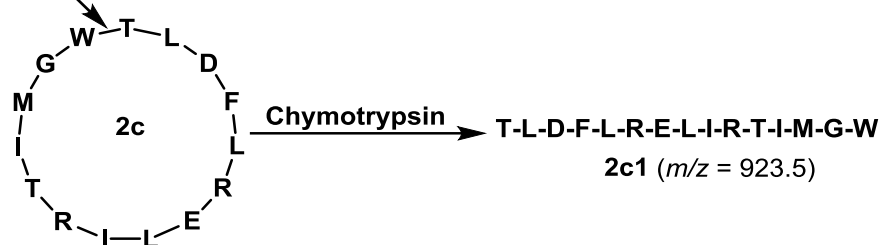


The peak of 924.0  $m/z$  could also represent the peptide in Figure 3.9 produced by cleavage of the peptide bond between Thr and Trp by chymotrypsin, in addition to elimination of a water molecule from one of the threonine residues as shown in Scheme 3.2 (peptide **2c1**).



**Figure 3.9:** Suggested structure of peptide **2c1** ( $m/z = 923.5$ ), in the +2 charge state produced from cyclic peptide (**2c**) by chymotrypsin catalysed hydrolysis of the peptide bond between Thr and Trp with elimination of a water molecule from one of the threonine residues.

Cleaved peptide bond



**Scheme 3.2:** Site of the cleaved peptide bond in 15-mer cyclic peptide (**2c**) by chymotrypsin at 10 °C and pH 8.6 for 20 min.

The MS<sup>2</sup> mass analysis for the precursor of 924.0  $m/z$  (Figure B.8 in Appendix B) supported the third-choice (peptide **2c1**) due to the fragmentation of this precursor ion to fragments that have peaks consistent with the theoretically calculated values for peptide **2c1** (Table 3.6). The structures of the suggested fragments are given in Table B.3 in Appendix B.

**Table 3.6:** The comparison between theoretically calculated peaks and the observed CID fragments of the precursor ion 924.0 *m/z* (peptide **2c1**) produced by hydrolysis of 15-mer cyclic peptide (**2c**) by chymotrypsin (See Figure B.8 in Appendix B).

No	Observed <i>m/z</i>	Calculated <i>m/z</i>	Suggested sequence
1	877.1	876.5	y <sub>7</sub>
2	590.0	590.3	b <sub>5</sub>
3	572.2	572.3	b <sub>5</sub> -H <sub>2</sub> O
4	562.0	562.3	a <sub>5</sub>
5	477.0	477.2	b <sub>4</sub>
6	330.0	330.2	b <sub>3</sub>
7	196.9	197.1	b <sub>2</sub> -H <sub>2</sub> O

It should be noted that the retention time of peptide **2c1** (924.0 *m/z*) was higher than the retention time of **2c**, although the total charge of **2c** is +2 while the full charge of peptide **2c1** is +3 in the acidic medium of the HPLC solvents. The restricted conformation of the 15-mer cyclic peptide (**2c**) was potentially enhancing the polarity of the compound that resulted in a lower retention time. In addition, peptide **2c1** (Figure 3.9) has greater HPLC retention time than that of **2b** (12.67 min) as in Figure 2.17, which has the same sequence but a different order of the amino acids. It appears that the different order of the amino acids for the same sequence of **2b** has a significant effect on the retention time of **2b**.

The other peaks of 386.9, 607.3, 773.5, 663.5 at 1.5, 10.1, 16.3, 31.5 min respectively in Figure 3.7 did not match the mass of any of the expected peptides produced by enzymatic hydrolysis of **2c** by chymotrypsin (See Table B.4 in Appendix B).

The *t*<sub>½</sub> of **2c** was calculated using the data in Table 3.7 by the same method that was used to calculate the *t*<sub>½</sub> of the 15-mer linear peptide (**2b**).



**Table 3.7:** Areas of 15-mer cyclic peptide (**2c**) peaks in the HPLC chromatograms during digestion with chymotrypsin at 10 °C and pH 8.6.

Time(min)	Area	ln(area)
0	549136	13.216
2	512582	13.147
4	497582	13.117
6	434692	12.982
8	343782	12.747
10	223228	12.315
15	211670	12.262
20	146052	11.891
30	96890	11.481

The linear regression shown in Figure 3.10 gave the value of  $k \text{ min}^{-1}$  (slope). Table 3.8 shows the value of  $t_{1/2}$  ( $11.07 \pm 0.9 \text{ min}$ ).

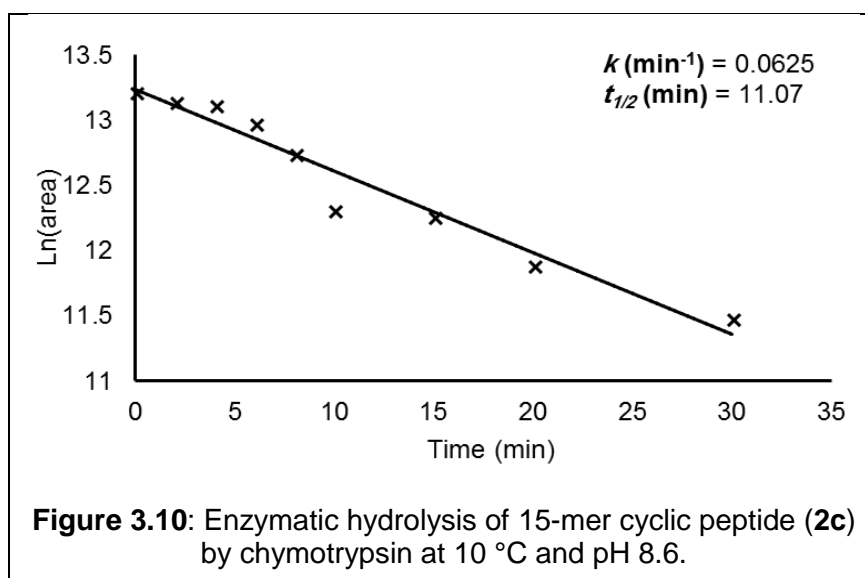


**Table 3.8:**  $t_{1/2}$  of 15-mer cyclic peptide (**2c**) during incubation with chymotrypsin at 10 °C and pH 8.6 including rate constant ( $k \text{ min}^{-1}$ ) and the standard error (SE).

$k (\text{min}^{-1})$	SE	%Error of $k$	$t_{1/2} (\text{min})$	Error of $t_{1/2} (\text{min})$
0.0626	0.005	8	11.07	0.9

It appears that the peptide bond between Phe and Asp in the two peptides (**2b**, **2c**) was not cleaved as rapidly by chymotrypsin as the peptide bond

between Trp and Thr. This result provides evidence that the conformation of the first peptide bond (Phe–Asp) has remained the same after cyclisation of the 15-mer linear peptide (**2b**) to form **2c** or the new orientation remains unsuitable as a substrate for the enzyme; consequently, it was not broken down by the enzyme. According to the HPLC chromatograms, the retention times for the peptides produced by hydrolysis of **2b** were less than the retention time of **2b**, while the retention time of the peptide that was generated by hydrolysis of **2c** was greater than the retention time of **2c**.

It should be noted that the  $t_{1/2}$  of **2c** ( $11.07 \pm 0.9$  min) was less than the  $t_{1/2}$  of **2b** ( $14.11 \pm 1.7$  min). It was concluded that the 15-mer cyclic peptide (**2c**) is less stable than its linear counterpart (**2b**) towards chymotrypsin-catalysed hydrolysis. This implies that cyclisation of **2b** did not boost the stability of the compound against the enzymatic hydrolysis by chymotrypsin. Potentially, the constricted conformation of the cyclic peptide (**2c**) was a more favourable substrate for chymotrypsin than its linear counterpart (**2b**). Consequently, in human serum the compound **2c** may stand less chance of reaching its target.

### 3.2.5 Enzymatic degradation and kinetic study of the 15-mer linear peptide (**2b**) in the presence of trypsin

Figure B.9 in Appendix B shows the HPLC chromatograms of the reaction between trypsin and 15-mer linear peptide (**2b**) over 0–20 min at 10 °C and pH 6.2. The purpose of these conditions was, as previously in the hydrolysis of **2b** by chymotrypsin, to retard degradation to more easily observable rates. The single sharp peak at the retention time 11.66 min is for the linear peptide (**2b**). As **2b** began to decrease, a new peak started to appear at the retention time 9.93 min. The intensity of the new peak reached approximately the same intensity as the linear peptide (**2b**) at 8 min, then it became greater at 10 min. The peak of **2b** disappeared completely at 15 min (See Figure 3.11).

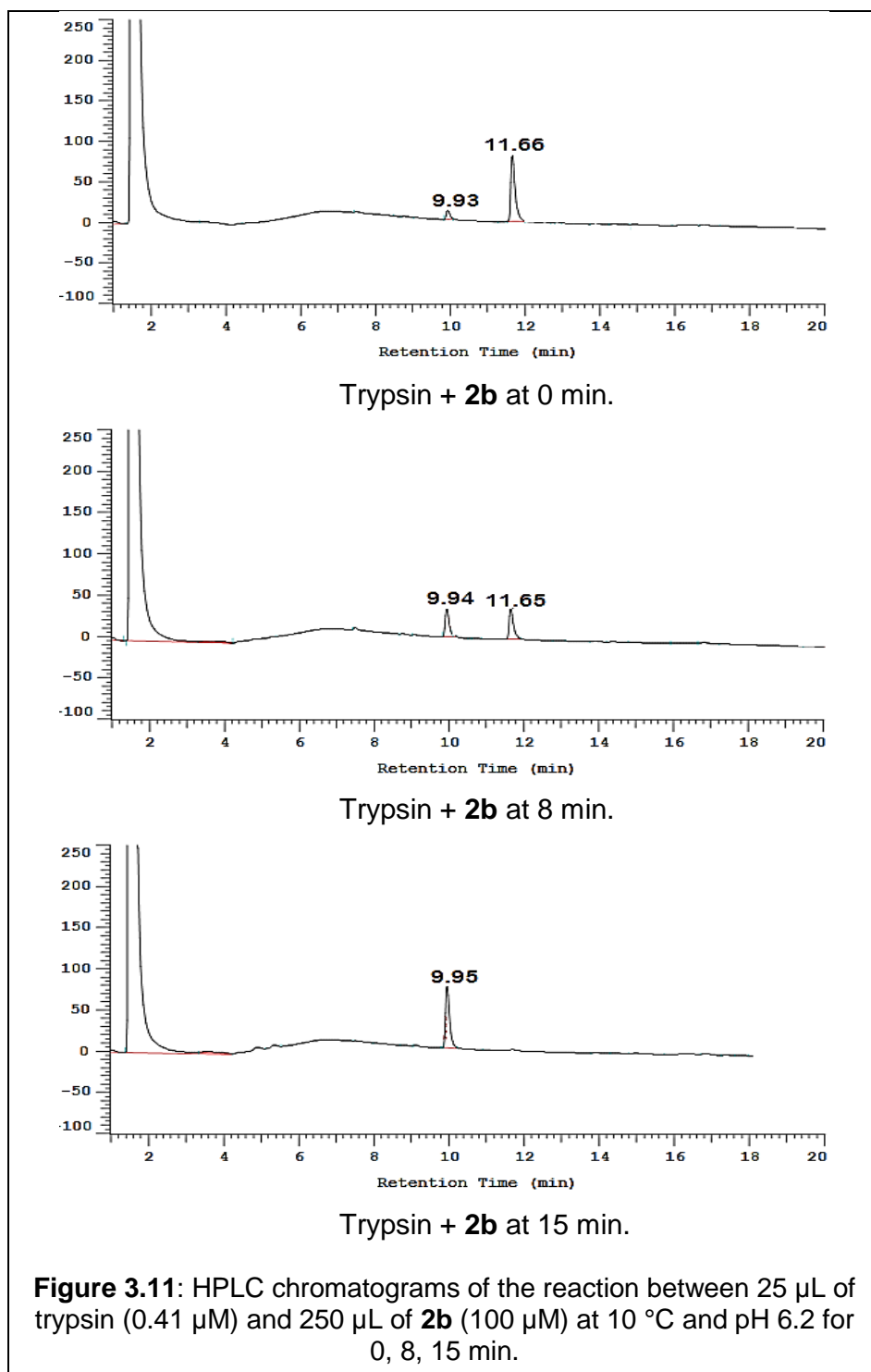
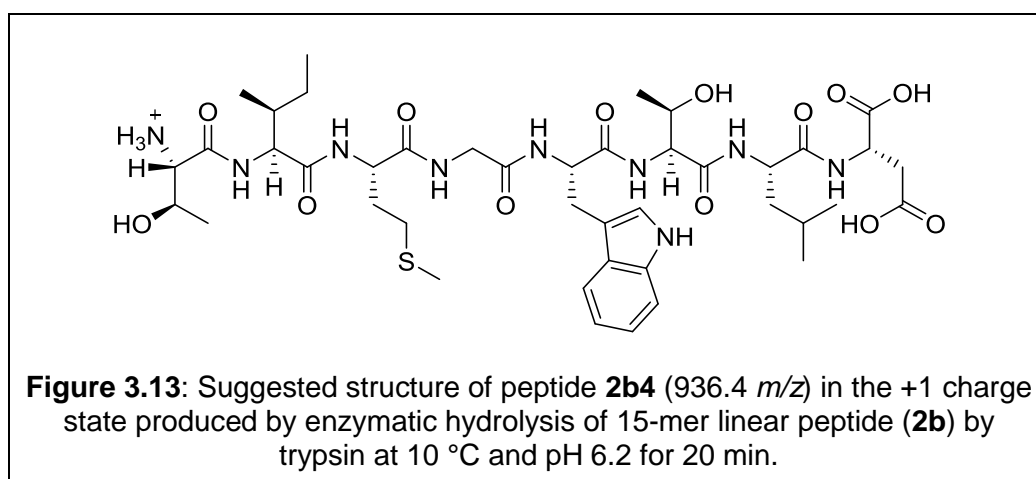
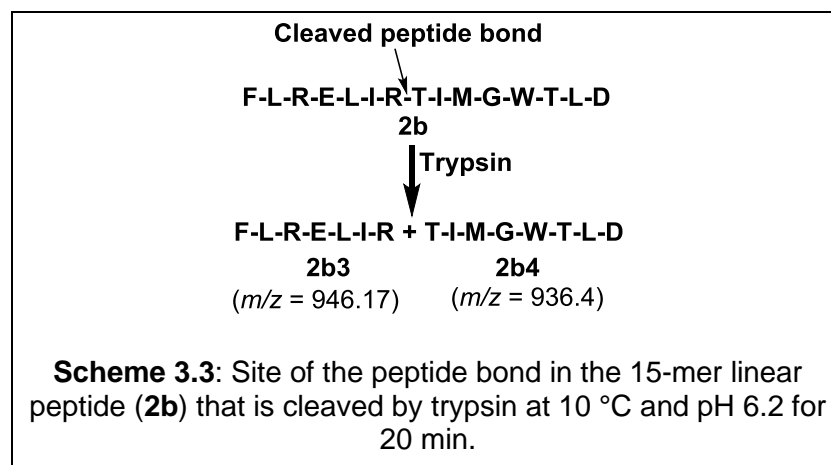
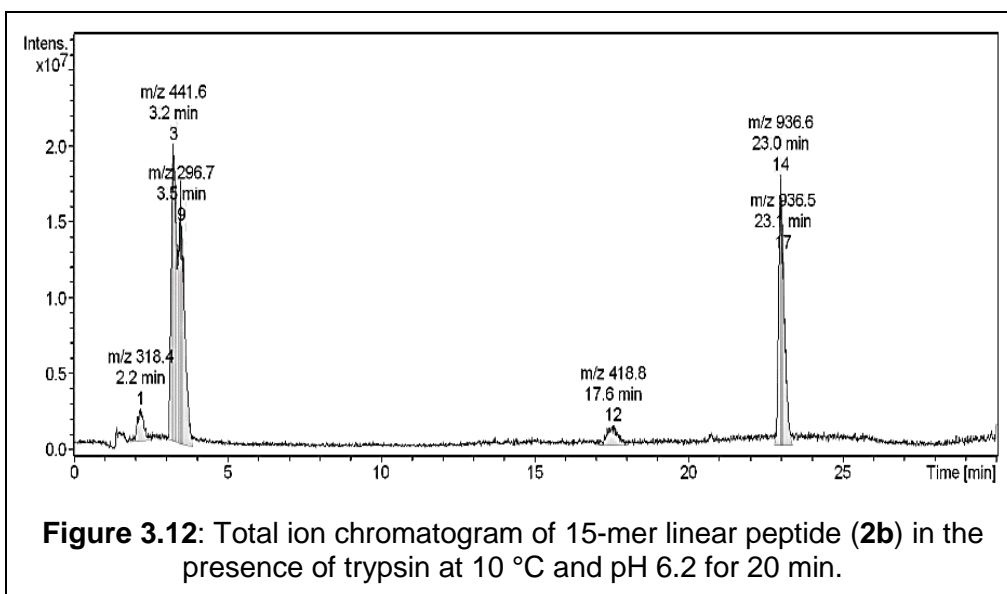


Figure 3.12 shows the total ion chromatogram of **2b** at a reaction time of 20 min in the presence of trypsin. The peak of 936.6  $m/z$  at the retention time 23.0 min was consistent with the theoretically calculated value of 936.4  $m/z$  for the protonated peptide (+1) which is peptide **2b4** in Scheme 3.3. As expected, trypsin cleaved the peptide bond between Arg and Thr; the suggested structure of peptide **2b4** is shown in Figure 3.13.



The MS<sup>2</sup> mass analysis for the precursor of 936.6 m/z (Figure B.10 in Appendix B) was evidence for the validity of the proposed structure of peptide

**2b4**, with the fragment peaks observed having masses consistent with the theoretical values (Table 3.9). All the structures of the proposed fragments for these peaks are shown in Table B.5 in Appendix B.

**Table 3.9:** The comparison between theoretically calculated peaks and the observed CID fragments of the precursor ion 936.6  $m/z$  (peptide **2b4**) produced by trypsin digestion of **2b** (Figure B.10 in Appendix B).

No	Observed $m/z$	Calculated $m/z$	Suggested sequence
1	918.4	918.4	MH-H <sub>2</sub> O
2	803.3	803.4	b <sub>7</sub>
3	785.3	785.4	b <sub>7</sub> -H <sub>2</sub> O
4	767.2	767.4	b <sub>7</sub> -2H <sub>2</sub> O
5	722.2	722.3	y <sub>6</sub>
6	690.1	690.3	b <sub>6</sub>
7	672.1	672.3	b <sub>6</sub> -H <sub>2</sub> O
8	573.0	573.3	y <sub>5</sub> -H <sub>2</sub> O

Peptide **2b3** (946.17  $m/z$ ), shown in Scheme 3.3, did not appear in the HPLC chromatograms or the total ion chromatogram. Potentially this compound eluted with the DMSO solvent front due to its polarity. The other peaks (318.4, 441.6, 296.7, 418.8  $m/z$  at 2.2, 3.2, 3.5, 17.6 min respectively) in Figure 3.12 did not match any expected  $m/z$  ratio. Table B.6 in Appendix B indicates all the expected masses produced by enzymatic hydrolysis of **2b** by trypsin.

The peptide bond between Arg and Glu did not hydrolyse. An adverse effect on enzymatic cleavage due to negatively charged amino acids such as Glu surrounding the cleavage site was previously observed during a study of protein identification in proteomics.<sup>194</sup> Furthermore, the intramolecular hydrogen bonds between the side groups of the two amino acids (Arg, Glu) may also shield the peptide bond from being cleaved by the trypsin.

A kinetic study of digestion of **2b** by trypsin was undertaken; the data are shown in Table 3.10. Areas of HPLC peaks of **2b** were determined during its enzymatic hydrolysis by trypsin at 10 °C and pH 6.2 for 0–10 min.

**Table 3.10:** Areas of 15-mer linear peptide (**2b**) peaks in the HPLC chromatograms during trypsin digestion at 10 °C and pH 6.2.

Time (min)	Area	ln(area)
0	572744	13.258
2	439664	12.993
4	346068	12.754
6	344968	12.751
8	259532	12.466
10	241908	12.396

The  $t_{1/2}$  of **2b** was computed in the same way that was used to calculate the  $t_{1/2}$  of the same compound in the presence of chymotrypsin.  $k \text{ min}^{-1}$  (slope) was obtained from Figure 3.14 (a plot of ln area versus time). Table 3.11 includes the value of  $t_{1/2}$  ( $8.23 \pm 0.8 \text{ min}$ ).

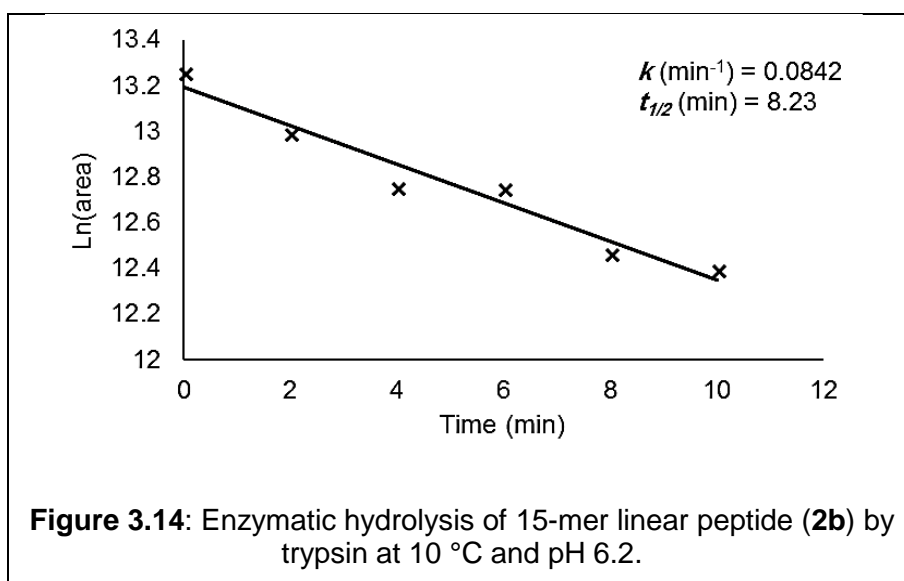


**Table 3.11:**  $t_{1/2}$  of 15-mer linear peptide (**2b**) in the presence of trypsin at 10 °C and pH 6.2, including the rate constant ( $k \text{ min}^{-1}$ ) and the standard error (SE).

$k \text{ (min}^{-1}\text{)}$	SE	%Error of $k$	$t_{1/2} \text{ (min)}$	Error of $t_{1/2} \text{ (min)}$
0.0842	0.009	10	8.23	0.8

### 3.2.6 Enzymatic degradation and kinetic study of the 15-mer cyclic peptide (**2c**) in the presence of trypsin and the comparison with its linear counterpart (**2b**)

Figure B.11 in Appendix B shows the HPLC chromatograms of the reaction between trypsin and **2c** at 10 °C and pH 6.2 over 0–30 min. The single peak at the retention time 11.75 min corresponds to **2c**. The effect of the trypsin on **2c** first became apparent at 2 min, where a new peak was visible at the retention time 12.48 min. By the time the intensity of **2c** peak began to drop, the intensity of the new peak had increased up until 10 min, when a second new peak appeared at the retention time 10.95 min. The intensity of the two new peaks continued to increase until after 30 min the first new peak (12.56 min) became more intense than the peak of **2c** (See Figure 3.15).

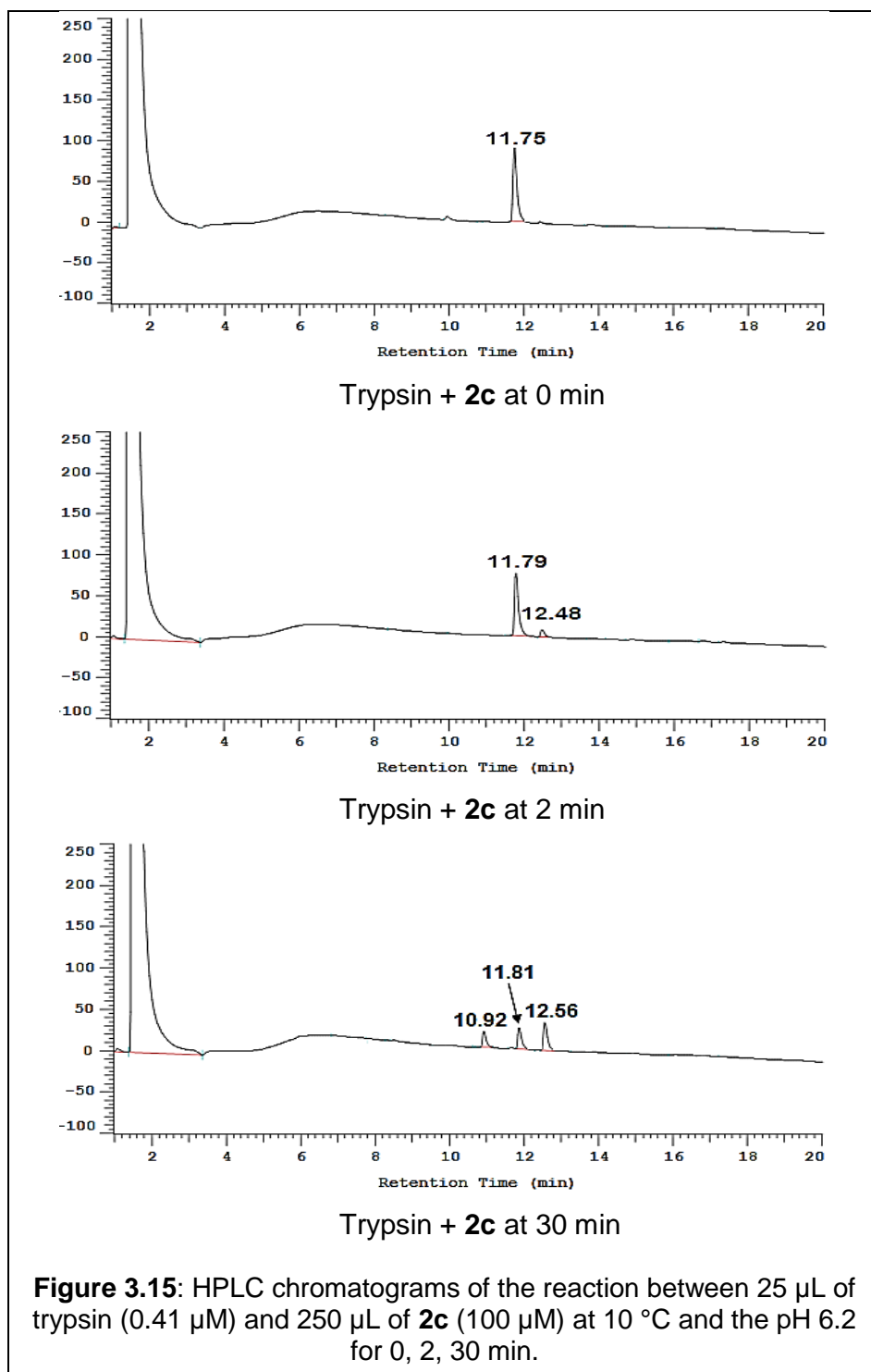
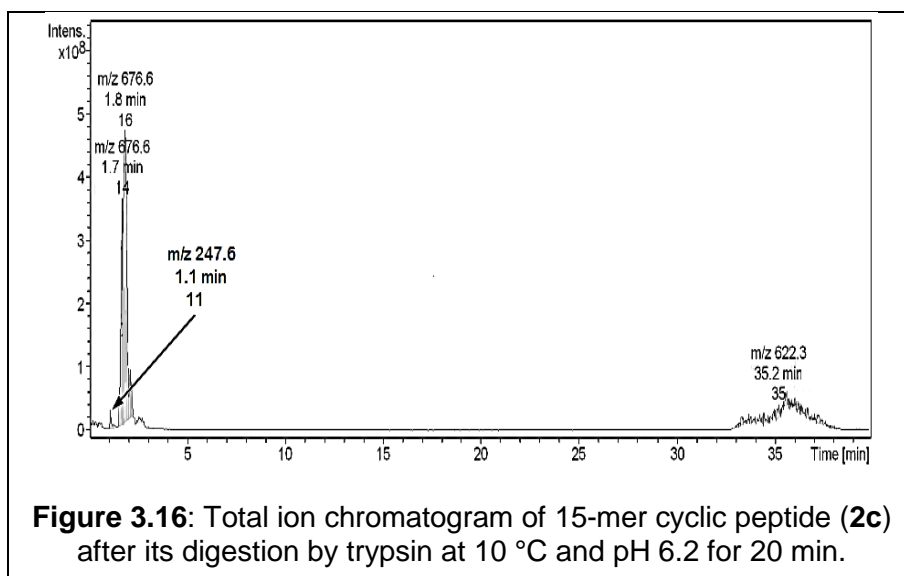
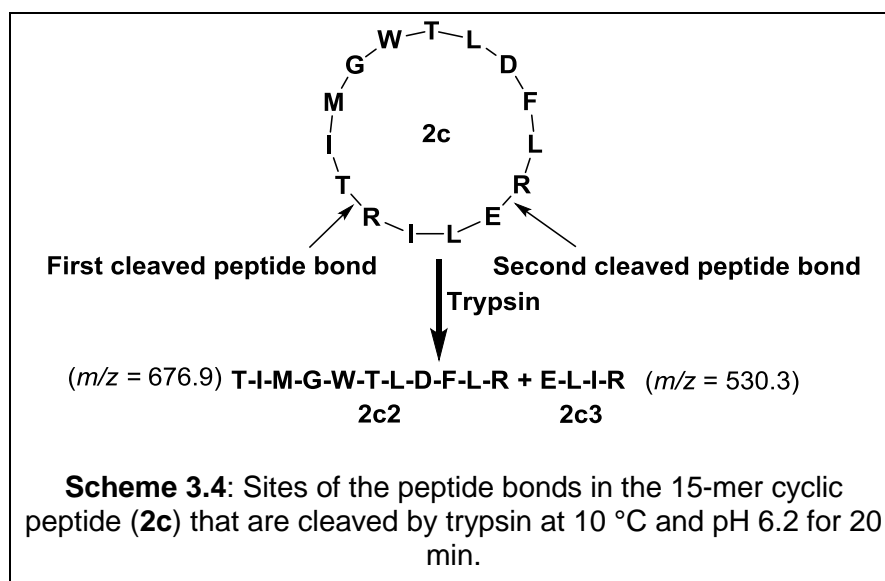


Figure 3.16 is the total ion chromatogram of **2c** after 20 min in the presence of trypsin. More than one peak appeared in this chromatogram; the peak of 676.6  $m/z$  at the retention time 1.8 min, which potentially represented the first new peak at 12.48 min in the HPLC chromatogram.





As was expected, the sites of the peptide bonds cleaved by trypsin in compound **2c** are between Arg and Thr, Arg and Glu. The sequence of the peptide which has a peak of 676.6  $m/z$  is shown in Scheme 3.4 (peptide **2c2**). The suggested structure of peptide **2c2** is given in Figure 3.17.



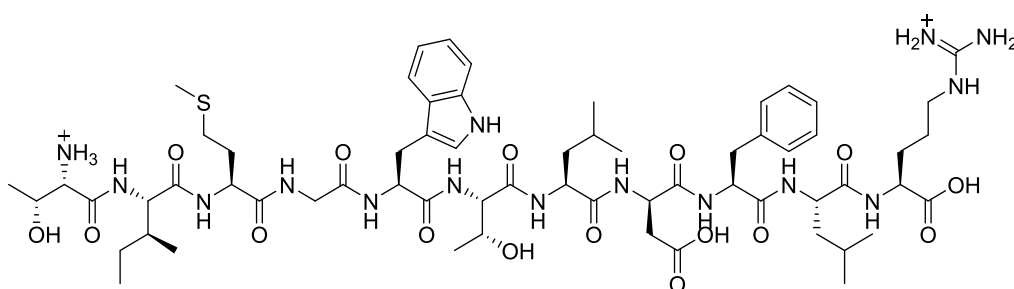


**Figure 3.17:** Suggested structure of peptide **2c2** (676.9  $m/z$ ) in the +2 charge state produced by enzymatic hydrolysis of 15-mer cyclic peptide (**2c**) in the presence of trypsin where the peptide bonds between Arg and Thr, Arg and Glu were cleaved.

The MS<sup>2</sup> mass analysis for the precursor ion (peptide **2c2**) which has the peak of 676.6  $m/z$  is illustrated in Figure B.12 in Appendix B and provided evidence for the validity of the proposed structure of peptide **2c2**, with peaks observed that have masses consistent with the theoretically calculated values (Table 3.12). All the structures of the proposed fragments for these peaks are in Table B.7 in Appendix B.

**Table 3.12:** The comparison between theoretically calculated peaks and the observed CID fragments of the precursor ion 676.6  $m/z$  (peptide **2c2**) produced by enzymatic hydrolysis of **2c** in the presence of trypsin (See Figure B.12 in Appendix B).

No	Observed $m/z$	Calculated $m/z$	Suggested sequence
1	1178.6	1178.6	b <sub>10</sub>
2	1160.7	1160.6	b <sub>10</sub> -H <sub>2</sub> O
3	1138.7	1138.6	y <sub>9</sub>
4	1121.7	1121.5	y <sub>9</sub> -NH <sub>3</sub>
5	1007.6	1007.5	y <sub>8</sub>
6	950.5	950.5	y <sub>7</sub>
7	803.2	803.4	b <sub>7</sub>
8	785.4	785.4	b <sub>7</sub> -H <sub>2</sub> O
9	764.3	764.4	y <sub>6</sub>

The peak of 247.6  $m/z$  at the retention time 1.1 min (Figure 3.16) has a mass that did not match the mass of the second expected peptide (530.3  $m/z$ )

produced by trypsin which has the sequence given in Scheme 3.4 (peptide **2c3**). The suggested structure for this second peptide is in Figure 3.18. The MS<sup>2</sup> mass for the precursor ion 247.6 *m/z* is illustrated in Figure B.13 in Appendix B.

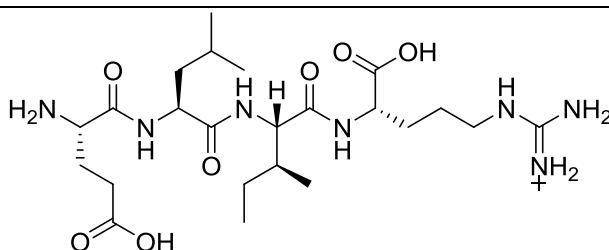


**Figure 3.18:** Suggested structure of peptide **2c3** (*m/z* = 530.3) in the +1 charge state produced by enzymatic hydrolysis of 15-mer cyclic peptide (**2c**) in the presence of trypsin where the peptide bonds between Arg and Thr, Arg and Glu were cleaved.

The third observed peak in the mass spectrum (Figure 3.16) is 622.3 *m/z* at the retention time 35.2 min. Although the mass of this peak is consistent with the mass of **2b** in the +3 charge state (Figure 3.19), the MS<sup>2</sup> mass spectrum (Figure B.14 in Appendix B) did not support this assignment. The observed peaks for the fragmentation of the precursor ion which has the peak of 622.0 *m/z* differ from theoretically calculated values for **2b** (See Table 2.8). Therefore, this peak was potentially due to contamination of the column.

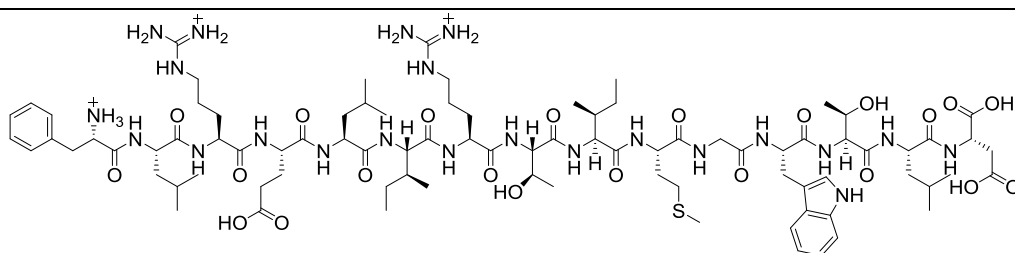


**Figure 3.19:** Structure of 15-mer linear peptide (**2b**) in the +3 charge state (*m/z* = 622.0).

The peak of 11.89 min in the HPLC chromatogram of 20 min for **2c** (Figure B.11 in Appendix B) did not appear in the mass spectrum. Possibly some of the trypsin remained active after conclusion of the reaction and storage for 24 h in the freezer, leading to the conversion of all the cyclic compound (**2c**) to the two new compounds.

A kinetic study for the 15-mer cyclic peptide (**2c**) during digestion with trypsin was performed and the data given in Table 3.13.

**Table 3.13:** Areas of 15-mer cyclic peptide (**2c**) peaks in the HPLC chromatograms during digestion with trypsin at 10 °C and pH 6.2.

Time(min)	Area	ln(area)
0	594329	13.295
2	509911	13.141
4	417448	12.941
6	414081	12.933
8	396831	12.891
10	387189	12.866
15	315297	12.661
20	177260	12.085
30	160943	11.988

The  $t_{1/2}$  of **2c** was computed in the same way that was used to calculate the  $t_{1/2}$  of the same compound in the presence of chymotrypsin.  $k \text{ min}^{-1}$ (slope) was obtained from Figure 3.20 (a plot of ln area versus time). Table 3.14 includes the value of  $t_{1/2}$ . ( $15.53 \pm 1.4 \text{ min}^{-1}$ ).

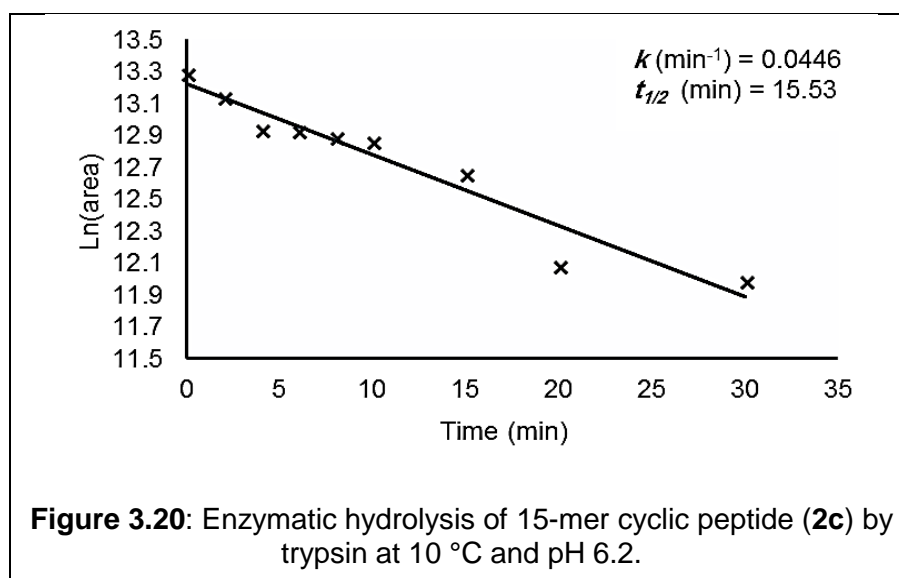


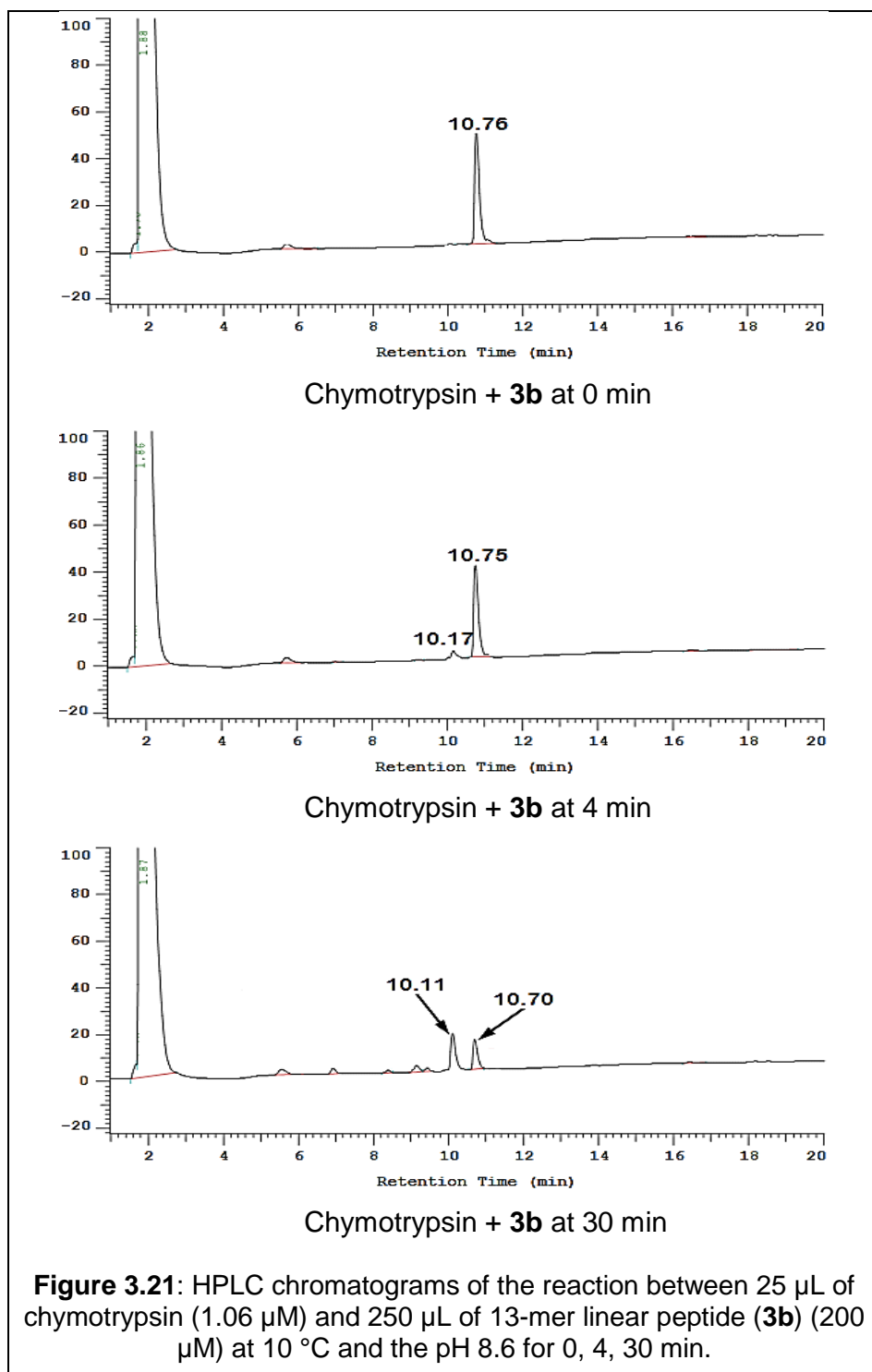
**Table 3.14:**  $t_{1/2}$  of 15-mer cyclic peptide (**2c**) during digestion with trypsin at 10 °C and pH 6.2, including the value of rate the constant ( $k \text{ min}^{-1}$ ) and the standard error (SE).

$k \text{ (min}^{-1}\text{)}$	SE	%Error of $k$	$t_{1/2} \text{ (min)}$	Error of $t_{1/2} \text{ (min)}$
0.0446	0.004	9	15.53	1.4

According to the results in the HPLC chromatograms for the two compounds (**2b**, **2c**), hydrolysis of the linear peptide (**2b**) by trypsin occurred at the peptide bond between Arg and Thr. The peptide identified in this reaction, **2b4** in Scheme 3.3, provided evidence for this cleaved peptide bond site, while the cyclic peptide (**2c**) was cleaved at the peptide bond between Arg and Thr in addition to Arg and Glu. The identified peptide **2c2** in Scheme 3.4 was evidence for these two cleaved peptide bond sites. It should be noted that the linear peptide (**2b**) disappeared completely after 20 min, while the cyclic peptide (**2c**) was still present at 30 min. This result indicated that the stability of the cyclic peptide (**2c**) against trypsin was greater than the stability of its linear counterpart (**2b**) at 10 °C and pH 6.2. The  $t_{1/2}$  of the two compounds (**2b**, **2c**) supported this result, with the  $t_{1/2}$  of **2c** ( $15.53 \pm 1.4 \text{ min}$ ) greater than the  $t_{1/2}$  of **2b** ( $8.23 \pm 0.8 \text{ min}$ ). Possibly the restricted conformation of **2c** rendered this compound less suitable as a substrate for the enzyme. Therefore, compound **2c** should have a greater chance of reaching the target than its linear counterpart (**2b**).

### 3.2.7 Enzymatic degradation and kinetic study of the 13-mer linear peptide (**3b**) in the presence of chymotrypsin

Figure B.15 in Appendix B shows the HPLC chromatograms of the reaction between chymotrypsin and 13-mer linear peptide (**3b**) at 10 °C and pH 8.6 over 0–30 min. The peak at the retention time 10.76 min is for **3b**. The effect of hydrolysis of **3b** became apparent at 4 min, where the first new peak was visible at the retention time 10.17 min. The intensity of the new peak increased and became more intense than the peak of **3b** after 30 min (See Figure 3.21).



As expected, chymotrypsin cleaved the peptide bond between Trp and Thr as shown in Scheme 3.5.

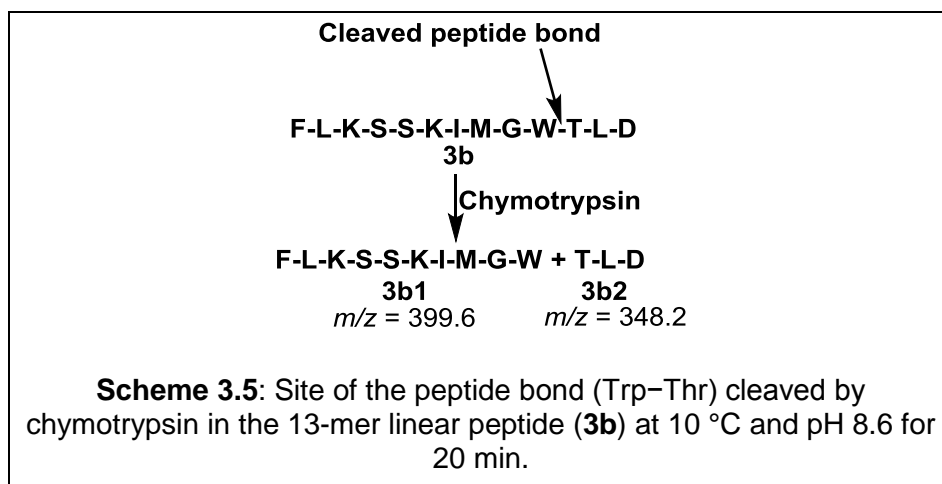
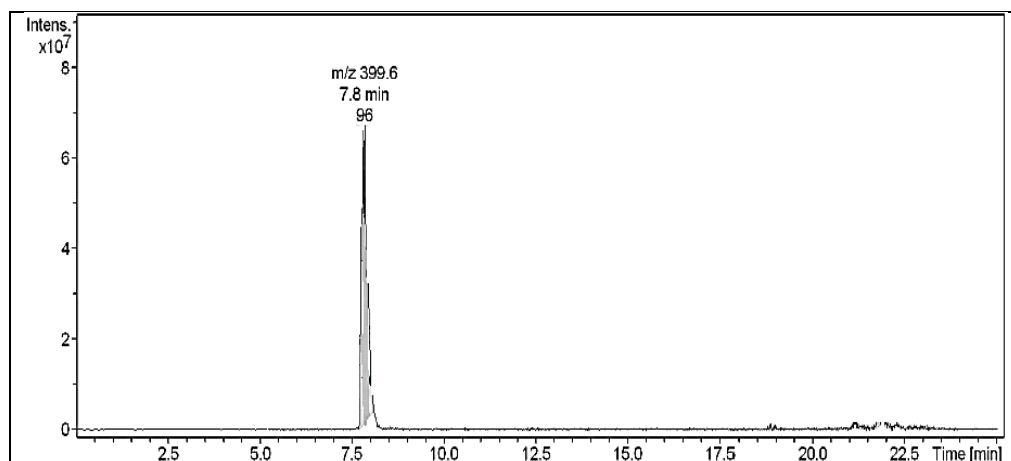
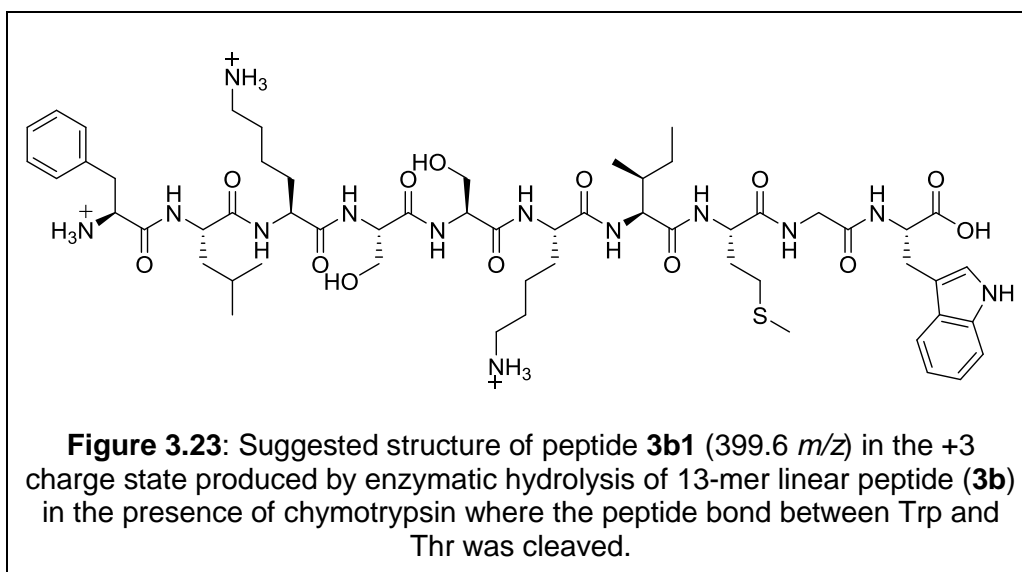


Figure 3.22 shows the total ion chromatogram of **3b** after 20 min of enzymatic reaction in the presence of chymotrypsin. The peak of 399.6  $m/z$  at the retention time 7.8 min was consistent with the theoretically calculated value of 399.6  $m/z$  for the compound in the +3 charge state (peptide **3b1** in Scheme 3.5). The suggested structure of this peptide is shown in Figure 3.23.



**Figure 3.22:** Total ion chromatogram of 13-mer linear peptide (**3b**) after digestion by chymotrypsin at 10 °C and pH 8.6 for 20 min.



The MS<sup>2</sup> mass spectrum for the precursor of 399.6 *m/z* (See Figure B.16 in Appendix B) provided evidence for the validity of the proposed structure for peptide **3b1**, due to the observed peaks that were consistent with the theoretically calculated values for the compound (Table 3.15). All the structures of these proposed fragments are in Table B.8 in Appendix B.

**Table 3.15:** The comparison between theoretically calculated peaks and the observed CID fragments of the precursor ion 399.6 *m/z* (peptide **3b1**) produced by enzymatic hydrolysis of 13-mer linear peptide (**3b**) in the presence of chymotrypsin (See Figure B.16 in Appendix B).

No	Observed <i>m/z</i>	Calculated <i>m/z</i>	Suggested sequence
1	344.2	344.2	a <sub>3</sub> -NH <sub>3</sub>
2	361.3	361.3	a <sub>3</sub>
3	389.3	389.3	b <sub>3</sub>
4	476.3	476.3	b <sub>4</sub>
5	546.3	546.3	b <sub>5</sub> -NH <sub>3</sub>
6	646.4	646.4	a <sub>6</sub> -NH <sub>3</sub>
7	663.3	663.3	a <sub>6</sub>
8	759.5	759.5	a <sub>7</sub> -NH <sub>3</sub>
9	776.5	776.5	a <sub>7</sub>
10	1179.6	1179.6	MH-NH <sub>3</sub>

A peak from remaining **3b** (Figure 3.21, peak 10.70 min) did not appear in the mass spectrum for the sample at 30 min (Figure 3.22). It is possible that



the enzyme was still active after completion of the reaction step for the chymotrypsin and 24 h storage in the freezer, leading to essentially complete conversion of **3b** to the product.

Peptide **3b2** (348.2 *m/z*), shown in Scheme 3.5, did not appear in the HPLC chromatograms and the total ion chromatogram; potentially this compound eluted with the DMSO solvent front due to its polarity.

The peptide bond between Phe and Leu in **3b** (Scheme 3.5) that was expected to be cleaved by chymotrypsin was left intact. During the entire time series, HPLC chromatograms did not show any second peak in addition to the new peak at the retention time 10.11 min (Figure 3.21). The conformation of the 13-mer linear peptide (**3b**) possibly prevented the peptide from occupying the active site. In addition, the presence of the charged amino group on the Phe residue at the *N*-terminus may have been negatively affecting the enzymatic interactions with neighbouring amino acids thus inhibiting the hydrolysis.

The  $t_{1/2}$  of **3b** was computed using the data in Table 3.16 in the same way that was used to calculate the  $t_{1/2}$  of the 15-mer linear peptide (**2b**) with the same enzyme.

**Table 3.16:** Areas of 13-mer linear peptide (**3b**) peaks in the HPLC chromatograms during digestion with chymotrypsin at 10 °C and pH 8.6.

Time (min)	Area	ln(area)
0	379560	12.846
2	353080	12.774
4	305907	12.631
6	247309	12.418
8	231773	12.353
10	203199	12.221
15	195252	12.182
20	118676	11.684
30	92130	11.430

Figure 3.24 (a plot of ln area versus time) gave the value of  $k$  ( $\text{min}^{-1}$ ). Table 3.17 includes the value of  $t_{1/2}$  ( $14.35 \pm 0.9$  min).

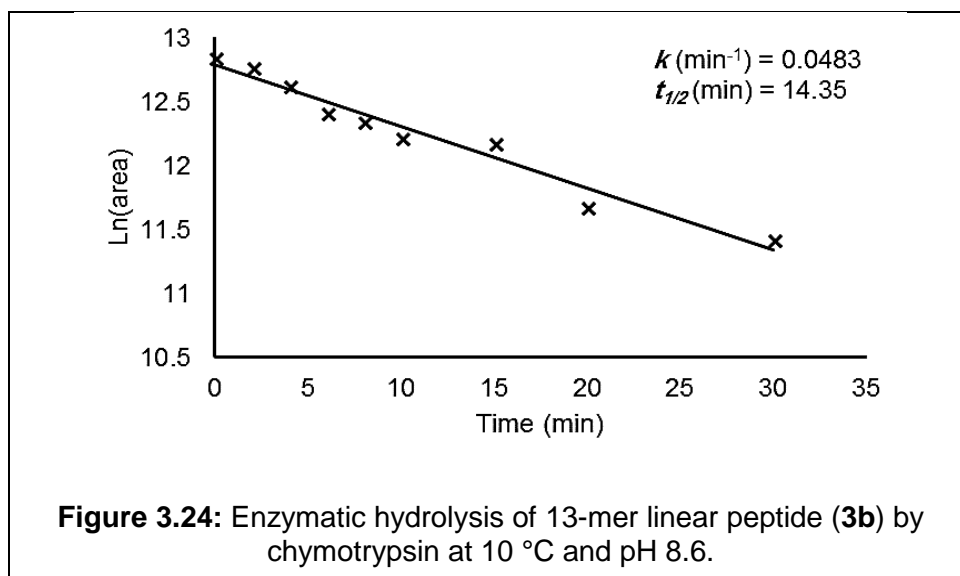


**Table 3.17:**  $t_{1/2}$  of 13-mer linear peptide (**3b**) during digestion with chymotrypsin at 10 °C and pH 8.6, including the value of the rate constant ( $k \text{ min}^{-1}$ ) and the standard error (SE).

$k \text{ (min}^{-1}\text{)}$	SE	%Error of $k$	$t_{1/2} \text{ (min)}$	Error of $t_{1/2} \text{ (min)}$
0.0483	0.003	6	14.35	0.9

### 3.2.8 Enzymatic degradation and kinetic study of the 13-mer cyclic peptide (**3c**) in the presence of chymotrypsin and the comparison with its linear counterpart (**3b**)

Figure B.17 in Appendix B shows the HPLC chromatograms of the reaction between the chymotrypsin and 13-mer cyclic peptide (**3c**) at 10 °C and pH 8.6 over 0–20 min. The peak at the retention time 14.71 min corresponds to the cyclic peptide (**3c**). The effect of hydrolysis by the chymotrypsin on **3c** is apparent after 4 min, where a new peak is visible at a retention time of 11.41 min. By the time that the intensity of **3c** began to decrease, the intensity of the new peak increases. The intensity of **3c** decreased to almost half of its value at 15 min, then less than half at 20 min (See Figure 3.25).

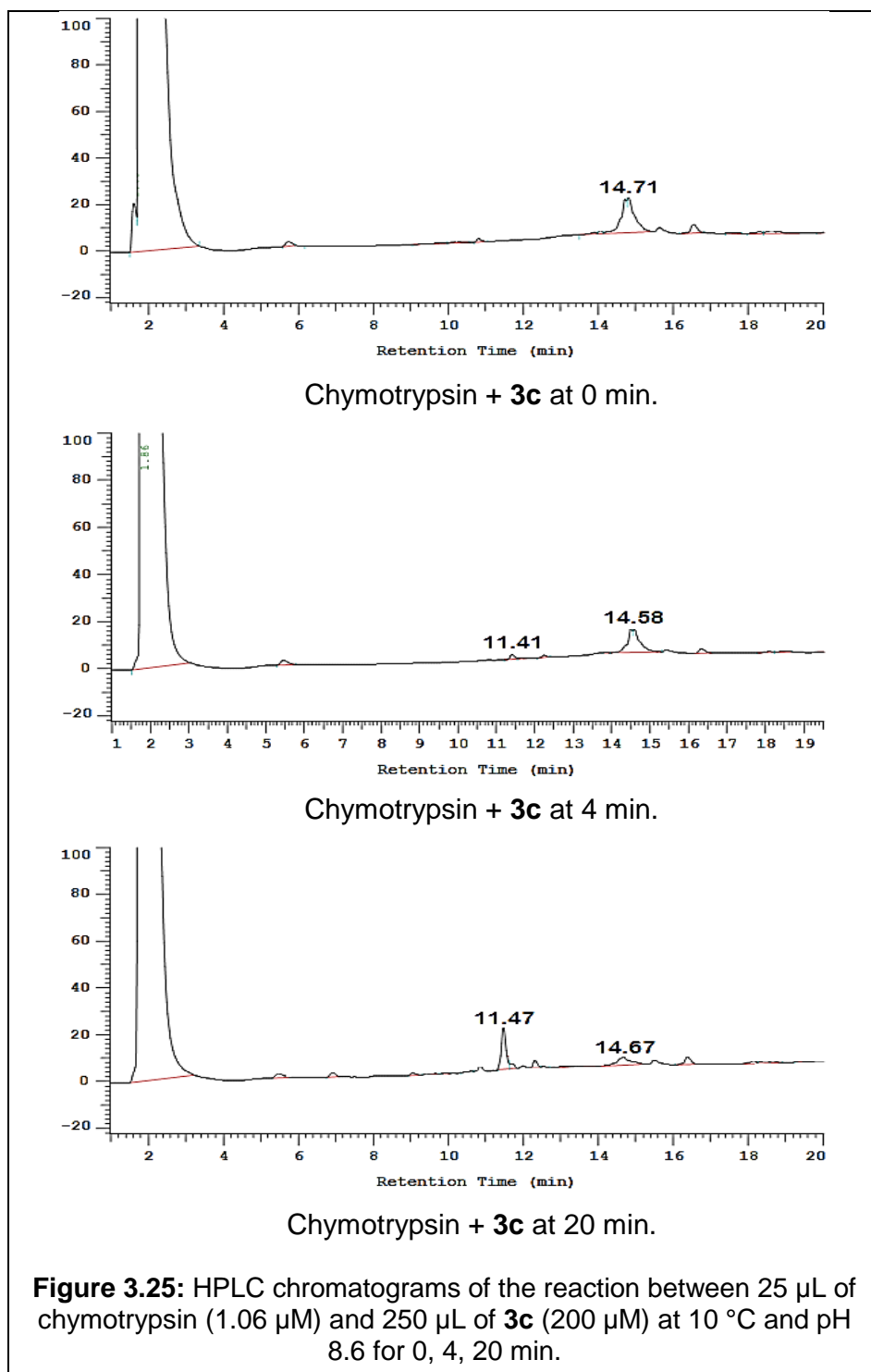


Figure 3.26 is a total ion chromatogram of the 13-mer cyclic peptide (**3c**) at 20 min of the enzymatic hydrolysis by chymotrypsin. As expected, chymotrypsin cleaved the peptide bond between Thr and Trp, as shown in Scheme 3.6. The peak of 763.5  $m/z$  at the retention time 5.2 min in Figure 3.26 was consistent with the theoretically calculated value of 763.4  $m/z$  for peptide



theoretically calculated values for the peptide (Table 3.18). The structures of all the suggested fragments from the precursor ion (peptide **3c1**) with 763.5  $m/z$  are shown in Table B.9 in Appendix B.

**Table 3.18:** The comparison between theoretically calculated peaks and the observed CID fragments of the precursor ion 763.5  $m/z$  (peptide **3c1**) produced by enzymatic hydrolysis of **3c** in the presence of chymotrypsin (See Figure B.18 in Appendix B).

No	Observed $m/z$	Calculated $m/z$	Suggested sequence
1	262.0	262.1	y <sub>2</sub>
2	330.2	330.2	b <sub>3</sub>
3	477.3	477.2	b <sub>4</sub>
4	572.3	572.3	b <sub>5</sub> -H <sub>2</sub> O
5	808.4	808.4	y <sub>7</sub>
6	875.6	875.5	b <sub>8</sub> -NH <sub>3</sub>
7	936.6	936.5	y <sub>8</sub>
8	1020.8	1020.6	b <sub>9</sub>
9	1133.8	1133.7	b <sub>10</sub>
10	1264.9	1264.7	b <sub>11</sub>

The peptide bond in **3c** between Phe and Leu that was expected to be cleaved by chymotrypsin to result in the peptide TLDF remained intact. The HPLC chromatograms for the entire time series (Figure B.17 in Appendix B) showed no additional peaks that could correspond to this peptide. It is possible that the conformation of the 13-mer cyclic peptide (**3c**) prevented it from occupying the active site of the enzyme, or potentially the enzymatic hydrolysis at this site was slow due to the same cause (local conformation of the peptide); thus, the HPLC detector was not sufficiently sensitive to detect this product. Moreover, the masses (495.2)<sup>1+</sup>, (477.2)<sup>1+</sup>  $m/z$  corresponding to the protonated peptide (TLDF) and protonated peptide with the elimination of a water molecule from the threonine residue respectively did not match with any one of the peaks 387.0, 896.3, 718.1, 415.3, 927.4  $m/z$  at 2.0, 5.5, 5.7, 6.4, 11.2 min respectively in Figure 3.26. These peaks were possibly due to contamination on the column.

The  $t_{1/2}$  of **3c** was computed in the same way used to calculate the  $t_{1/2}$  of the 15-mer linear peptide (**2b**) with the same enzyme using the data in Table 3.19.

**Table 3.19:** Areas of 13-mer cyclic peptide (**3c**) peaks in the HPLC chromatograms during digestion with chymotrypsin at 10 °C and pH 8.6.

Time	Area	ln(area)
0	207015	12.240
2	186115	12.134
4	122830	11.718
6	148703	11.909
8	120222	11.697
10	109000	11.599
15	107023	11.580
20	81239	11.305

The rate constant,  $k$  ( $\text{min}^{-1}$ ), was obtained from Figure 3.28 (a plot of  $\ln$  area versus time). Table 3.20 includes the value of  $t_{1/2}$  ( $16.9 \pm 2.8$  min).

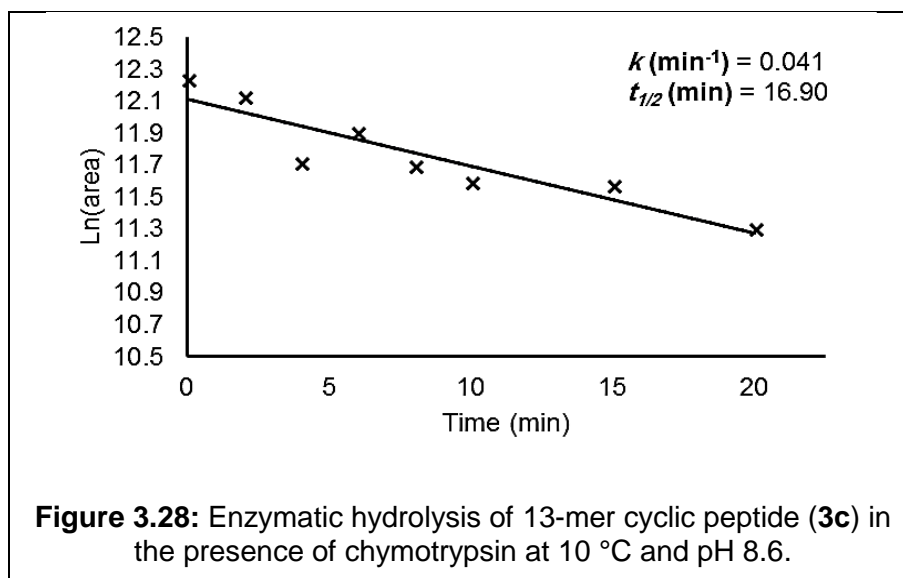


**Figure 3.28:** Enzymatic hydrolysis of 13-mer cyclic peptide (**3c**) in the presence of chymotrypsin at 10 °C and pH 8.6.

**Table 3.20:**  $t_{1/2}$  of 13-mer cyclic peptide (**3c**) during digestion with chymotrypsin at 10 °C and pH 8.6, including value of rate constant ( $k \text{ min}^{-1}$ ) and the standard error (SE).

$k (\text{min}^{-1})$	SE	%Error of $k$	$t_{1/2} (\text{min})$	Error of $t_{1/2} (\text{min})$
0.041	0.007	17	16.9	2.8

The effect of the chymotrypsin on the two peptides (**3c**, **3b**) was the same. The peptide bond between Trp and Thr was hydrolysed by the enzyme in the two compounds (**3c**, **3b**), while the peptide bond between Phe and Leu remained intact. It was possible that the conformation of the first site (Trp–Thr) was in a more susceptible orientation to hydrolysis by chymotrypsin than the second site (Phe–Leu). Therefore, the minor reaction products were not detected by the HPLC. The rate of enzymatic hydrolysis for **3b** ( $t_{1/2} = 14.35 \pm 0.9$  min) was close to **3c** ( $t_{1/2} = 16.90 \pm 2.8$  min). It was deduced that the conversion of the 13-mer linear peptide (**3b**) to the cyclic peptide (**3c**) did not significantly affect the stability of the peptide against chymotrypsin, considering the magnitude of error in the determination of  $t_{1/2}$ .

It is important to note that hydrolysis of **3c** by chymotrypsin produced linear peptide that has the same length but different sequence (Scheme 3.6, Figure 3.27) and greater retention time (11.47 min, Figure 3.25) than its linear peptide **3b** (10.76 min, Figure 3.21). There is a possibility that the sequence of the linear peptide (**3b**) with the new order and different polarity would give greater chance of reaching the target than the original linear peptide (**3b**).

### 3.2.9 Enzymatic degradation and kinetic study of the 13-mer linear peptide (**3b**) in the presence of trypsin

Figure B.19 in Appendix B shows the HPLC chromatograms of the reaction between trypsin and 13-mer linear peptide (**3b**) at 10 °C and pH 6.2 over 0–20 min. The peak at the retention time 8.61 min is **3b**. Enzymatic hydrolysis was detectable almost immediately, with a new peak beginning to appear at the retention time 9.55 min. The intensity of **3b** peak dropped to less than half at 8 min, then it almost disappeared, and the intensity of the new peak increased significantly at 20 min (Figure 3.29).

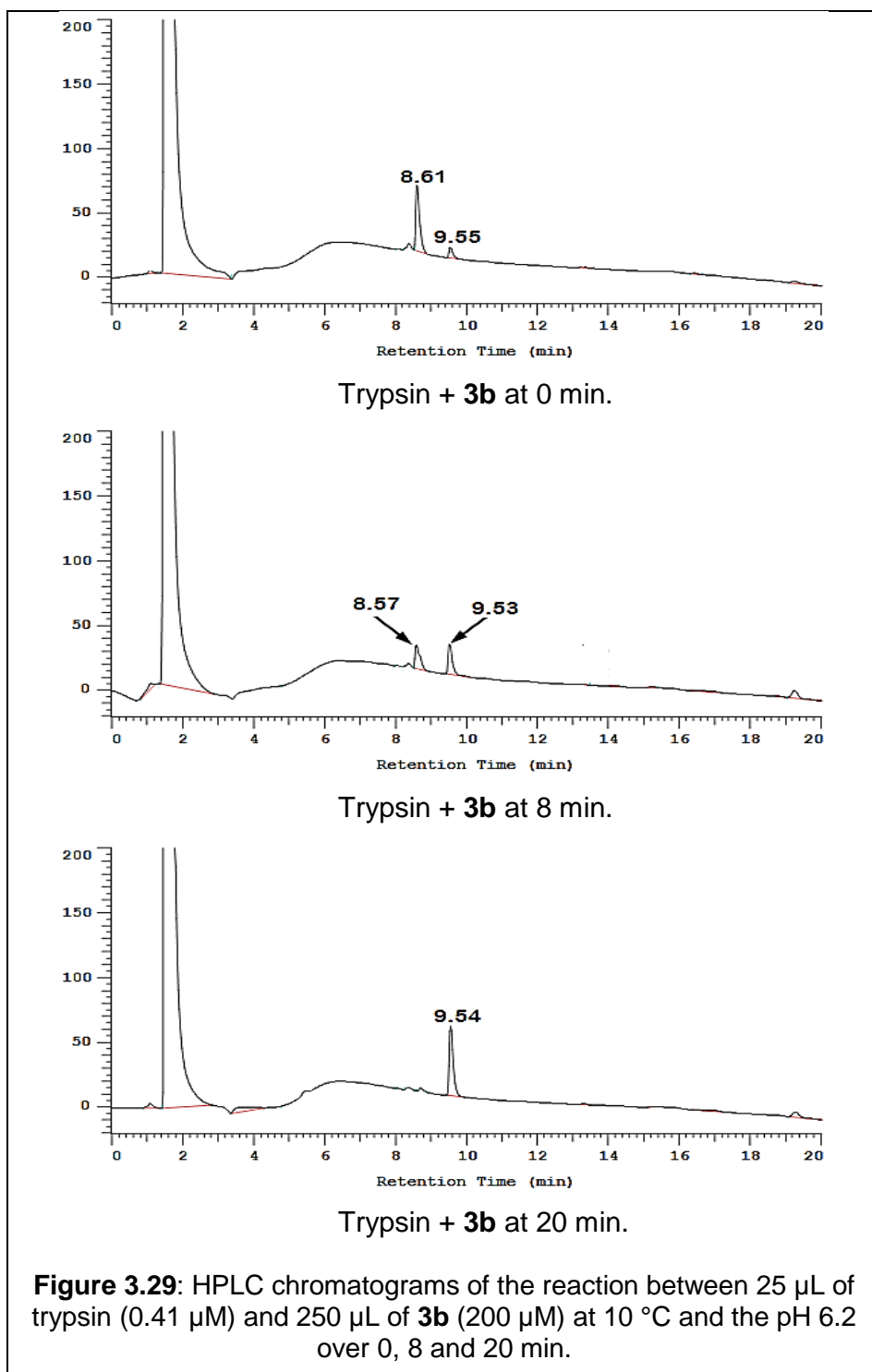
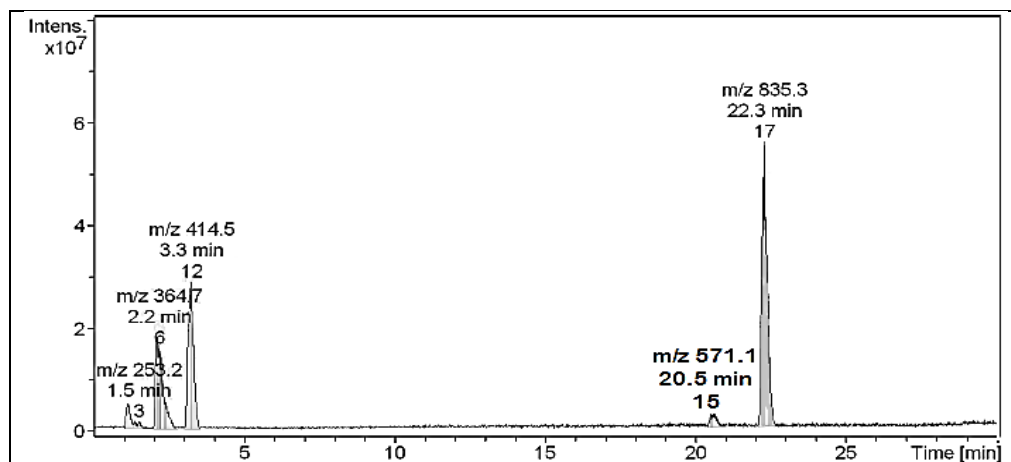


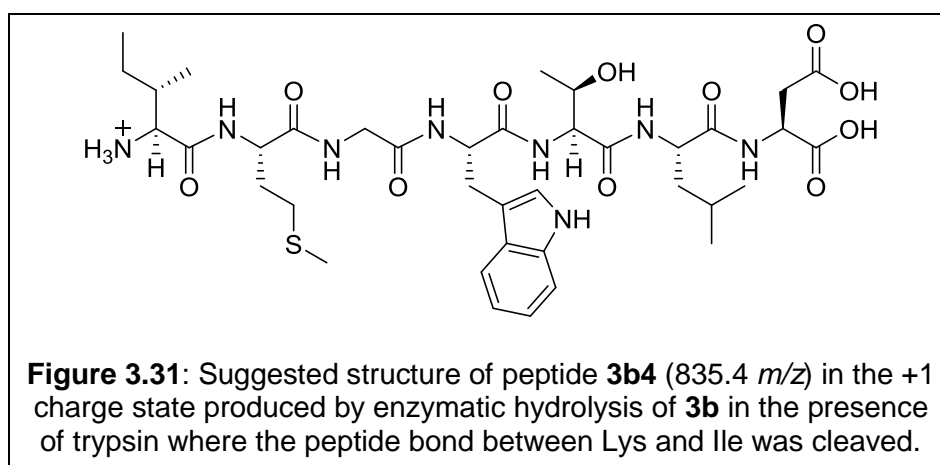
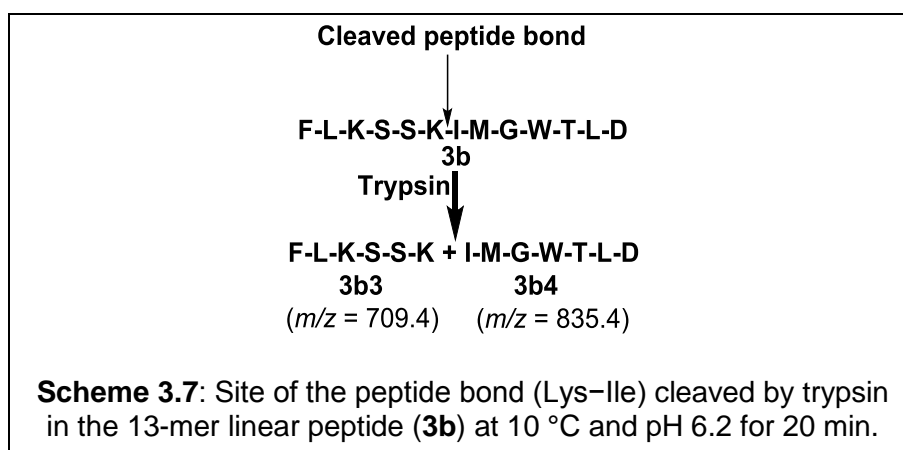
Figure 3.30 is the total ion chromatogram of **3b** at 20 min of the enzymatic hydrolysis in the presence of trypsin. The peak of 835.3  $m/z$  at the retention time 22.3 min was consistent with the theoretically calculated value of 835.4  $m/z$  for the protonated peptide in the +1 charge state. The sequence of this peptide is shown in Scheme 3.7 (peptide **3b4**). As was expected, trypsin



cleaved the peptide bond between Lys and Ile. The suggested structure of this peptide is shown in Figure 3.31.



**Figure 3.30:** Total ion chromatogram of 13-mer linear peptide (**3b**) during digestion by trypsin at 10 °C and pH 6.2 for 20 min.

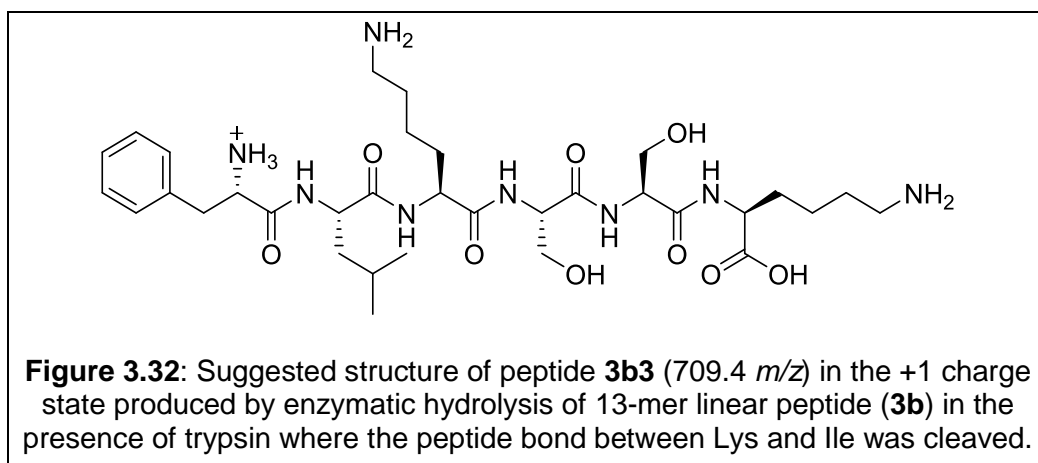


The MS<sup>2</sup> mass spectrum for the precursor of 835.3 *m/z* (Figure B.20 in Appendix B) supported the suggested structure of peptide **3b4**. The observed peaks were consistent with the theoretically calculated values (Table 3.21). All the structures of these proposed fragments are in Table B.10 in Appendix B.

**Table 3.21:** The comparison between theoretically calculated peaks and the observed CID fragments of the precursor ion 835.6 *m/z* (peptide **3b4**) produced by enzymatic hydrolysis of **3b** by trypsin (See Figure B.20 in Appendix B).

No	Observed <i>m/z</i>	Calculated <i>m/z</i>	Suggested sequence
1	330.0	330.2	y <sub>3</sub> -H <sub>2</sub> O
2	488.0	488.2	b <sub>4</sub>
3	573.0	573.3	y <sub>5</sub> -H <sub>2</sub> O
4	589.0	589.3	b <sub>5</sub>
5	684.1	684.4	b <sub>6</sub> -H <sub>2</sub> O
6	704.0	704.3	y <sub>6</sub> -H <sub>2</sub> O
7	817.2	817.4	MH-H <sub>2</sub> O

Peptide **3b3** (709.4 *m/z*) in Scheme 3.7 which has suggested structure shown in Figure 3.32 did not appear in the HPLC chromatograms (Figure B.19 in Appendix B) and the total ion chromatogram (Figure 3.30). There was the possibility that peptide **3b3** was eluted with the DMSO solvent due to the triply charged nature of the compound under acidic conditions. The other peaks 253.2, 364.7, 414.5, 571.1 at 1.5, 2.2, 3.3, 20.5 min respectively (Figure 3.30) did not match with a mass of any one of the expected peptides produced by trypsin hydrolysis of peptide **3b3** (Table B.11 in Appendix B). Thus, there could be contamination on the column.



The  $t_{1/2}$  of **3b** towards trypsin digestion at 10 °C and pH 6.2 was computed using the areas of the **3b** peak in the HPLC chromatograms (Table 3.22). The  $t_{1/2}$  was computed in the same way that had been used to calculate the  $t_{1/2}$  of the 15-mer linear peptide (**2b**) with chymotrypsin.

**Table 3.22:** Areas of 13-mer linear peptide (**3b**) peaks in the HPLC chromatograms during digestion with trypsin at 10 °C and pH 6.2.

Time(min)	Area	ln(area)
0	328008	12.700
2	270232	12.507
4	258916	12.464
6	183361	12.119
8	148347	11.907
10	72609	11.297
15	21304	9.966
20	19024	9.853

The rate constant  $k$  ( $\text{min}^{-1}$ ) was obtained from Figure 3.33 (a plot of  $\ln$  area versus time). Table 3.23 includes the value of  $t_{1/2}$  ( $4.22 \pm 0.6$  min).

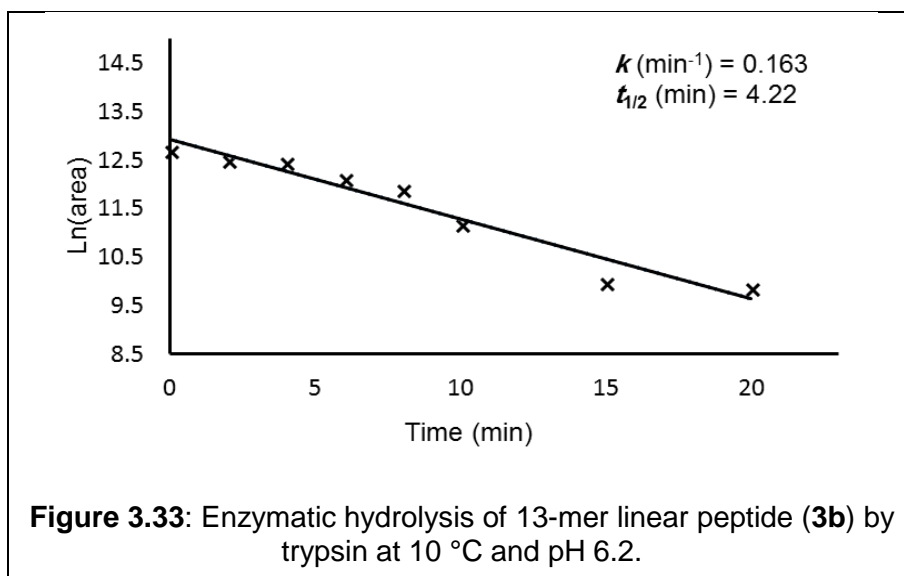


**Table 3.23:**  $t_{1/2}$  of 13-mer linear peptide (**3b**) during digestion with trypsin at 10 °C and pH 6.2, including the value of the rate constant ( $k \text{ min}^{-1}$ ) and the standard error (SE).

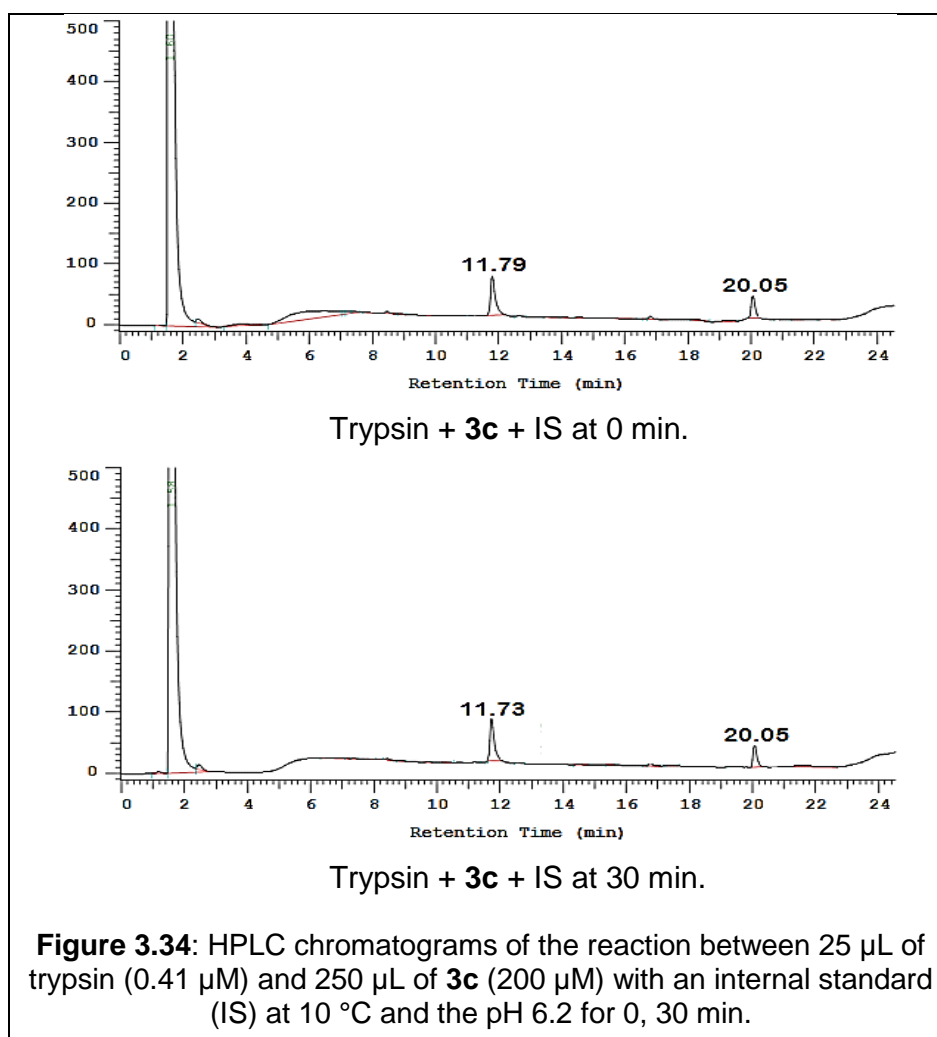
$k \text{ (min}^{-1}\text{)}$	SE	%Error of $k$	$t_{1/2} \text{ (min)}$	Error of $t_{1/2} \text{ (min)}$
0.163	0.023	14	4.22	0.6

### 3.2.10 Enzymatic degradation and kinetic study of the 13-mer cyclic peptide in the presence of trypsin and the comparison with its linear counterpart (**3b**)

Figure B.21 in Appendix B indicates the HPLC chromatograms of the reaction between trypsin and 13-mer cyclic peptide (**3c**) at 10 °C, and pH 6.2 over 0–30 min.  $2.7 \times 10^{-2} \text{ M}$  of Fmoc-tryptophan(Boc) compound was used as an internal standard (IS). The peak at the retention time 11.79 min is for **3c** and the second peak at the retention time 20.05 min is for the internal standard. Clearly, compound **3c** has significant stability against trypsin, due to the ratio of the intensity of **3c** peak to the intensity of the internal standard peak (**3c**/IS) which did not decrease ( $1.172 \pm 0.005$ ) until 30 min, as in Table 3.24 (See Figure 3.34). There was no new peak in the HPLC chromatograms during the entire time series (0–30 min) of the enzymatic hydrolysis.

**Table 3.24:** The ratio of areas of 13-mer cyclic peptide (**3c**) peaks to areas of the internal standard peaks in the HPLC chromatograms during digestion with trypsin at 10 °C and pH 6.2.

Time (min)	Area of 3c	Area of IS	3c/IS
0	578696	266196	2.173
2	525208	241173	2.177
4	547966	252684	2.168
6	575126	265486	2.166
8	542063	250446	2.164
10	561642	257867	2.178
15	591169	271162	2.180
20	611451	281008	2.175
30	559752	257509	2.173



There is the potential that the constricted conformation of this cyclic peptide (**3c**) in the solution negatively affected its ability to act as a substrate for trypsin. The sequence and the order of the residues in this cyclic peptide (**3c**) may also contribute to the stability of the compound (Figure 3.35). The presence of polar side groups, such as the Lys residues, possibly strengthened intramolecular hydrogen bonds as well as the intermolecular hydrogen bonds (with water) enhancing the folding of **3c** therefore making it less able to occupy the active site of the enzyme.

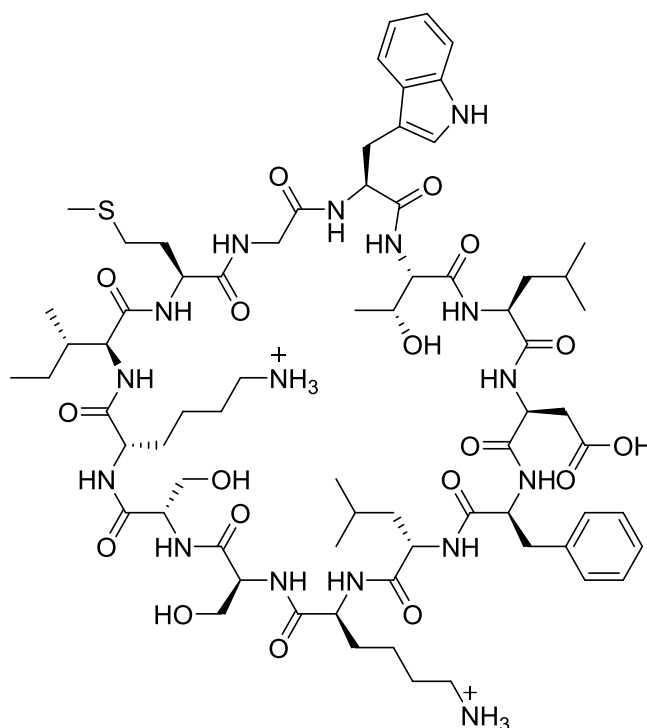
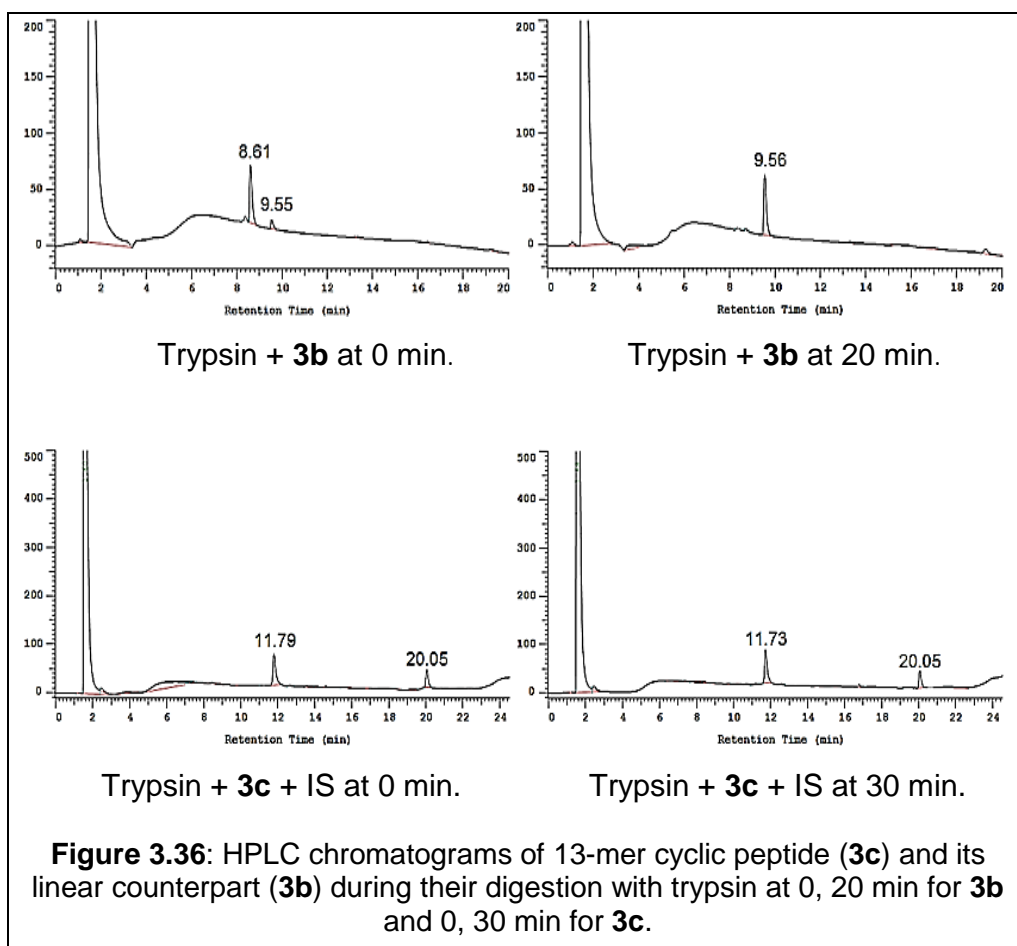


**Figure 3.35:** Structure of 13-mer cyclic peptide (**3c**) in the +2 charge state ( $m/z = 754.4$ ).

There is a significant contrast between 13-mer cyclic peptide (**3c**) and its linear counterpart (**3b**) in their stability towards the trypsin at 10 °C and pH 6.2 over 0–30 min. It was concluded that the stability of peptide bond between Lys and Ile in the two compounds (**3b**, **3c**) against trypsin was different. It was stable in the cyclic peptide (**3c**) until 30 min, while it was hydrolysed in the linear peptide (**3b**). The HPLC peak of **3b** disappeared within 20 min, while the HPLC peak of **3c** still remained at 30 min (See Figure 3.36).

Converting the 13-mer linear peptide (**3b**) to cyclic peptide (**3c**), with the KSSK fragment in the sequence, significantly increased the stability of the peptide against hydrolysis by trypsin. Thus, the cyclic compound (**3c**) may stand a greater chance than its linear counterpart (**3b**) to survive proteolysis in the body to reach an antigen presenting cell (B cell) that activates T-cells to destroy a tumour.



**Chapter 4**

**Study of the Stability  
of the Peptides in Fetal  
Calf Serum (FCS)**



## 4 Stability of the peptides in fetal calf serum

### 4.1 Introduction

The stability of the peptides (**2b**, **2c**, **3b**, **3c**) in fetal calf serum (FCS) was examined because this is the medium that is commonly used in immunological experiments to investigate T-cell activation by peptides. FCS contains growth factors, a low content of immunoglobulin and a lower level of complement in comparison to an adult. Complement proteins have an undesirable effect of inducing immunoglobulin aggregation which may produce false-positive tests in immunological assays and could negatively affect a variety of cell reactions.<sup>195</sup> Therefore, FCS was heated at 56 °C for 30 minutes to inactivate the complement proteins.

The measurement of the rates of peptide degradation is a relatively straightforward experiment, but some factors may lead to inconsistent results; for example, different results are obtained for *in vitro* peptide stabilities in non-human plasma which has varying levels of peptidases. Also, the results from plasma collected in different types of blood collection tube are complicated by the fact that peptidase inhibitors such as EDTA may be included in the tube.<sup>196</sup>

Benzoic acid was used as an internal standard in all the experiments because it has good solubility in water and acetonitrile (HPLC solvents). In addition to that, its HPLC peak has no overlap with the peaks of the peptides (**2b**, **2c**, **3b**, **3c**).

### 4.2 Stability of the 15-mer linear peptide (**2b**) in 20% FCS

Table 4.1 shows the values for the HPLC peak areas of 0.7 mM 15-mer linear peptide (**2b**) relative to the internal standard peak areas (benzoic acid) in 20% FCS at 37 °C, and pH 7.4 for 2, 6, 12, 24, 48 h. The experiment was performed in triplicate; for example, Figure C.1 in appendix C represents the first replicate. The highest peak at the retention time 9.85 min is for the 15-mer linear peptide (**2b**). The peak at the retention time 9.10 min is for the internal standard. The peak at the retention time 8.89 min is for the FCS (See chromatogram at 0 h in the same Figure in appendix C).

**Table 4.1:** HPLC peak areas for 15-mer linear peptide (**2b**) relative to the internal standard (IS) peak areas during incubation in 20% FCS at 37 °C and pH 7.4 for 0 – 48 h. Three replicates.

Time (h)	0	2	6	12	24	48
1- <b>2b</b> /IS	3.1428	2.9440	2.8504	2.6170	2.4862	2.4752
2- <b>2b</b> /IS	2.6216	2.6121	2.5786	2.3963	2.3635	2.1856
3- <b>2b</b> /IS	2.8181	2.8464	2.6764	2.3089	2.5766	2.2336
1-ln <b>2b</b> /IS)	1.1451	1.0797	1.0474	0.9620	0.9107	0.9063
2-ln( <b>2b</b> /IS)	0.9637	0.9601	0.9472	0.8739	0.8601	0.7818
3-ln( <b>2b</b> /IS)	1.0360	1.0460	0.984	0.8367	0.9464	0.8036

Over the whole period, there was a decrease in the peak area of the 15-mer linear peptide (**2b**). It appears that up to 12 h there was a slight drop in the peak area of **2b** relative to the internal standard (**2b**/IS). At 48 h the peak area of **3b** in the FCS reached the lowest value compared to its starting point. There were some small fluctuations in replicate 3 in Figure 4.1. The reasons for irregular fluctuations could be down to the measurement errors; for instance, small difference in volumes withdrawn from the reaction vial and transferred to the mass spectrum vial by micropipette at each particular time may lead to this variance. Also, an inconsistent amount of internal standard being added (pipetting errors) could have contributed to this variation.

The rate constant  $k$  was calculated from the slope of a straight line fitted to a plot of the logarithm of the peak area ratio **3b**/IS versus time using the Excel software as in Figure 4.1. The  $t_{1/2}$  (Table 4.2) of the 15-mer linear peptide (**2b**) was calculated for the triplicate using the following formula,

$$t_{1/2} = \ln 2 / k$$

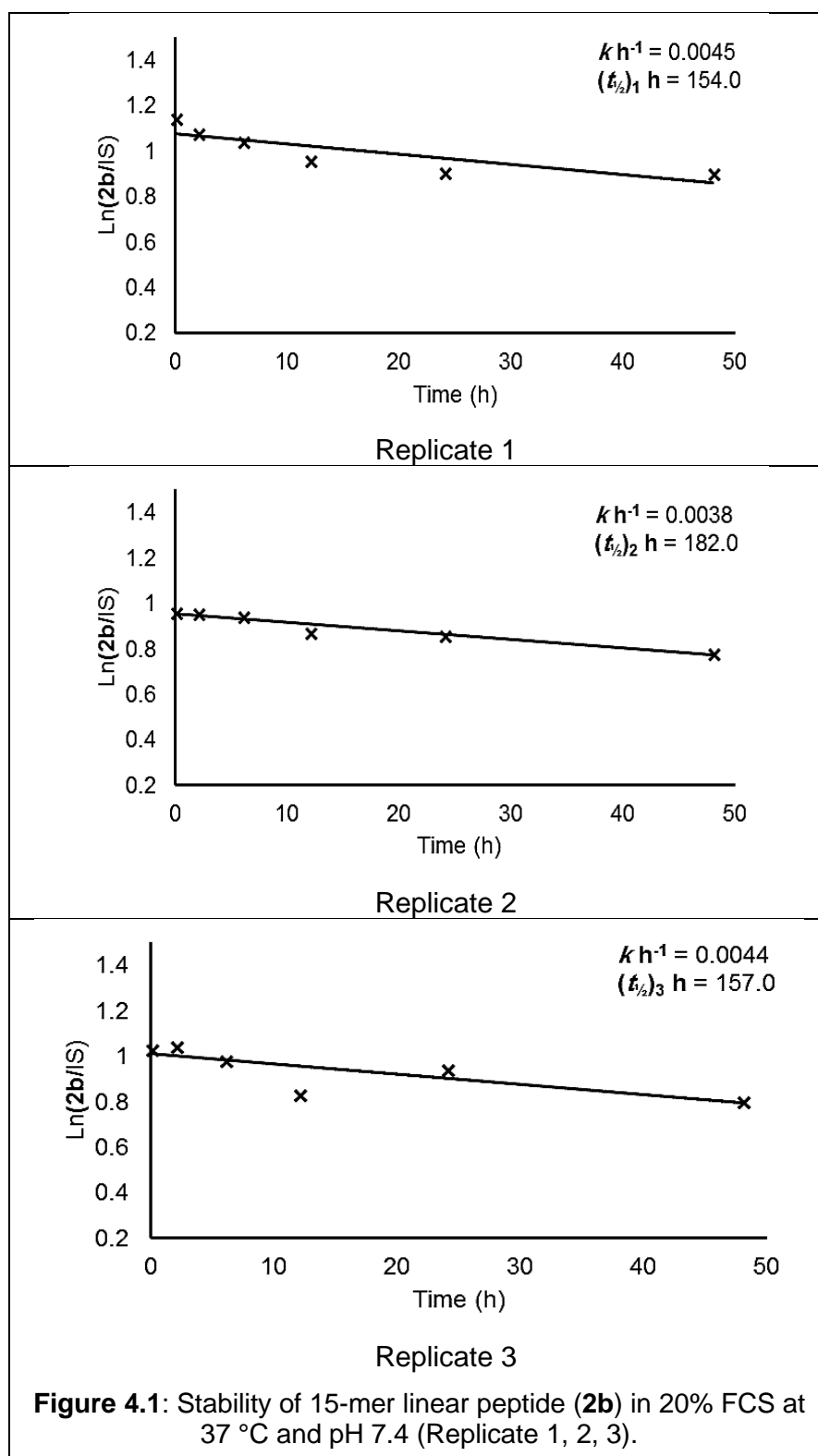


**Table 4.2:**  $t_{1/2}$  of 15-mer linear peptide (**2b**) in 20% FCS at 37 °C and pH 7.4 with the mean and standard deviation ( $\sigma$ ) of the triplicate.

No	$k$ (h <sup>-1</sup> )	$t_{1/2}$ (h)	Mean of $t_{1/2}$ (h)	$\sigma$
1	0.0045	154	165	15
2	0.0038	182		
3	0.0044	157		

### 4.3 Stability of the 15-mer cyclic peptide (**2c**) in 20% FCS

Table 4.3 shows the HPLC peak areas of 0.7 mM 15-mer cyclic peptide (**2c**) relative to the internal standard peak areas (**2c**/IS) in 20% FCS, at 37 °C, and pH 7.4 for 2, 6, 12, 24, 48 h. The experiment was repeated three times; for instance, Figure C.4 in appendix C represents the first replicate. The highest peak at the retention time 9.66 min is for the 15-mer cyclic peptide (**2c**). The peak at the retention time 8.92 min is for the internal standard. The peak at the retention time 8.69 min is for the FCS (See chromatogram at 0 h in the same Figure in appendix C).

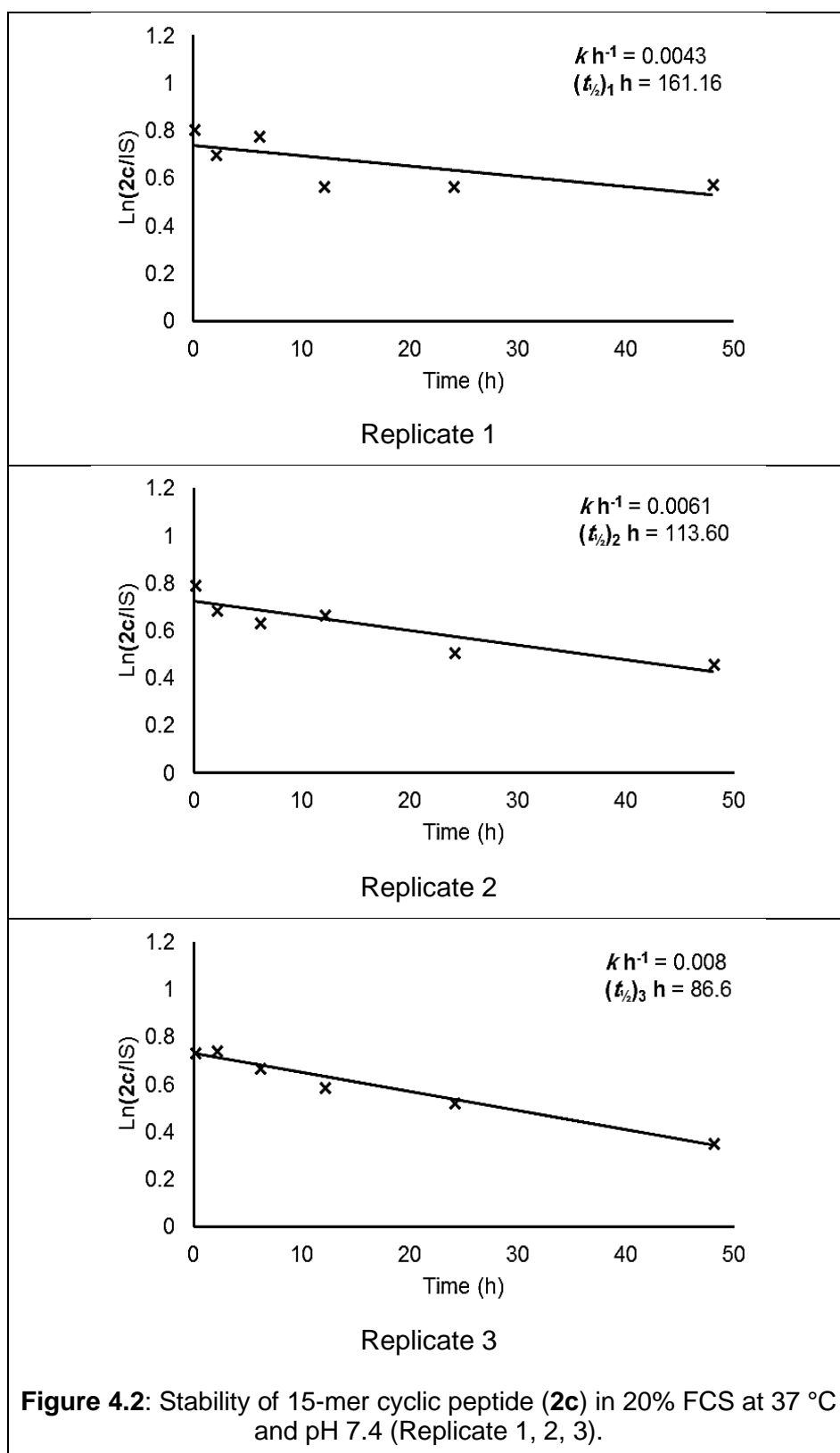
**Table 4.3:** HPLC peak areas for 15-mer cyclic peptide (**2c**) relative to the internal standard (IS) during incubation in 20% FCS at 37 °C and pH 7.4 for 0 – 48 h. Three replicates.

Time (h)	0	2	6	12	24	48
1- <b>2c</b> /IS	2.2528	2.0274	2.1849	1.7707	1.7692	1.78683
2- <b>2c</b> /IS	2.2202	1.9971	1.8952	1.9537	1.6680	1.5886
3- <b>2c</b> /IS	2.0906	2.1116	1.9596	1.8093	1.6913	1.4293
1-ln( <b>2c</b> /IS)	0.8122	0.7067	0.7815	0.5714	0.5705	0.5804
2-ln( <b>2c</b> /IS)	0.7976	0.6916	0.6393	0.6697	0.5116	0.4628
3-ln( <b>2c</b> /IS)	0.7374	0.7474	0.6727	0.5929	0.5255	0.3572

Over the entire period, there was a drop in the intensity of the peak of the 15-mer cyclic peptide (**2c**) relative to the peak area of the internal standard (**2c**/IS). There was a slight decrease, between 0 and 12 h. During the time

between 12 to 48 h, the rate of decline was accompanied by minimal fluctuation only in replicate 1, as in Figure 4.2. The peak area for **2c** reached the lowest value at 48 h compared to its initial value.

The small variation in the rate of decrease of the peak area of **2c** was possibly for the same reasons mentioned in the study of the stability of **2b** in the same medium. In addition, one of the potential causes leading to this variation was the peptide adhering to tips/vials.



After computing the values of  $k$  (gradient) of the 15-mer cyclic peptide (**2c**) using the Excel program as in Figure 4.2, the values of  $t_{1/2}$  and their mean and standard deviation ( $\sigma$ ) were calculated and are reported in Table 4.4.

**Table 4.4:**  $t_{1/2}$  of 15-mer cyclic peptide (**2c**) in 20% FCS at 37 °C and pH 7.4 with the mean and standard deviation ( $\sigma$ ) of the triplicate.

No	$k$ ( $\text{h}^{-1}$ )	$t_{1/2}$ (h)	Mean of $t_{1/2}$ (h)	$\sigma$
1	0.0043	161	120	38
2	0.0061	114		
3	0.008	87		

In a comparison between the  $t_{1/2}$  of the 15-mer cyclic peptide (**2c**) and the  $t_{1/2}$  of its linear counterpart (**2b**), it appears that the results of this experiment did not support the hypothesis that the cyclic peptide has the larger  $t_{1/2}$ . It was expected that the cyclic peptide would be an unsuitable substrate for exoprotease enzymes because it has no free terminus (*N* and *C*-terminus), while the linear peptide is more suitable as a substrate for the exoprotease enzymes because it has two free termini. Therefore, the expectation was that the  $t_{1/2}$  of **2c** would be larger than the  $t_{1/2}$  of **2b**, but the data of this experiment did not support the hypothesis. The results were that the  $t_{1/2}$  of **2c** is  $120 \pm 38$  h which was less than the  $t_{1/2}$  of **2b** ( $165 \pm 15$  h). Although there was a difference in the mean values of the  $t_{1/2}$  between **2c** and **2b**, the standard deviations are sufficiently high that it cannot be concluded that there is a significant difference between them. Within experimental error, the two peptides (**2c**, **2b**) have the same resistance against the protease enzymes in fetal calf serum. On the other hand, if this simple difference between them was real, it still does not support the hypothesis.

The constricted conformation of the cyclic peptide potentially influenced the  $t_{1/2}$  of the 15-mer cyclic peptide (**2c**) in the fetal calf serum. There are many possible conformations for the linear compound in solution and the number of conformations is reduced after cyclisation.<sup>4</sup> The constricted conformation of the cyclic structure was expected to make the compound an unsuitable substrate for protease (providing a high  $t_{1/2}$ ), but the converse may have occurred for peptide (**2c**) and the compound may instead have been held in a suitable conformation for cleavage resulting in a low  $t_{1/2}$  value.

#### 4.4 Stability of the 13-mer linear peptide (**3b**) in 20% FCS

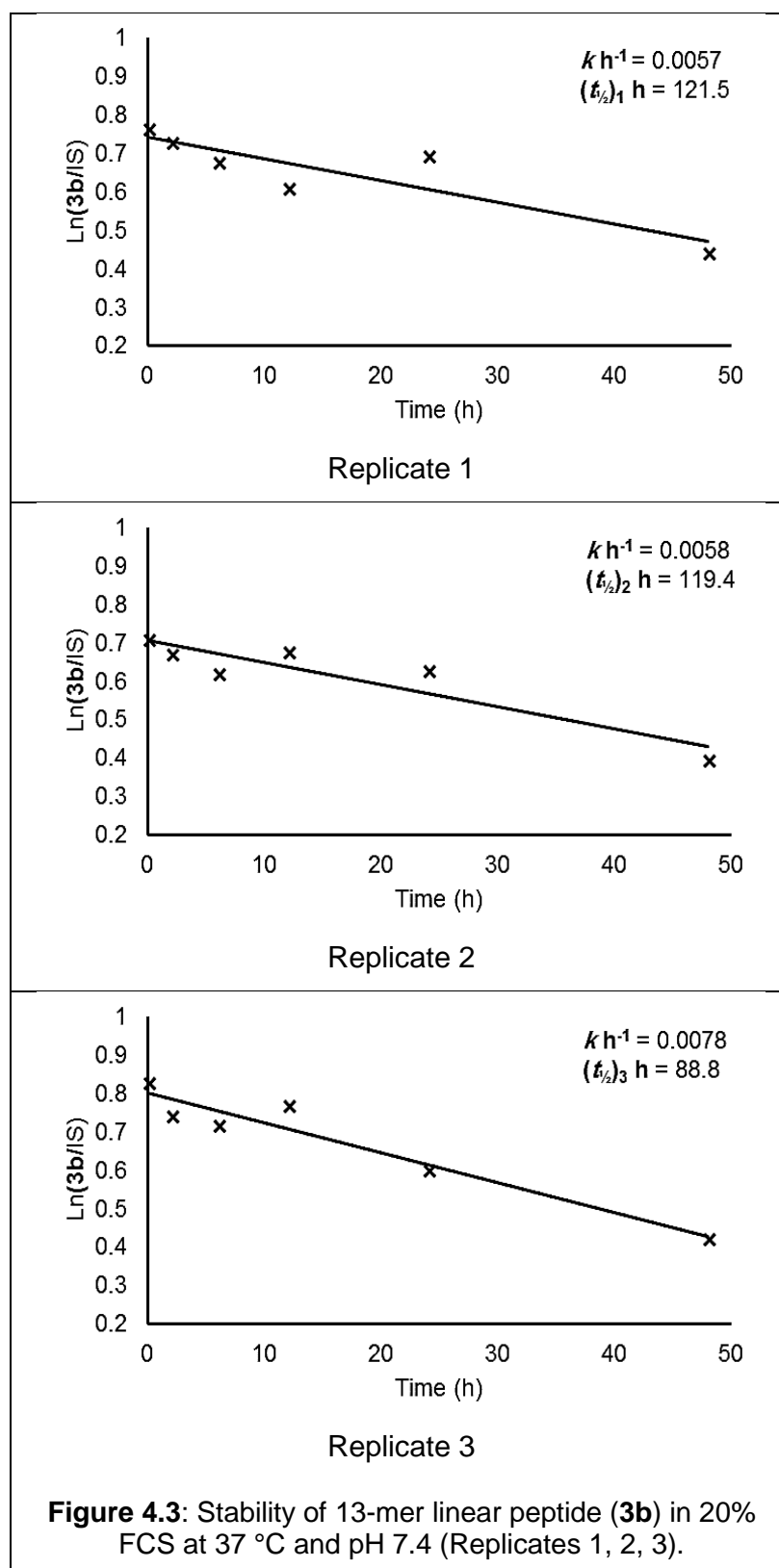
Table 4.5 shows the values for the HPLC peak areas of 0.7 mM 13-mer linear peptide (**3b**) relative to the internal standard peak areas (**3b**/IS) in 20% FCS, at 37 °C, and pH 7.4 for 2, 6, 12, 24, 48 h. The experiment was performed in triplicate; for example, Figure C.7 in appendix C represents the first replicate. The highest peak at the retention time 9.84 min is for the 13-mer linear peptide (**3b**). The peak at the retention time 10.61 min is for the internal standard. The broad peak at the retention time 11.35 min is for the fetal calf serum (See the chromatogram for 0 h in the same figure in appendix C).

**Table 4.5:** HPLC peak areas for the 13-mer linear peptide (**3b**) relative to the internal standard (IS) during incubation in 20% FCS at 37 °C and pH 7.4 for 0 – 48 h. Three replicates.

Time(h)	0	2	6	12	24	48
1- <b>3b</b> /IS	2.1533	2.0805	1.9752	1.8430	2.0048	1.5605
2- <b>3b</b> /IS	2.0359	1.9628	1.8608	1.9726	1.8767	1.4871
3- <b>3b</b> /IS	2.2962	2.1039	2.0515	2.1622	1.8292	1.5265
1-ln( <b>3b</b> /IS)	0.7670	0.7326	0.6806	0.6114	0.6955	0.4450
2-ln( <b>3b</b> /IS)	0.7109	0.6743	0.6210	0.6793	0.6295	0.3968
3-ln( <b>3b</b> /IS)	0.8312	0.7438	0.7185	0.7711	0.6039	0.4230

As shown in Figure 3.4, the plot is approximately linear but with some fluctuation that appeared over the period between 12 and 24 h (entry replicate 2, 3 in the same figure) but the peak area of **3b** remained less than the peak area of **3b** at 0 h. The peak area for **3b** reached its lowest value at 48 h in all three experiments. The fluctuation in the decrease of **3b** intensity was potentially for the same reasons that were mentioned in the study of the stability of **2b** and **2c** in the same reaction medium.





The  $t_{1/2}$  of the 13-mer linear peptide (**3b**) was calculated using the same equation that was used to calculate the  $t_{1/2}$  of **2b**. The results and the mean and standard deviation ( $\sigma$ ) for the three replicates are given in Table 4.6.

**Table 4.6:**  $t_{1/2}$  of 13-mer linear peptide (**3b**) in 20% FCS at 37 °C and pH 7.4 with the mean and standard deviation ( $\sigma$ ) of the triplicate.

No	$k$ ( $\text{h}^{-1}$ )	$t_{1/2}$ (h)	Mean of $t_{1/2}$ (h)	$\sigma$
1	0.0057	122	110	18
2	0.0058	119		
3	0.0078	89		

#### 4.5 Stability of the 13-mer cyclic peptide (**3c**) in 20% FCS

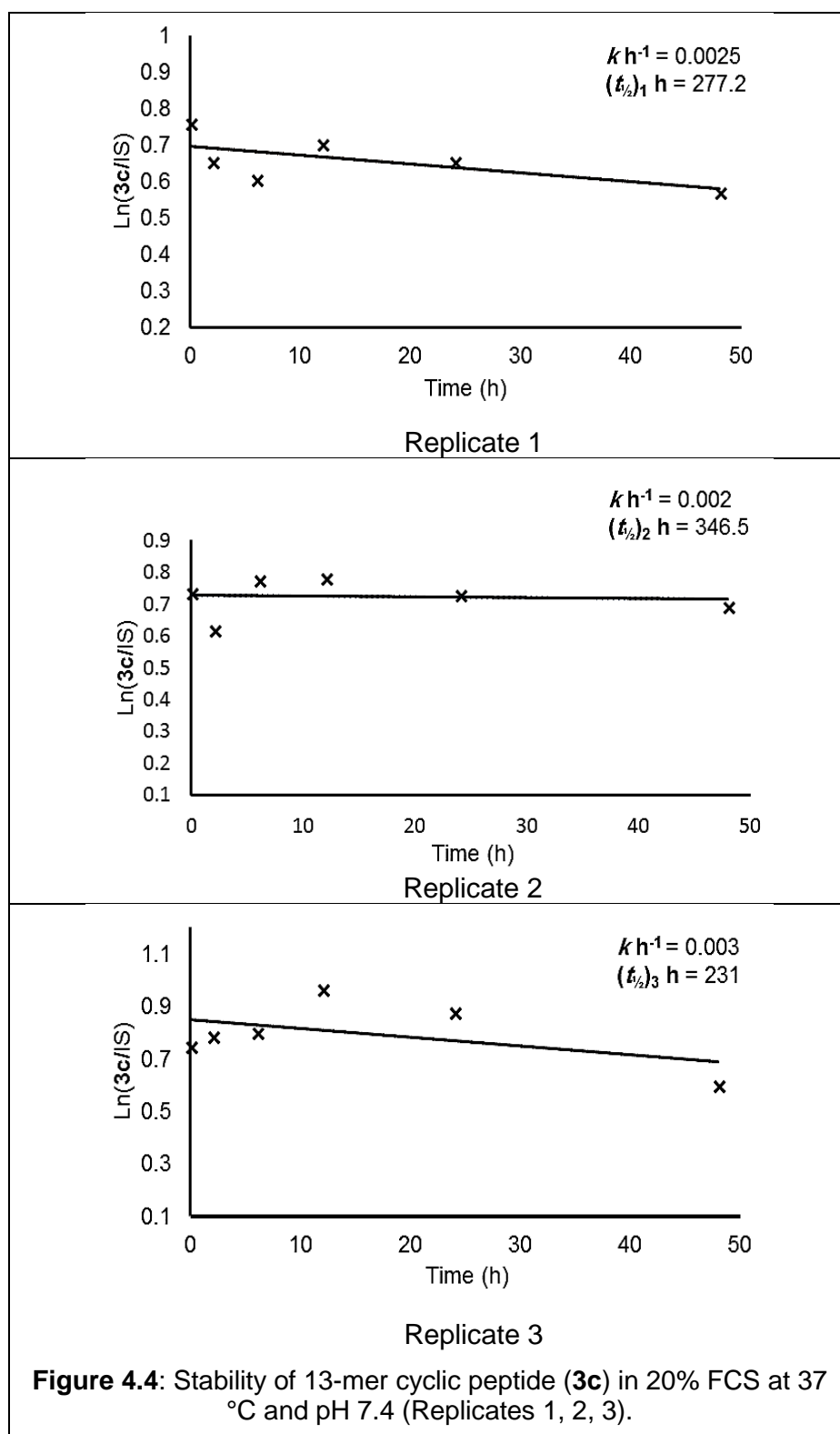
Table 4.7 indicates the areas of HPLC peaks of 0.7 mM 13-mer cyclic peptide (**3c**) in 20% FCS at 37 °C and pH 7.4 for 0, 2, 6, 12, 24, 48 h. The experiment was undertaken three times; for example, Figure C.10 in appendix C represents the first replicate. The highest peak at the retention time 12.26 min is for the 13-mer cyclic peptide (**3c**). The peak at the retention time 10.57 min is for the internal standard. The smallest peak at the retention time 11.29 min is for the fetal calf serum (See chromatogram for 0 h in the same Figure in appendix C).

**Table 4.7:** HPLC peak areas for 13-mer cyclic peptide (**3c**) relative to the internal standard (IS) during incubation in 20% FCS at 37 °C, and pH 7.4 for 0 – 48 h. Three replicates.

Time (h)	0	2	6	12	24	48
1- <b>3c</b> /IS	2.1427	1.9263	1.8343	2.0262	1.9255	1.7718
2- <b>3c</b> /IS	2.0890	1.8604	2.1732	2.1910	2.0751	2.0000
3- <b>3c</b> /IS	2.1152	2.2026	2.2327	2.6377	2.4098	1.8212
1-ln( <b>3c</b> /IS)	0.7620	0.6556	0.6066	0.7061	0.6552	0.5720
2-ln( <b>3c</b> /IS)	0.7367	0.6208	0.7762	0.7844	0.7300	0.6931
3-ln( <b>3c</b> /IS)	0.7491	0.7896	0.8032	0.9699	0.8795	0.5995

As shown in Figure 4.4, the peak area of the 13-mer cyclic peptide (**3c**) decreased to the lowest level in all three experiments at 48 h in comparison to its peak area at 0 h. The rate of decrease of the peak area for **3c** relative to the internal standard (**3c**/IS) was accompanied by some fluctuation in replicates 2 and 3 in Figure 4.4. The reasons for this variation in the peak areas could be the same reasons that were mentioned in the study of the stability of **2b** and **2c**

in the same medium reaction. Furthermore, adherence of peptide on tips or vials potentially caused irreproducible losses of compound, contributing towards variation within and between the replicates. In addition, this cyclic peptide appeared to be more resistant against proteases. Therefore, there was little decrease in its peak area over the course of the experiment, making fluctuations more evident.



The  $t_{1/2}$  of the 13-mer cyclic peptide (**3c**) for the three replicates and its standard deviation ( $\sigma$ ) were calculated using the same method that was used to calculate the  $t_{1/2}$  of the 13-mer linear peptide (**3b**) and the results are given in Table 4.8.

**Table 4.8:**  $t_{1/2}$  of 13-mer cyclic peptide (**3c**) in 20% FCS at 37 °C and pH 7.4 with the mean and standard deviation ( $\sigma$ ) of the triplicate.

No	$k$ ( $\text{h}^{-1}$ )	$t_{1/2}$ (h)	Mean of $t_{1/2}$ (h)	$\sigma$
1	0.0025	277	285	58
2	0.002	346.5		
3	0.003	231		

Although the standard deviation was quite high in the two experiments (Table 4.8 and Table 4.6), it could be said that there was a difference in the value of  $t_{1/2}$  between 13-mer cyclic peptide (**3c**) and its linear counterpart (**3b**). As a comparison between them, the result was the  $t_{1/2}$  of the former ( $285 \pm 58$  h) is greater than the  $t_{1/2}$  of the latter ( $110 \pm 18$  h). This result was as expected because the cyclic peptide has no free terminus (*N* and *C*-terminus) and so was not a suitable substrate for the exoprotease enzymes. Therefore, the cyclic peptide (**3c**) hydrolysis was delayed in comparison to its linear counterpart (**3b**) which has the two free termini, thus being a suitable substrate for exoprotease enzymes, and the hydrolysis was faster than the cyclic compound (**3c**) giving a lower value of  $t_{1/2}$ . Although the 13-mer cyclic peptide (**3c**) was not a substrate for the exopeptidases, it could still, however, be a substrate for endopeptidases. Thus, the measurement  $t_{1/2}$  of the two peptides (**3b**, **3c**) was evidence of the validity of the hypothesis that the cyclic peptide might be a poorer substrate for endopeptidases. Therefore, **3c** was more resistant against the two types of enzymes (endo and exopeptidase) in comparison to its linear counterpart (**3b**). Consequently, it could be said that 13-mer cyclic peptide (**3c**) may stand a greater chance of reaching a target *in vivo* than its linear counterpart (**3b**).

Although  $t_{1/2}$  ( $165 \pm 15$  h) of 15-mer linear peptide (**2b**) is greater than  $t_{1/2}$  ( $110 \pm 18$  h) of 13-mer linear peptide (**3b**) considering the magnitude of the standard deviations the results must be interpreted with caution. Potentially, the length of **2b** (15 residues) caused the increase in stability of the compound against the endo and exopeptidase enzymes by providing a degree of folding. Therefore, the termini of the peptide and the peptide bonds were potentially more shielded from the enzymes resulting in slower hydrolysis than the shorter and less structured 13-mer linear peptide (**3b**).

It is worth noting that the process of cyclisation for the 15-mer linear peptide (**2b**) led to a decrease in the  $t_{1/2}$  of the peptide (See Table 4.2 and Table 4.4). This observation implies that the constricted conformation of the cyclic peptide (**2c**) made the compound more accessible as a substrate for the protease enzymes, thus compound **2c** has less chance of reaching the target as a comparison to its linear counterpart (**2b**). However, the cyclisation process to form compound **3c** from precursor **3b** led to an increase in the  $t_{1/2}$  of **3c** as a comparison with the  $t_{1/2}$  of **3b**. Therefore, the constricted conformation of this cyclic peptide (**3c**) made the peptide less accessible as a substrate to protease enzyme giving a high  $t_{1/2}$  value. Consequently, compound **3c** has more chance to reach a biological target than its linear counterpart (**3b**).

According to these results, peptide cyclisation does not necessarily provide greater resistance to enzymatic hydrolysis but instead the effect will depend on the length and sequence of the peptide.

## **Chapter 5**

# **Conclusion**

## 5 Conclusion

### 5.1 Conclusion

#### 5.1.1 Synthesis of peptides

A Bax peptide (IMGWTLDFL) that has the ability to activate CD8<sup>+</sup> T-cells<sup>2</sup> was circularly permuted to obtain the sequence FLIMGWTLTD. The purpose of this change was to obtain a sequence that has an aspartic acid residue at the C-terminus of the peptide allowing the peptide to be anchored to a solid support through its side chain for head-to-tail cyclisation. Cyclisation restores the original Bax sequence. Therefore, the backbone and sequence of the cyclic peptide (**1c**) were the same as its linear counterpart (**1b**), thus allowing a direct comparison of the two peptides for evaluation of the effect of cyclisation.

There was no problem during synthesis of the 9-mer linear peptide allyl ester (**1a**) and converting it to 9-mer linear peptide (**1b**). Changing parameters such as reaction temperature, shaker RPM and coupling time during synthesis of the 9-mer linear peptide allyl ester (**1a**) did not yield significantly different results. In addition, identification of the two compounds (**1a**, **1b**) by HPLC and LCMS was successful. The solubility of the linear compounds in the solvents of the HPLC and LCMS was enhanced by the polar termini. Additionally, these two peptides were not long sequences which may have reduced their propensity to aggregate in the aqueous solvent mixtures used during chromatography.

The conversion of the linear peptide (**1b**) to cyclic peptide (**1c**) faced several problems that prevented sufficient quantity of the compound being obtained for further studies. The first main problem confronting synthesis of the cyclic peptide (**1c**) was failure of the cyclisation reaction. Possibly the length and sequence of the peptide resulted in conformations that failed to bring the termini sufficiently close together thus resulting in a sluggish cyclisation reaction. This problem could be overcome to an extent by using DEPBT as the coupling reagent. The second problem encountered was in the purification of the cyclic peptide (**1c**) by HPLC. Unfortunately, the solubility of this cyclic compound (**1c**) was very poor in the HPLC solvent, especially in water. Despite the cyclic peptide (**1c**) being dissolved in acetonitrile and a small amount of



DMSO then added to increase the solubility, the majority of **1c** precipitated during collection due to water being one of the HPLC solvents. Although many gradient methods were used for the HPLC solvents (water and acetonitrile) in addition to different organic solvents (methanol, isopropanol), a large amount of the cyclic peptide (**1c**) was lost. Consequently, the yield was very low.

The third problem was observed on two occasions when small amounts of **1c** had been successfully purified and lyophilised. This small amount was dissolved in DMSO, and then stored in a freezer at -20 °C. After 15 days there was more than one peak besides the cyclic peptide peak in the HPLC and LCMS chromatograms suggesting that the peptide had decomposed during storage. Possible strain due to the cyclisation might have been responsible for an increased rate of hydrolysis. Further purification of the compound was not deemed to be worthwhile due to the inevitable losses that this would entail.

Therefore, it was necessary to search for a linker that could be inserted into the sequence of the cyclic Bax peptide to increase its solubility without interfering with the residues that contact the HLA and TCR.

The length of the peptide was increased from a 9 to 15-mer by insertion of the residues RELIRT which form the flanking sequence from the Bax protein. This longer sequence was expected to be more flexible, increasing the likelihood of the termini colliding during the cyclisation reaction. The presence of the two Arg residues was expected to increase the positive charge of the compound and its ability to form hydrogen bonding.

The synthesis of the 15-mer cyclic peptide (**2c**) was successful using the same reagents and conditions as used for the 9-mer cyclic peptide (**1c**). The solubility of **2c** was acceptable in water and acetonitrile. Consequently, insertion of the fragment of RELIRT was a successful idea. Thus, sufficient quantity of the 15-mer purified cyclic peptide (**2c**) was obtained to perform enzymatic degradation studies and stability studies in FCS. However, the yield of **2c** was still very low. A possible reason for this low yield was an inefficient cyclisation reaction. In addition to that, the purification was wasteful, as it had to be repeated several times to obtain material of sufficient quality, losing an amount of **2c** each time.

The retention time of the 15-mer cyclic peptide (**2c**) was less than the retention time of the 9-mer cyclic peptide (**1c**) in the HPLC chromatogram with the same method for the two compounds. It is concluded from this result that the polarity of **2c** was greater than the polarity of **1c**. This result was clear evidence for improvement of the properties of the cyclic peptide.

The second fragment that was inserted into the sequence of the Bax peptide was KSSK. The motivation for the insertion of this fragment was that the two high hydrophilic residues (Lys) would increase the hydrophilicity of the peptide, and thus, increase solubility of the 13-mer cyclic peptide (**3c**) in HPLC and LCMS solvents.

Synthesis and purification of this cyclic peptide (**3c**) was superior to the 15-mer cyclic peptide (**2c**), and the evidence for this was that the yield (crude and purified) was greater than **2c**. Potentially, the cause for this improvement is that the solubility of **3c** in the HPLC solvents (water and acetonitrile) was greater than **2c**. In addition to that, the cyclic peptide required fewer HPLC runs to purify than compound **2c**. Consequently, loss of the cyclic compound (**3c**) during purification was reduced. However, the total yield was still very low. Possibly this was due to factors mentioned in synthesis of **2c** (inefficient cyclisation reaction, repeated purification, lyophilisation step).

It was concluded from this result that the insertion of the fragment (KSSK) in the Bax peptide sequence was a more successful proposal than the insertion of the RELIRT fragment. There is a possibility that the length of the peptide (13-mer) assisted in allowing the termini of the peptide to approach closer together. Also, the two protected lysine residues might form more intramolecular hydrogen bonds with carbonyl groups of the peptide bonds to draw the termini of the peptide closer together.

The storage of the two cyclic peptides (**2c**, **3c**) for six months inside a freezer at -20 °C without any hydrolysis was an indicator that the two compounds have acceptable stability and are better than compound **1c**. Probably, the two cyclic peptides (**2c**, **3c**) adopt a strain free conformation in solution that is not predisposed to hydrolysis. Therefore, in the solution, they were stable for a far greater time in comparison to compound **1c**.

No issues occurred in the synthesis, identification, purification, and lyophilisation of the linear peptides (**2b**, **3b**). This may be due to their acceptable solubility in the HPLC solvents because they have more than one free polar side group, in addition to the two free polar termini.

It was noticed that the retention time of the 15-mer cyclic peptide (**2c**) in the HPLC was very close to the retention time of its linear counterpart (**2b**). It is deduced from this value that the restricted conformation and lack of termini of the cyclic peptide (**2c**) had no significant effect on the polarity of the compound, while the difference between 13-mer cyclic peptide (**3c**) and its linear counterpart (**3b**) was observed clearly. The retention time of the cyclic compound (**3c**) was greater than the retention time of its linear counterpart (**3b**). It was concluded from this result that the loss of the termini and constricted conformation of **3c** had reduced its polarity relative to **3b**.

It was concluded from the study of the MS<sup>2</sup> mass spectra of compound **1c** and its linear counterpart (**1b**), that the main difference between them was a peak of 946.4 *m/z* in the spectrum of **2c** for the fragments of *b*<sub>8</sub> and *b*<sub>8</sub>-H<sub>2</sub>O. These fragments represented four different isobaric sequences, three for the fragment of *b*<sub>8</sub>-H<sub>2</sub>O and one for the fragment of *b*<sub>8</sub>, all of which included the peptide bond between Phe and Asp. As was expected, this fragment was not observed in the MS<sup>2</sup> mass spectrum of compound **1b** because there was no peptide bond between Phe (*N*-terminus) and Asp (*C*-terminus). This difference could be considered as evidence that the cyclic peptide (**1c**) had formed.

The main difference between the MS<sup>2</sup> spectrum of the cyclic peptide (**2c**) and its linear counterpart (**2b**) was a peak of 915.0 *m/z*. This mass was observed in the MS<sup>2</sup> mass spectrum of **2c** and was not observed in the MS<sup>2</sup> mass spectrum of its linear counterpart (**2b**) for the same reason that was mentioned in **1b**. This fragment represented five sequences, one of which (MH<sub>2</sub>-NH<sub>3</sub>) included the peptide bond between Phe and Asp. Therefore, this result was potential evidence for formation of the cyclic peptide (**2c**).

The main difference between the third cyclic peptide (**3c**) and its linear counterpart (**3b**) was the observed mass of 617.0 *m/z*. This mass was observed in the MS<sup>2</sup> mass spectrum of compound **3c**, whereas it was not observed in the MS<sup>2</sup> mass spectrum of its linear counterpart (**3b**) for the same reason that was

mentioned in **1b**. This mass represented two sequences ( $b_5$ ,  $y_5$ ) and because they included the peptide bond between Phe and Asp residues this result was potential evidence for formation of the cyclic peptide (**3c**).

### 5.1.2 Enzymatic degradation and kinetic study

It was noted that the chymotrypsin enzyme exhibited the same selectivity towards the two predicted cleavage sites (Trp–Thr and Phe–Leu) in the two compounds (**2b**, **2c**), leading to the cleaving of the peptide bond between Trp and Thr, but no cleavage between Phe and Leu. Potentially, the peptide bond of Phe–Leu did not hydrolyse due to the presence of the charged amino group on the *N*-terminal Phe residue that may have negatively affected the interactions with the enzyme.

The retention time of the peptide produced by chymotrypsin catalysed hydrolysis of **2c** was greater than the retention time of **2c**. This result was not expected because hydrolysis of compound **2c** generates two new polar groups at the termini. Possibly, the cause was the restricted conformation of **2c** enhancing the overall polarity of the compound by aligning polar groups. On the other hand, the free orientation of the polar groups in the linear peptide hydrolysis product (15-mer) may have resulted in the adoption of conformations that lowered the overall polarity of the molecule.

The retention times of all the peptides produced by hydrolysis of linear peptide **2b** were less than the retention time of **2b**. This result was expected because the generated peptides were polar (having two free polar termini in addition to internal polar side groups), in addition to the mass of these produced peptides being less than the mass of **2b**.

Surprisingly, the  $t_{\frac{1}{2}}$  of **2c** towards chymotrypsin hydrolysis was less than the  $t_{\frac{1}{2}}$  of **2b**. The cyclisation of peptide (**2c**) was potentially drawing compound **2c** into a conformation that was a more acceptable substrate for the chymotrypsin than its linear counterpart (**2b**).

The expected result was observed from hydrolysis of the peptide bond between Arg and Thr in compound **2b** by trypsin to afford a peptide with lower retention time and  $m/z$  than compound **2b**. The second susceptible peptide bond (Arg–Glu) did not hydrolyse; there was a possibility that the presence of

charged carboxyl group on the Glu residue might have negatively affected interactions with the enzyme.

The two susceptible peptide bonds (Arg–Thr, Arg–Glu) of **2c** were hydrolysed by trypsin. Two peptides products were observed. The first one had a lower retention time than **2c**, which was expected because this compound has more polar groups and lower mass than **2c**. The second peptide eluted with retention time greater than the retention time of the cyclic compound (**2c**), which was not predicted as it also has more polar groups and lower mass. Potentially, the cause was the conformation of this peptide. It was concluded that the second peptide bond (Arg–Glu) in the cyclic peptide (**2c**) was more suitable as a substrate for the enzyme than in linear peptide (**2b**).

The  $t_{1/2}$  of **2c** against trypsin was greater than the  $t_{1/2}$  of **2b** indicating greater stability of the cyclic peptide. There is the possibility that the cause was the constricted conformation of the cyclic compound (**2c**) preventing the compound occupying the active site of the enzyme. Consequently, relative to its linear counterpart (**2b**) it is predicted that the cyclic compound (**2c**) will stand an increased chance *in vivo* of reaching the target antigen presenting cells.

Hydrolysis of the peptide bond between Trp and Thr by chymotrypsin in the 13-mer linear and cyclic peptides (**3b**, **3c**) and non-hydrolysis of the peptide bond between Phe and Leu, were indicators that the effect of the chymotrypsin on the two compounds (**3c**, **3b**) was the same. It was possible that the constricted conformation of **2c** did not significantly change the orientation of the two peptide bonds in comparison with its linear counterpart.

As was expected, the peptide produced by chymotrypsin hydrolysis of **3b** had a retention time that was less than the retention time of **3b** as it was polar and lower molecular weight. The second peptide formed by hydrolysis of **3b** was not detected, possibly due to its high hydrophilicity leading to lack of retention on the chromatography column.

The linear peptide produced by hydrolysis of compound **3c** by chymotrypsin has the same length but a permuted sequence in comparison to **3b**; also, it has greater retention time than **3b**. The rate of enzymatic hydrolysis of the two compounds (**3b**, **3c**) by chymotrypsin was similar, since the  $t_{1/2}$  of **3b** was close to the  $t_{1/2}$  of **3c**. It is concluded from this result that the

conversion of the compound **3b** to **3c** did not significantly affect the stability of the peptide against chymotrypsin. The restricted conformation of the cyclic peptide (**3c**) appears to have made little difference to its ability to interact with the enzyme.

Regarding the stability of the two compounds (**3b**, **3c**) against trypsin, the cyclic peptide (**3c**) was very stable, while its linear counterpart was rapidly hydrolysed. It is deduced from this result that the restricted conformation of the cyclic peptide (**3c**) significantly changed the orientation of the peptide bond (Lys-Ile) to be in a conformation that was unsuitable as a substrate for trypsin. It is concluded that the conversion of compound **3b** to **3c** led to significant enhancement in the stability of the peptide. It is important to note that the second peptide bond (Lys-Ser) did not hydrolyse in either of the two compounds (**3b**, **3c**). Probably, this peptide bond was in a certain conformation that prevented it from occupying the active site of the enzyme.

### 5.1.3 Stability of the peptides (**2b**, **2c**, **3b**, **3c**) in fetal calf serum (FCS)

Some conclusions can be drawn from the study of the stability of the cyclic peptides (**2c**, **3c**) and their linear counterparts (**2b**, **3b**) in FCS.

Conversion of the 15-mer linear peptide (**2b**) to cyclic structure (**2c**) resulted in a decrease in the stability of the peptide. However, this decrease was not statistically significant. Therefore, there is no evidence that the constricted conformation of the cyclic peptide (**2c**) had boosted the stability of the peptide against the protease enzymes. It is deduced from this result that within experimental error the two peptides (**2c**, **2b**) have the same resistance against the protease enzymes in the FCS pool. Consequently, the cyclic compound (**2c**) has the same chance of its linear counterpart (**2b**) to reach the target cell.

Converting the 13-mer linear peptide (**3b**) to cyclic peptide (**3c**) increased the stability of the peptide. It is tentatively concluded from this result that the restricted conformation of the cyclic peptide (**3c**) was unsuitable as a substrate for the active site of the protease enzymes (greater resistance to the protease degradation). Therefore, it is possible that this cyclic peptide (**3c**) has a greater

chance of reaching the target cells than its linear counterpart (**3b**) thus leading to activation of CD8<sup>+</sup> T-cells.

## 5.2 Future work

Firstly, synthesis of an alternative compound to 9-mer cyclic peptide (**1c**), could be attempted using another method such as click reaction. The presence of a triazole group in the sequence of the cyclic peptide may increase the solubility of the peptide in HPLC solvents resulting in a higher yield. Also, synthesis of 9-mer cyclic peptide (**1c**) using another coupling reagent that yields a long lived active ester may increase the yield.

Preparation of larger amounts of 13-mer cyclic peptide (**3c**) and 15-mer cyclic peptide (**2c**) and their linear counterparts (**2b**, **3b**) is desirable to study their ability to activate T cells *in vitro*. In addition to that, synthesis of more derivatives of the 9-mer cyclic peptide (**1c**) with insertion of new fragments that conferring high aqueous solubility and cell permeability would facilitate study of the enzymatic degradation and stability in the serum, followed by T cell activity. Furthermore, study of the stability of the cyclic peptides (**2c**, **3c**) in the FCS could be performed for a longer time such as weeks or months, with additional studies of the stability of these two cyclic peptides in human serum. Following the fate of a cyclic peptide once it has been taken up by an antigen presenting cell would be another significant area of interest. The products of intracellular peptide cleavage could be investigated by mass spectrometry and the sub-cellular location of fluorescently labelled peptides tracked by confocal microscopy.

## **Chapter 6**

# **Experimental Section**



## 6 Methods

### 6.1 Analytical methods

#### 6.1.1 RP-HPLC

HPLC analysis was performed on a Merck–Hitachi LaChrom D–7000 instrument with a Merck (Germany) Chromolith RP–C18E, 4.6 × 10 mm column, a 50 µL injection and a flow rate of 1 cm<sup>3</sup> min<sup>−1</sup>. The detector wavelength was set at 220 nm. The column oven temperature was set at 30 °C. Unless stated otherwise, solvent A was H<sub>2</sub>O with 0.1% TFA and solvent B was MeCN with 0.1% TFA.

#### 6.1.2 LC-MS

Mass spectrometry analysis was predominantly conducted on a Bruker Amazon SL ion trap system (Bruker Daltonics), instrument including a Thermo Ultimate 3000, ACQUITY UPLC, and using a Waters BEH C18 1.7 µm, 2.1 × 100 mm column, with a 10 µL injection and flow rate 0.5 cm<sup>3</sup> min<sup>−1</sup>. The temperature was set at 40 °C.

Mass spectrometry of BSA samples was performed by Dr Thomas Williams on a Waters Synapt G2-Si instrument with Acquity H class UPLC System and Waters BEH C18 Column, 130 Å, 1.7 µm, 2.1 mm × 50 mm, 40 °C, flow rate 0.25 ml/min.

For both systems, solvent A was H<sub>2</sub>O with 0.1% formic acid and solvent B was MeCN with 0.1% formic acid.

#### 6.1.3 Glass and plasticware

**Table 6.1:** Names of the suppliers of glassware and plasticware.

Supplier	Glass and plastics
Fisher Scientific	Disposable sterile centrifuge tube (15, 50 mL), beakers (25, 100, 250, 1000 mL), conical flask (100, 250 mL)
Kinesis	Autosampler vial (1.5 mL, 250 µL)
Eppendorf	Microcentrifuge vial (1.5, 2.5 mL)

## 6.1.4 Chemicals

**Table 6.2:** Names of the chemical suppliers.

Supplier	Material
Fisher Scientific	HPLC water, HPLC acetonitrile, TFA, LiCl, DIPEA
Novabiochem	All Fmoc-amino acids, Fmoc-Trp(Boc)-Thr(ψMe, Mepro)-OH, Fmoc-Asp(Resin)-Allyl
Sigma Aldrich	Trypsin, chymotrypsin, chloroform, ether, methanol
Acros Organics	DEPBT, piperidine, Parafilm
Alfa Aesar	Pd(PPh <sub>3</sub> ) <sub>4</sub> , 4-methylmorpholine, sodium dimethyl dithiocarbamate hydrate
AGTC Bioproducts	<i>N</i> -methylpyrrolidone, PyBOP, HOBt (anhydrous)

## 6.1.5 Instruments

**Table 6.3:** Suppliers of instruments.

Supplier	Instrument
Kern	ALS 220-4N balance
Grant	Ultrasonic bath
Sorval	Microcentrifuge
Eppendorf	Heat block
Hettich	Rotina 38 R centrifuge
Medline Scientific Ltd.	Shaker
Prestige Medical	Autoclave
Thermo Electron Corporation	Freeze dryer
Shimadzu Corporation	2401PC UV visible spectrometer

## 6.2 Method to synthesise the cyclic peptide and their linear counterparts

### 6.2.1 Method to synthesise the linear peptide allyl esters (1a, 2a, 3a)

Resin preloaded with Fmoc-Asp-OAllyl (catalogue number 8560250001) (0.1 g, 0.02 mmol) was placed into a 5 mL filter tube and peptide synthesis grade NMP (3–4 mL) was added. The resin was left for 1 h to swell. Meanwhile, suitable amounts of reagents PyBOP (51 mg, 0.1 mmol) and HOBt (15 mg, 0.1

mmol) were added to eight Eppendorf tubes, and into each tube the required amount of amino acid (five molar equivalents excess relative to the resin) was added, taking into account the sequence of the amino acids. An excess amount (3–4 mL) of 20% piperidine in NMP was added to the filter tube containing the swollen resin, the resin was agitated for 10 min using the vortex mixer and filtered. The piperidine treatment was performed three times to cleave the Fmoc protecting group. The resin was then washed NMP (3 × 3 mL) by shaking it gently for 3 min to remove the remainder of the piperidine. NMP (500 µL) and DIPEA (38 µL) were added to the next amino acid in sequence in the Eppendorf tube, and this was mixed strongly by vortexing the tube. This mixture was added to the resin in the filter tube. The mixture was agitated for 1 h at 25 °C in a shaker. The solution was filtered using vacuum filtration, and the resin washed with NMP (3 × 3 mL) for 3 min to remove the excess activated amino acid, HOBt, and DIPEA. The process of deprotection of the Fmoc group by piperidine, the activation and coupling of the next amino acid in the sequence, and the washing with NMP was repeated for all the remaining amino acids. After addition of the final amino acid, its Fmoc group was left attached until immediately before the cyclisation step was performed.

Once the resin-bound linear peptide allyl ester had been synthesised, a few mg of resin was removed for analysis of the cleaved and deprotected allyl ester peptides **1a**, **2a** and **3a**. The Fmoc deprotection reaction was performed on this sample after washing with 3 × 1 mL portions of NMP, chloroform, ethanol, and diethyl ether for 3 min. After drying the diethyl ether using nitrogen gas, the small sample was placed inside a vacuum oven at 30 °C for 15 min. Finally, the cleavage reaction was conducted by adding 1 µL of water, 1 µL of triisopropyl silane, and 100 µL of TFA, then leaving for 1 hour at room temperature. After evaporating more than half of the TFA by nitrogen blow-down, 250 µL of acetonitrile or water was added to the sample then it was vortexed, centrifuged and analysed by HPLC and LC–MS.

### 6.2.2 Method to deprotect the allyl ester from the C-terminus

The resin loaded with the peptide allyl ester was soaked in 3–2 mL of chloroform for 10 min, during which time a solution of catalytic Pd(PPh<sub>3</sub>)<sub>4</sub> (70 mg, 0.06 mmol), in chloroform (950 µL), glacial acetic acid (100 µL) and

*N*-methyl morpholine (50  $\mu$ L) was prepared in a small pear-shaped flask. This solution was then freeze-pump-thaw degassed. The filter tube containing the peptide-loaded resin was closed with a rubber septum and was flushed with nitrogen for 5 min. The solution of Pd(PPh<sub>3</sub>)<sub>4</sub> was transferred to the resin by syringe and needle. This was left with gentle agitation for 2 h in the shaker at 20 °C, using a rubber septum to exclude air. The resin was washed with 3  $\times$  1 mL portions of NMP, chloroform, ethanol, sodium diethyldithiocarbamate solution (1 g/100 mL in NMP) and diethyl ether for 3 min. A few mg of resin was removed to produce samples of linear peptides (**1b**, **2b**, **3b**) for analysis. The Fmoc deprotection reaction was performed. After the washing with 3  $\times$  1 mL portions of NMP, chloroform, ethanol, and diethyl ether for 3 min, a cleavage reaction was conducted, as was mentioned in the synthesis of linear peptide allyl ester; then, a sample was taken for analysis by HPLC and LC-MS.

### 6.2.3 Cyclisation of the linear peptide (**1c**, **2c**, **3c**)

After deprotection of the allyl group, the final Fmoc protecting group was removed using three portions of 20% piperidine in NMP (3 mL), each for 10 min. The resin was then washed with 3  $\times$  1 mL portions of NMP for 3 min. Further washing was carried out with 3  $\times$  1 mL 10% DIPEA in NMP and then 3  $\times$  1 mL portions of LiCl (339 mg, 0.8 M in NMP) for 3 min. A solution of DEPBT (25 mg, 0.084 mmol) and DIPEA (35  $\mu$ L) in NMP (500  $\mu$ L) was added to the resin and gently agitated for 2 h in the shaker at 20 °C. The solution was then drained and another identical portion of the coupling reagent solution was added; this was then left overnight, and finally the resin was washed with 3  $\times$  3 mL NMP; a small amount of resin was then removed, and a Fmoc deprotection reaction was performed prior to washing with 3  $\times$  1 mL portions of NMP, chloroform, ethanol, and diethyl ether for 3 min. Finally, a cleavage reaction was conducted, as was described in the synthesis of linear peptide allyl ester, and a sample taken for analysis by HPLC and LC-MS.

### 6.2.4 Method to synthesise linear peptide (**1b**, **2b**, **3b**)

Three steps were used in the synthesis of the three compounds (**1b**, **2b**, **3b**). The assembly of the peptide chain was as in the procedure for the synthesis of linear peptide allyl ester (2.6.1); then the second step was as in the procedure for the deprotection of allyl group (6.2.2); the cleavage and side chain

deprotection followed the same procedure as cleavage of the cyclised peptide (2.6.5).

### 6.2.5 Cleavage of the cyclised peptide

The peptide-loaded resin was firstly washed with an excess amount (3–4 mL) of chloroform, methanol and diethyl ether. Next, the resin was dried in a vacuum oven for 15 min to evaporate the ether. Water (25  $\mu$ L), ethane-1,2-dithiol (25  $\mu$ L), triisopropyl silane (10  $\mu$ L) and TFA (950  $\mu$ L) were then added to the Eppendorf vial containing the resin by micropipette using a disposable tip. Any apparatus and all the tips that had touched the mixture were immediately put into a beaker (500 mL) of bleach and left for at least 12 h to oxidise the mixture for neutralisation purposes. The reaction was left for 2 h with gentle agitation. At this point, 2  $\times$  12 mL of diethyl ether was put into centrifuge tubes (15 mL) and placed into an ice bath to cool. After the reaction had taken place, the solution of the peptide was poured into the first tube of ice cold diethyl ether (12 mL). The peptide was then obtained as a milky cream precipitate, and the tube was centrifuged for 5 min at 19450 RCF using the second diethyl ether tube (12 mL) as a balance for the centrifuge. After this, the ether was eliminated through careful decantation into a waste beaker. The process of adding diethyl ether and its removal was repeated one further time; then, 2 mL of water was added to dissolve the peptide. The solution was also vortexed to ensure the pellet of peptide had completely dissolved. The solution was stored at 4 °C and LC-MS and HPLC analyses were run.

### 6.3 HPLC purification of the peptides

The cyclic peptides (**1c**, **2c**, **3c**) were purified using a Merck (Germany) Chromolith RP-C18E, 100  $\times$  4.6 mm column, via a 100  $\mu$ L injection and a flow rate of 1 mL min<sup>-1</sup>. The column oven was set at 30 °C. Unless stated otherwise, solvent A was H<sub>2</sub>O with 0.1% TFA and solvent B was MeCN with 0.1% TFA. The method which was used to purify the 9-mer cyclic peptide (**1c**) has retention time 17.23 min as shown in Table 6.4.

**Table 6.4:** HPLC method for purification of 9-mer cyclic peptide (**1c**), which has retention time 17.23 min.

Time (min)	% Water	% Acetonitrile
0	95	5
1	95	5
25	5	95
30	5	95
33	95	5

The fraction containing the cyclic peptide (**1c**) was lyophilised to remove the HPLC solvents. The solid sample was then weighed and dissolved in dimethylsulfoxide (DMSO) to prepare a concentration of 10 mg/mL as a stock solution. 1  $\mu$ L was taken from the stock solution and added to 50  $\mu$ L of acetonitrile for analysis. Finally, HPLC and LC-MS analyses were performed, and the stock solution was stored at  $-20^{\circ}\text{C}$ . Compound **2c**, which has retention time 12.29 min, was purified (three times) using the method as shown in Table 6.5. Using the same method as for the 9-mer cyclic peptide (**1c**), the 15-mer cyclic peptide (**2c**) was dried, weighed, re-dissolved, analysed and stored.

**Table 6.5:** HPLC method for purification of 15-mer cyclic peptide (**2c**), which has retention time 12.29 min.

Time (min)	% Water	% Acetonitrile
0	95	5
1	95	5
20	5	95
23	5	95
24	95	5
25	95	5

The method which was used to collect the 15-mer linear peptide (**2b**), which has retention time 12.67 min, is the same as the method used for the 15-mer cyclic peptide (**2c**). Again, the 15-mer linear peptide (**2b**) was dried, weighed, re-dissolved, analysed and stored. The method used to purify the 13-mer cyclic peptide (**3c**), which has retention time 14.49 min, is described in Table 6.6.

**Table 6.6:** HPLC method for the purification of 13-mer cyclic peptide (**3c**), which has retention time 14.49 min.

Time (min)	% Water	% Acetonitrile
0	95	5
1	95	5
25	5	95
30	5	95
34	95	5
35	95	5

The 13-mer cyclic peptide (**3c**) was purified (two times), dried using the same method that was utilised in the 9-mer cyclic peptide: weighed, re-dissolved, analysed by HPLC and LC-MS and stored.

Finally, the method used to collect the 13-mer linear peptide (**3b**), which has retention time 10.68 min, is the same as the method employed for the 13-mer cyclic peptide (**3c**) and the 9-mer cyclic peptide. Then, the same final five steps for the 13-mer cyclic peptide (**3c**) were undertaken for its linear counterpart (**3b**).

## 6.4 Fragmentation of the peptides

The same samples of the cyclic peptides (9, 13, 15-mer) and their linear counterparts, which were used to run MS analysis, were used to run the MS<sup>2</sup> analysis via the LC-MS. The selection of the precursor ion for fragmentation by the MS<sup>2</sup> method for all the peptides depended on the peak observed in the MS scan. Therefore, the precursor ions were as described in Table 6.7. Collision induced dissociation was used for fragmentation, with the collision energy set automatically by the instrument control software.

**Table 6.7:** Precursor ion  $m/z$  for the MS<sup>2</sup> analysis which were obtained from MS scan.

Peptide	Precursor ion ( $m/z$ )
9-mer linear peptide ( <b>1b</b> )	1095.7
9-mer cyclic peptide ( <b>1c</b> )	1077
15-mer linear peptide ( <b>2b</b> )	933.0
15-mer cyclic peptide ( <b>2c</b> )	923.5
13-mer linear peptide ( <b>3b</b> )	509.6
13-mer cyclic peptide ( <b>3c</b> )	754.9

## 6.5 Preparation of the buffer solution

Ammonium bicarbonate ( $\text{NH}_4\text{HCO}_3$ ) was used as a buffer solution in the enzyme degradation experiments and for checking the stability of the peptides in FCS.  $\text{NH}_4\text{HCO}_3$  (39.5 mg) was dissolved in 50 mL of distilled water to prepare a 0.01 M concentration of the buffer solution, the pH of which was then adjusted by 3–5 drops of the concentrated ammonia solution until a pH of 8.6 was achieved. The buffer was then stored at room temperature.

## 6.6 Calculating the concentration of the peptides (2b, 2c, 3b, 3c)

### 6.6.1 The 13-mer cyclic peptide (3c)

2.7 mg of the 13-mer purified cyclic peptide (**3c**) was dissolved in 270  $\mu\text{L}$  of DMSO solvent to obtain a 10 mg/mL stock solution. 1  $\mu\text{L}$  of the stock solution was added to 999  $\mu\text{L}$  of the ammonium bicarbonate buffer solution inside the UV cuvette. After mixing the solution, the absorbance was measured at wavelengths from 200–600 nm at a temperature of 25 °C. This measurement was repeated twice and the concentration of the cyclic peptide in the cuvette was calculated at the wavelength 280 nm by the following equation:

$$C = A/\epsilon$$

$$\epsilon(\text{Trp}) = 5690 \text{ M}^{-1}\text{cm}^{-1}$$

Then the concentration of the stock solution (270  $\mu\text{L}$ ) was calculated by the following equation:

$$C_1 \times V_1 = C_2 \times V_2$$

### 6.6.2 The 13-mer linear peptide (3b)

0.74 mg of the linear peptide was dissolved in 74  $\mu\text{L}$  of dimethyl sulfoxide (DMSO) to obtain a 10 mg/mL stock solution. 10  $\mu\text{L}$  of this stock solution was added to 990  $\mu\text{L}$  of the ammonium bicarbonate buffer solution, inside a spectrophotometer cuvette. After mixing the solution, the absorbance was measured at wavelengths between 200–600 nm at a temperature of 25 °C. This



measurement was repeated twice, and the concentration of the linear peptide was calculated using the absorbance at 280 nm using the equation mentioned previously.

### **6.6.3 The 15-mer cyclic peptide (2c) and its linear counterpart (2b)**

The same method as for the previous peptide (**3b**) was applied to prepare the stock solution (10 mg/mL) and compute the concentration of the 15-mer cyclic peptide (**2c**) and its linear counterpart (**2b**).

### **6.6.4 Calculation of the percentage yield of the peptides (2b, 2c, 3b, 3c)**

The general method that was used to calculate the percentage for the yield of the synthesised peptide is as follows:

$$\text{Resin substitution (mmol/g)} = 0.2$$

$$\text{Amount of resin (g)} = 0.1$$

$$\text{Meq of resin (mmol)} = 0.2 \times 0.1 = 0.02$$

$$\text{Yield of the synthesised peptide (mmol)} = \text{mass (by UV method)} / \text{MW}$$

$$\% \text{ of the peptide} = 100 \times \text{yield of the synthesised peptide (mmol)} / \text{Meq of resin (mmol)}$$

## **6.7 Calculation of the concentration of the enzymes**

1 mg of each enzyme, trypsin and chymotrypsin, was dissolved in 1 mL of buffer solution ( $\text{NH}_4\text{HCO}_3$ ) in a 1.5 mL Eppendorf tube for use as a stock solution. A Bradford assay for the quantity of the protein in the solution was used to measure the absorbance of each enzyme.<sup>197</sup> Bovine serum albumin (BSA) was used as a protein standard to generate a calibration plot. An aliquot of BSA stock solution was diluted to a volume of 200  $\mu\text{L}$  with water, then Bradford reagent was added to give a total volume of 1.0 mL. The absorbance at a wavelength of 595 nm was measured at a temperature of 25 °C. Measurements were performed in an identical way for the trypsin and chymotrypsin stock solutions. The BSA calibration graph was used to determine the amount of each

enzyme present in the diluted volume (200  $\mu\text{L}$ ), from which the stock solution (1.0 mL) concentration was calculated.

## **6.8 Preparation of the BSA solution**

BSA protein (2 mg,  $15 \times 10^{-3}$  M) was weighed and dissolved in 2 mL of buffer solution ( $\text{NH}_4\text{HCO}_3$ ); then, 10  $\mu\text{L}$  was taken from the solution and diluted to 500  $\mu\text{L}$  by the buffer solution to obtain BSA concentration ( $3 \times 10^{-4}$  M) as a stock solution.

## **6.9 Checking the activity of the enzymes**

### **6.9.1 Activity of the chymotrypsin**

BSA was used to check the activity of the chymotrypsin enzyme. 10  $\mu\text{L}$  of chymotrypsin stock solution was added to 100  $\mu\text{L}$  of BSA stock solution inside an Eppendorf tube. The reaction was incubated at 37  $^{\circ}\text{C}$  for 30 min, after which the reaction was stopped by heating for 5 min in a boiling water bath (100  $^{\circ}\text{C}$ ) followed by cooling with liquid nitrogen for 1 min. MS analysis was then performed after centrifuging of the sample.

### **6.9.2 Activity of the trypsin**

10  $\mu\text{L}$  of trypsin stock solution was added to 100  $\mu\text{L}$  of BSA stock solution inside an Eppendorf tube, Then, the same methodology was used as described when studying the activity of chymotrypsin to examine the activity of the trypsin.

## **6.10 Enzymatic degradation and kinetics for the hydrolysis of peptides**

### **6.10.1 Enzymatic degradation and calculation of the $t_{1/2}$ of 13-mer linear peptide (3b) in the presence of chymotrypsin**

25  $\mu\text{L}$  of chymotrypsin (1.06  $\mu\text{M}$ ) was added to 250  $\mu\text{L}$  of **3b** (200  $\mu\text{M}$ , pH 8.6) inside a 0.5 mL Eppendorf tube; this tube was then incubated inside a heat block at 10  $^{\circ}\text{C}$ . A small sample (25  $\mu\text{L}$ ) was then taken and transferred to another Eppendorf tube after 0, 2, 4, 6, 8, 10, 15, 20, 30 min and the reaction stopped by heating in a boiling water bath (100  $^{\circ}\text{C}$ ) for 4 min then freezing in a

bath of liquid nitrogen for 1 min. Finally, LC–MS and HPLC (10 µL as injection volume, 30 °C column temperature and the method shown in Table 6.8) analysis was performed after centrifuging of the sample.

**Table 6.8:** General HPLC method used to study the enzymatic degradation and  $t_{1/2}$  of 13-mer cyclic peptide (**3c**) and its linear counterpart (**3b**) in the presence of chymotrypsin and trypsin.

Time (min)	% Water	% Acetonitrile
0	95	5
1	95	5
25	5	95
30	5	95
34	95	5
35	95	5

The areas of the 13-mer linear peptide (**3b**) peaks in the chromatograms of HPLC for 0–30 min were used to calculate the  $t_{1/2}$  of compound **3b**, by plotting  $\ln$  area against the time. The LINEST function in Excel was used to obtain the gradient ( $k$ ) and its standard error (SE). The gradient was used in the following equation to calculate the  $t_{1/2}$ .

$$t_{1/2} = \ln 2 / k$$

### 6.10.2 Enzymatic degradation and calculation of the $t_{1/2}$ of the 13-mer cyclic peptide (**3c**) in the presence of chymotrypsin

25 µL of chymotrypsin (1.06 µM) was added to 250 µL of **3c** (200 µM, pH 8.6) inside a 0.5 mL Eppendorf tube. The degradation was then achieved, using the same methodology as described for the enzymatic degradation of the 13-mer linear peptide (**3b**) in the presence of chymotrypsin, to perform the experiment. LC–MS and HPLC were again performed using the same conditions and solvent gradient as for **3b** in the presence of chymotrypsin.

The areas of the 13-mer cyclic peptide (**3c**) peaks in the chromatograms of HPLC for 0–30 min and the same functions in the Excel program and the equation, as was mentioned in the study of the  $t_{1/2}$  of the 13-mer linear peptide (**3b**) in the presence of chymotrypsin, were used to calculate the  $t_{1/2}$  of **3c**.

### 6.10.3 Enzymatic degradation and calculation of the $t_{1/2}$ of the 13-mer linear peptides (**3b**) in the presence of trypsin

25  $\mu$ L of trypsin (0.41  $\mu$ M) was added to a 0.5 mL Eppendorf tube containing 250  $\mu$ L of **3b** (200  $\mu$ M, pH 6.2). The tube was then incubated inside a heat block at 10 °C. The experiment was then prepared in the same way as described previously (section 6.10.2) but with the presence of trypsin. Finally, LC-MS and HPLC analyses were performed with the HPLC methodology as shown in Table 6.8.

The same procedure was used to study the  $t_{1/2}$  of the 13-mer linear peptide (**3b**) in the presence of chymotrypsin. The areas of **3b** peaks in the HPLC chromatograms resulting from the reaction of the 13-mer linear peptide (**3b**) with trypsin for 0–30 min were used to calculate the  $t_{1/2}$ .

### 6.10.4 Enzymatic degradation and calculation of the $t_{1/2}$ of the 13-mer cyclic peptide (**3c**) in the presence of trypsin

This is the same procedure, that was used in the study of the degradation of the linear peptide (**3b**) in the presence of trypsin. In addition, 3  $\mu$ L of Fmoc-tryptophan(Boc) ( $2.7 \times 10^{-2}$  M) was added to each sample after stopping the reaction (heating in a boiling water bath at 100 °C for 4 min then freezing in a bath of liquid nitrogen for 1 min). The ratio of peak area of peptide to internal standard (**3c**/IS) was calculated for each time point to study the stability of **3c** against trypsin.

### 6.10.5 Enzymatic degradation and calculation of the $t_{1/2}$ of the 15-mer linear peptide (**2b**) in the presence of chymotrypsin

Inside a 0.5 mL Eppendorf tube, 25  $\mu$ L of chymotrypsin (1.06  $\mu$ M) was added to 250  $\mu$ L of **2b** (100  $\mu$ M pH 8.6). This tube was incubated inside a heat block at 10 °C and then a small portion of the sample (25  $\mu$ L) was taken and moved to another Eppendorf tube after 0, 2, 4, 6, 8, 10, 15, 20, 30 min. At this point, the enzyme reaction was stopped by heating in a boiling water bath (100 °C) for 4 min followed by freezing in a bath of liquid nitrogen for 1 min. LC-MS and HPLC were then performed with the HPLC conditions listed in Table 6.9.

The areas of the 15-mer linear peptide (**2b**) peaks in the HPLC chromatograms for 0–30 min were used to calculate the  $t_{1/2}$  of **2b**, using the same functions in the Excel program and the equation as were mentioned in the study of the  $t_{1/2}$  of the 13-mer linear peptide (**3b**) in the presence of the same enzyme.

**Table 6.9:** General HPLC method used to study the enzymatic degradation and  $t_{1/2}$  of 15-mer cyclic peptide (**2c**) and its linear counterpart (**2b**) in the presence of chymotrypsin and trypsin.

Time (min)	% Water	% Acetonitrile
0	95	5
1	95	5
20	5	95
21	5	95
23	95	5

#### 6.10.6 Enzymatic degradation and calculation of the $t_{1/2}$ of the 15-mer cyclic peptide (**2c**) in the presence of chymotrypsin

The same procedure and conditions that were used in the hydrolysis of the 15-mer linear peptide (**2b**) by chymotrypsin were then employed in this experiment to undertake the degradation and LC–MS, HPLC analysis of the 15-mer cyclic peptide (**2c**) with the same enzyme.

The areas of the 15-mer cyclic peptide (**2c**) peaks in the chromatograms of HPLC for 0–30 min were used to calculate the  $t_{1/2}$  of **2c**, using the same methodology applied for determining  $t_{1/2}$  of the 13-mer linear peptide (**3b**) in the presence of chymotrypsin.

#### 6.10.7 Enzymatic degradation and calculation of the $t_{1/2}$ of the 15-mer linear peptide (**2b**) in the presence of trypsin

25  $\mu$ L of trypsin (0.41  $\mu$ M) was added to a 0.5 mL Eppendorf tube containing 250  $\mu$ L of **2b** (100  $\mu$ M pH 6.2). The tube was then incubated inside a heat block at 10 °C. The experiment was then prepared in the same way as described previously (section 6.10.5) but in the presence of trypsin. Finally, LC–MS and HPLC analyses were performed with the HPLC method shown in Table 6.9.

Using the method described previously, the  $t_{1/2}$  of the 15-mer linear peptide (**2b**) was calculated from the areas of **2b** peaks in the HPLC chromatograms for 0–30 min of reaction between trypsin and compound **2b**.

#### **6.10.8 Enzymatic degradation and calculation of the $t_{1/2}$ of the 15-mer cyclic peptide (2c) in the presence of trypsin**

The same procedure and conditions that were used in the hydrolysis of **2b** by trypsin and the conditions of the LC–MS and HPLC (Table 6.9) analysis were used in this experiment to study the degradation of **2c** with the same enzyme.

The  $t_{1/2}$  of **2c** was determined from the areas of **2c** peaks in the HPLC chromatograms of HPLC for 0–30 min reaction time using the previously described method.

#### **6.11 General procedures to study the stability of the peptides (2b, 3b, 2c, 3c) in fetal calf serum (FCS)**

##### **6.11.1 Preparation of 20% FCS solution**

The stored frozen serum (supplied by Sigma–Aldrich) was prepared by centrifugation at 9450 RCF at 8 °C, for 10 min. Then 200  $\mu$ L of the clear solution was taken by micropipette and added to 800  $\mu$ L of the HEPES buffer solution (1 M in H<sub>2</sub>O, pH 7.4) inside a 1.5 mL Eppendorf tube to obtain 20% serum solution.

##### **6.11.2 Studying the stability of the 13-mer linear peptide (3b) in the presence of FCS**

226  $\mu$ L of **3b** (0.7 mM) was added to 226  $\mu$ L of serum (20%) inside a 0.5 mL Eppendorf tube; this tube was then incubated inside a heat block at 37 °C. Aliquots (24  $\mu$ L) were taken after 0, 2, 6, 12, 24, 48 h, following which, the enzymatic reaction was stopped by heating the sample in a boiling water bath (100 °C) for 5 min followed by freezing in a bath of liquid nitrogen for 1 min. 1  $\mu$ L of benzoic acid (8.1 mmole), used as an internal standard, was then added, followed by vortexing and centrifugation of the sample. HPLC analysis was performed with a 10  $\mu$ L injection volume and column temperature of 30 °C. The

solvent gradient used in the HPLC analysis is shown in Table 6.10. This experiment was repeated a further two times.

**Table 6.10:** General HPLC method used to study the stability of 13-mer cyclic peptide (**3c**) and its linear counterpart (**3b**) in 20% FCS.

Time (min)	% Water	% Acetonitrile
0	95	5
1	95	5
12	5	95
30	5	95
33	95	5

**Table 6.11:** General HPLC method used to study the stability of 15-mer cyclic peptide (**2c**) and its linear counterpart (**2b**) in 20% FCS.

Time (min)	% Water	% Acetonitrile
0	95	5
1	95	5
12	5	95
23	5	95

### 6.11.3 Studying the stability of the 13-mer cyclic peptide (**3c**) in the presence of FCS

226  $\mu$ L of **3c** (0.7 mM) was added to 226  $\mu$ L of serum (20%) inside a 0.5 mL Eppendorf tube. The experiment was then achieved using the same methodology as described in the study of the stability of **3b**.

### 6.11.4 Studying the stability of the 15-mer linear peptide (**2b**) in the presence of FCS

226  $\mu$ L of **2b** (0.7 mM) was added to 226  $\mu$ L of 20% serum inside a 0.5 mL Eppendorf tube. The enzymatic degradation was then allowed to occur as previously described. However, the HPLC conditions required for this peptide were different and are described in Table 6.11.

### 6.11.5 Studying the stability of the 15-mer cyclic peptide (**2c**) in the presence of FCS

226  $\mu$ L of **2c** (0.7 mM) was added to 226  $\mu$ L of serum (20%) inside a 0.5 mL Eppendorf tube. Using the same methodology as previously described, the sample was analysed with the same injection volume, temperature and HPLC method (Table 6.11).

### 6.11.6 General procedure to calculate the $t_{1/2}$ of the peptides (**2b**, **2c**, **3b**, **3c**) in the presence of FCS

The ratio of the area of the peptide peak (**2b**, **2c**, **3b**, **3c**) in the HPLC chromatogram at 0, 2, 6, 12, 24, 48 h to the internal standard peak (benzoic acid) was used to calculate the  $t_{1/2}$  of each peptide.  $\ln$  (area of peptide peak/area of the internal standard peak) was plotted against time and a linear trendline fitted using the Excel software. The first order rate constant,  $k$ , is the negative of the gradient of the trendline. The equation that was used to calculate the  $t_{1/2}$  of the peptide is as mentioned in the calculation of the  $t_{1/2}$  of 13-mer linear peptide (**3b**) in the presence of chymotrypsin (section 6.10.1). The mean of the  $t_{1/2}$  values for the three replicates was calculated, in addition to the standard deviation ( $\sigma$ ) by the Excel program.



# References

## 7 References

- 1 K. G. Wolter, Y.-T. Hsu, C. L. Smith, A. Nechushtan, X. G. Xi and R. J. Youle, *J. Cell Biol.*, 1997, **139**: 1281–1292.
- 2 S. G. Agrawal, F. T. Liu, C. Wiseman, S. Shirali, H. Liu, D. Lillington, M. Q. Du, D. S. Court, A. C. Newland, J. G. Gribben and L. Jia, *Blood*, 2008, **111**(5): 2790–2796.
- 3 C. T. Nunes, K. L. Miners, G. Dolton, C. Pepper, C. Fegan, M. D. Mason and S. Man, *Cancer Res.*, 2011, **71**(16): 5435–5444.
- 4 Á. Roxin and G. Zheng, *Future Med. Chem.*, 2012, **4**: 1601–1618.
- 5 H. Zha, H. A. Fisk, M. P. Yaffe, N. Mahajan, B. Herman and J. C. Reed, *Mol. Cell. Biol.*, 1996, **16**: 6494–6508.
- 6 S. Cory and J. M. Adams, *Nat. Rev. Cancer*, 2002, **2**(9): 647–656.
- 7 B. Li and Q. P. Dou, *Proc. Natl. Acad. Sci. U. S. A.*, 2000, **97**: 3850–3855.
- 8 M. Weimershaus, I. Evnouchidou, L. Saveanu and P. V. Endert, *Curr. Opin. Immunol.*, 2013, **25**: 90–96.
- 9 B. Alberts, A. Johnson, J. Lewis, M. Raff, D. Morgan, K. Roberts and P. Walter, *Molecular Biology of the Cell*, Garland Science, New York 6<sup>th</sup> edition, 2015, 1324-1234.
- 10 N. Rezaei, S. H. Aalaei-Andabili, H. L. Kaufman, *Cancer Immunology*, Springer, Verlag-Berlin, Heidelberg, 2015, 1–8.
- 11 V. Brusic, V. B. Bajic and N. Petrovsky, *Methods*, 2004, **34**: 436–443.
- 12 J. A. Berzofsky, J. D. Ahlers and I. M. Belyakov, *Nat. Rev. Immunol.*, 2001, **1**(3): 209–219.
- 13 P. Cresswell, M. J. Turner and J. L. Strominger, *Proc. Natl. Acad. Sci. U. S. A.*, 1973, **70**(5):1603–1607.
- 14 L. Trägårdh, L. Rask, K. Wiman, J. Fohlman and P. A. Peterson, *Proc. Natl. Acad. Sci. U. S. A.*, 1979, **76**(11): 5839–5842.

- 15 H. M. Grew, R. T. Kubo, S. M. Colon, M. D. Poulik, P. Cresswell, T. Springer, M. Turner and J. L. Strominger, *J. Exp. Med.*, 1973, **138**: 1608–1612.
- 16 <https://www.rcsb.org/3d-view/5EU4/1>, [Accessed 20/03/2018].
- 17 D. H. Fremont, M. Matsumura, E. A. Stura, P. A. Peterson and I. A. Wilson, *Science*, 1992, **257**(5072): 919–927.
- 18 M. Matsumura, D. H. Fremont, P. A. Peterson and I. A. Wilson, *Science*, 1992, **257**(5072): 927–934.
- 19 C. DeLisi and J. A. Berzofsky, *Proc. Natl. Acad. Sci. U. S. A.*, 1985, **82**(20): 7048–7052.
- 20 P. J. Bjorkman, M. A. Saper, B. Samraoui, W. S. Bennett, J. L. Strominger and D. C. Wiley, *Nature*, 1987, **329**: 512–518.
- 21 J. B. Rothbard and W. R. Taylor, *EMBO J.*, 1988, **7**(1): 93–100.
- 22 P. J. Bjorkman and P. Parham, *Annu. Rev. Biochem.*, 1990, **59**: 253–288.
- 23 S. H. Joo, *Biomol. Ther.*, 2012, **20**(1): 19–26.
- 24 M. Chang, X. Li, Y. Sun, F. Cheng, Y. Li, W. Zhao and Q. Wang, *Biol. Pharm. Bull.*, 2013, **36**(10): 1602–1607.
- 25 P. M. Small and H. F. Chambers, *Antimicrob. Agents Chemother.*, 1990, **34**(6): 1227–1231.
- 26 R. J. Clark, N. L. Daly and D. J. Craik, *Biochem. J.*, 2006, **394**(1): 85–93.
- 27 S. Fernandez-Lopez, H. Kim, E. C. Choi, M. Delgado, J. R. Granja, A. Khasanov, K. Kraehenbuehl, G. Long, D. A. Weinberger, K. M. Wilcoxon and M. R. Ghadiri, *Nature*, 2001, **412**: 452–455.
- 28 M. Ali, M. Amon, V. Bender, A. Bolte, F. Separovic, H. Benson and N. Manolios, *Clin. Immunol.*, 2014, **150**(1): 121–133.
- 29 C. N. Birts, S. K. Nijjar, C. A. Mardle, F. Hoakwie, P. J. Duriez, J. P. Blaydes and A. Tavassoli, *Chem. Sci.*, 2013, **4**: 3046–3057.

- 30 L. Pollaro and C. Heinis, *Med. Chem. Commun.*, 2010, **1**: 319–324.
- 31 L. Feliu, G. Oliveras, A. D. Cirac, E. Besalu, C. Roses, R. Colomer, E. Bardaji, M. Planas and T. Puig, *Peptides*, 2010, **31**: 2017–2026.
- 32 M. Franchini and P. M. Mannucci, *Br. J. Clin. Pharmacol.*, 2011, **72**: 553–562.
- 33 O. L. Franco, *FEBS Lett.*, 2011, **585**(7): 995–1000.
- 34 M. Y. Yeshak, U. Göransson, R. Burman and B. Hellman, *Mutat. Res.*, 2012, **747**(2): 176–181.
- 35 A. Ehrlich, H. U. Heyne, R. Winter, M. Beyermann, H. Haber, L. A. Carpino and M. Bienert, *J. Org. Chem.*, 1996, **61**(25): 8831–8838.
- 36 T. Satoh, S. Li, T. M. Friedman, R. Wiaderkiewicz, R. Korngold and Z. Huang, *Biochem. Biophys. Res. Commun.*, 1996, **224**(2): 438–443.
- 37 L. Yang and G. Morriello, *Tetrahedron Lett.*, 1999, **40**(47): 8197–8200.
- 38 K. D. Kopple, P. W. Baures, J. W. Bean, C. A. D'Ambrosio, J. L. Hughes, C. E. Peishoff and D. S. Eggleston, *J. Am. Chem. Soc.*, 1992, **114**(24): 9615–9623.
- 39 A. Piserchio, G. D. Salinas, T. Li, J. Marshall, M. R. Spaller and D. F. Mierke, *Chem. Biol.*, 2004, **11**(4): 469–473.
- 40 D. J. Craik, N. L. Daly, T. Bond and C. Waine, *J. Mol. Biol.*, 1999, **294**(5): 1327–1336.
- 41 D. J. Craik, J. E. Swedberg, J. S. Mylne and M. Cemazar, *Expert Opin. Drug Discov.*, 2012, **7**: 179–194.
- 42 N. L. Daly, K. J. Rosengren and D. J. Craik, *Adv. Drug Deliv. Rev.*, 2009, **61**(11): 918–930.
- 43 L. Skjeldal, L. Gran, K. Sletten and B. F. Volkman, *Arch. Biochem. Biophys.*, 2002, **399**(2): 142–148.
- 44 R. E. W. Hancock and M. G. Scott, *Proc. Natl. Acad. Sci. U. S. A.*, 2000, **97**(16): 8856–8861.
- 45 M. Zasloff, *Nature*, 2002, **415**: 389–395.

- 46 F. Milletti, *Drug Discov. Today*, 2012, **17**: 850–860.
- 47 T. Rezai, J. E. Bock, M. V. Zhou, C. Kalyanaraman, R. S. Lokey and M. P. Jacobson, *J. Am. Chem. Soc.*, 2006, **128**(43): 14073–14080.
- 48 S. Qu, Y. Chen, X. Wang, S. Chen, Z. Xu and T. Ye, *Chem. Commun.*, 2015, **51**(13): 2510–2513.
- 49 S. Matthew, V. J. Paul and H. Luesch, *Planta Med.*, 2009, **75**(5): 528–533.
- 50 A. Isidro-Llobet, M. Alvarez and F. Albericio, *Chem. Rev.*, 2009, **109**(6) 2455–2504.
- 51 J. Tulla-Puche and G. Barany, *J. Org. Chem.*, 2004, **69**(12): 4101–4107.
- 52 F. W. Lichtenthaler, *European J. Org. Chem.*, 2002, **2002**: 4095–4122.
- 53 M. Goodman, W. Cai and N. D. Smith, *J. Pept. Sci.*, 2003, **9**(9): 594–603.
- 54 G. W. Anderson and A. C. McGregor, *J. Am. Chem. Soc.*, 1957, **79**(23): 6180–6183.
- 55 R. B. Merrifield, *J. Am. Chem. Soc.*, 1963, **85**(14): 2149–2154.
- 56 L. A. Carpino and G. Y. Han, *J. Am. Chem. Soc.*, 1970, **92**(19): 5748–5749.
- 57 T. Lescrinier, R. Busson, J. Rozenski, G. Janssen, A. V. Aerschot and P. Herdewijn, *Tetrahedron*, 1996, **52**(20): 6965–6972.
- 58 C. D. Chang, M. Waki, M. Ahmad, J. Meienhofer, E. O. Lundell and J. D. Haug, *Int. J. Pept. Protein Res.*, 1980, **15**(1): 59–66.
- 59 G. B. Fields and C. G. Fields, *J. Am. Chem. Soc.*, 1991, **113**(11): 4202–4207.
- 60 T. P. Curran, M. P. Pollastri, S. M. Abelleira, R. J. Messier, T. A. McCollum and C. G. Rowe, *Tetrahedron Lett.*, 1994, **35**(30): 5409–5412.

- 61 E. Kaiser, F. Picart, T. Kubiak, J. P. Tam and R. B. Merrifield, *J. Org. Chem.*, 1993, **58**(19): 5167–5175.
- 62 K. J. Jensen, J. Alsina, M. F. Songster, J. Vágner, F. Albericio and G. Barany, *J. Am. Chem. Soc.*, 1998, **120**(22): 5441–5452.
- 63 S. A. Kates, N. A. Solé, C. R. Johnson, D. Hudson, G. Barany and F. Albericio, *Tetrahedron Lett.*, 1993, **34**(10): 1549–1552.
- 64 S. Bräse, J. H. Kirchhoff and J. Kobberling, *Tetrahedron*, 2003, **59**: 885–939.
- 65 T. Berthelot, M. Gonçalves, G. Laïn, K. Estieu–Gionnet and G. Délérís, *Tetrahedron*, 2006, **62**(6): 1124–1130.
- 66 M. Cudic, J. D. Wade and L. Otvos, *Tetrahedron Lett.*, 2000, **41**(23): 4527–4531.
- 67 K. Borsuk, F. L. Van Delft, I. F. Eggen, P. B. W. Kortenaar, A. Petersen and F. P. J. T. Rutjes, *Tetrahedron Lett.*, 2004, **45**(18): 3585–3588.
- 68 B. W. Erickson and R. B. Merrifield, *Isr. J. Chem.*, 1974, **12**: 79–85.
- 69 G. B. Fields and R. L. Noble, *Int. J. Pept. Protein Res.*, 1990, **35**(3): 161–214.
- 70 J. Green, O. M. Ogunjobi, R. Ramage, A. S. J. Stewart, S. McCurdy and R. Noble, *Tetrahedron Lett.*, 1988, **29**(34): 4341–4344.
- 71 L. A. Carpino, H. Shroff, S. A. Triolo, E. M. E. Mansour, H. Wenschuh and F. Albericio, *Tetrahedron Lett.*, 1993, **34**(49): 7829–7832.
- 72 M. Gairí, P. Lloyd–Williams, F. Albericio and E. Giralt, *Tetrahedron Lett.*, 1994, **35**(1): 175–178.
- 73 H. Yajima, J. Kanaki, M. Kitajima and S. Funakoshi, *Chem. Pharm. Bull.*, 1980, **28**: 1214–1218.
- 74 F. Albericio, *Biopolym. - Pept. Sci.*, 2000, **55**: 123–139.
- 75 S. Akabori, S. Sakakibara, Y. Shimonishi and Y. Nobuhara, *Bull. Chem. Soc. Jpn.*, 1964, **37**(3): 433–434.

- 76 D. F. Veber, J. D. Milkowski, S. L. Varga, R. G. Denkwalter and R. Hirschmann, *J. Am. Chem. Soc.*, 1972, **94**(15): 5456–5461.
- 77 M. C. Munson, C. Garcia-Echeverria, F. Albericio and G. Barany, *J. Org. Chem.*, 1992, **57**(11): 3013–3018.
- 78 M. Royo, J. Alsina, E. Giralt, U. Slomczynska and F. Albericio, *J. Chem. Soc. Perkin Trans. 1*, 1995, 1095–1102.
- 79 R. Behrendt, S. Huber, R. Martí and P. White, *J. Pept. Sci.*, 2015, **21**(8): 680–687.
- 80 R. S. Feinberg and R. B. Merrifield, *J. Am. Chem. Soc.*, 1975, **97**(12): 3485–3496.
- 81 J. N. Lambert, J. P. Mitchell and K. D. Roberts, *J. Chem. Soc. Perkin Trans. 1*, 2001, 471–484.
- 82 V. D. Vigneaud, C. Ressler, C. J. M. Swan, C. W. Roberts, P. G. Katsoyannis and S. Gordon, *J. Am. Chem. Soc.*, 1953, **75**(19): 4879–4880.
- 83 L. A. Carpino, S. Ghassemi, D. Ionescu, M. Ismail, D. Sadat-Aalae, G. A. Truran, E. M. E. Mansour, G. A. Siwruk, J. S. Eynon and B. Morgan, *Org. Process Res. Dev.*, 2003, **7**(1): 28–37.
- 84 V. D. Vigneaud, C. Ressler, J. M. Swan, C. W. Roberts and P. G. Katsoyannis, *J. Am. Chem. Soc.*, 1954, **76**(12): 3115–3121.
- 85 J. M. Stewart, *J. Macromol. Sci. Part A - Chem.*, 1976, **10**: 259–288.
- 86 K. C. Nicolaou, N. Winssinger, J. Pastor and F. DeRoose, *J. Am. Chem. Soc.*, 1997, **119**(2): 449–450.
- 87 S. L. Beaucage and R. P. Iyer, *Tetrahedron*, 1992, **48**(12): 2223–2311.
- 88 V. K. Sarin, S. B. H. Kent, A. R. Mitchell and R. B. Merrifield, *J. Am. Chem. Soc.*, 1984, **106**(25): 7845–7850.
- 89 V. K. Sarin, S. B. Kent and R. B. Merrifield, *J. Am. Chem. Soc.*, 1980, **102**(17): 5463–5470.
- 90 K. D. Kopple, *J. Pharm. Sci.*, 1972, **61**(9): 1345–1356.

- 91 S. L. Pedersen, A. P. Tofteng, L. Malik and K. J. Jensen, *Chem. Soc. Rev.*, 2012, **41**(5): 1826–1844.
- 92 V. Santagada, F. Frecentese, E. Perissutti, F. Fiorino, B. Severino and G. Caliendo, *Mini-Reviews Med. Chem.*, 2009, **9**(3): 340–358.
- 93 R. Behrendt, P. White and J. Offer, *J. Pept. Sci.*, 2016, **22**: 4–27.
- 94 M. C. Alcaro, G. Sabatino, J. Uziel, M. Chelli, M. Ginanneschi, P. Rovero and A. M. Papini, *J. Pept. Sci.*, 2004, **10**(4): 218–228.
- 95 D. P. Fairlie, J. D. A. Tyndall, R. C. Reid, A. K. Wong, G. Abbenante, M. J. Scanlon, D. R. March, D. A. Bergman, C. L. L. Chai and B. A. Burkett, *J. Med. Chem.*, 2000, **43**(7): 1271–1281.
- 96 J. Rizo and L. M. Gierasch, *Annu. Rev. Biochem.*, 1992, **61**: 387–416.
- 97 R. L. A. Dias, R. Fasan, K. Moehle, A. Renard, D. Obrecht and J. A. Robinson, *J. Am. Chem. Soc.*, 2006, **128**(8): 2726–2732.
- 98 A. R. Horswill and S. J. Benkovic, *Cell Cycle*, 2005, **4**(4): 552–555.
- 99 J. S. Davies, *J. Pept. Sci.*, 2003, **9**(80): 471–501.
- 100 S. A. Kates, N. A. Solé, C. R. Johnson, D. Hudson, G. Barany and F. Albericio, *Tetrahedron Lett.*, 1993, **34**(10): 1549–1552.
- 101 J. Zhang, M. Mulumba, H. Ong and W. D. Lubell, *Angew. Chem.*, 2017, **129**: 6381–6385.
- 102 S. Ma, H. Zhang, X. Dong, L. Yu, J. Zheng and Y. Sun, *Front. Chem. Sci. Eng.*, 2018, **42**: 1–13.
- 103 J. A. Camarero and T. W. Muir, *J. Am. Chem. Soc.*, 1999, **121**(23): 5597–5598.
- 104 U. Schmidt and J. Langner, *J. Pept. Res.*, 1997, **49**(1): 67–73.
- 105 E. Gross and J. Meienhofer, *The peptides: Analysis, synthesis, biology*, Elsevier Inc., New Jersey, 1<sup>st</sup> edition, 1979, 315–338.
- 106 P. E. Dawson, T. W. Muir I. Clark-Lewis, and S. B. H. Kent, *Science*, 1994, **266**(5186): 776–779.



- 107 D. S. Kemp, S. L. Leung and D. J. Kerkman, *Tetrahedron Lett.*, 1981, **22**(3): 181–184.
- 108 J. Blake, *Int. J. Pept. Protein Res.*, 1981, **17**(2): 273–274.
- 109 P. E. Dawson and S. B. H. Kent, *Annu. Rev. Biochem.*, 2000, **69**: 923–960.
- 110 W. Zhong, M. Skwarczynski, Y. Fujita, P. Simerska, M. F. Good and I. Toth, *Aust. J. Chem.*, 2009, **62**: 993–999.
- 111 J. B. Blanco–Canosa and P. E. Dawson, *Angew. Chem. Int. Ed. Eng.*, 2008, **47**(36): 6851–6855.
- 112 A. Brik, E. Keinan and P. E. Dawson, *J. Org. Chem.*, 2000, **65**(12): 3829–3835.
- 113 G. M. Fang, Y. M. Li, F. Shen, Y. C. Huang, J. B. Li, Y. Lin, H. K. Cui and L. Liu, *Angew. Chem. Int. Ed. Eng.*, 2011, **50**(33): 7645–7649.
- 114 L. D. Rosa, A. L. Cortajarena, A. Romanelli, L. Regan and L. D. D'Andrea, *Org. Biomol. Chem.*, 2012, **10**(2): 273–280.
- 115 E. Saxon, J. I. Armstrong and C. R. Bertozzi, *Org. Lett.*, 2000, **2**(14): 2141–2143.
- 116 N. A. McGrath and R. T. Raines, *Acc. Chem. Res.*, 2011, **44**(9): 752–761.
- 117 R. Jagasia, J. M. Holub, M. Bollinger, K. Kirshenbaum and M. G. Finn, *J. Org. Chem.*, 2009, **74**(8): 2964–2974.
- 118 P. Li and L. Wang, *Lett. Org. Chem.*, 2007, **4**(1): 23–26.
- 119 H. C. Kolb, M. G. Finn and K. B. Sharpless, *Angew. Chem. Int. Ed. Eng.*, 2001, **40**: 2004–2021.
- 120 P. Li, P. P. Roller and J. Xu, *Curr. Org. Chem.*, 2002, **6**(5): 411–440.
- 121 V. J. Hruby, F. Al–Obeidi and W. Kazmierski, *Biochem. J.*, 1990, **268**(2): 249–262.
- 122 H. E. Blackwell and R. H. Grubbs, *Angew. Chem. Int. Ed. Eng.*, 1998, **37**(23): 3281–3284.

- 123 A. L. C. Isaad, A. M. Papini, M. Chorev and P. Rovero, *J. Pept. Sci.*, 2009, **15**(7): 451–454.
- 124 R. S. Harrison, N. E. Shepherd, H. N. Hoang, G. Ruiz-Gómez, T. A. Hill, R. W. Driver, V. S. Desai, P. R. Young, G. Abbenante and D. P. Fairlie, *Proc. Natl. Acad. Sci. U. S. A.*, 2010, **107**(26): 11686–11691.
- 125 H. X. Zhou, P. C. Lyu, D. E. Wemmer and N. R. Kallenbach, *J. Am. Chem. Soc.*, 1994, **116**(3): 1139–1140.
- 126 J. W. Taylor, *Biopolym.-Pept. Sci.*, 2002, **66**(1): 49–75.
- 127 G. Bulaj, *Biotechnol. Adv.*, 2005, **23**(1): 87–92.
- 128 A. Caporale, M. Sturlese, L. Gesiot, F. Zanta, A. Wittelsberger and C. Cabrele, *J. Med. Chem.*, 2010, **53**(22): 8072–8079.
- 129 A. A. Aimetti, R. K. Shoemaker, C. C. Lin and K. S. Anseth, *Chem. Commun.*, 2010, **46**(23): 4061–4063.
- 130 Y. C. Tang, H. B. Xie, G. Tian and Y. H. Ye, *J. Pept. Res.*, 2002, **60**(2): 95–103.
- 131 Z. E. Perlman, J. E. Bock, J. R. Peterson and R. S. Lokey, *Bioorg. Med. Chem. Lett.*, 2005, **15**(23): 5329–5334.
- 132 I. Daidone, H. Neuweiler, S. Doose, M. Sauer and J. C. Smith, *PLoS Comput. Biol.*, 2010, **6**(1): 1–9.
- 133 M. Tamaki, S. Akabori and I. Muramatsu, *J. Am. Chem. Soc.*, 1993, **115**(23): 10492–10496.
- 134 Y. Takeuchi and G. R. Marshall, *J. Am. Chem. Soc.*, 1998, **120**(22): 5363–5372.
- 135 A. B. Yongye, Y. Li, M. A. Giulianotti, Y. Yu, R. A. Houghten and K. Martínez-Mayorga, *J. Comput. Aided. Mol. Des.*, 2009, **23**(9): 677–689.
- 136 M. Favre, K. Moehle, L. Jiang, B. Pfeiffer and J. A. Robinson, *J. Am. Chem. Soc.*, 1999, **121**(12): 2679–2685.

- 137 J. Jacob, H. Duclohier and D. S. Cafiso, *Biophys. J.*, 1999, **76**(3): 1367–1376.
- 138 Y. H. Ye, X. M. Gao, M. Liu, Y. C. Tang and G. L. Tian, *Lett. Pept. Sci.*, 2003, **10**: 571–579.
- 139 T. Wöhr, F. Wahl, A. Nefzi, B. Rohwedder, T. Sato, X. Sun and M. Mutter, *J. Am. Chem. Soc.*, 1996, **118**(39): 9218–9227.
- 140 D. Skropeta, K. A. Jolliffe and P. Turner, *J. Org. Chem.*, 2004, **69**(25): 8804–8809.
- 141 P. Dumy, M. Keller, D. E. Ryan, B. Rohwedder, T. Wöhr and M. Mutter, *J. Am. Chem. Soc.*, 1997, **119**(5): 918–925.
- 142 X. M. Gao, Y. H. Ye, M. Bernd and B. Kutscher, *J. Pept. Sci.*, 2002, **8**(8): 418–430.
- 143 A. R. Vaino and K. D. Janda, *J. Comb. Chem.*, 2000, **2**(6): 579–596.
- 144 Z. Ö. Özdemir, E. Karabulut, M. Topuzoğullari and Z. Mustafaev, *Hacettepe J. Biol. and Chem.*, 2008, **36**(4): 329–337.
- 145 D. Vogel, R. Schmidt, K. Hartung, H. U. Demuth, N. N. Chung and P. W. Schiller, *Int. J. Pept. Protein Res.*, 1996, **48**(6): 495–502.
- 146 T. I. Al-Warhi, H. M. A. Al-Hazimi and A. El-Faham, *J. Saudi Chem. Soc.*, 2012, **16**(2): 97–116.
- 147 O. F. Luna, J. Gomez, C. Cárdenas, F. Albericio, S. H. Marshall and F. Guzmán, *Molecules*, 2016, **21**(11): 1542–1554.
- 148 C. A. Guy and G. B. Fields, *Methods Enzymol.*, 1997, **289**: 67–83.
- 149 <https://www.sigmaaldrich.com/content/dam/docs/Supelco/Bulletin/44>, [Accessed 14/3/2018].
- 150 R. K. Murray, D. K. Granner and V. W. Rodwell, *Harper's Illustrated Biochemistry*, Mc Graw Hill, New York, 27<sup>th</sup> edition, 2003, 14.
- 151 V. A. Davankov and M. P. Tsyurupa, *React. Polym.*, 1990, **13**: 27–42.
- 152 K. C. Pugh, E. J. York and J. M. Steward, *Int. J. Pept. Protein Res.*, 1992, **40**: 208–213.

- 153 B. Yan, N. Nguyen, L. Liu, G. Holland and B. Raju, *J. Comb. Chem.*, 2000, **2**(1): 66–74.
- 154 R. De Marco, A. Tolomelli, A. Greco and L. Gentilucci, *ACS Sustain. Chem. Eng.*, 2013, **1**(6): 566–569.
- 155 Y. García-Ramos, M. Paradís-Bas, J. Tulla-Puche and F. Albericio, *J. Pept. Sci.*, 2010, **16**(12): 675–678.
- 156 A. Nefzi, J. M. Ostresh and R. A. Houghten, *Chem. Rev.*, 1997, **97**(2): 449–472.
- 157 C. X. Fan, X. L. Hao and Y. H. Ye, *Synth. Commun.*, 1996, **26**(7): 1455–1460.
- 158 Y. Han, F. Albericio and G. Barany, *J. Org. Chem.*, 1997, **62**(13): 4307–4312.
- 159 M. Slebioda, Z. Wodecki and A. M. Kolodziejczyk, *Int. J. Pept. Protein Res.*, 1990, **35**(6): 539–541.
- 160 D. Sarantakis, J. Teichman, E. L. Lien and R. L. Fenichel, *Biochem. Biophys. Res. Commun.*, 1976, **73**(2): 336–342.
- 161 L. A. Carpino, *J. Am. Chem. Soc.*, 1993, **115**(10): 4397–4398.
- 162 J. Coste, D. Le-Nguyen and B. Castro, *Tetrahedron Lett.*, 1990, **31**(2): 205–208.
- 163 S. Y. Han and Y. A. Kim, *Tetrahedron*, 2004, **60**: 2447–2467.
- 164 B. Castro, J. Dormoy, G. Evin and C. Selve, *Tetrahedron Lett.*, 1975, **16**(14): 1219–1222.
- 165 M. H. Kim and D. V. Patel, *Tetrahedron Lett.*, 1994, **35**(31): 5603–5606.
- 166 R. Knorr, A. Trzeciak, W. Bannwarth and D. Gillesen, *Tetrahedron Lett.*, 1989, **30**(15): 1927–1930.
- 167 H. Li, X. Jiang, Y. H. Ye, C. Fan, T. Romoff and M. Goodman, *Org. Lett.*, 1999, **1**(1): 91–94.
- 168 K. C. Parker, M. A. Bednarek, L. K. Hull, U. Utz, B. Cunningham, H. J. Zweerink, W. E. Biddison and J. E. Coligan, *J. Immunol.*, 1992,

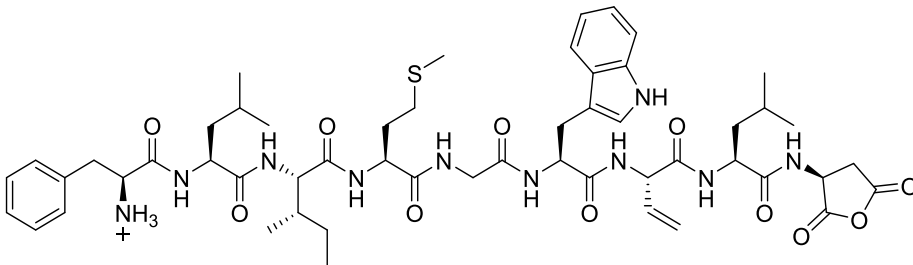
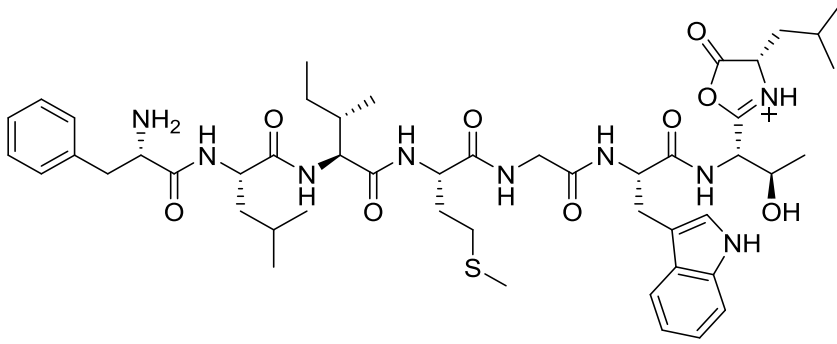
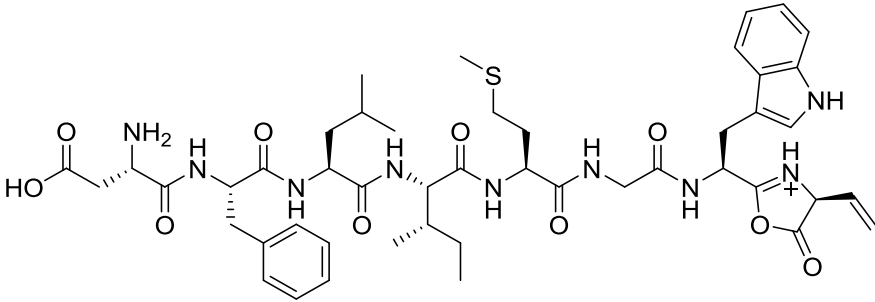
**149**(11): 3580–3587.

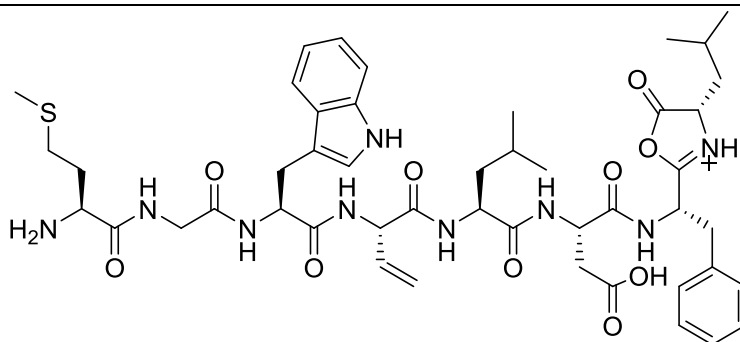
- 169 D. R. Madden, D. N. Garboczi and D. C. Wiley, *Cell*, 1993, **75**(4): 693–708.
- 170 I. A. Doytchinova, P. Guan and D. R. Flower, *BMC Bioinformatics*, 2006, **7**: 1–11.
- 171 <http://www.rcsb.org/structure/1F16>, [Accessed 10/06/2018].
- 172 K. L. Smith, A. Tristram, K. M. Gallagher, A. N. Fiander and S. Man, *Int. Immunol.*, 2004, **17**(2): 167–176.
- 173 C. A. Romos, N. Narala, G. M. Vyas, A. M. Leen, U. Gerdemann, E. M. Sturgis, M. L. Anderson, B. Savoldo, H. E. Heslop, M. K. Brenner and C. M. Rooney, *J. Immunother*, 2013, **36**(1): 66–76.
- 174 R. A. Reid, J. E. Redman, P. Rizkallah, C. Fegan, C. Pepper and S. Man, *Immunology*, 2014, **144**: 495–505.
- 175 M. L. Salgaller, A. Afshar, F. M. Marincola, L. Rivoltini, Y. Kawakami and S. A. Rosenberg, *Cancer Res.*, 1995, **55**(1): 4972–4979.
- 176 S. A. Wheaten, F. D. O. Ablan, B. L. Spaller, J. M. Trieu and P. F. Almeida, *J. Am. Chem. Soc.*, 2013, **135**(44): 16517–16525.
- 177 F. M. Menger, V. A. Seredyuk, M. V. Kitaeva, A. A. Yaroslavov and N. S. Melik–Nubarov, *J. Am. Chem. Soc.*, 2003, **125** (10): 2846–2847.
- 178 T. H. Evers, E. M. W. M. Van Dongen, A. C. Faesen, E. W. Meijer and M. Merks, *Biochemistry*, 2006, **45**(44): 13183–13192.
- 179 J. Bedford, C. Hyde, T. Johnson, W. Jun, D. Owen, M. Quibell and R. C. Sheppard, *Int. J. Pept. Protein Res.*, 1992, **40**: 300–307.
- 180 H. Edelhoch, *Biochemistry*, 1967, **6**(7): 1948–1954.
- 181 J. B. Fenn, M. Mann, C. K. Meng, S. F. Wong and C. M. Whitehouse, *Science*, 1989, **246**(4926): 64–71.
- 182 M. Karas and F. Hillenkamp, *Anal. Chem.*, 1988, **60**(20): 2299–2301.
- 183 J. A. Siepen, E. J. Keevil, D. Knight and S. J. Hubbard, *J. Proteome Res.*, 2007, **6**(1): 399–408.

- 184 H. Mohimani, Y. L. Yang, W. T. Liu, P. W. Hsieh, P. C. Dorrestein and P. A. Pevzner, *Proteomics*, 2011, **11**(18): 3642–3650.
- 185 I. P. Csonka, B. Paizs, G. Lendvay and S. Suhai, *Rapid Commun. Mass Spectrom.*, 2001, **15**(16): 1457–1472.
- 186 B. Paizs and S. Suhai, *Mass Spectrom. Rev.*, 2005, **24**(4): 508–548.
- 187 I. P. Csonka, B. Paizs, G. Lendvay and S. Suhai, *Rapid Commun. Mass Spectrom.*, 2001, **15**(16): 1457–1472.
- 188 P. D. Schnier, W. D. Price, R. A. Jockusch and E. R. Williams, *J. Am. Chem. Soc.*, 1996, **118**(30): 7178–7189.
- 189 K. D. Ballard and S. J. Gaskell, *J. Am. Soc. Mass Spectrom.*, 1993, **4**(6): 477–481.
- 190 W. Yu, J. E. Vath, M. C. Huberty and S. A. Martin, *Anal. Chem.*, 1993, **65**(21): 3015–3023.
- 191 C. López-Otín and J. S. Bond, *J. Biol. Chem.*, 2008, **283**(45): 30433–30437.
- 192 J. V. Olsen, S. E. Ong and M. Mann, *Mol. Cell. Proteomics*, 2004, **3**(6): 608–614.
- 193 U. Boominadhan, R. Rajakumar, P. K. V. Sivakumaar and M. M. Joe, *Bot. Res. Int.*, 2009, **2**(2): 83–87.
- 194 J. A. Siepen, E. J. Keevil, D. Knight and S. J. Hubbard, *J. Proteome Res.*, 2007, **6**(1): 399–408.
- 195 R. D. Soltis, D. Hasz, M. J. Morris and I. D. Wilson, *Immunology*, 1979, **36**(1): 37–45.
- 196 R. A. R. Bowen and A. T. Remaley, *Biochem. Medica*, 2014, **24**(1): 31–44.
- 197 M. M. Bradford, *Anal. Biochem.*, 1976, **72**: 248–254.

## 8 Appendix A

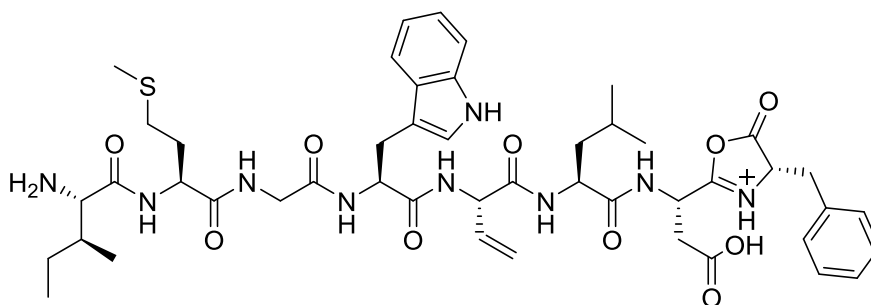
**Table A.1:** Suggested structures produced by fragmentation of the precursor ion 9-mer cyclic peptide (**1c**)  $[M+H]^+$   $m/z$  1077 using MS<sup>2</sup>.

No	Structure of the fragment and site of cleaved peptide bond
1	 <p style="text-align: center;"><math>MH-H_2O</math> (<math>m/z = 1059.5</math>)</p> <p>1) Cleavage of the amide bond between D and F in <b>1c</b>. 2) Loss of H<sub>2</sub>O molecule from T.</p>
2	 <p style="text-align: center;"><math>b_8</math> (<math>m/z = 962.5</math>)</p> <p>1) Cleavage of the amide bond between F and D in <b>1c</b>. 2) Cleavage of the amide bond between L and D in the linear fragment (loss of D).</p>
3	 <p style="text-align: center;"><math>1-b_8-H_2O</math> (<math>m/z = 946.4</math>)</p> <p>1) Cleavage of the amide bond between D and L in <b>1c</b>. 2) Cleavage of the amide bond between T and L in the linear fragment (loss of L). 3) Loss of H<sub>2</sub>O molecule from T.</p>



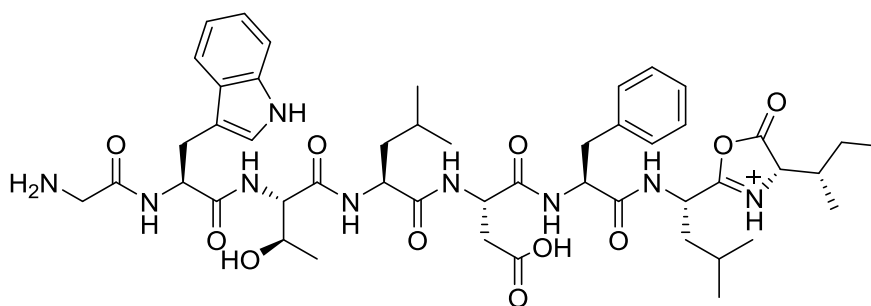
2-b<sub>8</sub>-H<sub>2</sub>O ( $m/z = 946.4$ )

- 1) Cleavage of the amide bond between M and I in **1c**. 2) Cleavage of amide bond between L and I in the linear fragment (loss of I). 3) Loss of H<sub>2</sub>O molecule from T.



3-b<sub>8</sub>-H<sub>2</sub>O ( $m/z = 946.4$ )

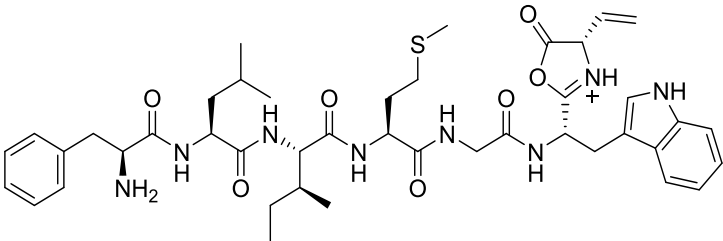
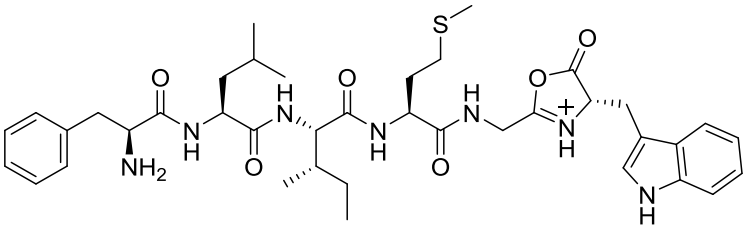
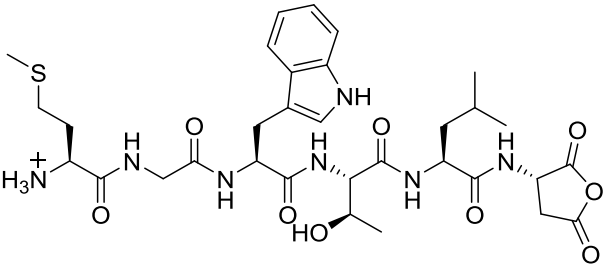
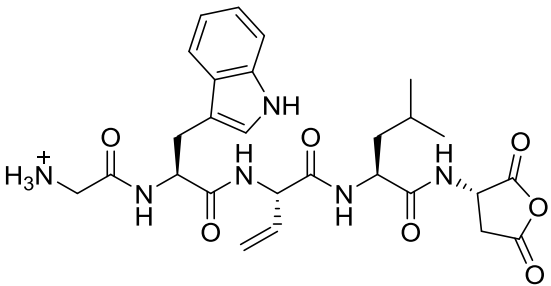
- 1) Cleavage of the amide bond between L and I in **1c**. 2) Cleavage of the amide bond between F and L in the linear fragment (loss of L). 3) Loss of H<sub>2</sub>O molecule from T.



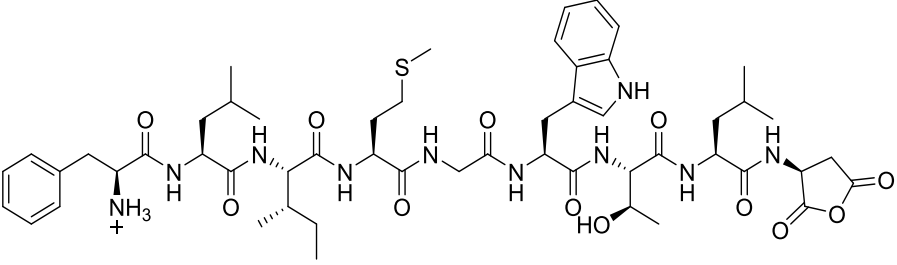
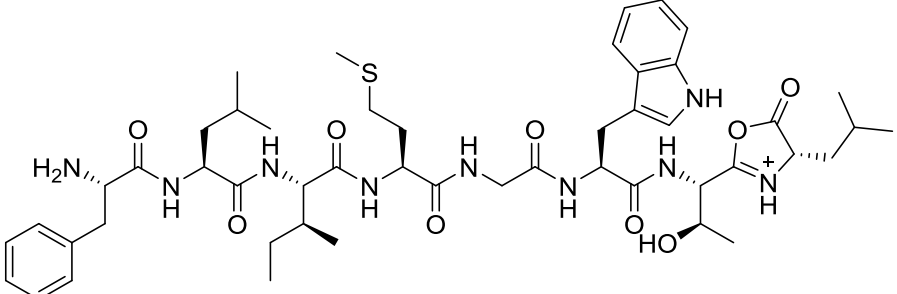
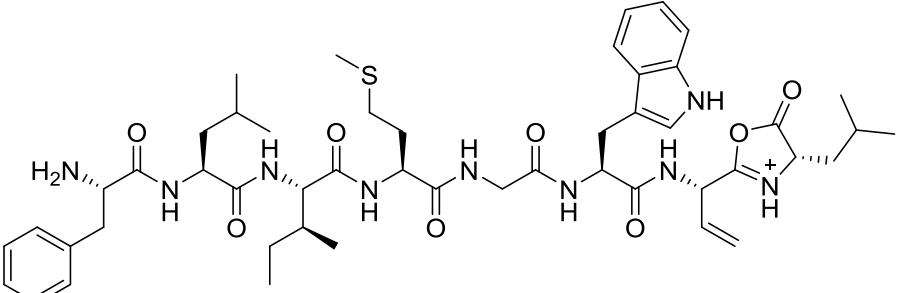
4-b<sub>8</sub> ( $m/z = 946.5$ )

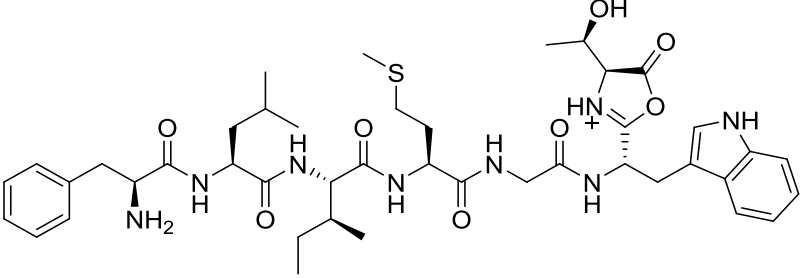
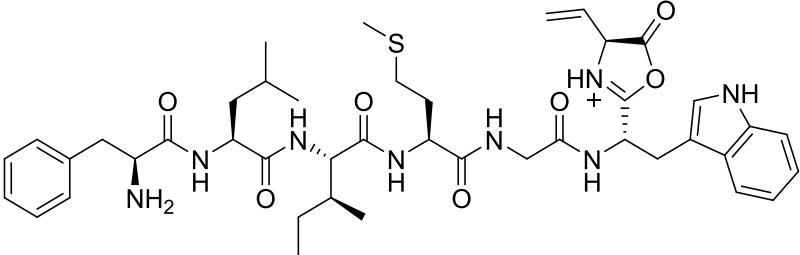
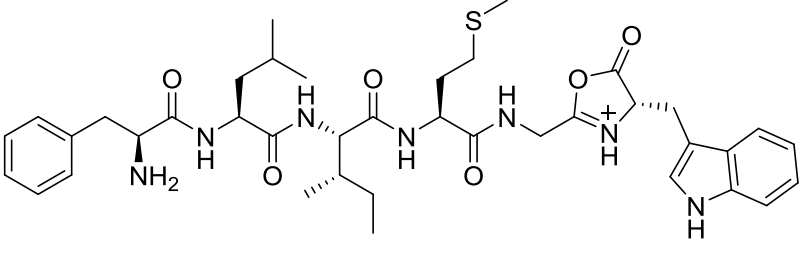
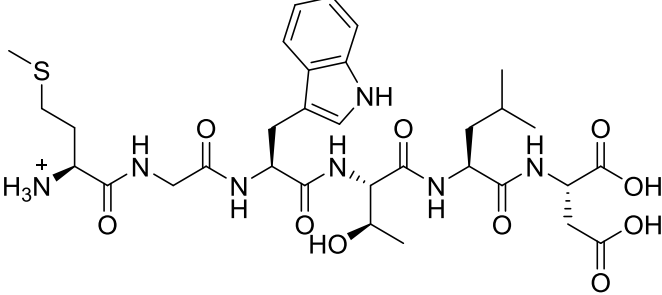
- 1) Cleavage of the amide bond between G and M in **1c**. 2) Cleavage of the amide bond between I and M in the linear fragment (loss of M).



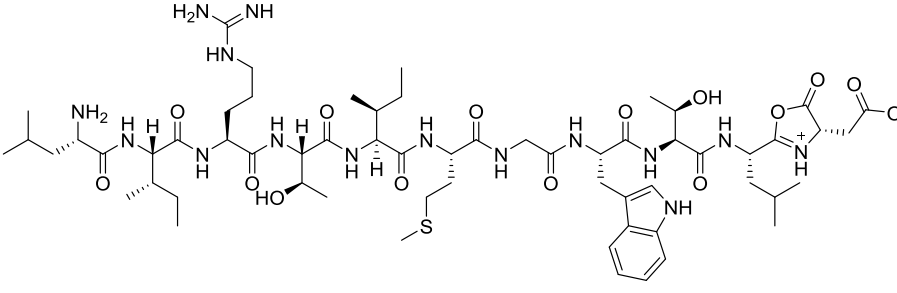
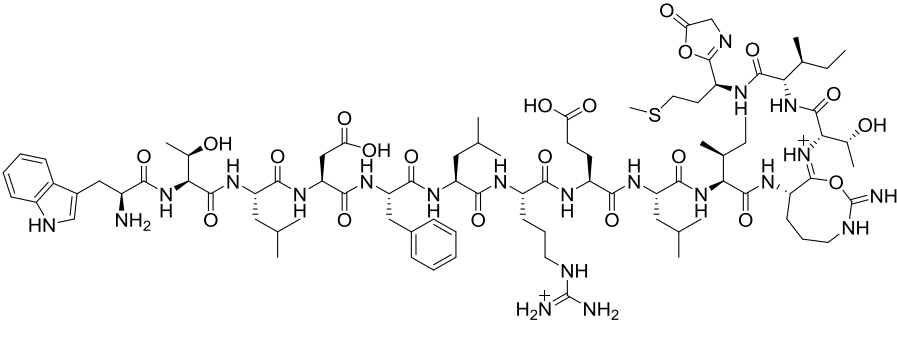
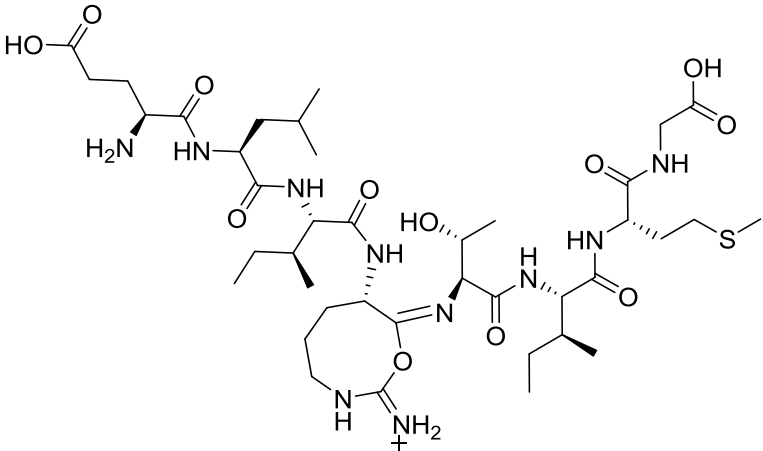
4	 <p style="text-align: center;"><math>b_7\text{-H}_2\text{O}</math> (<math>m/z = 831.4</math>)</p> <p>1) Cleavage of the amide bond between F and D in <b>1c</b>. 2) Cleavage of the amide bond between T and L in the linear fragment (loss of the fragment of LD). 3) Loss of H<sub>2</sub>O molecule from T.</p>
5	 <p style="text-align: center;"><math>b_6</math> (<math>m/z = 748.4</math>)</p> <p>1) Cleavage of the amide bond between F and D in <b>1c</b>. 2) Cleavage of the amide bond between W and T in the linear fragment (loss of the fragment of TLD).</p>
6	 <p style="text-align: center;"><math>b_6</math> (<math>m/z = 704.3</math>)</p> <p>1) Cleavage of the amide bond between M and I in <b>1c</b>. 2) Cleavage of the amide bond between D and F in the linear fragment (loss of the fragment of FLI).</p>
7	 <p style="text-align: center;"><math>b_5\text{-H}_2\text{O}</math> (<math>m/z = 555.3</math>)</p> <p>1) Cleavage of the amide bond between D and F in <b>1c</b>. 2) Cleavage of the amide bond between M and G in the linear fragment (loss of the fragment of FLIM). 3) Loss of H<sub>2</sub>O molecule from T.</p>

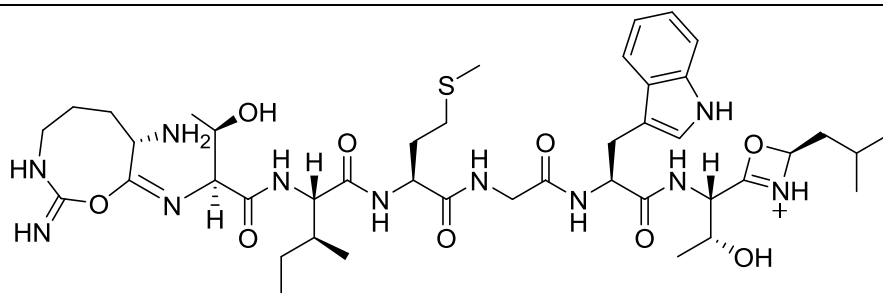
**Table A.2:** Suggested structures produced by fragmentation of the precursor ion 9-mer linear peptide (**1b**) [ $M+H$ ]<sup>+</sup>  $m/z$  1096 using MS<sup>2</sup>.

No	Structure of the fragment and site of cleaved peptide bond
1	 <p style="text-align: center;"><math>MH-H_2O</math> (<math>m/z = 1077.5</math>)</p> <p style="text-align: center;">Loss of H<sub>2</sub>O molecule from D, without any cleavage in the amide bonds of the linear compound (<b>1b</b>).</p>
2	 <p style="text-align: center;"><math>b_8</math> (<math>m/z = 962.5</math>)</p> <p style="text-align: center;">Cleavage of the amide bond between L and D in <b>1b</b> (loss of D).</p>
3	 <p style="text-align: center;"><math>b_8-H_2O</math> (<math>m/z = 944.5</math>)</p> <p style="text-align: center;">1) Cleavage of the amide bond between L and D in <b>1b</b> (loss of D). 2) Loss of H<sub>2</sub>O molecule from T.</p>

4	 <p><math>b_7</math> (<math>m/z = 849.4</math>)</p> <p>Cleavage of the peptide bond between T and L in <b>1b</b> (loss of the fragment of LD).</p>
5	 <p><math>b_7-H_2O</math> (<math>m/z = 831.4</math>)</p> <p>1) Cleavage of the amide bond between T and L in <b>1b</b> (loss of the fragment of LD). 2) Loss of H<sub>2</sub>O molecule from T.</p>
6	 <p><math>b_6</math> (<math>m/z = 748.4</math>)</p> <p>Cleavage of the amide bond between W and T in <b>1b</b> (loss of the fragment of TLD).</p>
7	 <p><math>y_6</math> (<math>m/z = 722.3</math>)</p> <p>Cleavage of the amide bond between M and I in <b>1b</b> (loss of the fragment of FLI).</p>

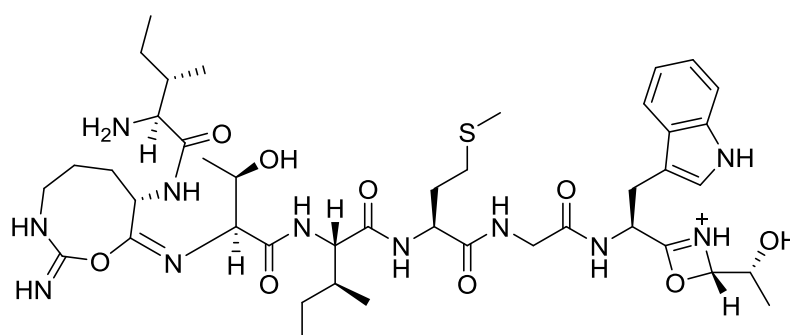
**Table A.3:** Suggested structures produced by fragmentation of the precursor ion 15-mer cyclic peptide (**2c**)  $[M+2H]^{2+}$   $m/z$  924 using MS<sup>2</sup>.

No	Structure of the fragment and site of cleaved peptide bond
1	 <p style="text-align: center;"><math>b_{11}</math> (<math>m/z = 1300.7</math>)</p> <p>1) Cleavage of the amide bond between L and E in <b>2c</b>. 2) Cleavage of the amide bond between D and F in the linear fragment (loss of the fragment of FLRE).</p>
2	 <p style="text-align: center;">1-MH<sub>2</sub>-NH<sub>3</sub> (<math>m/z = 915.0</math>)</p> <p>1) Cleavage of the amide bond between W and G in <b>2c</b>. 2) Loss of NH<sub>3</sub> molecule from one of the two R residues.</p>  <p style="text-align: center;">2-y<sub>8</sub>-NH<sub>3</sub> (<math>m/z = 915.5</math>)</p> <p>1) Cleavage of the amide bond between G and W in <b>2c</b>. 2) Cleavage of the amide bond between R and E in the linear fragment (loss of the fragment of WTLDFLR). 3) Loss of NH<sub>3</sub> molecule from R.</p>



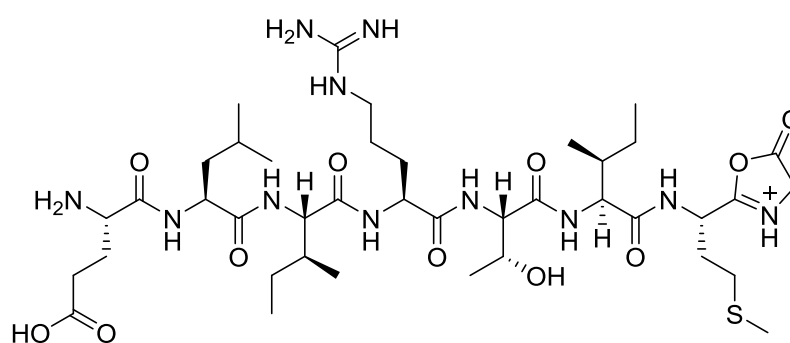
3-a<sub>8</sub>-NH<sub>3</sub> ( $m/z = 914.5$ )

1) Cleavage of the amide bond between R and I in **2c**. 2) Cleavage of the amide bond between L and D in the linear fragment (loss of the fragment of DFLRELI). 3) Loss of NH<sub>3</sub> molecule from R.



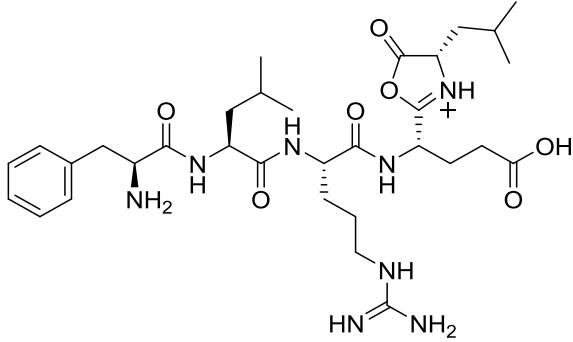
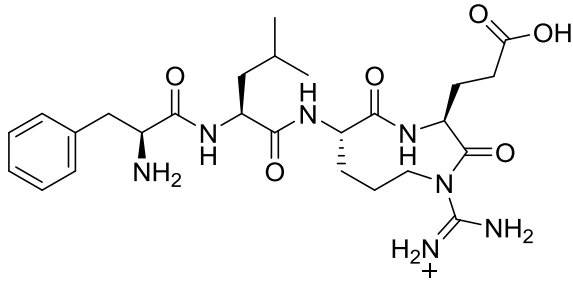
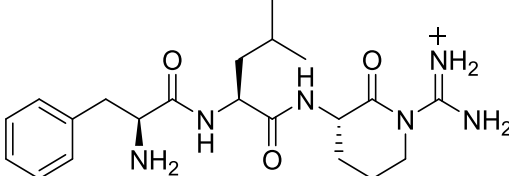
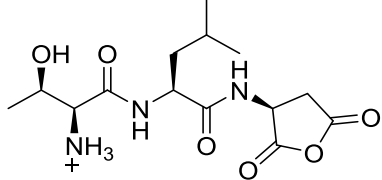
4-a<sub>8</sub>-NH<sub>3</sub><sup>\*</sup> ( $m/z = 914.5$ )

1) Cleavage of the amide bond between L and I in **2c**. 2) Cleavage of the amide bond between T and L in the linear fragment (loss of the fragment of LDFLREL). 2) Loss of NH<sub>3</sub> molecule from R.

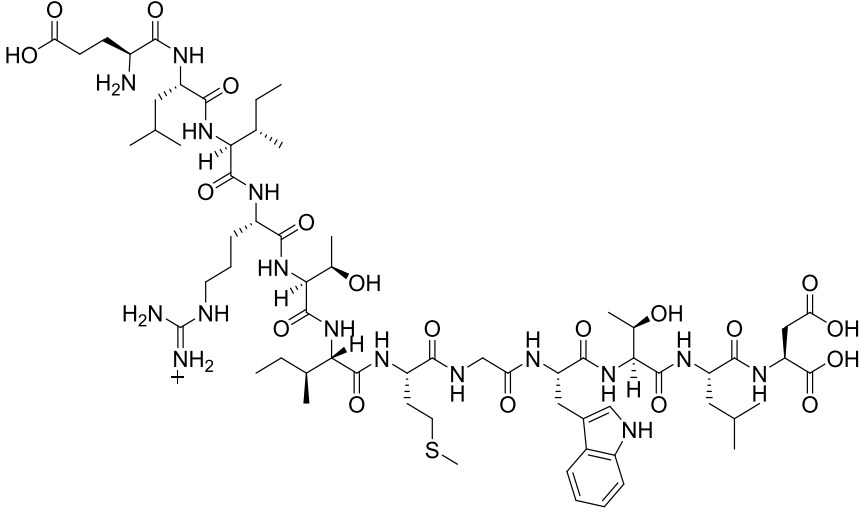
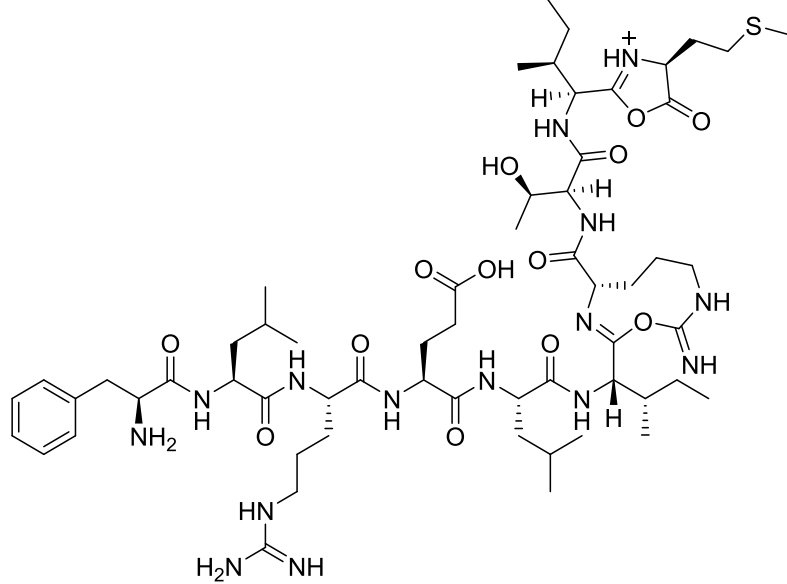


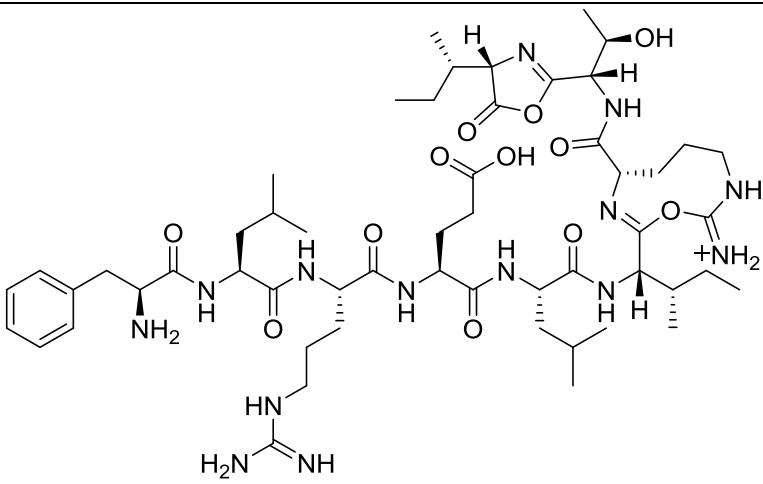
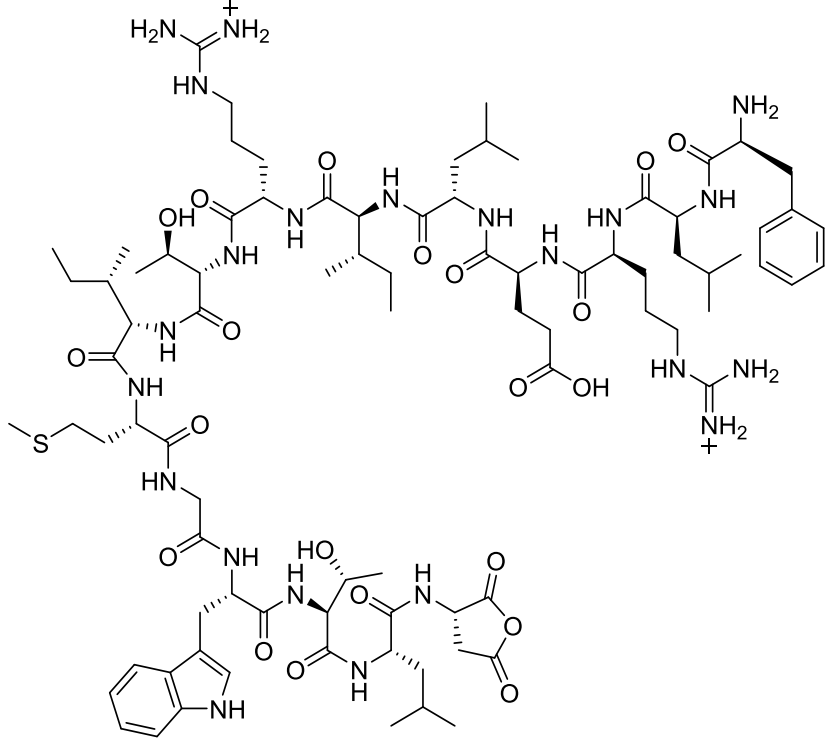
5-b<sub>8</sub> ( $m/z = 914.5$ )

1) Cleavage of amide bond between R and E in **2c**. 2) Cleavage of the amide bond between G and W in the linear fragment (loss of the fragment of WTLDFLR).

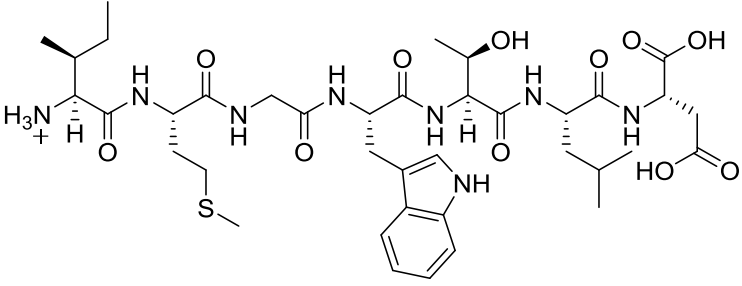
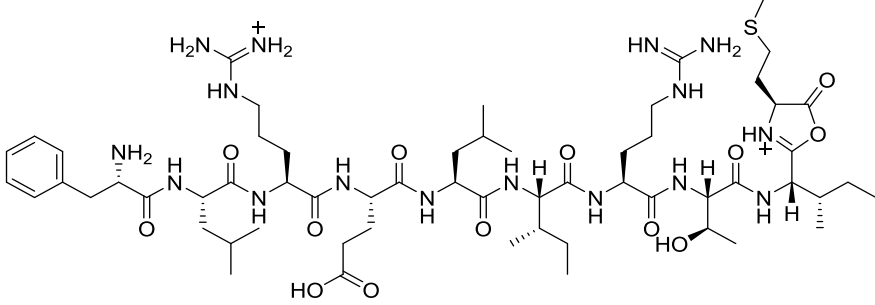
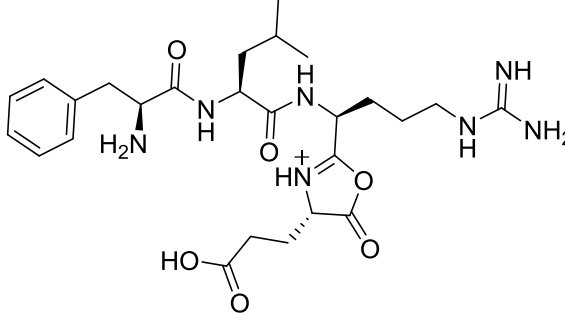
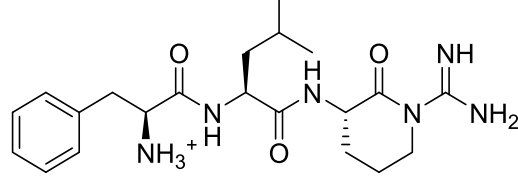
3	 <p><math>b_5</math> (<math>m/z</math> = 659.4)</p> <p>1) Cleavage of the amide bond between F and D in <b>2c</b>. 2) Cleavage of the amide bond between L and I in the linear fragment (loss of the fragment of IRTIMGWTLTD).</p>
4	 <p><math>b_4</math> (<math>m/z</math> = 546.3)</p> <p>1) Cleavage of the amide bond between F and D in <b>2c</b>. 2) Cleavage of the amide bond between E and L in the linear fragment (loss of the fragment of LIRTIMGWTLTD).</p>
5	 <p><math>b_3</math> (<math>m/z</math> = 417.3)</p> <p>1) Cleavage of the amide bond between F and D in <b>2c</b>. 2) Cleavage of the amide bond between R and E in the linear fragment (loss of the fragment of ELIRTIMGWTLTD).</p>
6	 <p><math>b_3</math> (<math>m/z</math> = 330.2)</p> <p>1) Cleavage of the amide bond between T and W in <b>2c</b>. 2) Cleavage of the amide bond between D and F in the linear fragment (loss of the fragment of FLRELIRTIMGW).</p>

**Table A.4:** Suggested structures produced by fragmentation of the precursor ion 15-mer linear peptide (**2b**)  $[M+2H]^{2+}$   $m/z$  933 using MS<sup>2</sup>.

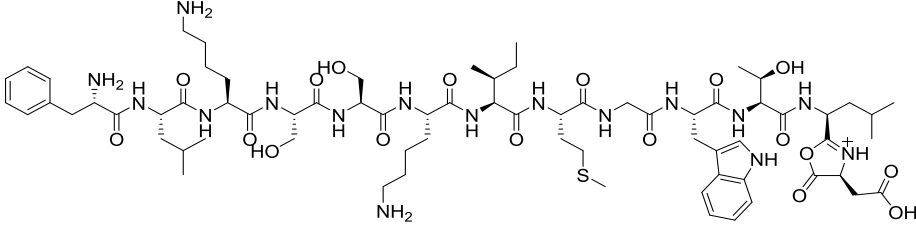
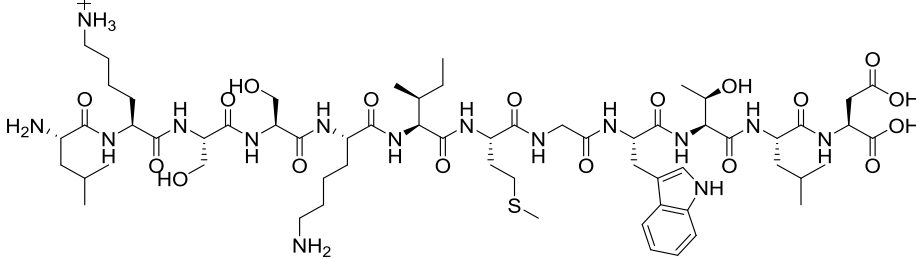
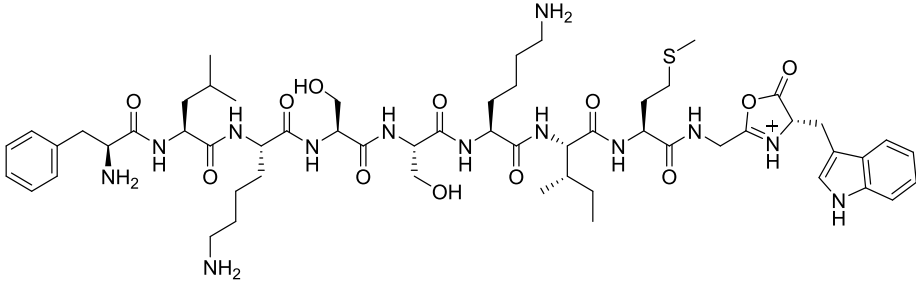
No	Structure of the fragment and site of cleaved peptide bond
1	 <p style="text-align: center;"><math>y_{12}</math> (<math>m/z = 1447.8</math>)</p> <p style="text-align: center;">Cleavage of the amide bond between G and R in <b>2b</b> (loss of the fragment of FLR).</p>
2	 <p style="text-align: center;"><math>b_{10}\text{-NH}_3</math> (<math>m/z = 1256.7</math>)</p> <p style="text-align: center;">Cleavage of the amide bond between M and G in <b>2b</b> (loss of the fragment of GWTLTD).</p>

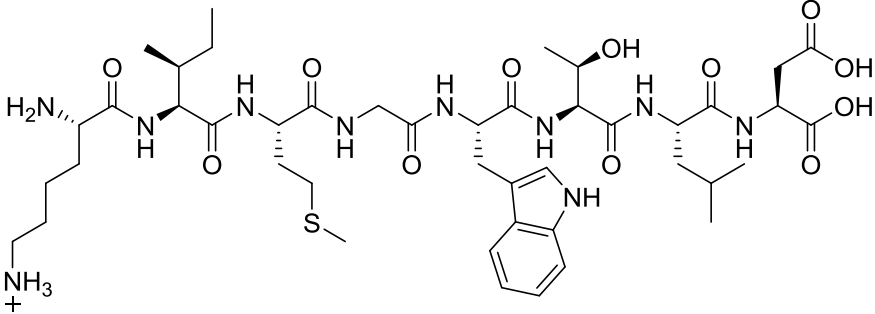
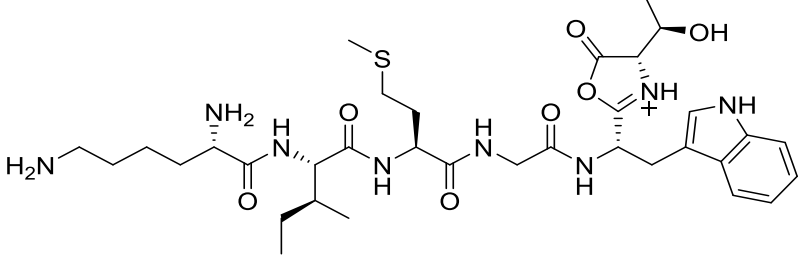
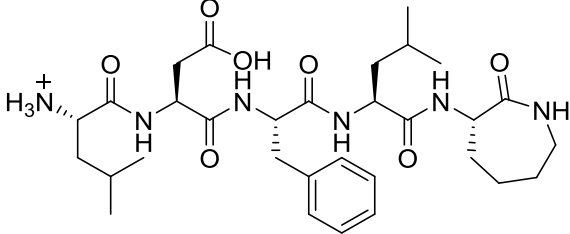
3	 <p><math>b_9\text{-NH}_3</math> (<math>m/z = 1125.7</math>)</p> <p>Cleavage of the amide bond between M and I in <b>2b</b> (loss of the fragment of MGWTLD).</p>
4	 <p><math>\text{MH}_2\text{-H}_2\text{O}</math> (<math>m/z = 923.5</math>)</p> <p>Loss of <math>\text{H}_2\text{O}</math> molecule from D residue in <b>2b</b>.</p>

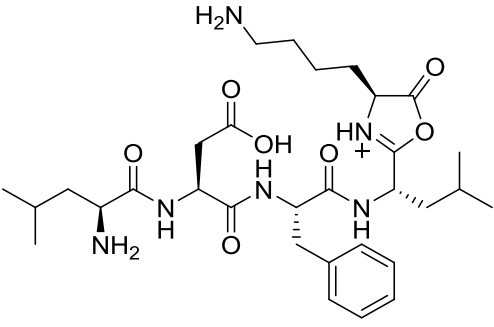
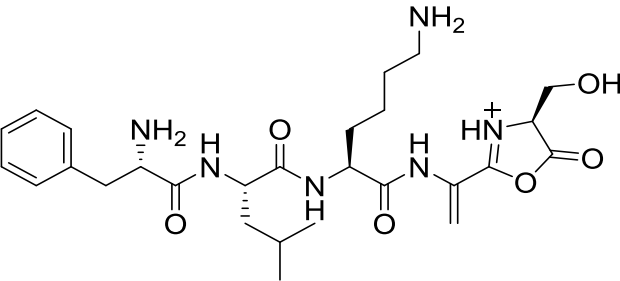
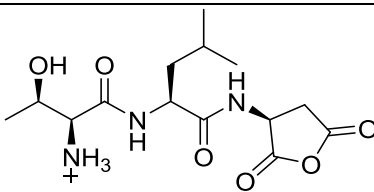


5	 <p style="text-align: center;"><math>y_7</math> (<math>m/z = 835.4</math>)</p> <p style="text-align: center;">Cleavage of the amide bond between T and I in <b>2b</b> (loss of the fragment of FLRELIRT).</p>
6	 <p style="text-align: center;"><math>b_{10}</math> (<math>m/z = 637.4</math>)</p> <p style="text-align: center;">Cleavage of the amide bond between G and M in <b>2b</b> (loss of the fragment of GWTLTD).</p>
7	 <p style="text-align: center;"><math>b_4</math> (<math>m/z = 546.3</math>)</p> <p style="text-align: center;">Cleavage of the amide bond between L and E in <b>2b</b> (loss of the fragment of LIRTIMGWTLTD).</p>
8	 <p style="text-align: center;"><math>b_3</math> (<math>m/z = 417.3</math>)</p> <p style="text-align: center;">Cleavage of the amide bond between R and E in <b>2b</b> (loss of the fragment of ELIRTIMGWTLTD).</p>

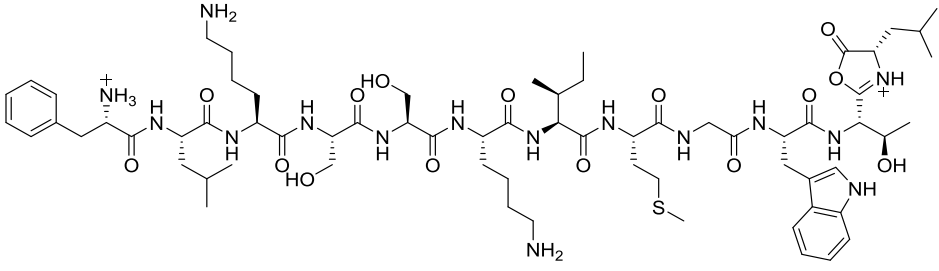
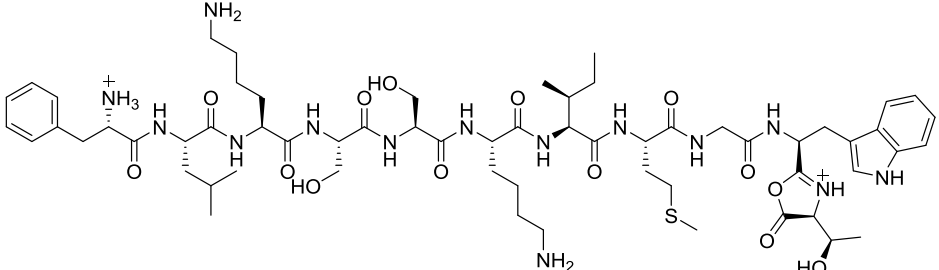
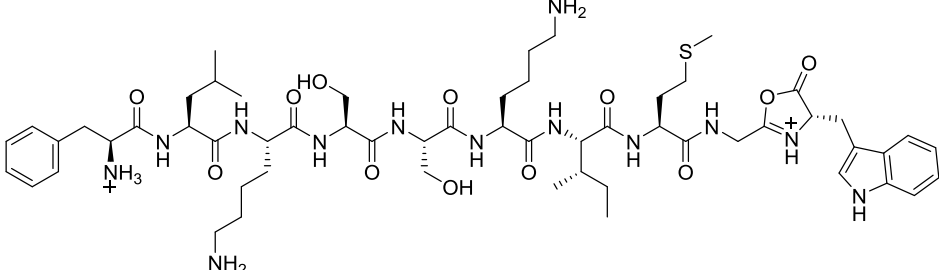
**Table A.5:** Suggested structures produced by fragmentation of the precursor ion 13-mer cyclic peptide (**3c**) [ $M+2H$ ] $^{2+}$   $m/z$  755 using MS $^2$ .

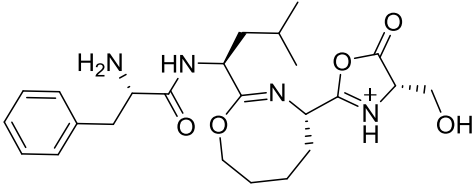
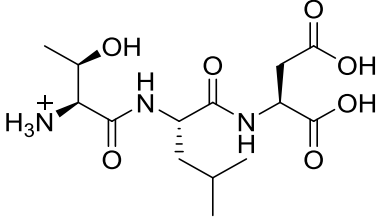
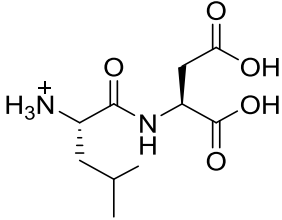
No	Structure of the fragment and site of cleaved peptide bond
1	 <p style="text-align: center;"><math>MH</math> (<math>m/z = 1507.8</math>)</p> <p style="text-align: center;">Cleavage of the amide bond between F and D in <b>3c</b> without losing any fragment.</p>
2	 <p style="text-align: center;"><math>y_{12}+H_2O</math> (<math>m/z = 1378.7</math>)</p> <p style="text-align: center;">1) Cleavage of the amide bond between F and D in <b>3c</b>. 2) Cleavage of the amide bond between F and L in the linear fragment (loss of F).</p>
3	 <p style="text-align: center;"><math>b_{10}</math> (<math>m/z = 1178.6</math>)</p> <p style="text-align: center;">1) Cleavage of the amide bond between F and D in <b>3c</b>. 2) Cleavage of the amide bond between W and T in the linear fragment (loss of the fragment of TLD).</p>

4	 <p style="text-align: center;"><math>y_8</math> (<math>m/z = 963.5</math>)</p> <p>1) Cleavage of the amide bond between F and D in <b>3c</b>. 2) Cleavage of the amide bond between K and S in the linear fragment (loss of the fragment of FLKSS).</p>
5	 <p style="text-align: center;"><math>b_6</math>, (<math>m/z = 717.4</math>)</p> <p>1) Cleavage of the amide bond between S and K in <b>3c</b>. 2) Cleavage of the amide bond between T and L in the linear fragment (loss of the fragment of LDFLKSS).</p>
6	 <p style="text-align: center;"><math>1-y_5</math> (<math>m/z = 617.4</math>)</p> <p>1) Cleavage of the amide bond between S and K in <b>3c</b>. 2) Cleavage of the amide bond between T and L in the linear fragment (loss of the fragment of SSKIMGWT).</p>

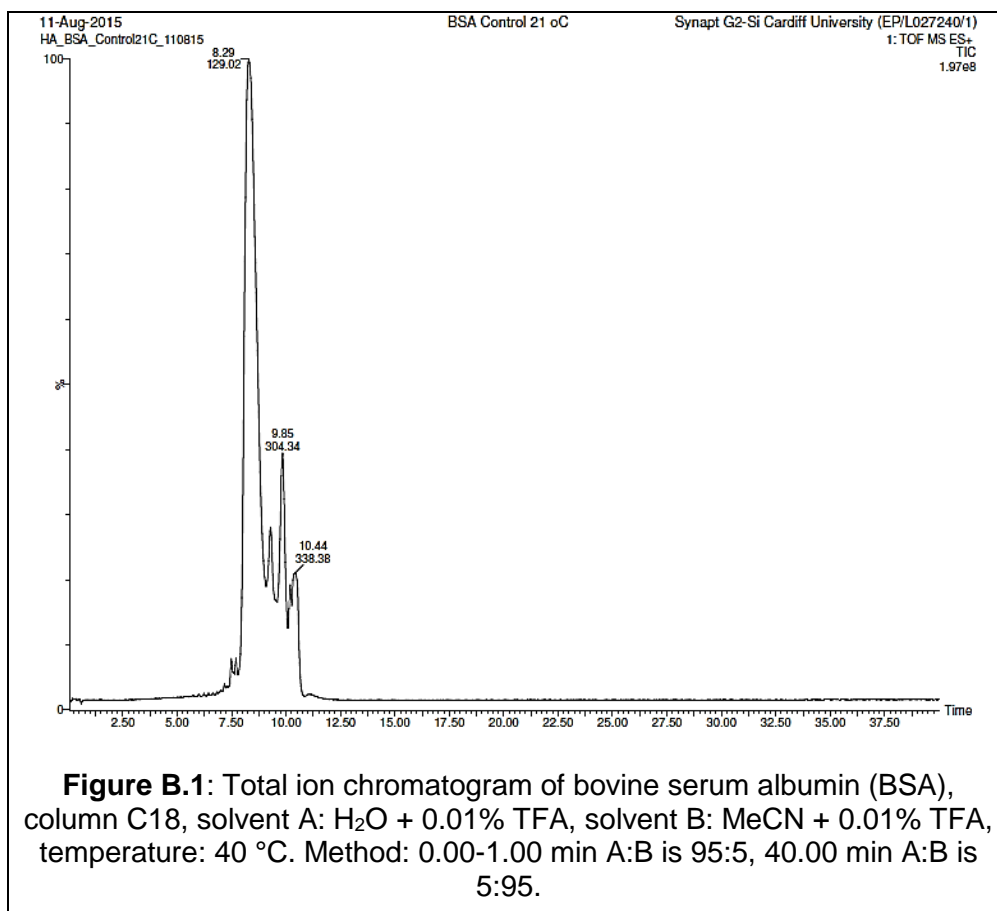
	 <p>2-b<sub>5</sub> (<math>m/z</math> = 617.4)</p> <p>1) Cleavage of the amide bond between T and L in <b>3c</b>. 2) Cleavage of the amide bond between K and S in the linear fragment (Loss of the fragment of SSKIMGWT).</p>
7	 <p>b<sub>5</sub>-H<sub>2</sub>O (<math>m/z</math> = 545.3)</p> <p>1) Cleavage of the amide bond between F and D in <b>3c</b>. 2) Cleavage of the amide bond between S and K in the linear fragment (Loss of the fragment of KIMGWTLTLD). 3) Loss of H<sub>2</sub>O molecule from T.</p>
8	 <p>y<sub>3</sub> (<math>m/z</math> = 330.2)</p> <p>1) Cleavage of the amide bond between F and D in <b>3c</b>. 2) Cleavage of the amide bond between W and T in the linear fragment (loss of the fragment of FLSSKLIMGW).</p>

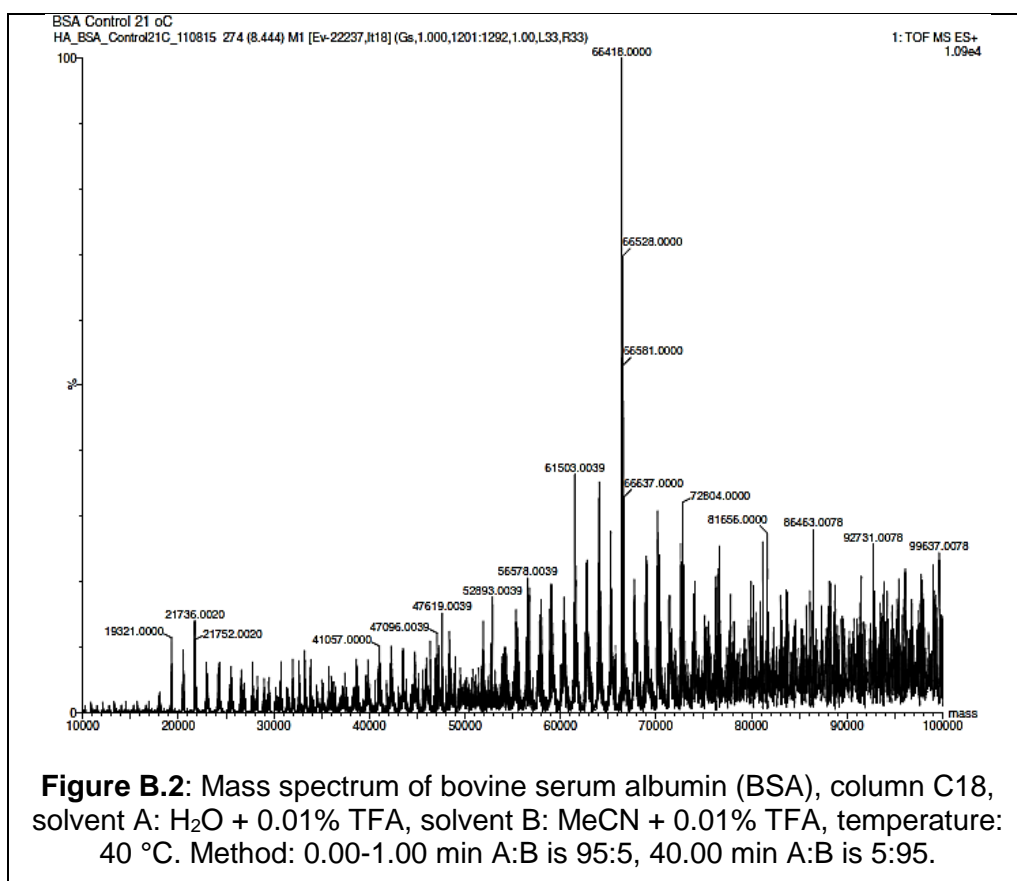
**Table A.6:** Suggested structures produced by fragmentation of the precursor ion 13-mer linear peptide (**3b**) [ $M+3H$ ] $^{3+}$   $m/z$  510 using MS $^2$ .

No	Structure of the fragment and site of cleaved peptide bond
1	 <p style="text-align: center;"><math>b_{12}</math> (<math>m/z</math> = 696.9)</p> <p style="text-align: center;">Cleavage of the amide bond between F and D in <b>3b</b> (loss of D).</p>
2	 <p style="text-align: center;"><math>b_{11}</math> (<math>m/z</math> = 640.3)</p> <p style="text-align: center;">Cleavage of the amide bond between T and L in <b>3b</b> (loss of the fragment of LD).</p>
3	 <p style="text-align: center;"><math>b_{10}</math> (<math>m/z</math> = 589.8)</p> <p style="text-align: center;">Cleavage of the amide bond between W and T in <b>3b</b> (loss of the fragment of TLD).</p>

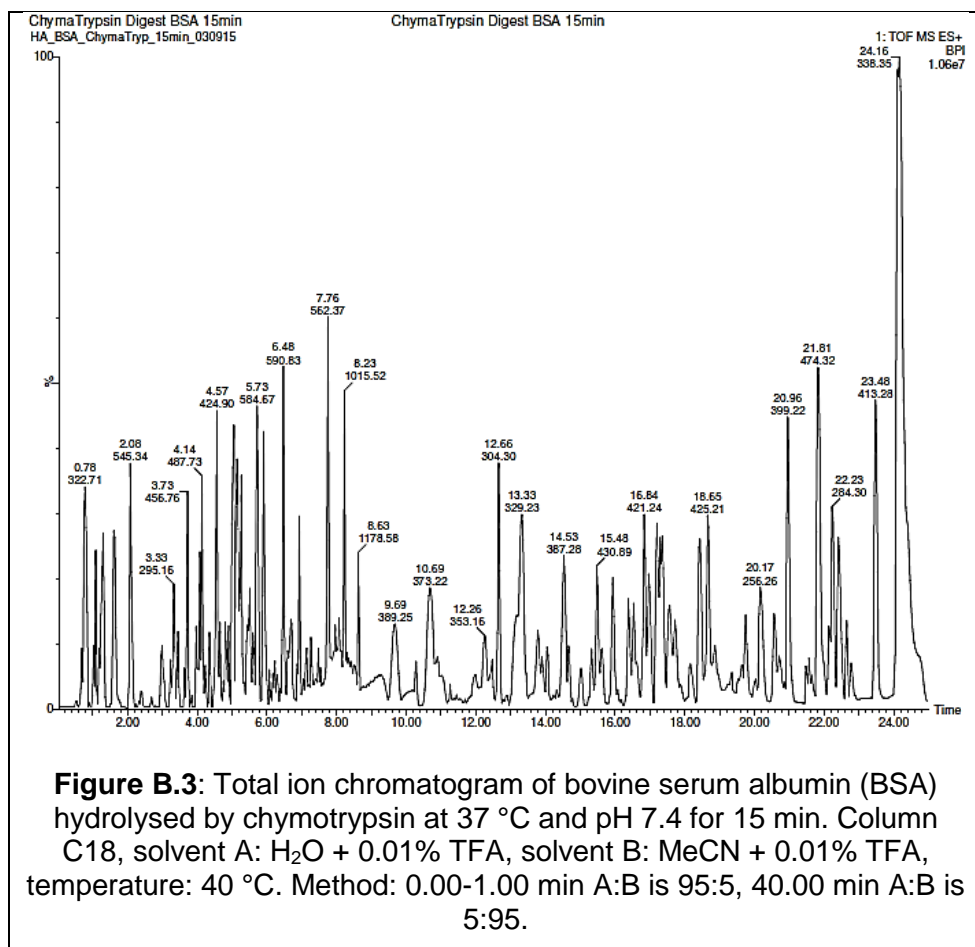
4	 <p><math>b_4\text{-NH}_3</math> (<math>m/z = 459.3</math>)</p> <p>1) Cleavage of the amide bond between S and S in <b>3b</b> (loss of the fragment of SKIMGWTLD. 2) Loss of <math>\text{NH}_3</math> molecule from K.</p>
5	 <p><math>y_3</math> (<math>m/z = 348.2</math>)</p> <p>Cleavage of the amide bond between W and T in <b>3b</b> (loss of the fragment of FLKSSKIMGW).</p>
6	 <p><math>y_2</math> (<math>m/z = 247.1</math>)</p> <p>Cleavage of the amide bond between T and L in <b>3b</b> (loss of the fragment of FLKSSKIMGWT).</p>

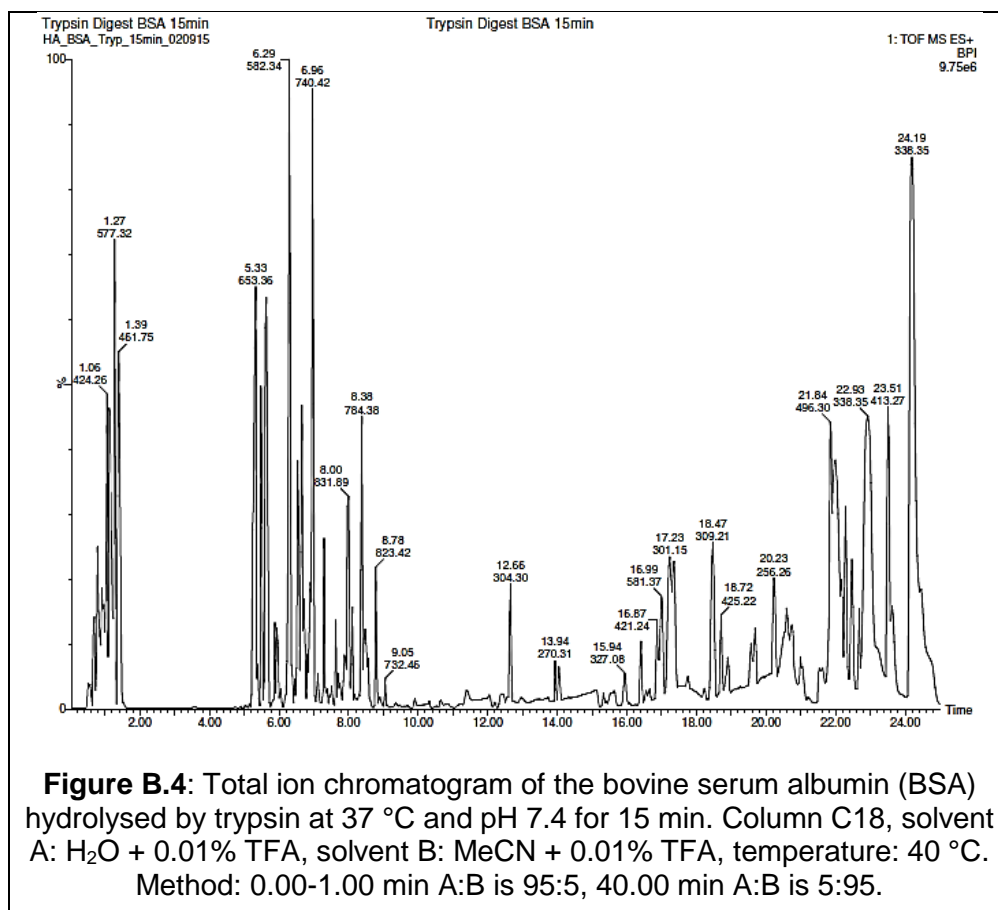
## 9 Appendix B

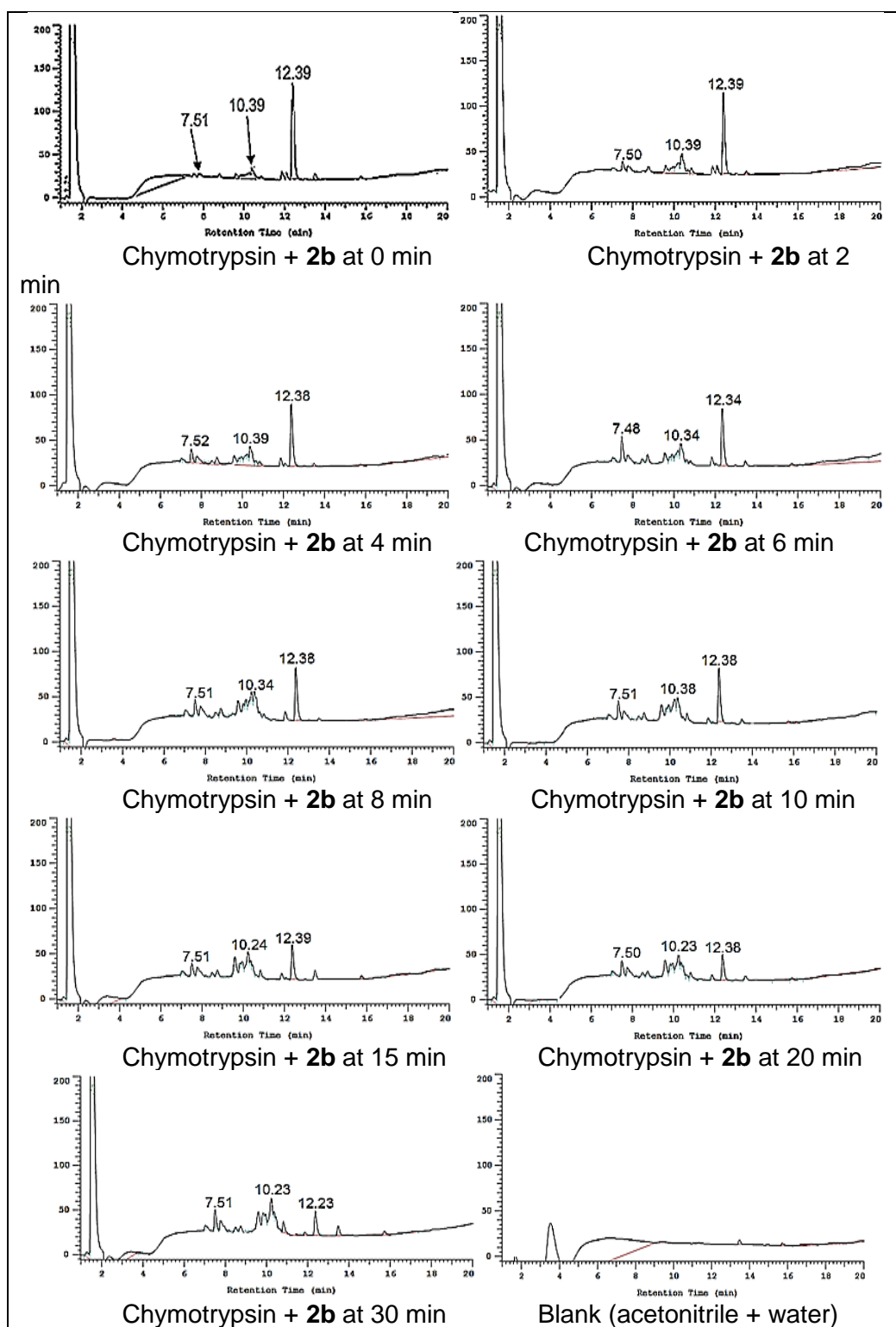




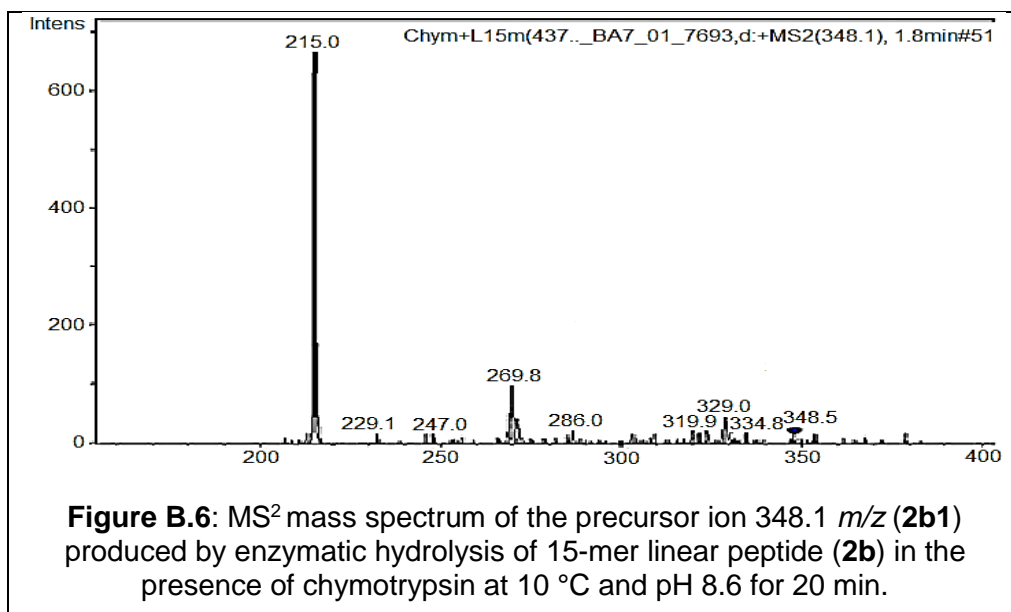








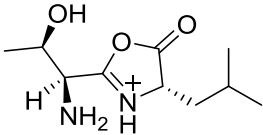
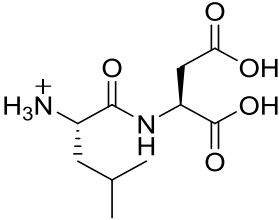
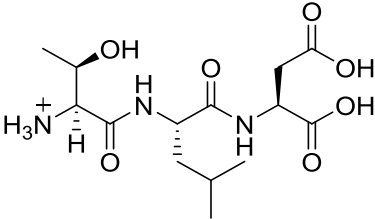
**Figure B.5:** HPLC chromatograms of the reaction between 25  $\mu\text{L}$  of chymotrypsin (1.06  $\mu\text{M}$ ) and 250  $\mu\text{L}$  of **2b** (100  $\mu\text{M}$ ) at 10  $^{\circ}\text{C}$  and pH 8.6 for 0, 2, 4, 6, 8, 10, 15, 20, 30 min.

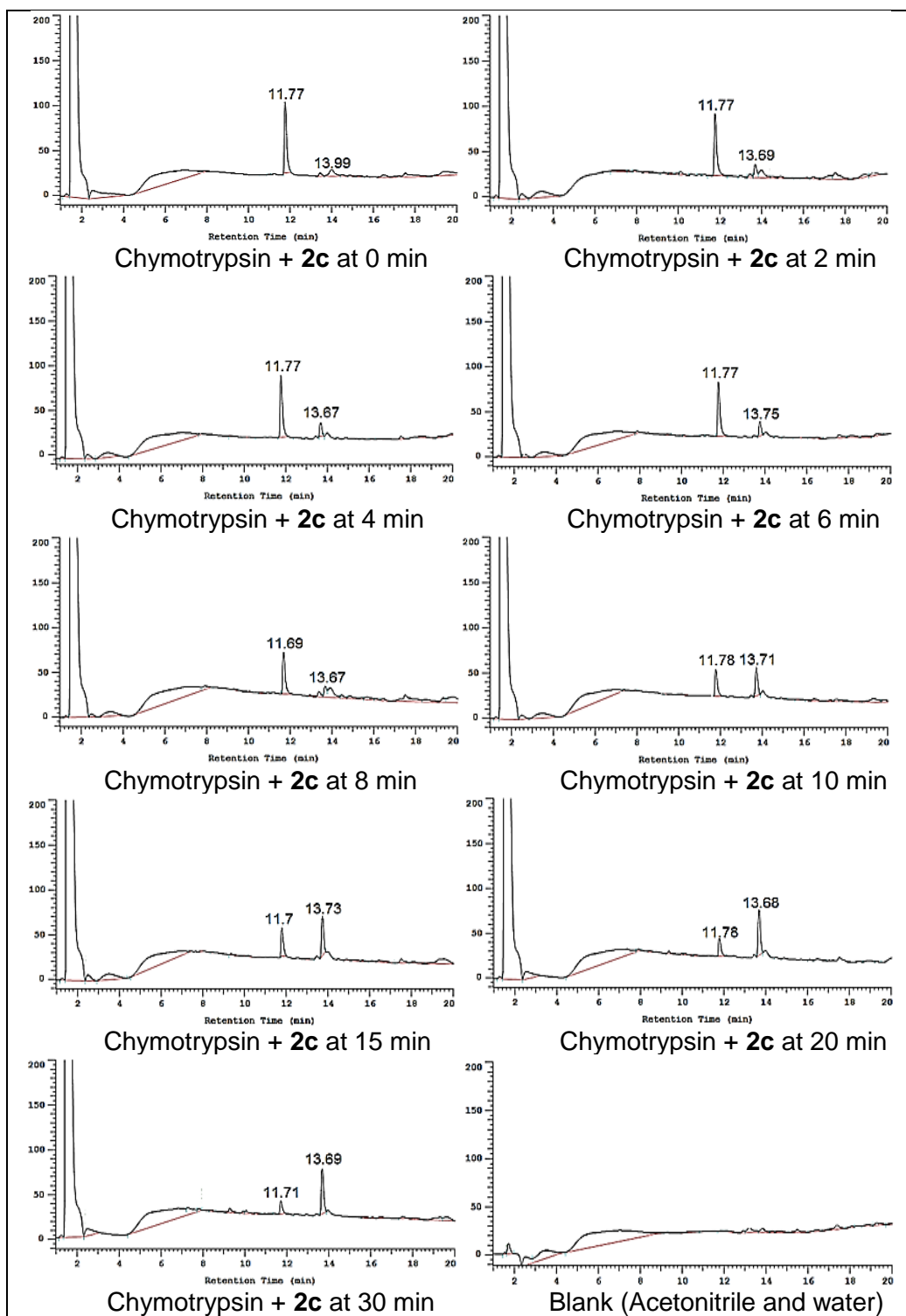


**Table B.1:** The expected mass of the peptides (*m/z*) produced by enzymatic hydrolysis of 15-mer linear peptide (**2b**) in the presence of chymotrypsin at 10 °C and pH 8.6 for 20 min.

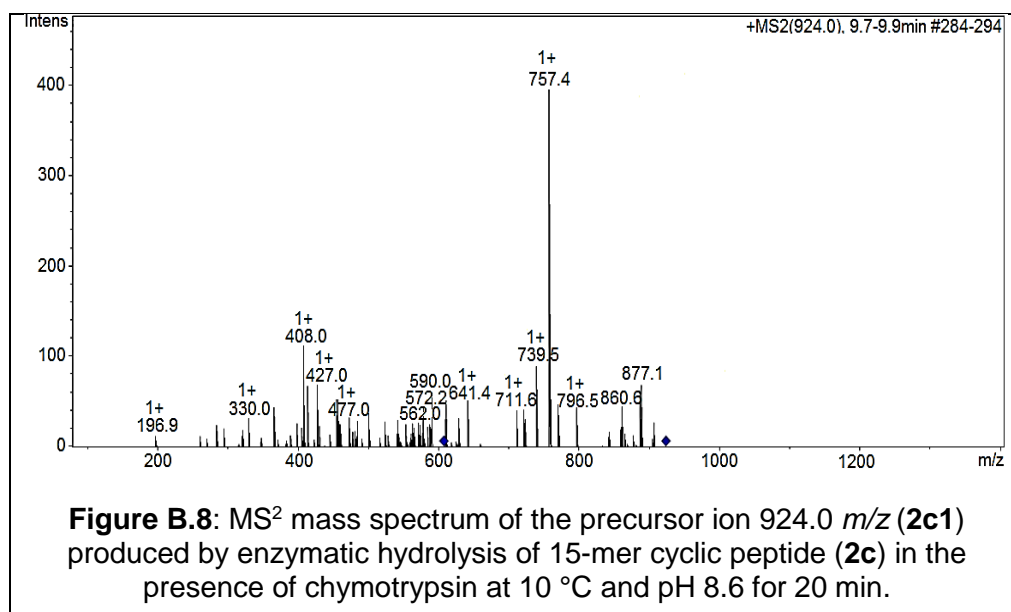
F-L-R-E-L-I-R-T-I-M-G-W-T-L-D		
No	Site of the cleaved peptide bond	<i>m/z</i> of the expected peptide
1	F-L	(166.1) <sup>1+</sup> , (1716.9) <sup>1+</sup> , (859) <sup>2+</sup> , (573) <sup>3+</sup>
2	W-T	(348.2) <sup>1+</sup> , (1534.9) <sup>1+</sup> , (767.9) <sup>2+</sup> , (512.3) <sup>3+</sup>
3	F-L, W-T	(166.1) <sup>1+</sup> , (348.2) <sup>1+</sup> , (1387.8) <sup>1+</sup> , (694.4) <sup>2+</sup> , (463.3) <sup>3+</sup>

**Table B.2:** Suggested structures for observed peaks (fragments) in the MS<sup>2</sup> mass spectrum of precursor ion 348.1 *m/z* (**2b1**) produced by enzymatic hydrolysis of 15-mer linear peptide (**2b**) in the presence of chymotrypsin at 10 °C and pH 8.6 for 20 min.

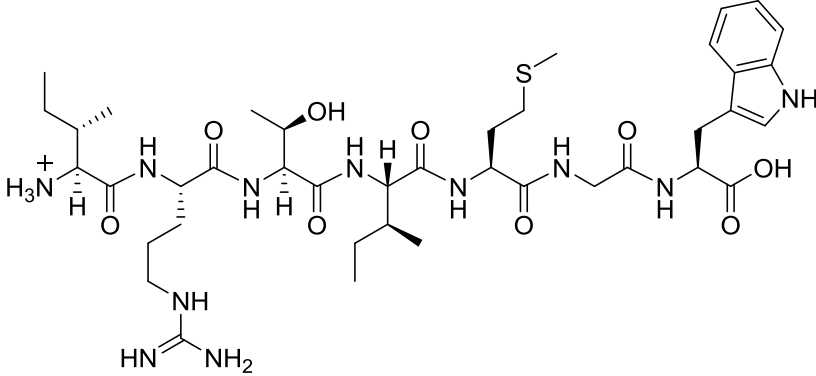
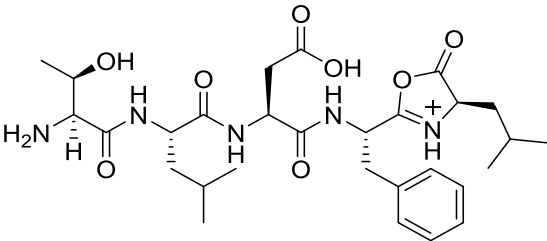
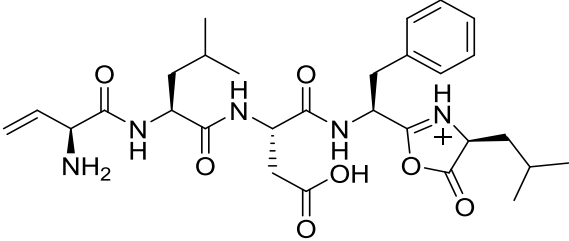
No	Structure of the fragment and site of the cleaved peptide bond in <b>2b1</b> (T-L-D)
1	 <p><math>b_2</math> (<math>m/z = 215.1</math>)</p> <p>Cleavage of the peptide bond between L and D in <b>2b1</b> (loss of D).</p>
2	 <p><math>y_2</math> (<math>m/z = 247.1</math>)</p> <p>Cleavage the peptide bond between T and L in <b>2b1</b> (loss of T).</p>
3	 <p>MH (<math>m/z = 348.2</math>)</p> <p>No cleavage at any of the peptide bonds of the precursor ion (<b>2b1</b>).</p>



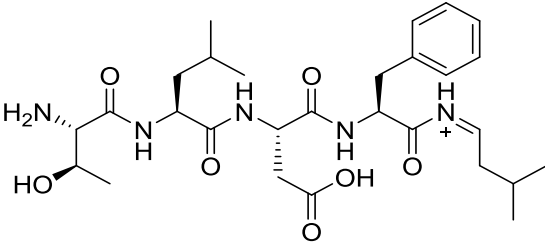
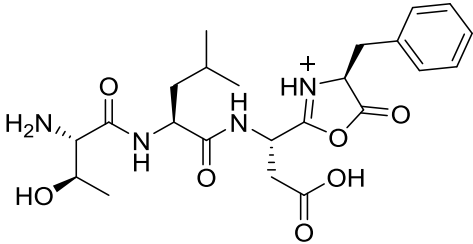
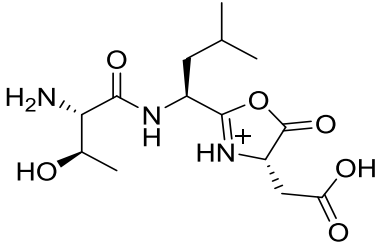
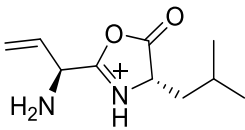
**Figure B.7:** HPLC chromatograms of the reaction between 25  $\mu\text{L}$  of chymotrypsin (1.06  $\mu\text{M}$ ) and 250  $\mu\text{L}$  of **2c** (100  $\mu\text{M}$ ) at 10  $^{\circ}\text{C}$  and pH 8.6 for 0, 2, 4, 6, 8, 10, 15, 20, 30 min.



**Table B.3:** Suggested structures for observed peaks (fragments) in the MS<sup>2</sup> mass spectrum of precursor ion 924.0 *m/z* (**2c1**) produced by enzymatic hydrolysis of 15-mer cyclic peptide (**2c**) in the presence of chymotrypsin at 10 °C and pH 8.6 for 20 min.

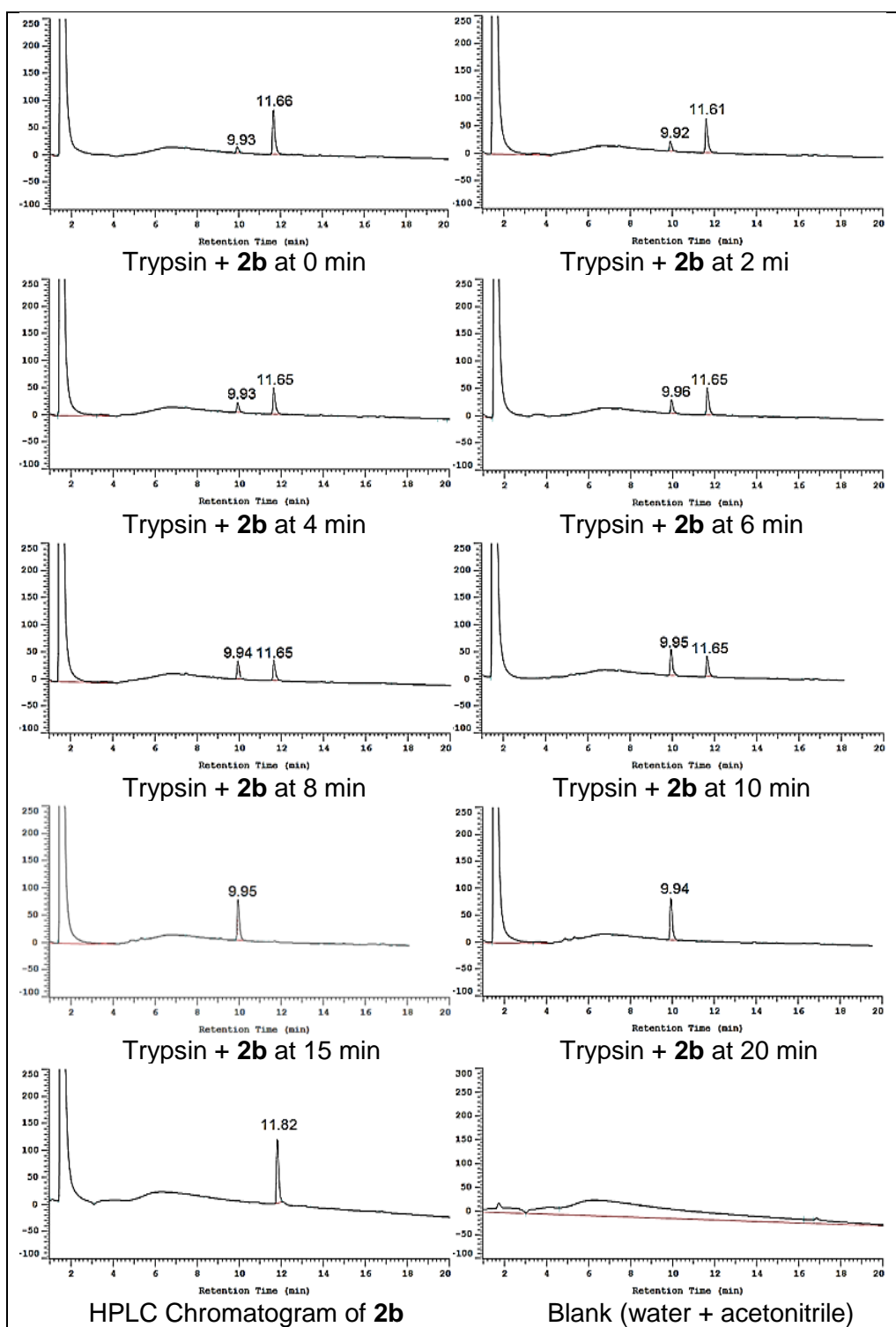
No	Structure of the fragment and site of the cleaved peptide bond in <b>2c1</b> (T-L-D-F-L-R-E-L-I-R-T-I-M-G-W)
1	 <p style="text-align: center;"><i>y</i><sub>7</sub> (<i>m/z</i> = 876.5)</p> <p>Cleavage of the peptide bond between L and I in <b>2c1</b> (loss of the fragment of TLDFLREL).</p>
2	 <p style="text-align: center;"><i>b</i><sub>5</sub> (<i>m/z</i> = 590.3)</p> <p>Cleavage of the peptide bond between L and R in <b>2c1</b> (loss of the fragment of RELIRTIMGW).</p>
3	 <p style="text-align: center;"><i>b</i><sub>5</sub>-H<sub>2</sub>O (<i>m/z</i> = 572.3)</p> <p>1) Cleavage of the peptide bond between L and R in <b>2c1</b> (loss of the fragment of RELIRTIMGW). 2) Loss of H<sub>2</sub>O molecule from T.</p>



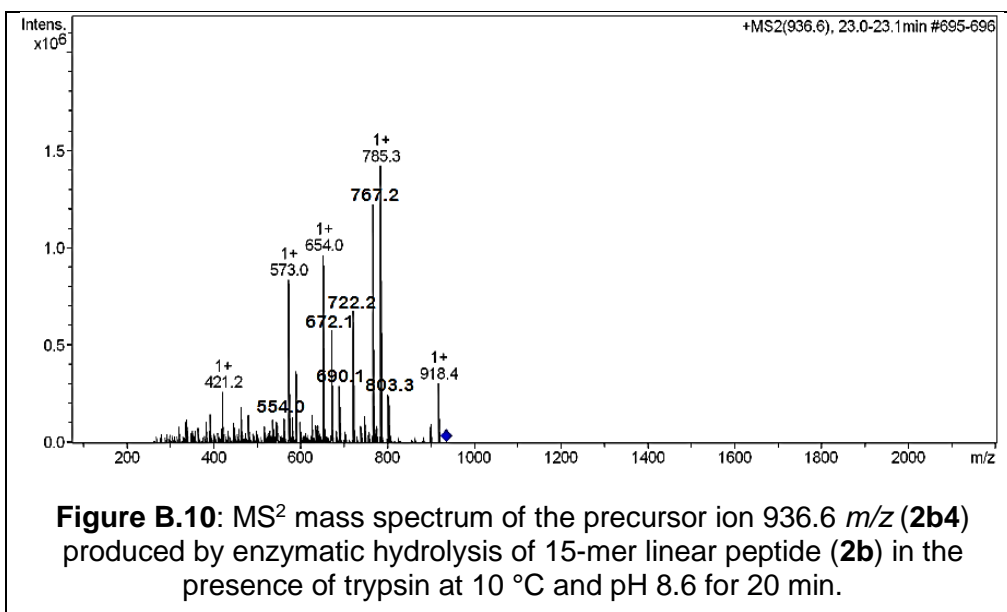
4	 <p style="text-align: center;"><math>a_5</math> (<math>m/z = 562.3</math>)</p> <p>Cleavage of the peptide bond between L and R in <b>2c1</b> (loss of the fragment of RELIRTIMGW).</p>
5	 <p style="text-align: center;"><math>b_4</math> (<math>m/z = 477.2</math>)</p> <p>Cleavage of the peptide bond between F and L in <b>2c1</b> (loss of the fragment of LRELIRTIMGW).</p>
6	 <p style="text-align: center;"><math>b_3</math> (<math>m/z = 330.2</math>)</p> <p>Cleavage of the peptide bond between D and F in <b>2c1</b> (loss of the fragment of FLRELIRTIMGW).</p>
7	 <p style="text-align: center;"><math>b_2-H_2O</math> (<math>m/z = 197.1</math>)</p> <p>1) Cleavage of the peptide bond between L and D in <b>2c1</b> (loss of the fragment of DFLRELIRTIMGW). 2) Loss of H<sub>2</sub>O molecule from T.</p>

**Table B.4:** The expected mass of the peptides ( $m/z$ ) produced by enzymatic hydrolysis of 15-mer cyclic peptide (**2c**) in the presence of chymotrypsin at 10 °C and pH 8.6 for 20 min.

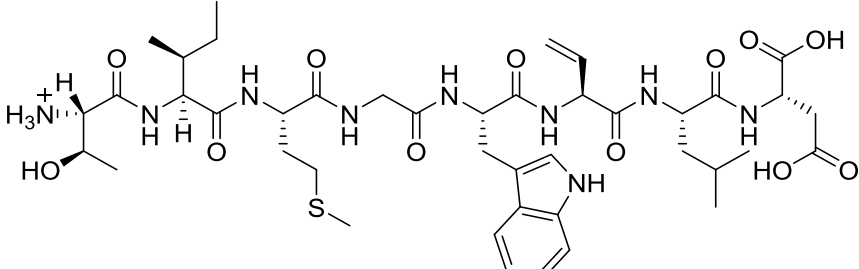
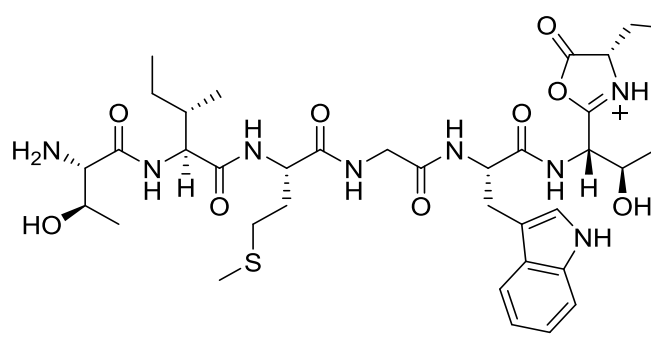
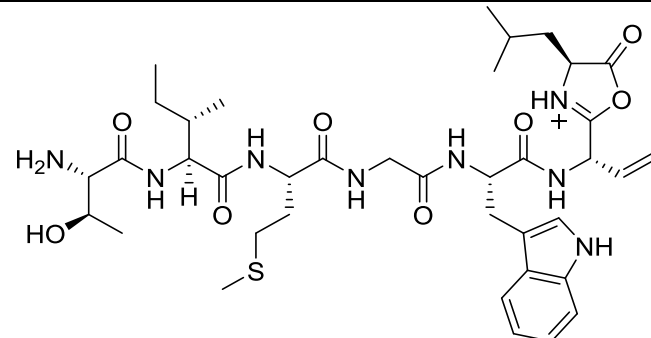
T-L-D-F-L-R-E-L-I-R-T-I-M-G-W		
No	Site of cleaved peptide bond	$m/z$ of the expected peptide
1	F-L	(1864.0) <sup>1+</sup> , (932.5) <sup>2+</sup> , (622) <sup>3+</sup>
2	W-T	(1864.0) <sup>1+</sup> , (932.5) <sup>2+</sup> , (622.5) <sup>3+</sup>
3	W-T, F-L	(495.2) <sup>1+</sup> , (1387.8) <sup>1+</sup> , (694.4) <sup>2+</sup> , (463.3) <sup>3+</sup>

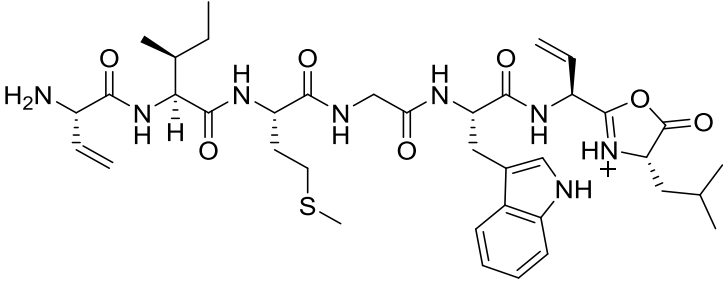
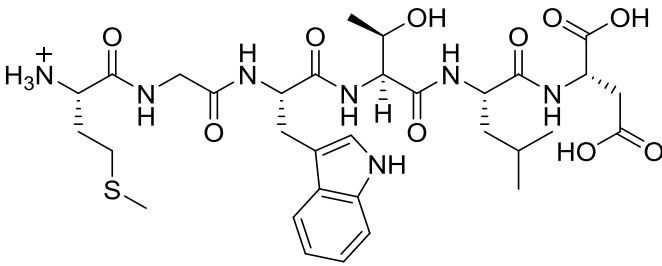
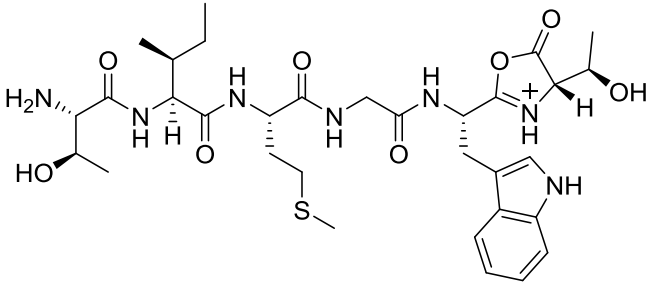
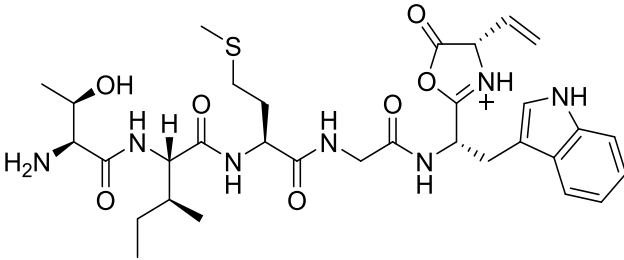


**Figure B.9:** HPLC chromatograms of the reaction between 25  $\mu\text{L}$  of trypsin (0.41  $\mu\text{M}$ ) and 250  $\mu\text{L}$  of **2b** (100  $\mu\text{M}$ ) at 10 °C and pH 6.2 for 0, 2, 4, 6, 8, 10, 15, 20 min.



**Table B.5:** Suggested structures for observed peaks (fragments) in the MS<sup>2</sup> mass spectrum of precursor ion 936.6 *m/z* (**2b4**) produced by enzymatic hydrolysis of 15-mer linear peptide (**2b**) in the presence of trypsin at 10 °C and pH 8.6 for 20 min.

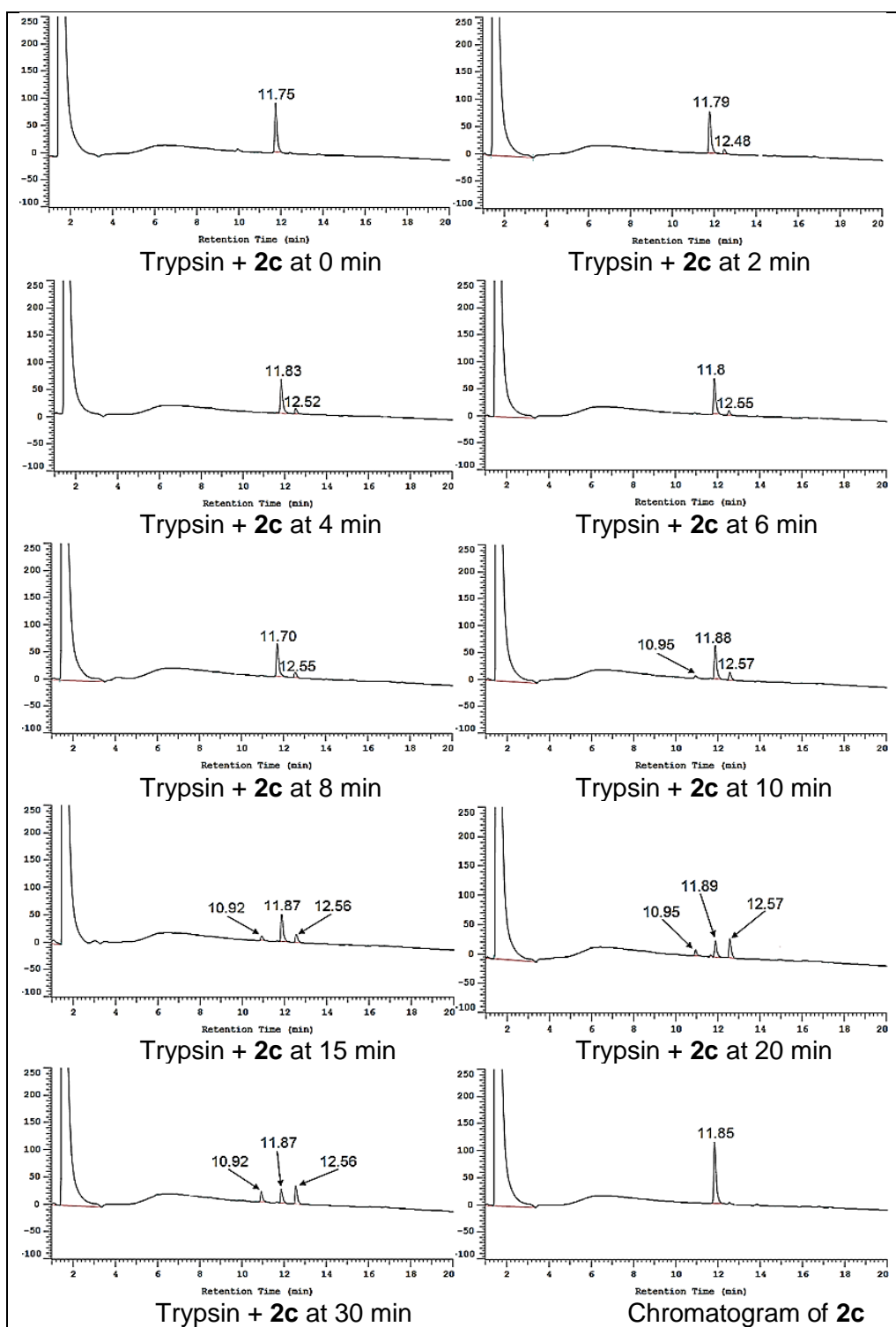
No	Structure of the fragment and site of the cleaved peptide bond in <b>2b4</b> (T-I-M-G-W-T-L-D)
1	 <p style="text-align: center;">MH-H<sub>2</sub>O (<i>m/z</i> = 918.4)</p> <p style="text-align: center;">Loss of H<sub>2</sub>O molecule from one of the two T residues in <b>2b4</b>.</p>
2	 <p style="text-align: center;"><i>b</i><sub>7</sub> (<i>m/z</i> = 803.4)</p> <p style="text-align: center;">Cleavage of the peptide bond between L and D in <b>2b4</b> (loss of D).</p>
3	 <p style="text-align: center;"><i>b</i><sub>7</sub>-H<sub>2</sub>O (<i>m/z</i> = 785.4)</p> <p style="text-align: center;">1) Cleavage of the peptide bond between L and D in <b>2b4</b> (loss of D). 2) Loss of H<sub>2</sub>O molecule from one of the two T residues.</p>

4	 <p style="text-align: center;"><math>b_7-2H_2O</math> (<math>m/z = 767.4</math>)</p> <p>1) Cleavage of the peptide bond between L and D in <b>2b4</b> (loss of D). 2) Loss of 2 H<sub>2</sub>O molecules from the two T residues.</p>
5	 <p style="text-align: center;"><math>y_6</math> (<math>m/z = 722.3</math>)</p> <p>1) Cleavage of the peptide bond between I and M in <b>2b4</b> (loss of the fragment of TI).</p>
6	 <p style="text-align: center;"><math>b_6</math> (<math>m/z = 690.3</math>)</p> <p>1) Cleavage of the peptide bond between T and L in <b>2b4</b> (loss of the fragment of LD).</p>
7	 <p style="text-align: center;"><math>b_6-H_2O</math> (<math>m/z = 672.3</math>)</p> <p>1) Cleavage of the peptide bond between T and L in <b>2b4</b> (loss of the fragment of LD). 2) Loss of H<sub>2</sub>O molecule from T.</p>

8	<p><math>y_5\text{-H}_2\text{O}</math> (<math>m/z = 573.3</math>)</p> <p>1) Cleavage of the peptide bond between M and G in <b>2b4</b> (loss of the fragment of TIM). 2) Loss of <math>\text{H}_2\text{O}</math> molecule from T.</p>
---	---

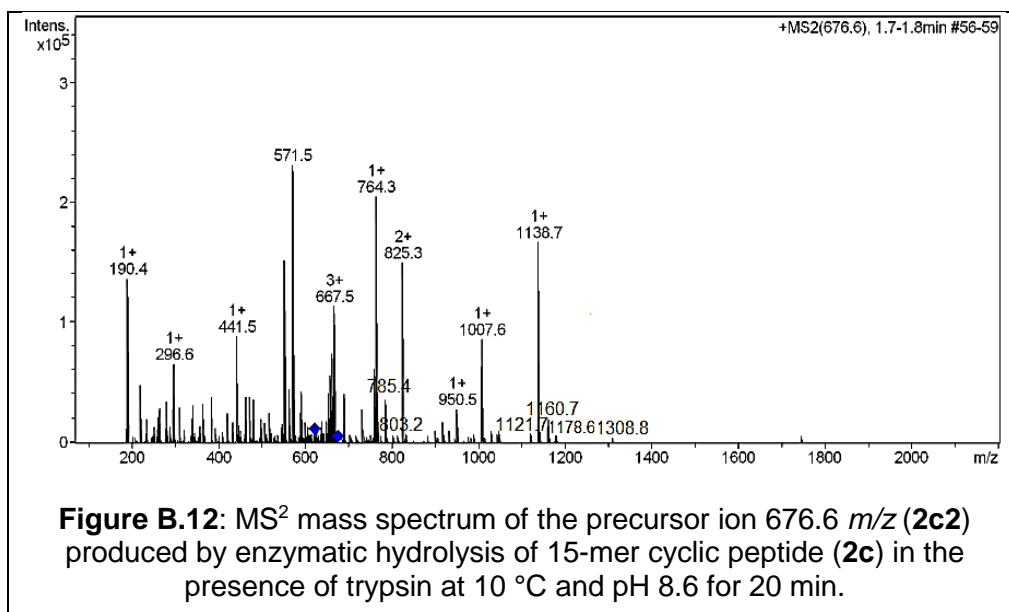
**Table B.6:** The expected mass of the peptides ( $m/z$ ) produced by enzymatic hydrolysis of 15-mer linear peptide (**2b**) in the presence of trypsin at 10 °C and pH 8.6 for 20 min.

F-L-R-E-L-I-R-T-I-M-G-W-T-L-D		
No	Site of cleaved peptide bonds	$m/z$ of the expected peptide
1	R-T	(936.4) <sup>1+</sup> , (946.6) <sup>1+</sup> , (473.8) <sup>2+</sup> , (316.2) <sup>3+</sup>
2	R-E	(435.5) <sup>1+</sup> , (218.1) <sup>2+</sup> , (1447.8) <sup>1+</sup> , (724.4) <sup>2+</sup>
3	R-T, R-E	(435.5) <sup>1+</sup> , (218.1) <sup>2+</sup> , (530.3) <sup>1+</sup> , (265.7) <sup>1+</sup> , (936.4) <sup>1+</sup>

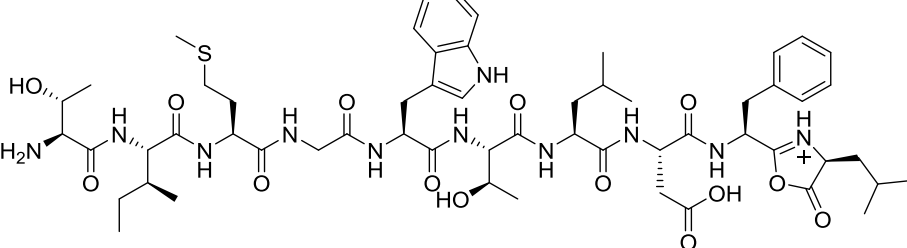
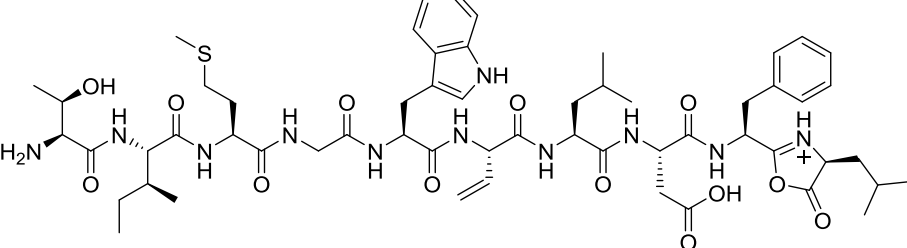
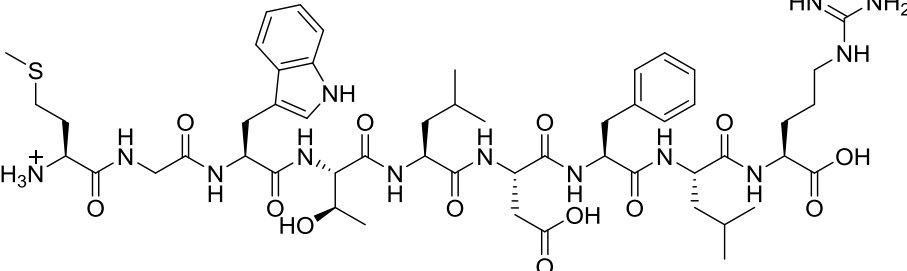


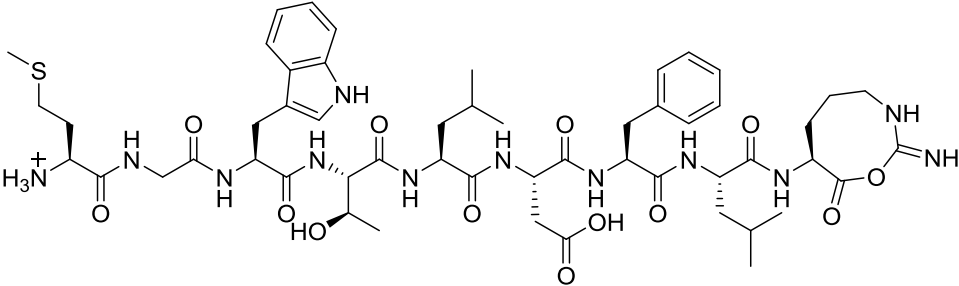
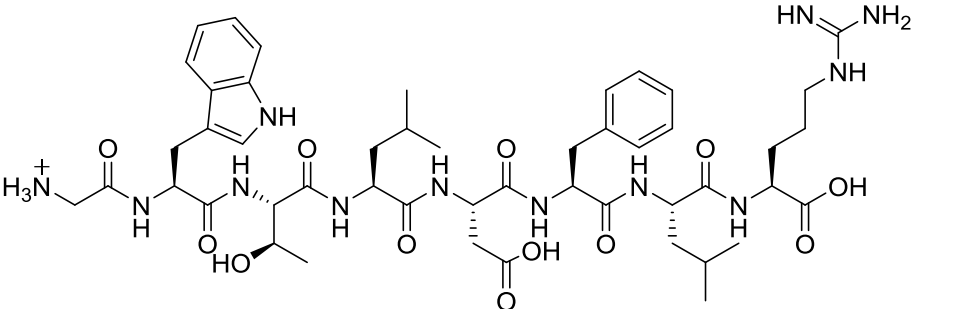
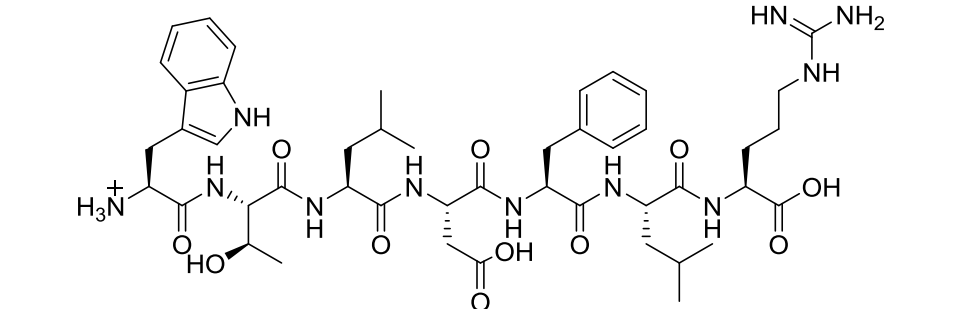
**Figure B.11:** HPLC chromatograms of the reaction between 25  $\mu\text{L}$  of trypsin (0.58  $\mu\text{M}$ ) and 250  $\mu\text{L}$  of **2c** (100  $\mu\text{M}$ ) at 10  $^{\circ}\text{C}$  and pH 6.2 over 0, 2, 4, 6, 8, 10, 15, 20, 30 min.

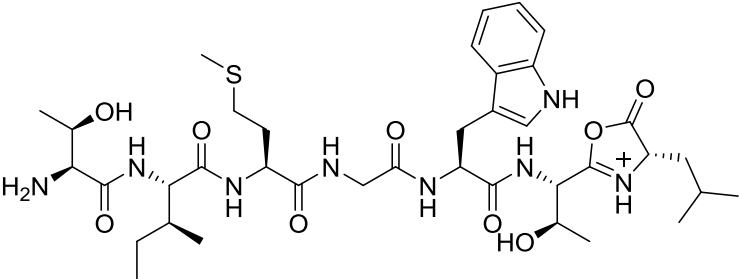
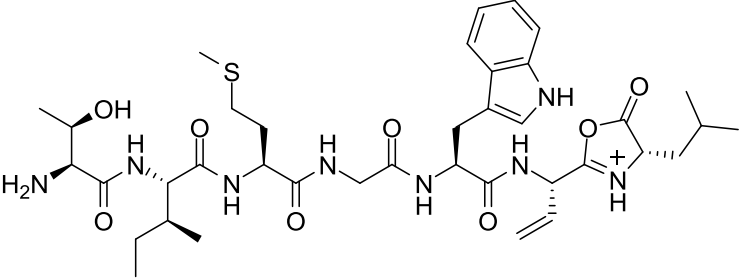
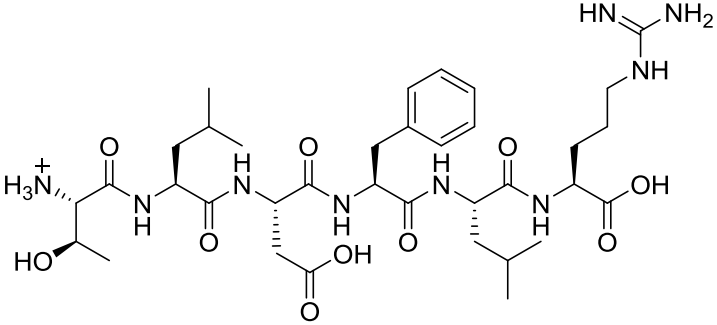


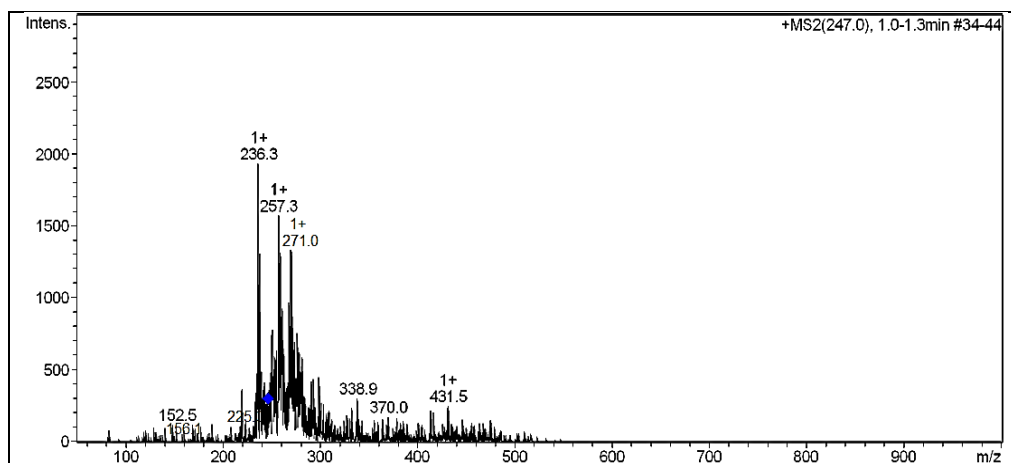


**Table B.7:** Suggested structures for observed peaks (fragments) in the MS<sup>2</sup> mass spectrum of precursor ion 676.6 *m/z* (**2c2**) produced by enzymatic hydrolysis of 15-mer cyclic peptide (**2c**) in the presence of trypsin at 10 °C and pH 8.6 for 20 min.

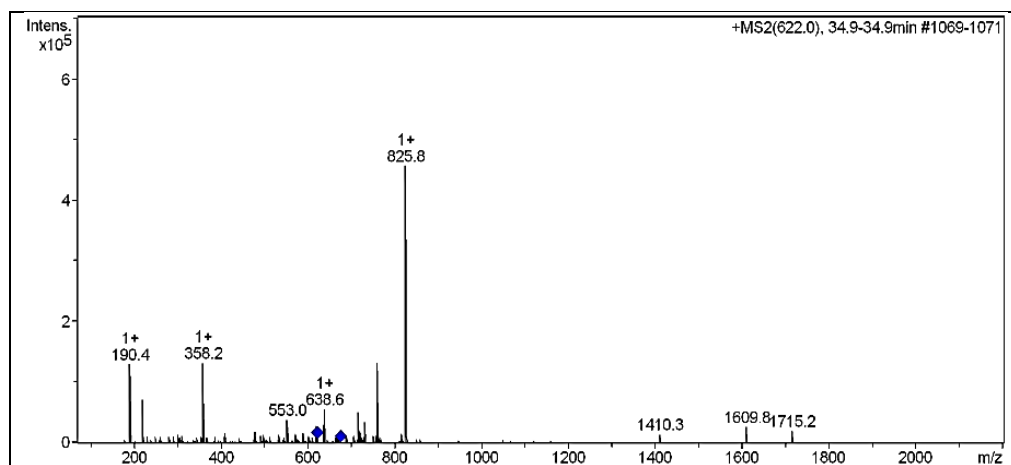
No	Structure of the fragment and site of the cleaved peptide bond in <b>2c2</b> (T-I-M-G-W-T-L-D-F-L-R)
1	 <p style="text-align: center;"><math>b_{10}</math> (<math>m/z = 1178.6</math>)</p> <p style="text-align: center;">Cleavage of the peptide bond between L and R in <b>2c2</b> (loss of R).</p>
2	 <p style="text-align: center;"><math>b_{10}-H_2O</math> (<math>m/z = 1160.6</math>)</p> <p style="text-align: center;">1) Cleavage of the peptide bond between L and R in <b>2c2</b> (loss of R). 2) Loss of H<sub>2</sub>O molecule from one of the two T residues.</p>
3	 <p style="text-align: center;"><math>y_9</math> (<math>m/z = 1138.6</math>)</p> <p style="text-align: center;">Cleavage of the peptide bond between I and M in <b>2c2</b> (loss of the fragment of TI).</p>

4	 <p style="text-align: center;"><math>y_9\text{-NH}_3</math> (<math>m/z = 1121.5</math>)</p> <p>1) Cleavage of the peptide bond between I and M in <b>2c2</b> (loss of the fragment of TI). 2) Loss of <math>\text{NH}_3</math> molecule from R.</p>
5	 <p style="text-align: center;"><math>y_8</math> (<math>m/z = 1007.5</math>)</p> <p>Cleavage of the peptide bond between M and G in <b>2c2</b> (loss of the fragment of TIM).</p>
6	 <p style="text-align: center;"><math>y_7</math> (<math>m/z = 950.5</math>)</p> <p>Cleavage of the peptide bond between G and W in <b>2c2</b> (loss of the fragment of TIMG).</p>

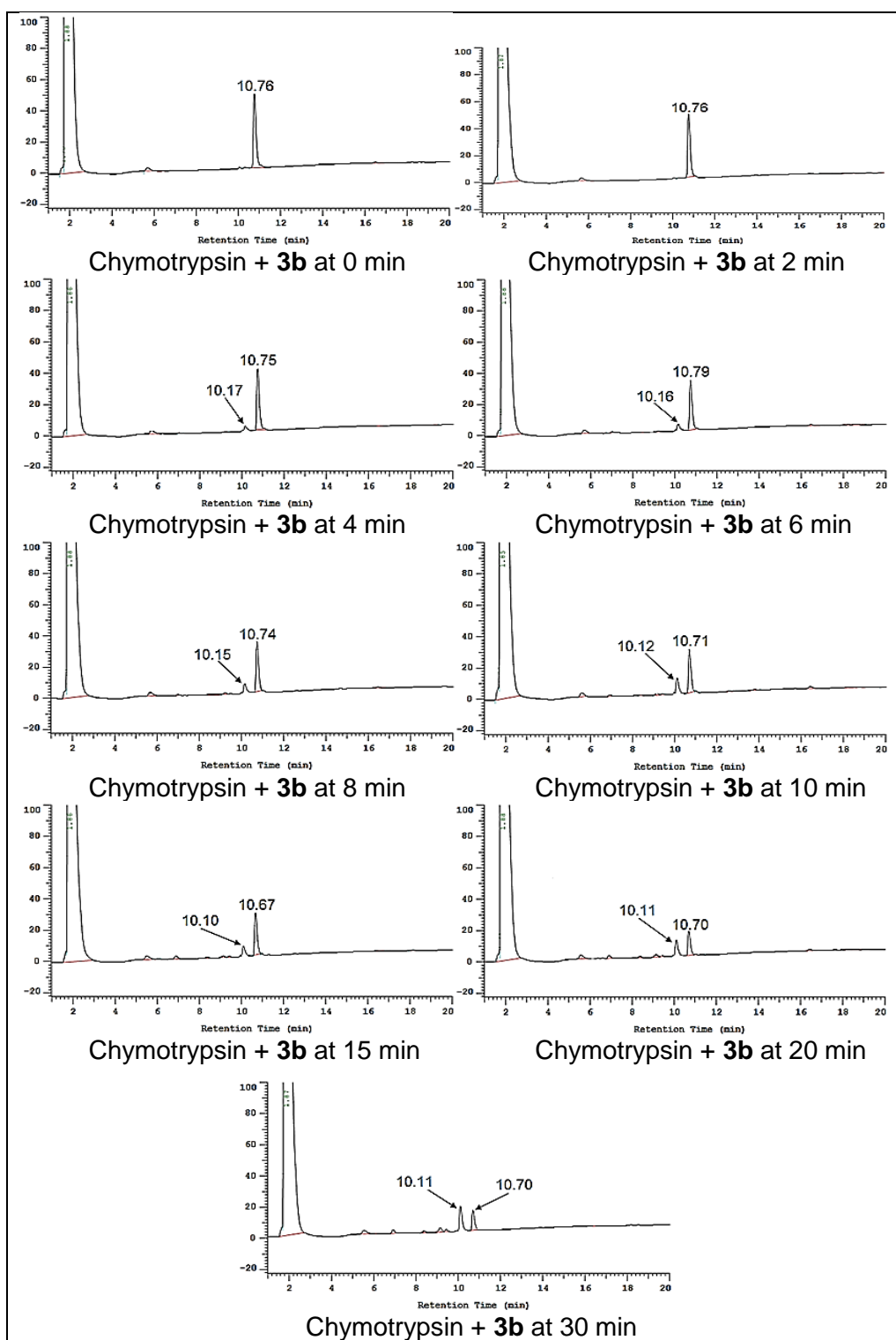
7	 <p><math>b_7</math> (<math>m/z = 803.4</math>)</p> <p>Cleavage of the peptide bond between L and D in <b>2c2</b> (loss of the fragment of DFLR).</p>
8	 <p><math>b_7-H_2O</math> (<math>m/z = 785.4</math>)</p> <p>1) Cleavage of the peptide bond between L and D in <b>2c2</b> (loss of the fragment of DFLR). 2) Loss of H<sub>2</sub>O molecule from one of the two T residues.</p>
9	 <p><math>y_6</math> (<math>m/z = 764.4</math>)</p> <p>Cleavage of the peptide bond between W and T in <b>2c2</b> (loss of the fragment of TIMGW).</p>



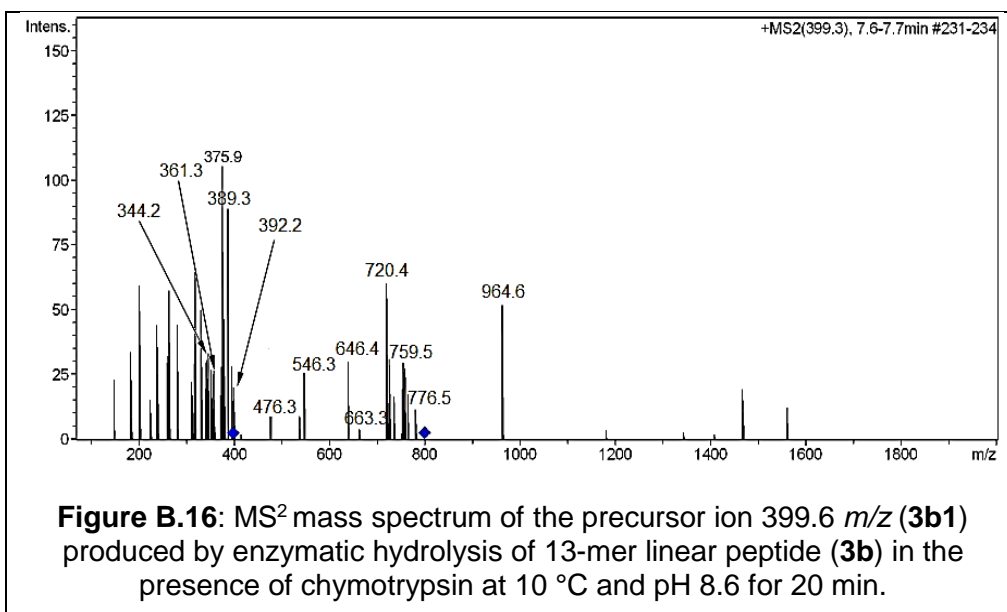
**Figure B.13:** MS<sup>2</sup> mass spectrum of the precursor ion 247.0 *m/z* produced by enzymatic hydrolysis of 15-mer cyclic peptide (**2c**) in the presence of trypsin at 10 °C and pH 8.6 for 20 min.



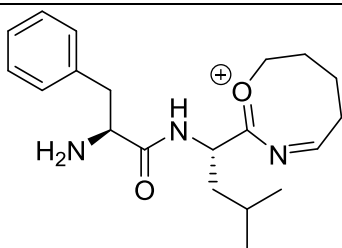
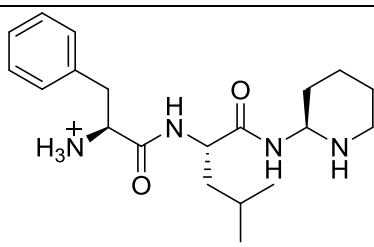
**Figure B.14:** MS<sup>2</sup> mass spectrum of the precursor ion 622 *m/z* produced by enzymatic hydrolysis of 15-mer cyclic peptide (**2c**) in the presence of trypsin at 10 °C and pH 8.6 for 10 min.

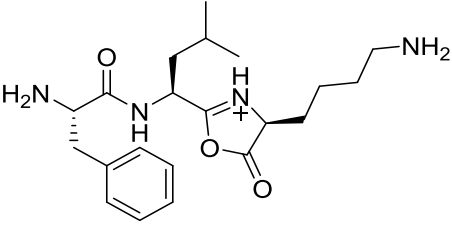
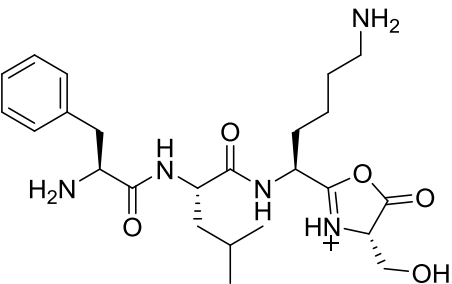
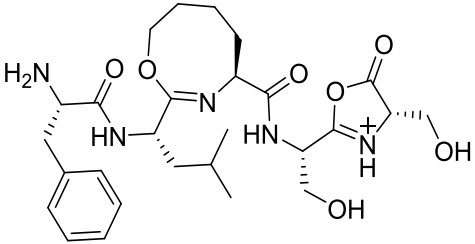
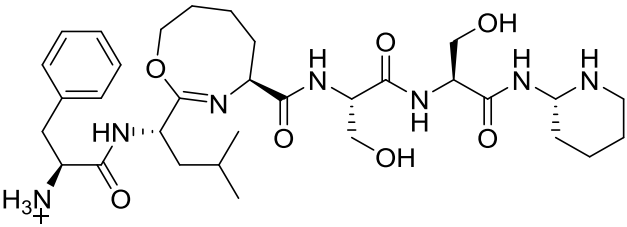


**Figure B.15:** HPLC chromatograms of the reaction between 25  $\mu\text{L}$  of chymotrypsin (1.06  $\mu\text{M}$ ) and 250  $\mu\text{L}$  of **3b** (200  $\mu\text{M}$ ) at 10  $^{\circ}\text{C}$  and pH 8.6 over 0, 2, 4, 6, 8, 10, 15, 20, 30 min.

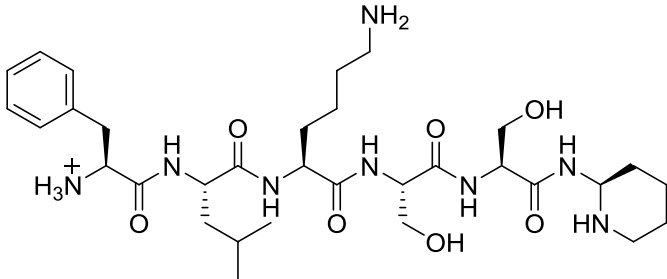
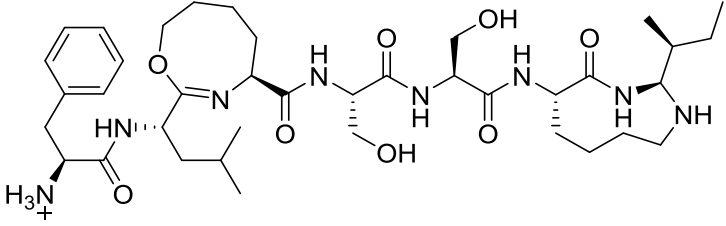
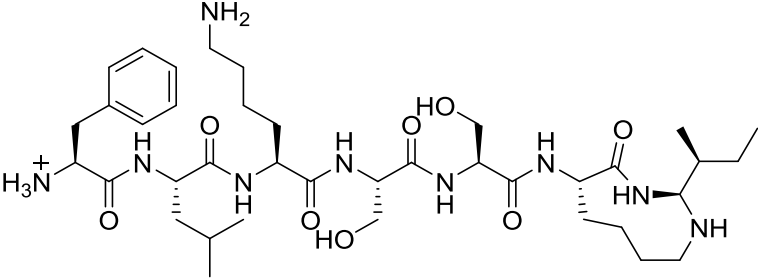
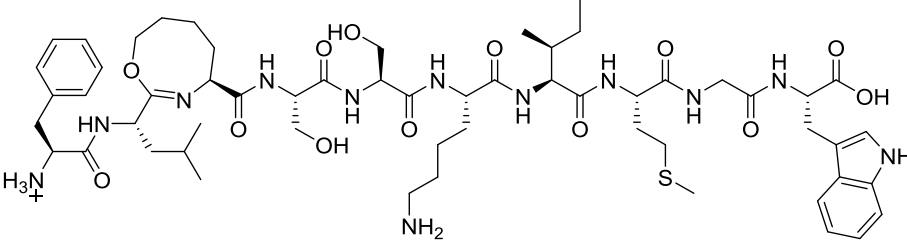


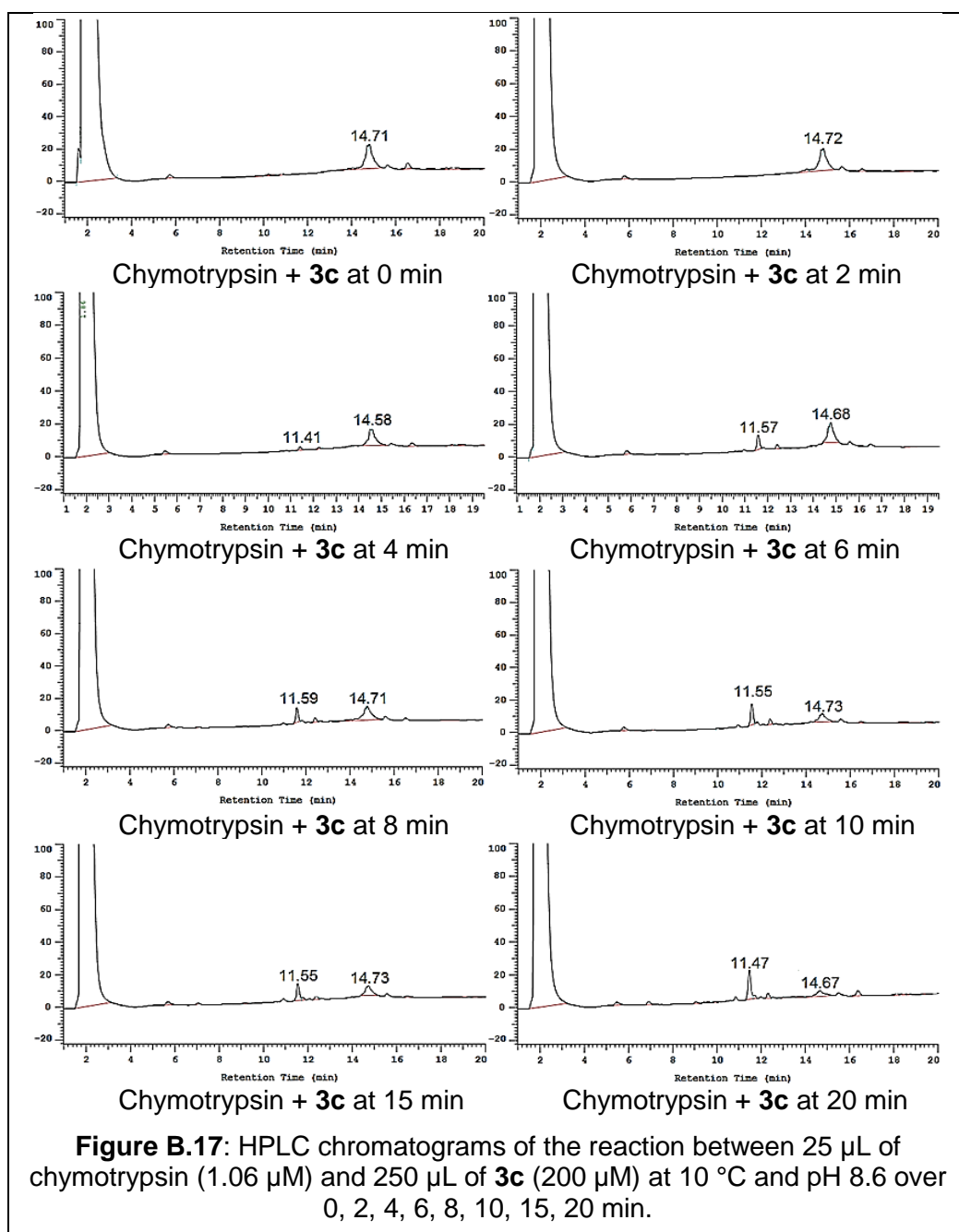
**Table B.8:** Suggested structures for observed peaks (fragments) in the MS<sup>2</sup> mass spectrum of precursor ion 399.6 *m/z* (**3b1**) produced by enzymatic hydrolysis of 13-mer linear peptide (**3b**) in the presence of chymotrypsin at 10 °C and pH 8.6 for 20 min.

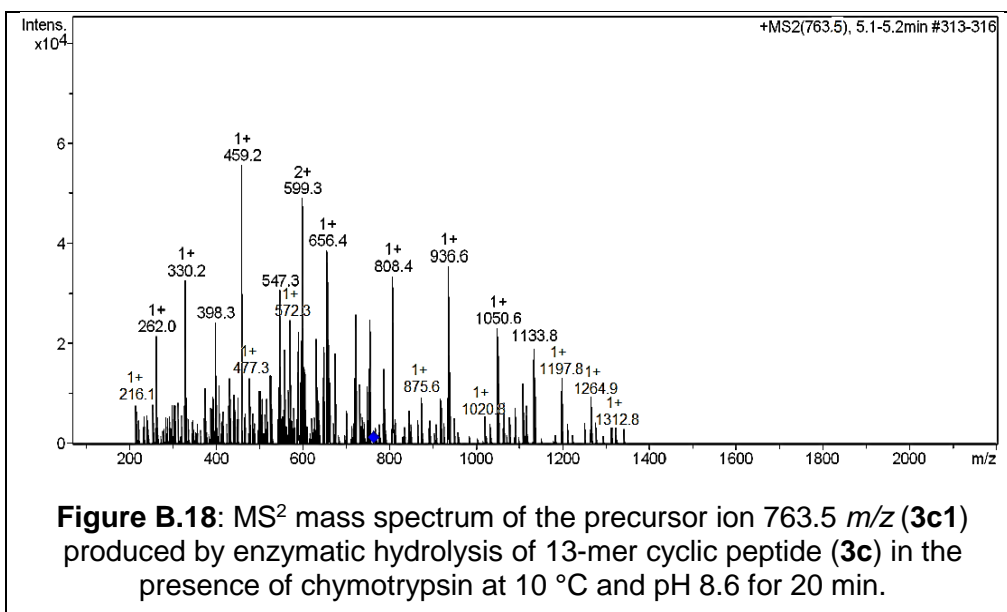
No	Structure of the fragment and site of the cleaved peptide bond in <b>3b1</b> (F-L-K-S-S-K-I-M-G-W)
1	 <p><math>a_3\text{-NH}_3</math> (<i>m/z</i> = 344.2)</p> <p>1) Cleavage of the peptide bond between K and S in <b>3b1</b> (loss of the fragment of SKIMGW). 2) Loss of NH<sub>2</sub> molecule from S.</p>
2	 <p><math>a_3</math> (<i>m/z</i> = 361.3)</p> <p>Cleavage of the peptide bond between K and S in <b>3b1</b> (loss of the fragment of SSKIMGW).</p>

3	 <p><math>b_3</math> (<math>m/z = 389.3</math>)</p> <p>Cleavage of the peptide bond between K and S in <b>3b1</b> (loss of the fragment of SSKIMGW).</p>
4	 <p><math>b_4</math> (<math>m/z = 476.3</math>)</p> <p>Cleavage of the peptide bond between S and S in <b>3b1</b> (loss of the fragment of SKIMGW).</p>
5	 <p><math>b_5\text{-NH}_3</math> (<math>m/z = 546.3</math>)</p> <p>1) Cleavage of the peptide bond between S and K in <b>3b1</b> (loss of the fragment of KIMGW). 2) Loss of <math>\text{NH}_3</math> molecule from K.</p>
6	 <p><math>a_6\text{-NH}_3</math> (<math>m/z = 646.4</math>)</p> <p>1) Cleavage of the peptide bond between K and I in <b>3b1</b> (loss of the fragment of IMGW). 2) Loss of <math>\text{NH}_3</math> molecule from one of the two K residues.</p>



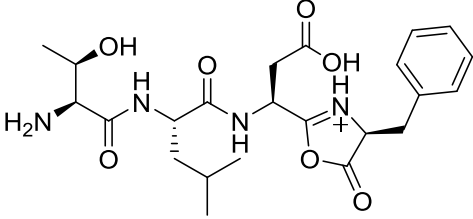
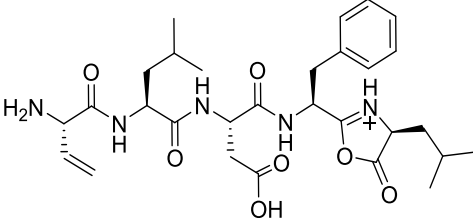
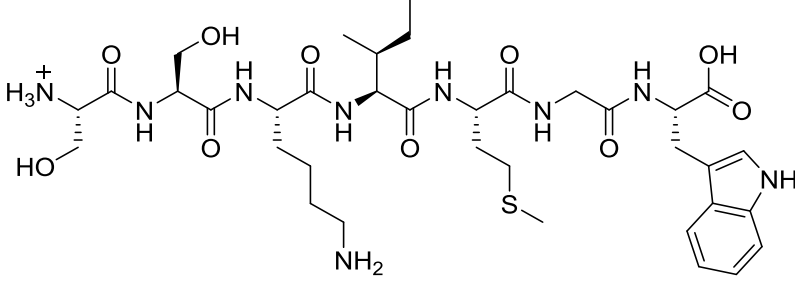
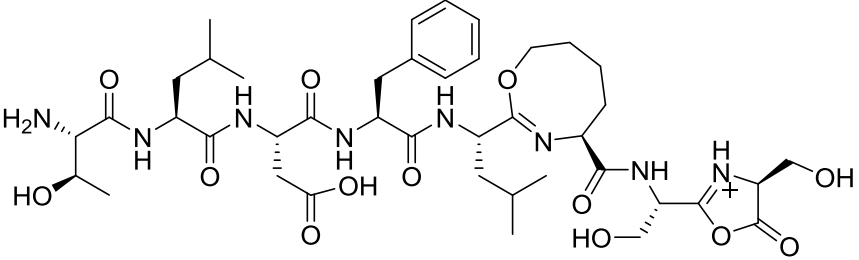
7	 <p><math>a_6</math> (<math>m/z = 663.4</math>)</p> <p>Cleavage of the peptide bond between K and I in <b>3b1</b> (loss of the fragment of IMGW).</p>
8	 <p><math>a_7\text{-NH}_3</math> (<math>m/z = 759.5</math>)</p> <p>1) Cleavage of the peptide bond between I and M in <b>3b1</b> (loss of the fragment of MGW). 2) Loss of <math>\text{NH}_3</math> molecule from one of the two K residues.</p>
9	 <p><math>a_7</math> (<math>m/z = 776.5</math>)</p> <p>Cleavage of the peptide bond between I and M in <b>3b1</b> (loss of the fragment of MGW).</p>
10	 <p><math>\text{MH-NH}_3</math> (<math>m/z = 1179.6</math>)</p> <p>Loss of <math>\text{NH}_3</math> molecule from one of the two K residues in <b>3b1</b>.</p>

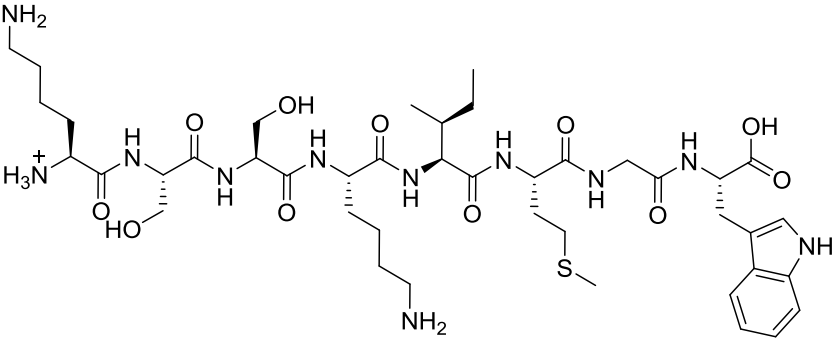
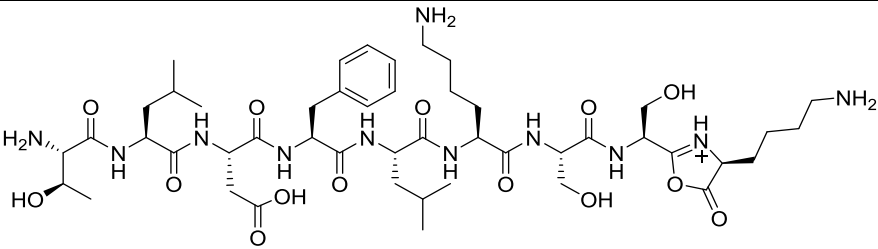
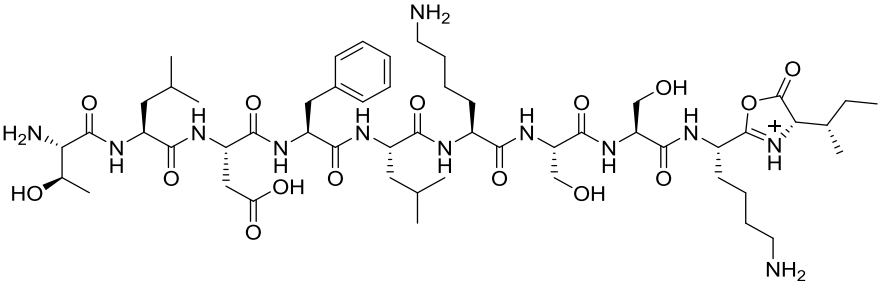
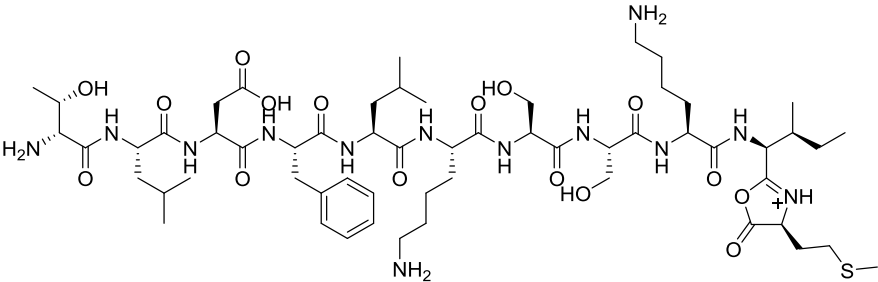


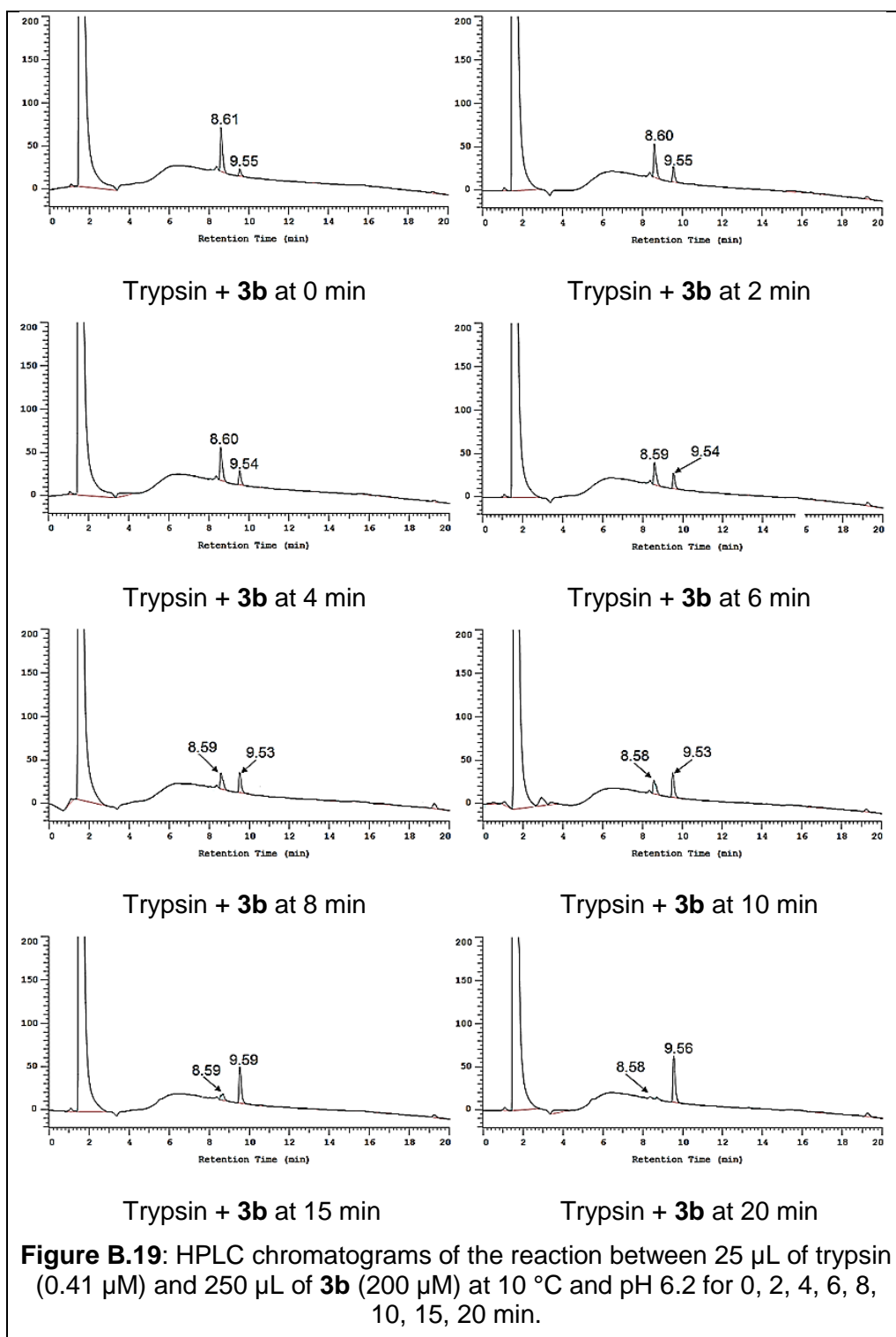


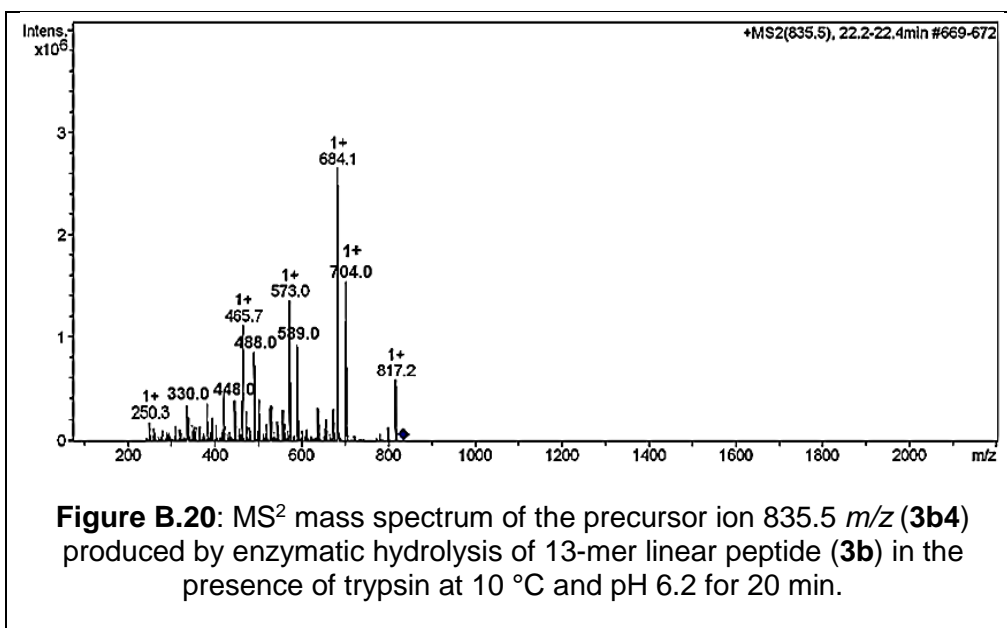
**Table B.9:** Suggested structures for observed peaks (fragments) in the MS<sup>2</sup> mass spectrum of precursor ion 763.5 *m/z* (**3c1**) produced by enzymatic hydrolysis of 13-mer cyclic peptide (**3c**) in the presence of chymotrypsin at 10 °C and pH 8.6 for 20 min.

No	Structure of the fragment and site of the cleaved peptide bond in peptide <b>3c1</b> (T-L-D-F-L-K-S-S-K-I-M-G-W)
1	<p><math>y_2</math> (<math>m/z = 262.1</math>)</p> <p>Cleavage of the peptide bond between M and G in <b>3c1</b> (loss of the fragment of TLDFLKSSKIM).</p>
2	<p><math>b_3</math> (<math>m/z = 330.2</math>)</p> <p>Cleavage of the peptide bond between D and F in <b>3c1</b> (loss of the fragment FLKSSKIMGW).</p>

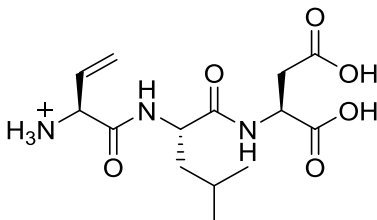
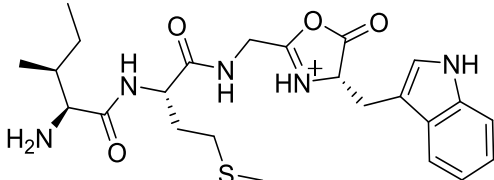
3	 <p style="text-align: center;"><math>b_4</math> (<math>m/z = 477.2</math>)</p> <p>Cleavage of the peptide bond between F and L in <b>3c1</b> (loss of the fragment of LKSSKIMGW).</p>
4	 <p style="text-align: center;"><math>b_5-H_2O</math> (<math>m/z = 572.3</math>)</p> <p>1) Cleavage of the peptide bond between L and K in <b>3c1</b> (loss of the fragment of KSSKIMGW). 2) Loss of H<sub>2</sub>O molecule from T.</p>
5	 <p style="text-align: center;"><math>y_7</math> (<math>m/z = 808.4</math>)</p> <p>Cleavage of the peptide bond between K and S in <b>3c1</b> (loss of the fragment of TLDFLK).</p>
6	 <p style="text-align: center;"><math>b_8-NH_3</math> (<math>m/z = 875.5</math>)</p> <p>1) Cleavage of the peptide bond between S and K in <b>3c1</b> (loss of the fragment of KIMGW). 2) Loss of NH<sub>3</sub> molecule from K.</p>

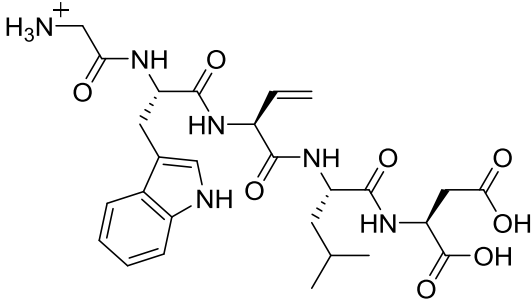
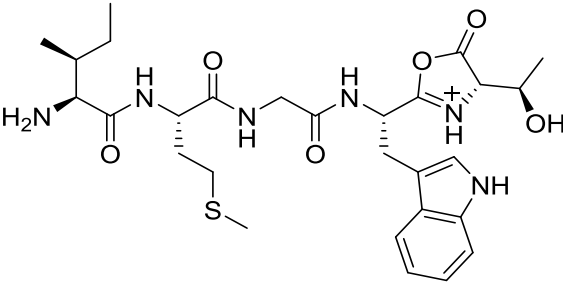
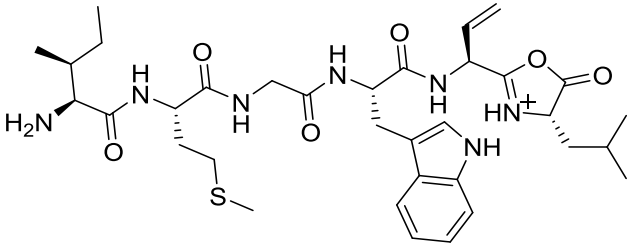
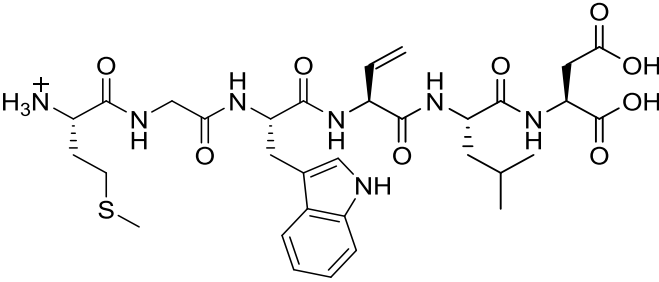
7	 <p><math>y_8</math> (<math>m/z = 936.5</math>)</p> <p>Cleavage of the peptide bond between L and K in <b>3c1</b> (loss of the fragment of TLDLFL).</p>
8	 <p><math>b_9</math> (<math>m/z = 1020.6</math>)</p> <p>Cleavage of the peptide bond between K and I in <b>3c1</b> (loss of the fragment of IMGW).</p>
9	 <p><math>b_{10}</math> (<math>m/z = 1133.7</math>)</p> <p>Cleavage of the peptide bond between I and M in <b>3c1</b> (loss of the fragment of MGW).</p>
10	 <p><math>b_{11}</math> (<math>m/z = 1264.7</math>)</p> <p>Cleavage of the peptide bond between M and G in <b>3c1</b> (loss of the fragment of GW).</p>



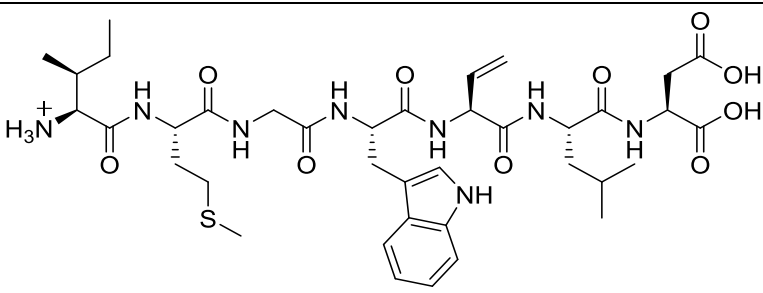


**Table B.10:** Suggested structures for observed peaks (fragments) in the MS<sup>2</sup> mass spectrum of precursor ion 835.5 *m/z* (**3b4**) produced by enzymatic hydrolysis of 13-mer linear peptide (**3b**) in the presence of trypsin at 10 °C and pH 6.2 for 20 min.

No	Structure of the fragment and site of the cleaved peptide bond in <b>3b4</b> (I-M-G-W-T-L-D)
1	 <p><math>y_3\text{-H}_2\text{O}</math> (<math>m/z = 330.2</math>)</p> <p>1) Cleavage of the peptide bond between W and T in <b>3b4</b> (loss of the fragment of IMGW). 2) Loss of H<sub>2</sub>O molecule from T.</p>
2	 <p><math>b_4</math> (<math>m/z = 488.2</math>)</p> <p>Cleavage of the peptide bond between W and T in <b>3b4</b> (loss of the fragment of TLD).</p>

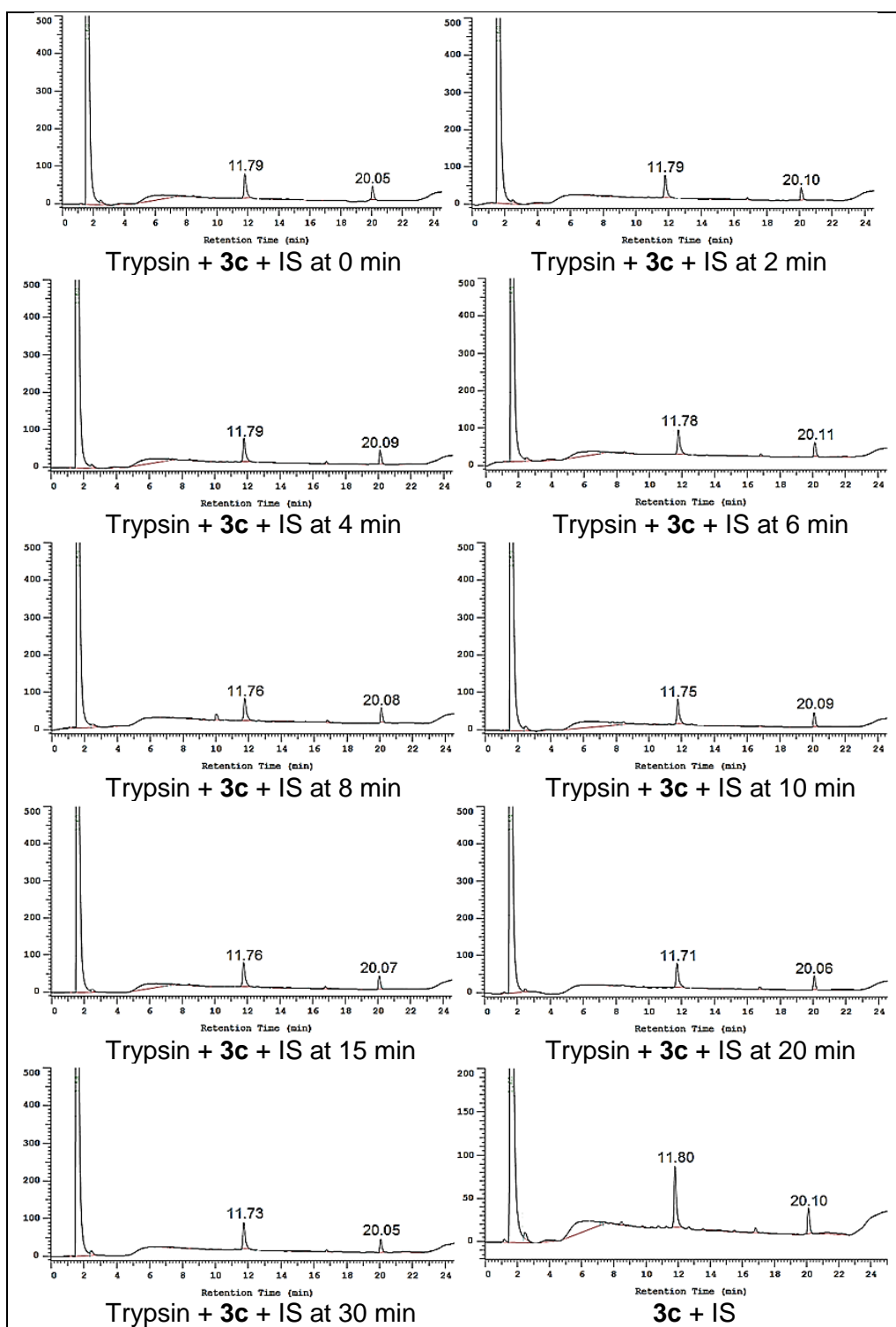
3	 <p><math>y_5\text{-H}_2\text{O}</math> (<math>m/z = 573.3</math>)</p> <p>1) Cleavage of the peptide bond between M and G in <b>3b4</b> (loss of the fragment of IM). 2) Loss of H<sub>2</sub>O molecule from T.</p>
4	 <p><math>b_5</math> (<math>m/z = 589.3</math>)</p> <p>1) Cleavage of the peptide bond between T and L in <b>3b4</b> (loss of the fragment of LD).</p>
5	 <p><math>b_6\text{-H}_2\text{O}</math> (<math>m/z = 684.4</math>)</p> <p>1) Cleavage of the peptide bond between L and D in <b>3b4</b> (loss of D residue). 2) Loss of H<sub>2</sub>O molecule from T.</p>
6	 <p><math>y_6\text{-H}_2\text{O}</math> (<math>m/z = 704.3</math>)</p> <p>1) Cleavage of the peptide bond between I and M in <b>3b4</b> (loss of I residue). 2) Loss of H<sub>2</sub>O molecule from T.</p>



7	 <p style="text-align: center;">MH-H<sub>2</sub>O (<math>m/z</math> = 817.4) Loss of H<sub>2</sub>O molecule from T in <b>3b4</b>.</p>
---	--

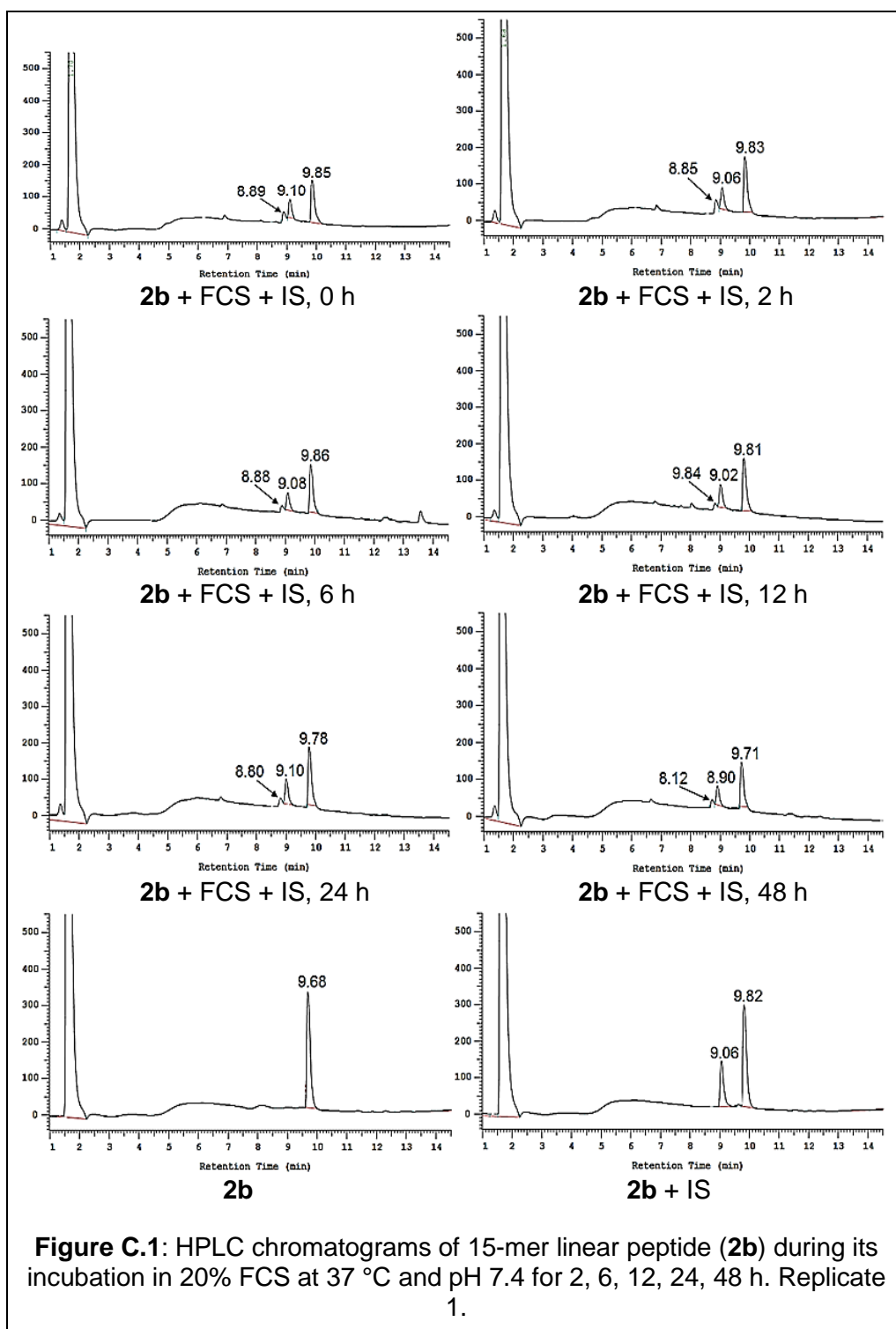
**Table B.11:** Expected mass of the peptides ( $m/z$ ) produced by enzymatic hydrolysis of **3b3** which one of the two peptides was produced by enzymatic hydrolysis of 13-mer linear peptide (**3b**) in the presence of trypsin.

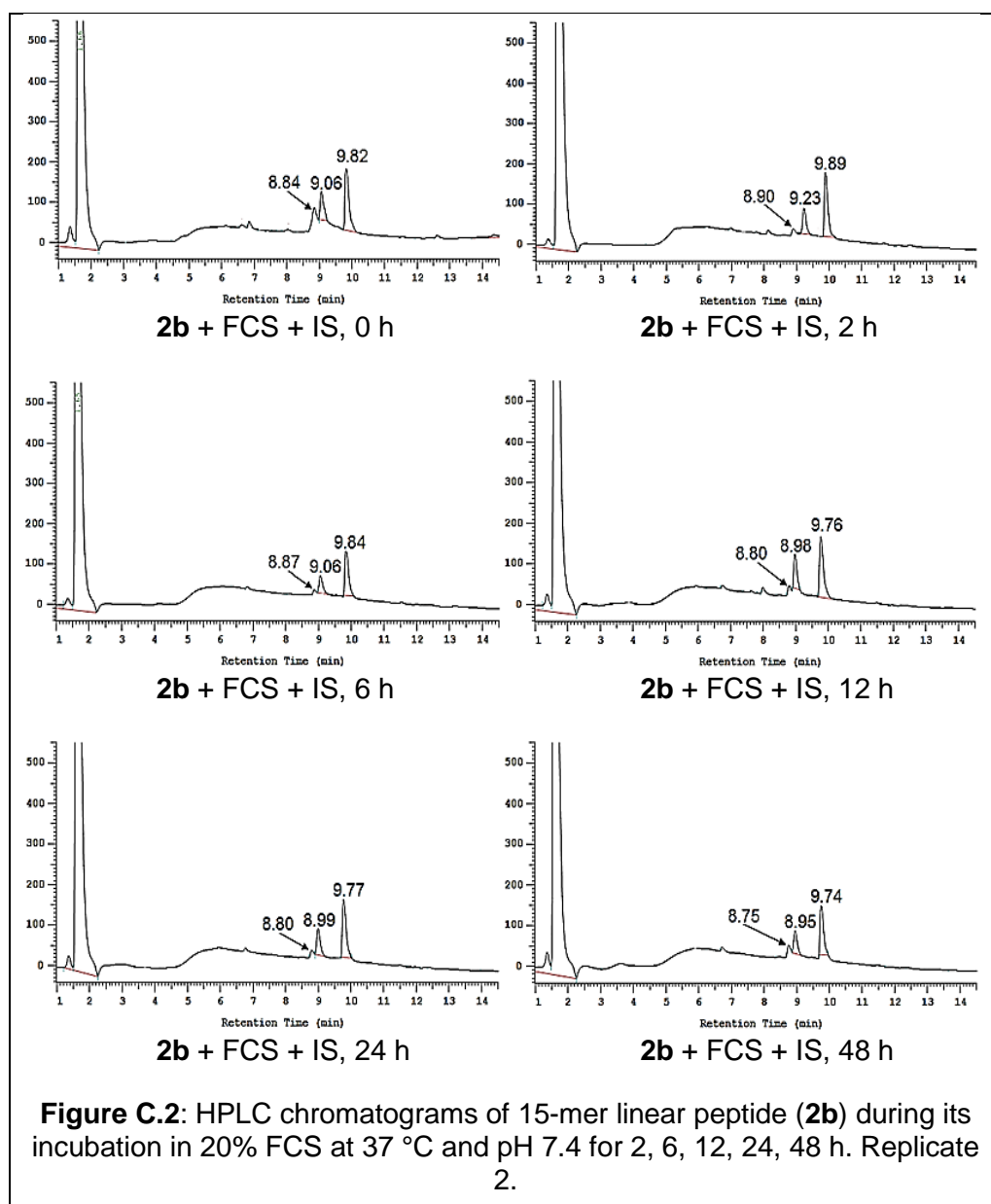
F-L-K-S-S-K		
No	Sequence	Expected $m/z$
1	F-L-K-S-S-K	(709.4) <sup>1+</sup> , (355.2) <sup>2+</sup> , (237.1) <sup>3+</sup>
2	F-L-K	(407.3) <sup>1+</sup> , (204.1) <sup>1+</sup>
3	S-S-K	(321.2) <sup>1+</sup> , (161.1) <sup>2+</sup>

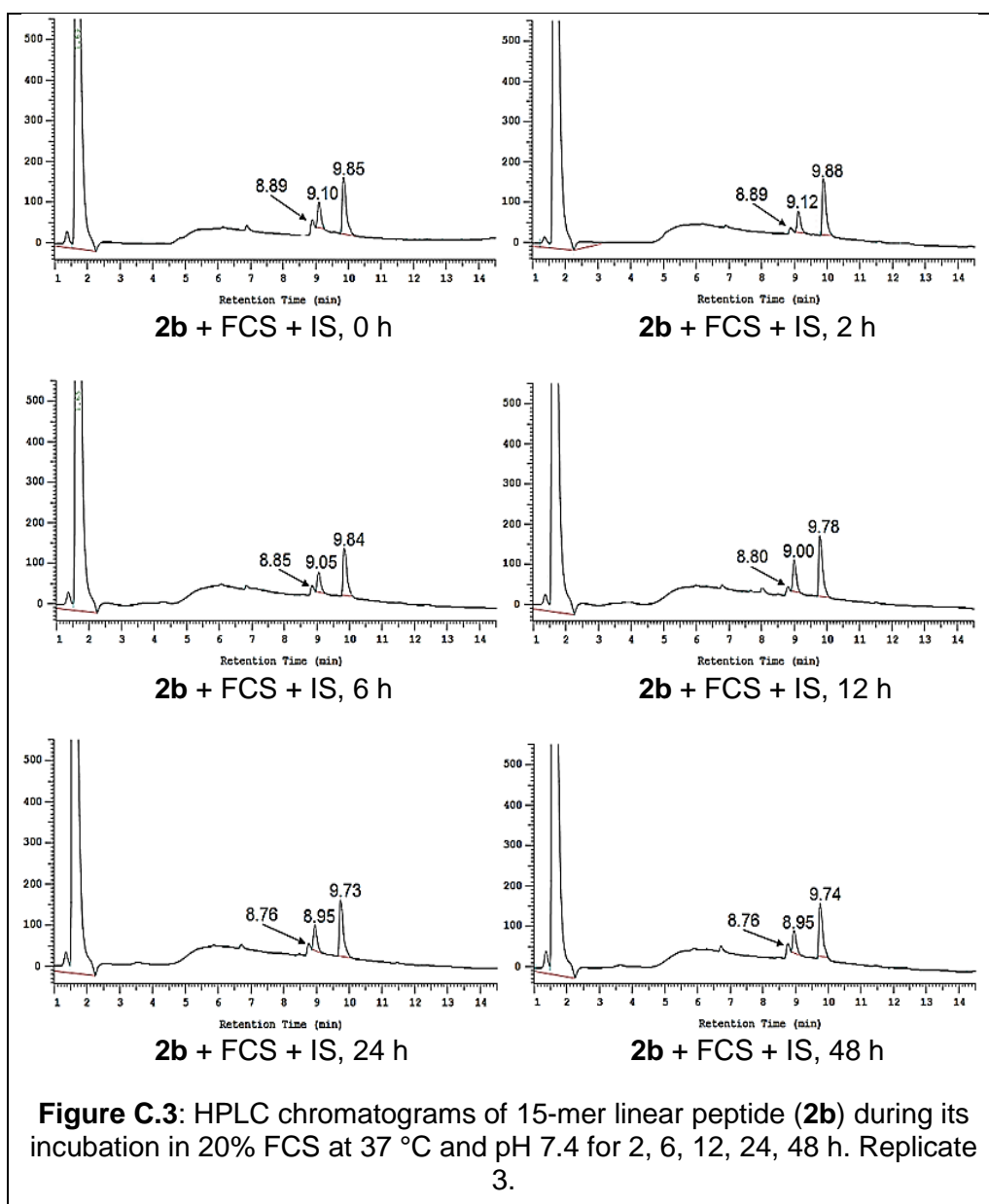


**Figure B.21:** HPLC chromatograms of the reaction between 25  $\mu\text{L}$  of trypsin (0.41  $\mu\text{M}$ ) and 250  $\mu\text{L}$  of **3c** (200  $\mu\text{M}$ ) over 0, 2, 4, 6, 8, 10, 15, 20, 30 min at 10  $^{\circ}\text{C}$  and pH 6.2.

## 10 Appendix C

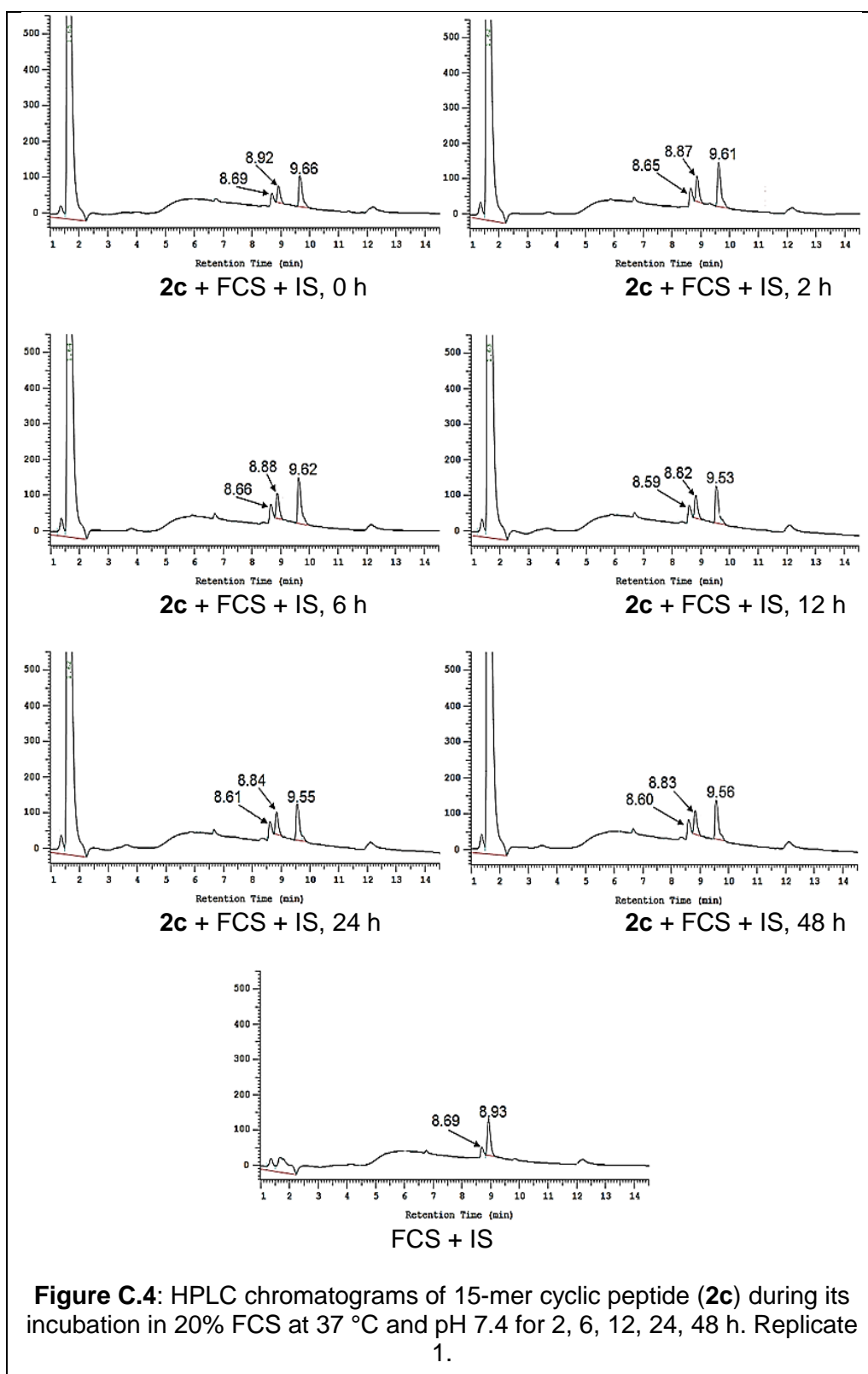


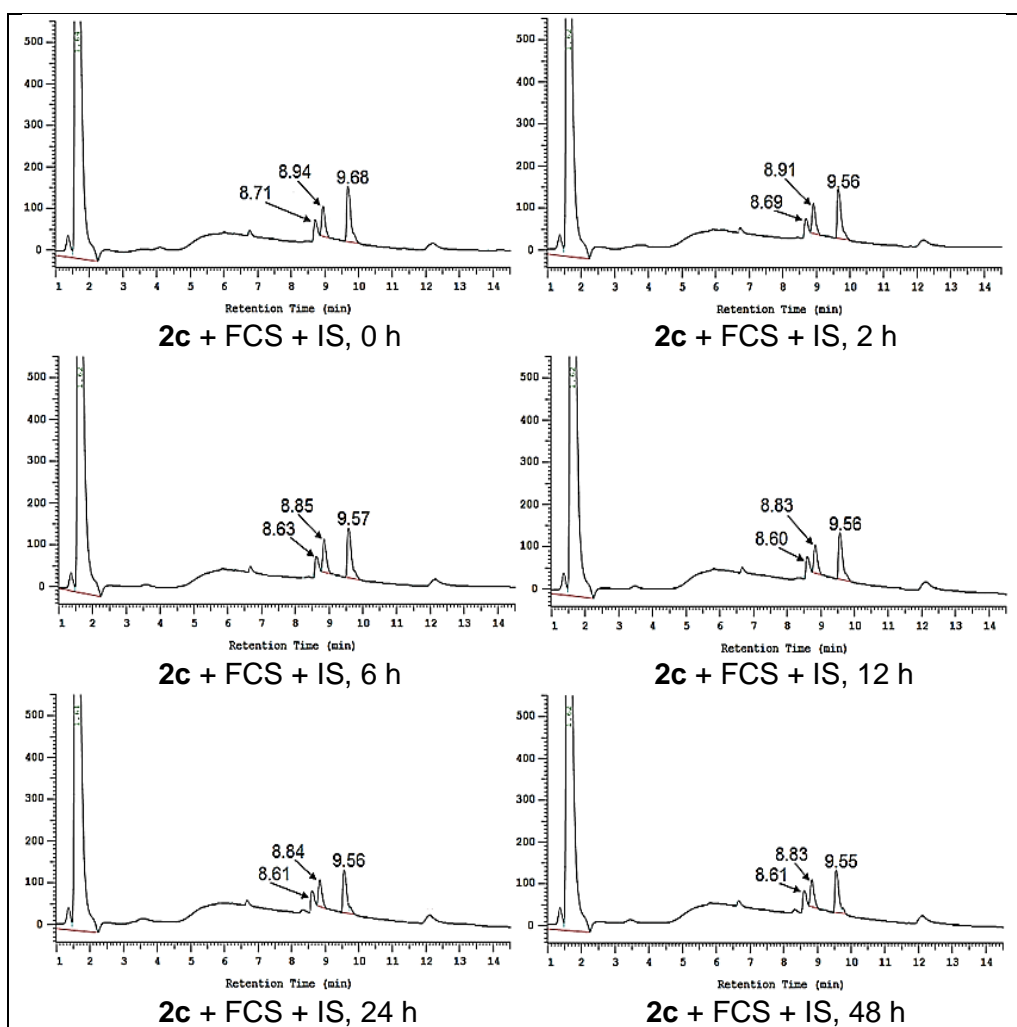




**Table C.1:** Areas of HPLC peaks for 15-mer linear peptide (**2b**) during its incubation in 20% FCS over 0, 2, 6, 12, 24, 48 h, in addition to areas of internal standard peaks (IS). Three replicates.

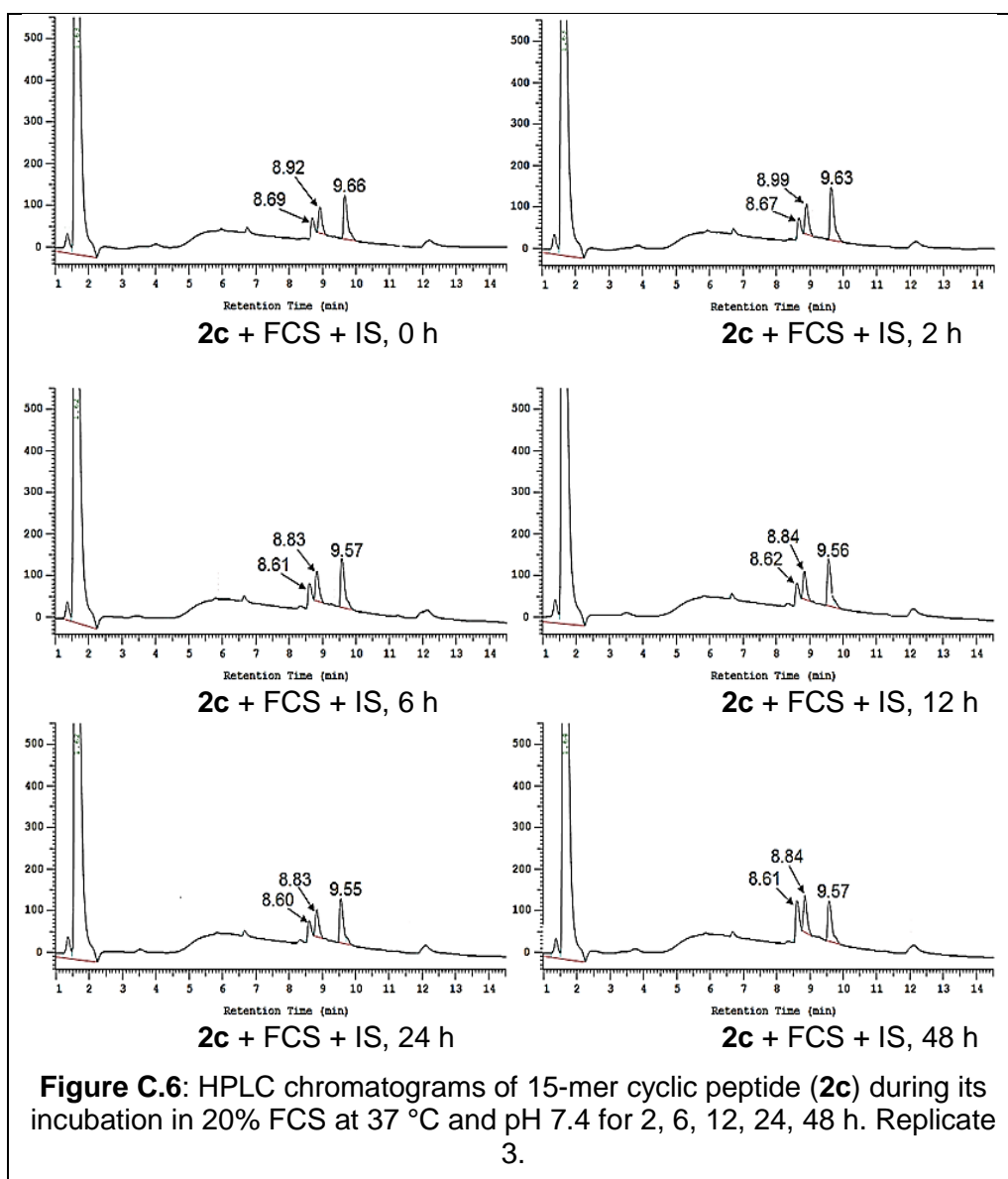
Time (h)	0	2	6	12	24	48
1- <b>2b</b> area	1060353	1152794	921894	1096403	1144630	824034
2- <b>2b</b> area	1216151	1076991	786427	1174472	1044862	811560
3- <b>2b</b> area	1091345	1010859	857342	1157014	1053747	829166
1-IS area	337382	391568	323417	418947	460375	332907
2-IS area	463892	412304	304971	490114	442073	371319
3-IS area	387259	355134	320334	501109	408962	371213





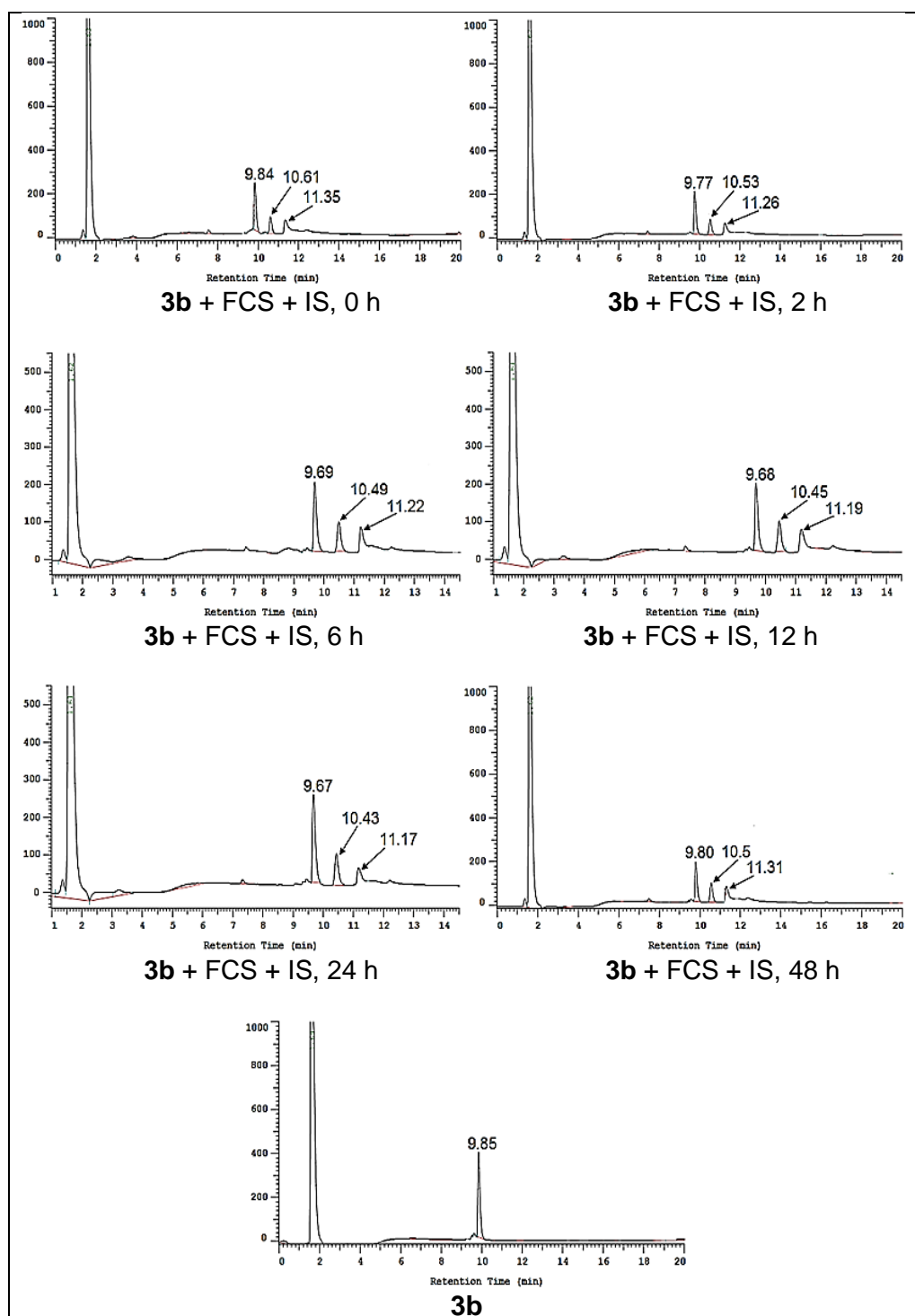
**Figure C.5:** HPLC chromatograms of 15-mer cyclic peptide (**2c**) during its incubation in 20% FCS at 37 °C and pH 7.4 for 2, 6, 12, 24, 48 h. Replicate 2.



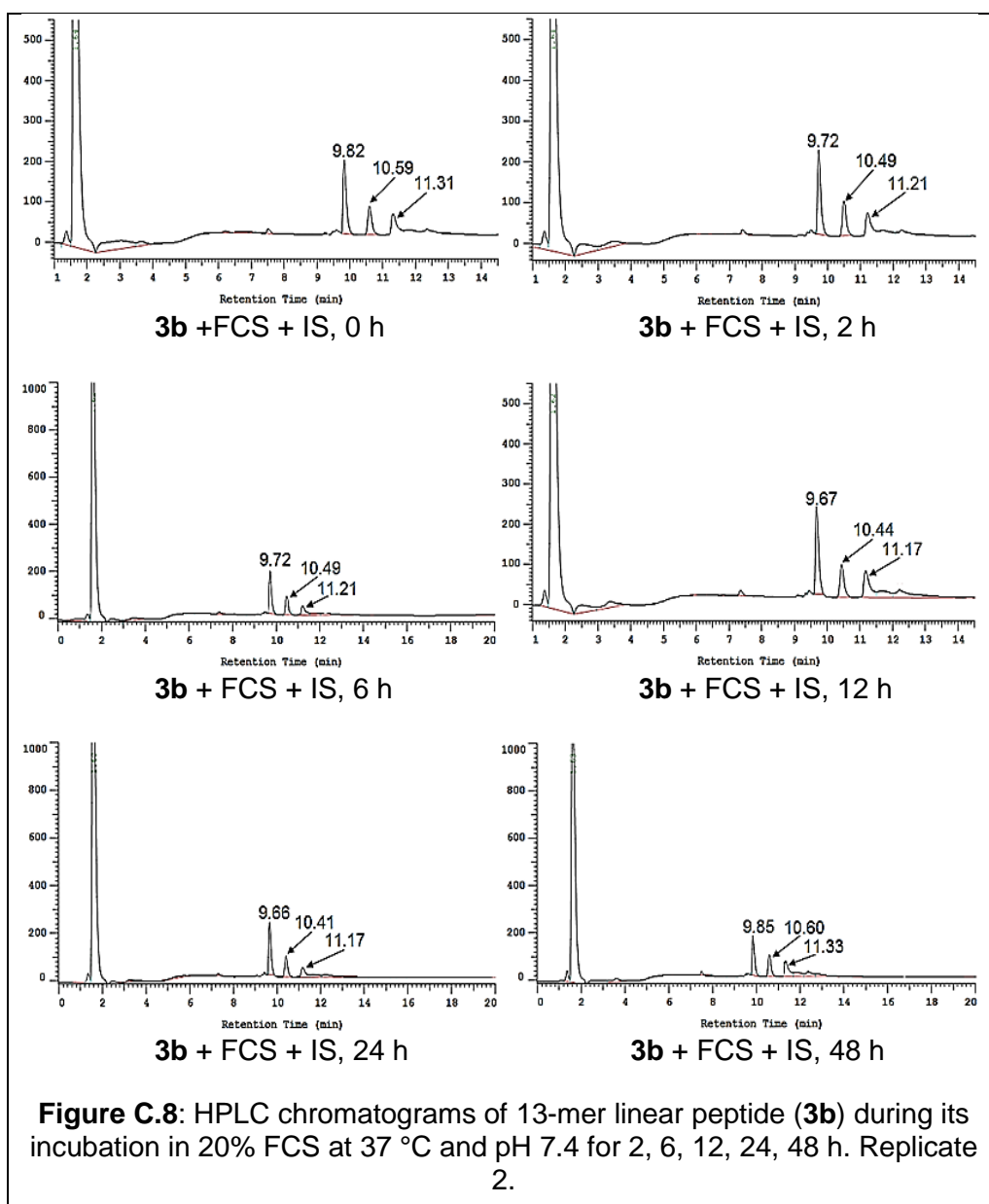


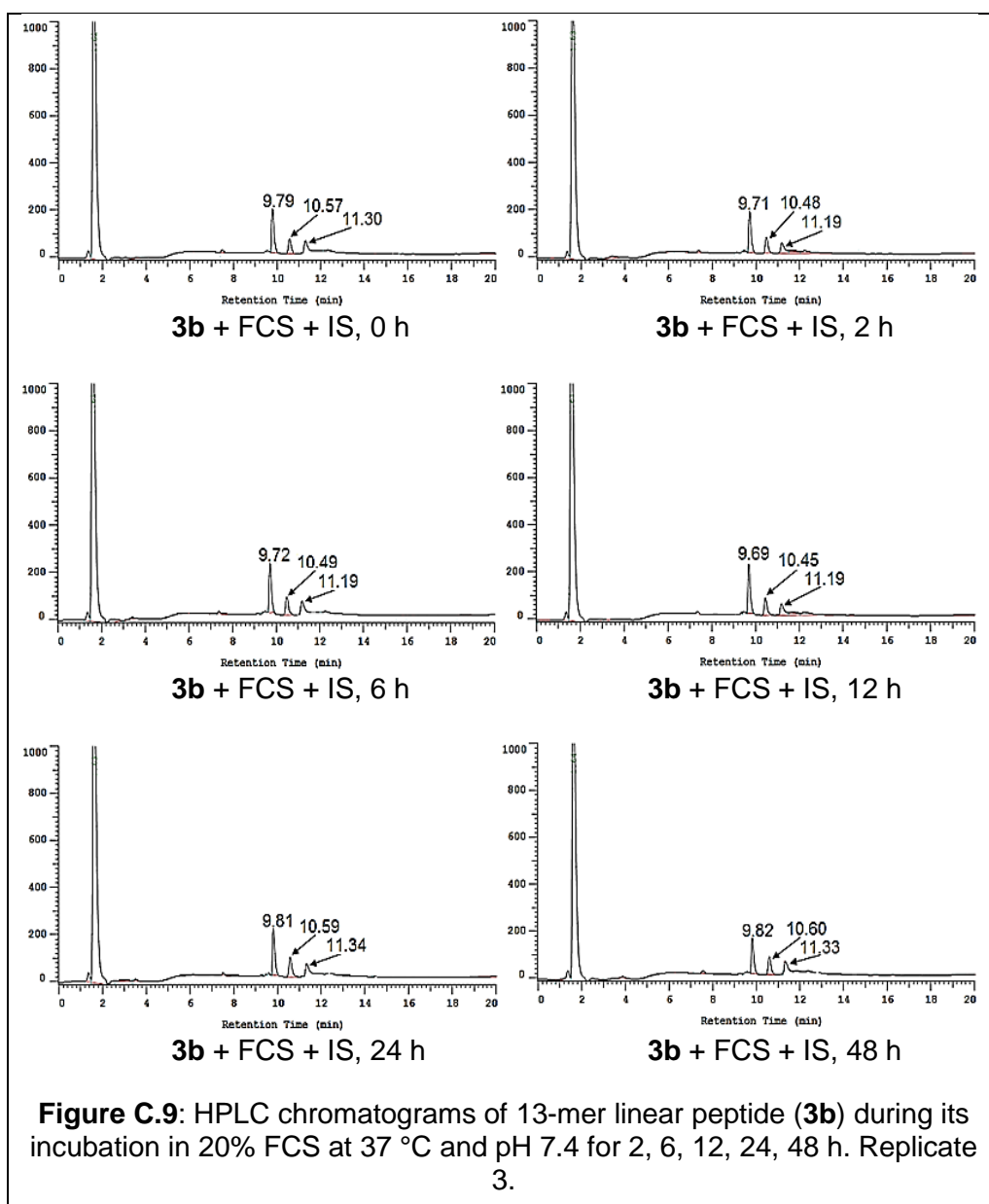
**Table C.2:** Areas of HPLC peaks for 15-mer cyclic peptide (**2c**) during its incubation in 20% FCS over 0, 2, 6, 12, 24, 48 h, in addition to areas of internal standard peaks (IS). Three replicates.

Time (h)	0	2	6	12	24	48
1- <b>2c</b> area	676318	945920	1012279	740087	710622	795148
2- <b>2c</b> area	103559	909394	954278	859237	709379	682021
3- <b>2c</b> area	796171	1001370	917499	797369	730446	778714
1-IS area	300203	466554	463299	417952	401657	445004
2-IS area	466436	455357	503516	439796	425282	429319
3-IS area	380832	474202	468205	440702	431867	544811



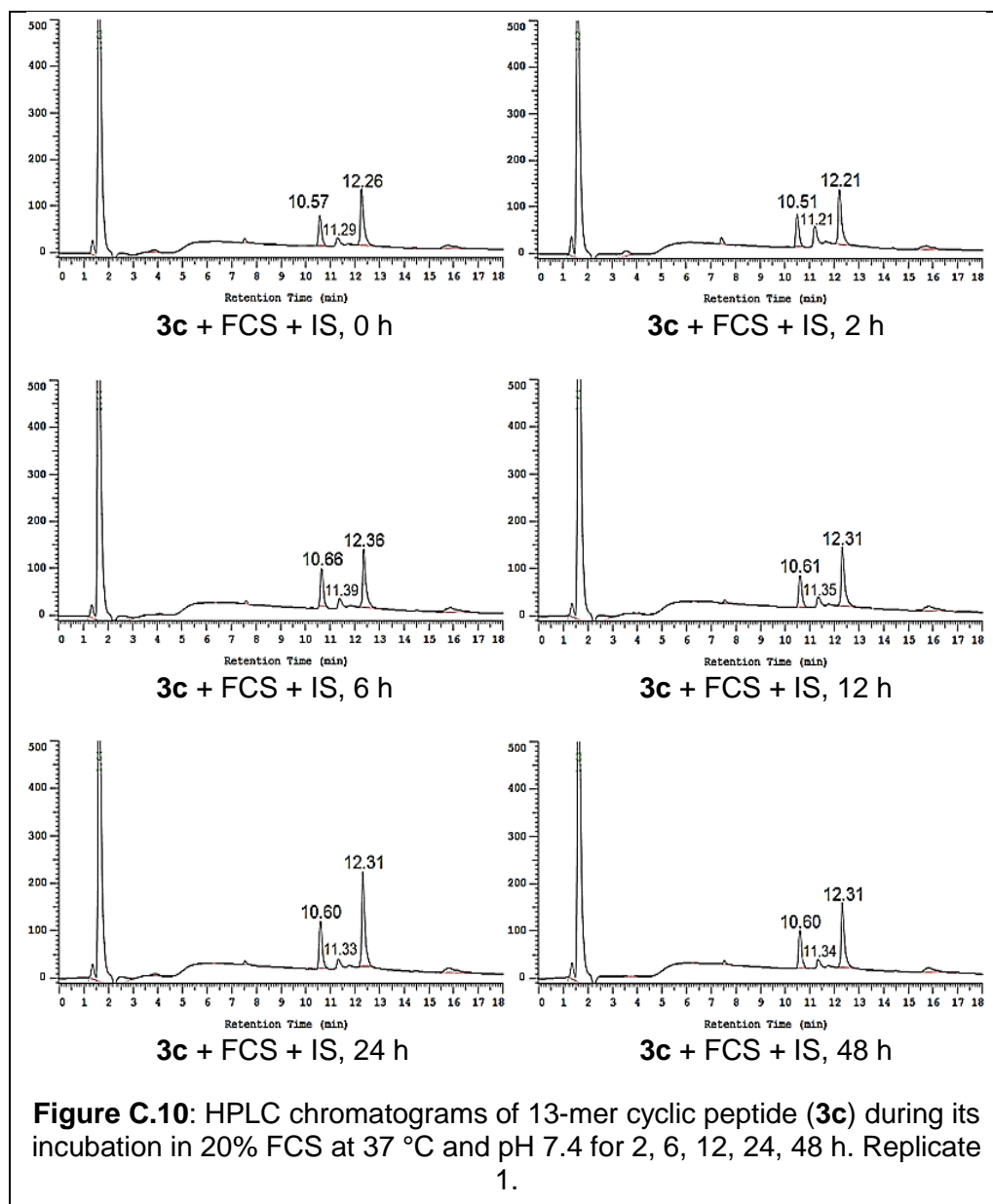
**Figure C.7:** HPLC chromatograms of 13-mer linear peptide (**3b**) during its incubation in 20% FCS at 37 °C and pH 7.4 for 2, 6, 12, 24, 48 h. Replicate 1.

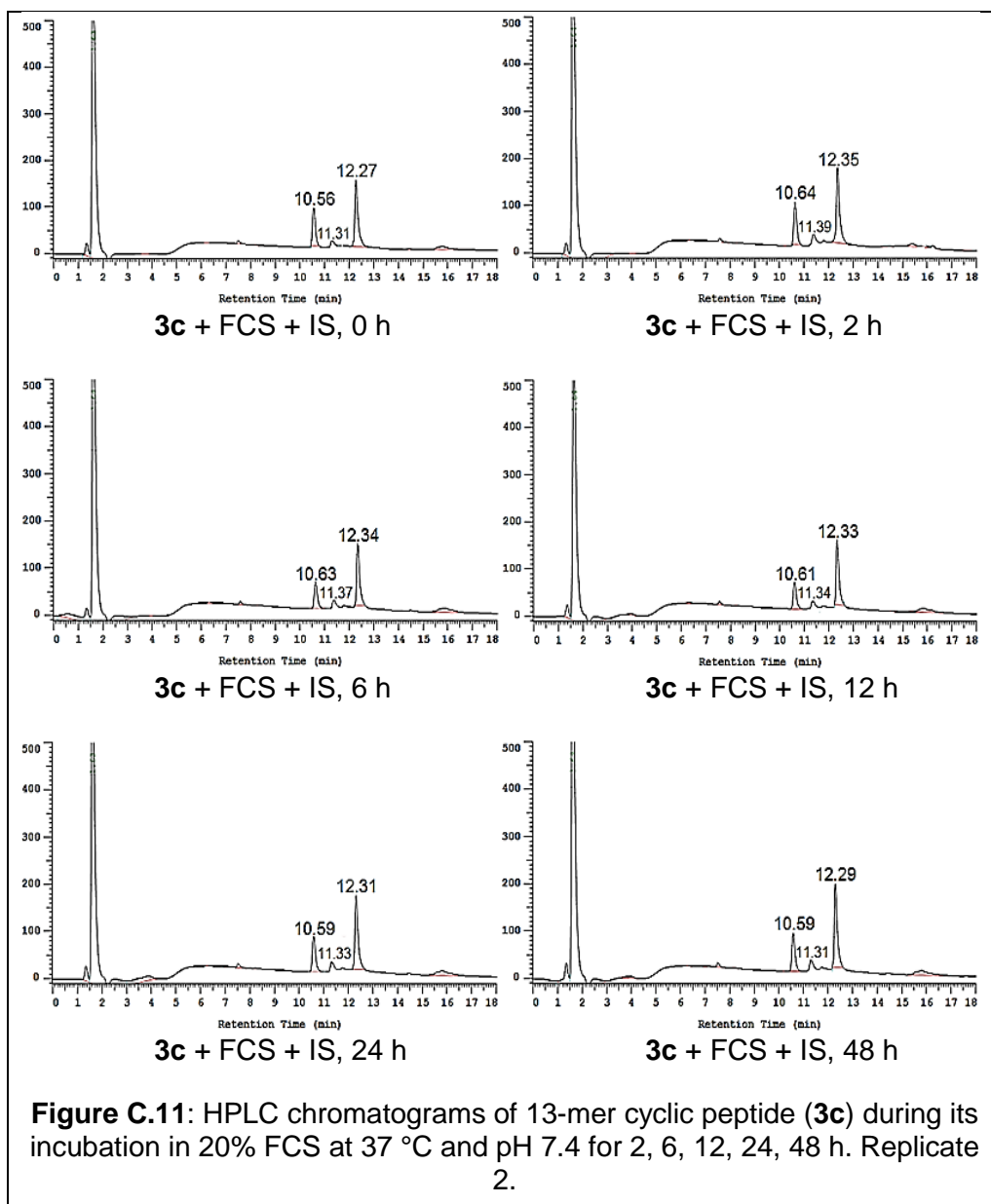




**Table C.3:** Areas of HPLC peaks for 13-mer linear peptide (**3b**) during its incubation in 20% FCS for 0, 2, 6, 12, 24, 48 h, in addition to areas of internal standard peaks (IS). Three replicates.

Time(h)	0	2	6	12	24	48
1- <b>3b</b> area	126132	119566	115087	113814	141978	114460
2- <b>3b</b> area	110195	125733	113038	133019	137947	105792
3- <b>3b</b> area	114453	108317	126577	128848	124263	950324
1-IS area	585737	574695	582656	617520	708190	733461
2-IS area	541253	640569	607461	674307	735035	711365
3-IS area	498432	514838	616992	595893	679315	622519







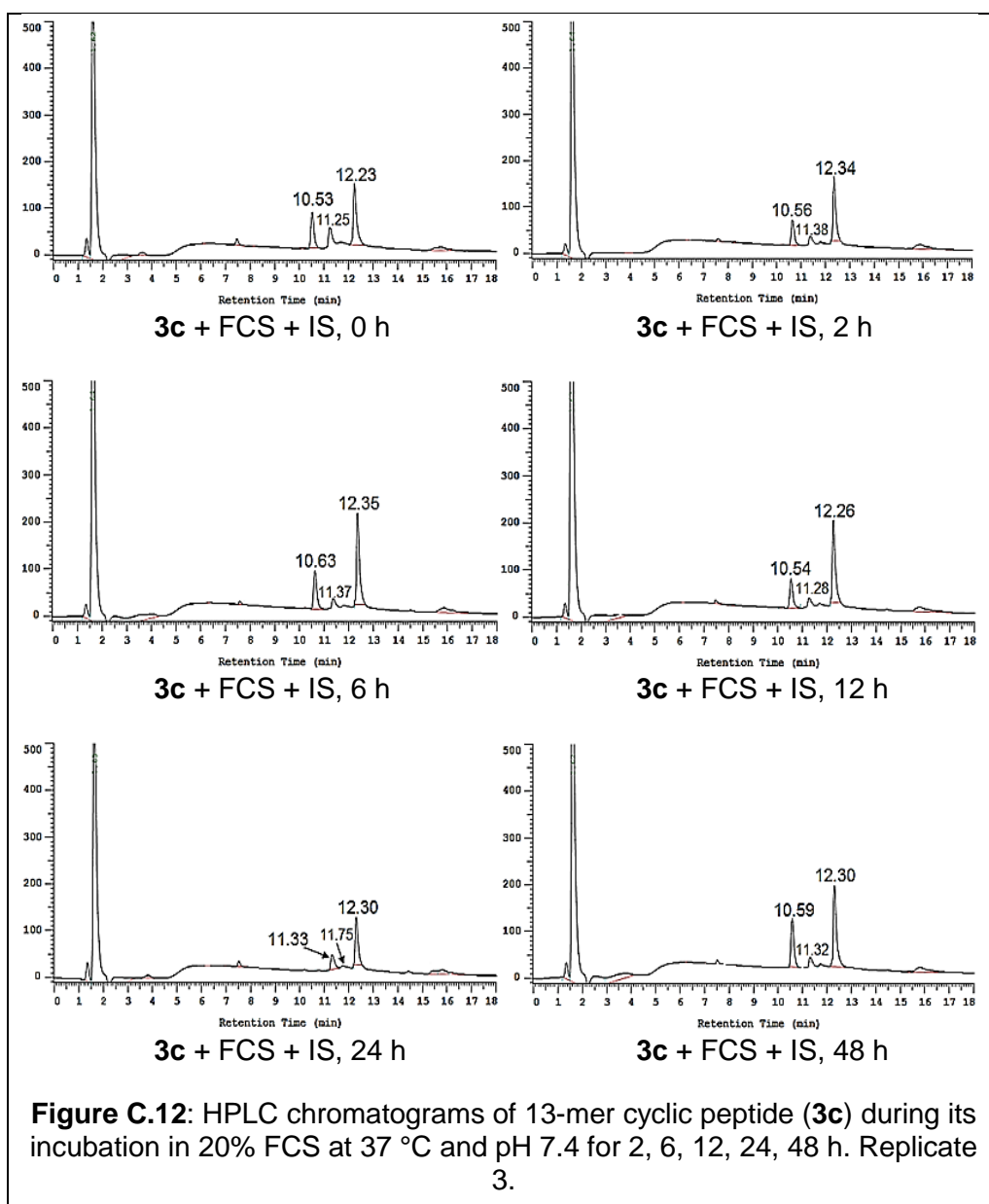


**Table C.4:** Areas of HPLC peaks for 13-mer cyclic peptide (**3c**) during its incubation in 20% FCS for 0, 2, 6, 12, 24, 48 h, in addition to areas of internal standard peaks (IS). Three replicates.

Time (h)	0	2	6	12	24	48
1- <b>3c</b> area	104506	102887	103335	109229	145597	108236
2- <b>3c</b> area	120395	131932	100142	985131	127776	131245
3- <b>3c</b> area	114401	960511	147288	129664	721572	143802
1-IS area	487721	534109	563335	539081	756118	610875
2-IS area	576304	709146	460786	449606	615745	656197
3-IS area	540835	436066	659662	491577	299432	789580